Etching of Wood by Glow-discharge Plasma

by

Arash Jamali

M.Sc. University of Tehran, 2005

A THESIS SUBMITTED IN PARTIAL FULFILLMENT OF
THE REQUIREMENTS FOR THE DEGREE OF

DOCTOR OF PHILOSOPHY

in

THE FACULTY OF GRADUATE STUDIES

(Forestry)

THE UNIVERSITY OF BRITISH COLUMBIA
(Vancouver)

December 2011

Abstract

In this thesis I hypothesize that plasma will etch wood surfaces, produce new cell wall microstructures, and change the surface chemistry of wood because of differential etching of wood's polymeric constituents. I also examine factors affecting the etching of wood by plasma, and applications of plasma etching for wood processing. Scanning electron and light microscopy and white light confocal profilometry were used to examine etching of wood surfaces. Wet chemical analysis, FTIR and XPS spectroscopy were used to analyze chemical changes at the surface of plasma-treated wood. Experiments were also performed to examine the effect of plasma treatments on the color of blue-stained wood, the morphology of fungal hyphae and the adhesion and performance of coatings on hot-oil modified wood. Exposure of wood to plasma caused etching of wood cell walls and created new surface microstructures. Regions of cell walls that were rich in lignin such as the middle lamella were etched more slowly by plasma. Confocal profilometry of wood exposed to plasma revealed a strong relationship between plasma treatment time and etching of cell walls, and same technique found that lignin pellets were etched more slowly than cellulose pellets. Plasma reduced the levels of carbohydrate at the surface of modified wood, which resulted in a relative increase in lignin content. Plasma treatment improved the effectiveness of hypochlorite bleach at removing blue-stain from wood and it prevented the discoloration of a white acrylic paint on hot-oil modified wood exposed to natural weathering. However, plasma treatment of hot-oil modified wood did not have positive effects on the adhesion and exterior performance of a range of other coatings (mainly semi-transparent stains). I conclude that prolonged exposure to plasma can etch wood cell walls, but cell wall layers that are rich in lignin are degraded more slowly. Plasma etching of wood mainly depends on treatment time and also on the structure and chemical composition of wood. Plasma treatment is an efficient pre-treatment for bleaching of blue-stained wood and reducing the discoloration of white acrylic paint on hot-oil modified wood.

Preface

Parts of Chapters 3 and 4 have been published in an international journal. The original publication is available at www.springerlink.com. Jamali, A. and Evans, P.D. *Etching of wood surfaces by glow discharge plasma*. Wood Science and Technology. Volume 45, Issue 1 (2011), Pages 169-182. I conducted all the experimental research described and discussed in this paper and I wrote the manuscript. Experimental design, statistical analysis and preparation of the final draft relied on the input of my co-author Professor Philip D. Evans.

Part of Chapter 7 can be found in a published report prepared for FPInnovations-Forintek. *Plasma treatment of oil-modified MPB wood*. Jamali, A. and Evans, P.D. In: Coatability of thermal-oil-treated post-MPB, FPInnovations-Forintek Division, Canada (2008), pp. 48-58. I conducted the experimental research described and discussed in this report and I wrote the report. My supervisor Professor Philip D. Evans contributed to the design of the experiments and analysis of results.

Table of contents

Abstract ..... *ii*

Preface ..... *iii*

Table of contents ..... *iv*

List of tables ..... *xi*

List of figures ..... *xiii*

Acknowledgements ..... *xxii*

Dedication ..... *xxiii*

1 General introduction *1*

1.1 Introduction **1**

1.2 General hypothesis **3**

1.3 Outline of study **4**

2 Literature review *5*

2.1 Introduction **5**

2.2 Plasma **7**

2.2.1 Introduction 7

2.2.1.1 Plasma types 8

2.2.1.2 Plasma generation 9

2.2.2 Glow-discharge plasma 10

2.2.3 Effects of plasma on the surface of materials 11

2.2.3.1 Plasma functionalization (activation) 13

2.2.3.2 Plasma deposition (coating) 14

2.2.3.3 Plasma etching (ablation) 15

2.3 Wood surface properties and modification 19

2.3.1 Introduction 19

2.3.2 Wood surfaces 21

2.3.3 Modification of wood surfaces 25

2.3.3.1 Mechanical treatments 27

2.3.3.2 Biological treatments 28

2.3.3.3 Chemical treatments 31

2.3.3.4 High energy treatments 33

2.4 Plasma modification of wood 36

2.4.1 Introduction 36

2.4.2 Plasma modification and wood composites 37

2.4.3 Plasma treatment of solid wood 41

2.4.3.1 Effect on chemical properties 41

2.4.3.2 Effects of plasma on wood structure and physical properties 43

2.4.4 Processing of solid wood with plasma 44

2.4.4.1 Glue bonding 44

2.4.4.2 Coating 47

2.5 Overview 50

3 Effects of plasma etching on the microstructure of wood 53

3.1 Introduction 53

3.2 Materials and methods 55

3.2.1 Wood samples and specimen preparation 55

3.2.2 Plasma treatments 57

3.2.3 Scanning electron microscopy 60

3.2.4 Light microscopy 60

3.3 Results 61

3.3.1 Effect of plasma on microstructure of wood cell walls 61

3.3.2 Effect of plasma etching on the microstructure of pits 76

3.4 Discussion 82

3.5 Conclusions 85

4 Quantification of etching of wood and its polymeric components using confocal profilometry 86

4.1 Introduction 86

4.2 Materials and methods 88

4.2.1 Experimental design and statistical analysis 88

4.2.2 Wood samples 90

4.2.2.1 Normal wood 90

4.2.2.2 Compression wood 91

4.2.3 Preparation of cellulose/lignin pellets 92

4.2.4 Plasma treatments 93

4.2.5 Surface confocal profilometry and data acquisition 94

4.2.5.1 Profilometry of wood samples 94

4.2.5.2 Profilometry of cellulose and lignin pellets 95

4.2.6 Light and scanning electron microscopy 96

4.3 Results 98

4.3.1 Use of white light confocal profilometry to image the surface structure of wood 98

4.3.2 Quantification of plasma etching of radial and tangential cell walls of yellow cedar and poplar 102

4.3.3 Etching of compression wood 104

4.3.4 Etching of cellulose and lignin pellets 107

4.4 Discussion 114

4.5 Conclusions 117

5 Effects of plasma etching on chemical composition of wood 119

5.1 Introduction 119

5.2 Materials and methods 120

5.2.1 Experimental design and statistical analysis 120

5.2.2 Wood samples 121

5.2.3 Wet chemical analysis 121

5.2.3.1 Veneer preparation and treatment 121

5.2.3.2 Acid insoluble (Klason) lignin 122

5.2.3.3 Acid soluble lignin 123

5.2.3.4 High performance liquid chromatography 123

5.2.3.5 Analysis of aqueous extract 125

5.2.4 Fourier transform infra-red spectroscopy (FTIR) 126

5.2.5 X-ray photoelectron spectroscopy (XPS) 127

5.3 Results 130

5.3.1 Wet chemical analysis 130

5.3.1.1 Lignin content 131

5.3.1.2 Sugar content 132

5.3.1.3 Chemical composition of aqueous extracts 135

5.3.2 FTIR analysis 136

5.3.3 XPS analysis 144

5.4 Discussion 146

5.4.1 Hypothesis 146

5.4.2 Relationship of findings to other studies 150

5.4.3 Limitations 152

5.5 Conclusions 154

6 Plasma etching and bleaching to remove blue-stain from lodgepole pine 156

6.1 Introduction 156

6.2 Materials and methods 158

6.2.1 Experimental design and statistical analysis 158

6.2.2 Wood samples 158

6.2.3 Contact angle 159

6.2.4 Bleaching 160

6.2.5 Color measurement 160

6.2.5.1 Light microscopy 161

6.2.5.2 Hyphae collection and analyses 162

6.3 Results 164

6.3.1 Effect of plasma on contact angle and color of blue-stained wood before and after bleaching..... 164

6.3.2 Effect of plasma treatment on the structure of fungal hyphae 172

6.4 Discussion 176

6.5 Conclusions 178

7 Effect of plasma etching on surface properties of hot-oil modified blue-stained wood…… ..... ……..180

7.1 Introduction 180

7.2 Materials and methods 182

7.2.1 Experimental design and statistical analysis 182

7.2.2 Wood samples 183

7.2.3 Hot-oil modification of blue-stained sapwood and plasma treatments 185

7.2.4 Contact angle measurement 186

7.2.5 Scanning electron microscopy and confocal profilometry 186

7.2.6 Application of coatings and measurement of coating adhesion 187

7.2.7 Exposure of specimens to natural weathering and evaluation of coating performance 190

7.3 Results 193

7.3.1 Effect of hot-oil modification and plasma treatment on the appearance and microstructure of wood……. 193

7.3.2 Wettability, water uptake and adhesion of coatings 196

7.3.2.1 Exterior performance of coatings on hot-oil modified and plasma treated blue-stained sapwood……. 200

7.4 Discussion 207

7.5 Conclusions 210

8 General discussion, conclusions and suggestions for further research 212

8.1 General discussion 212

8.2 Conclusions 215

8.3 Suggestions for further research 216

References *219*

Appendices *242*

Appendix 1 - Collection of SEM and light microscopy images of untreated and plasma treated samples of studied species **242**

Appendix 2 - Statistical analysis: Chapter 4 ..... **243**

Appendix 3 - Statistical analysis: Chapter 5 ..... **244**

Appendix 4 - Statistical analysis: Chapter 6 ..... **245**

Appendix 5 - Statistical analysis: Chapter 7 ..... **246**

List of tables

Table 3.1: Wood species treated with glow-discharge plasma and examined using scanning electron microscopy or light microscopy 55

Table 4.1: Summary of the statistical significance of species type, cell wall type and plasma treatment time on ratio of cell wall removed during plasma to their initial volume and mass losses of the cell walls 102

Table 4.2: Roughness parameters (S_a, S_q and S_t) of lignin/cellulose pellet surface before and after exposure to plasma for 667 s 108

Table 5.1: The effects of and interactions between experimental factors on chemical constituents of lodgepole pine and poplar wood samples 130

Table 5.2: Dry mass of phenolics and sugars in aqueous extract of plasma treated and untreated poplar and lodgepole pine wood veneers 135

Table 5.3: Ratios of the bands associated with lignin and carbohydrates in FTIR spectra of lodgepole pine 140

Table 5.4: Ratios of the bands associated with lignin and carbohydrates in FTIR spectra of poplar 143

Table 5.5: O/C ratio and fractional area percent of C1s components for untreated and plasma-treated lodgepole pine and poplar wood specimens 145

Table 6.1: Summary of the results of analyses of variance of the effects plasma treatment on response variables: contact angle, bleach uptake and CIE Lab color parameters 164

Table 7.1: Selected coatings that were applied to hot-oil modified blue-stained wood after treating the surface with plasma for different periods of time 187

Table 7.2: Description of ASTM (D 3359) classifications for the cross-cut adhesion of coatings to tested substrates 188

Table 7.3: Selected coatings for the outdoor weathering test that were applied to the blue-stained lodgepole pine sapwood samples, including untreated, hot-oil modified, plasma treated and hot-oil/plasma treated wood 189

Table 7.4: Meteorological conditions at the site in Vancouver where coated specimens were exposed to the weather (August 2007 to March 2009) 191

Table 7.5: List of parameters that were used to assess the performance of modified and coated blue-stained wood specimens exposed to natural weathering 192

Table 7.6: Summary of the statistical significance of plasma treatment (T) and coating type (C) on surface wettability, water uptake, and adhesion of coatings to hot-oil modified wood 196

Table 7.7: Summary of statistical significance of treatment (T), coating (C) and treatment x coating interactions on response variables measured on coatings on modified blue-stained lodgepole pine wood samples exposed to 18 months of outdoor weathering. Total color change of surface calculated from CIE Lab color parameters on weathered and nonweathered samples; surface

gloss and water uptake are expressed as ratios of weathered values to nonweathered values; and crack percent represent the measured values on weathered samples 201

List of figures

Figure 2.1: Has been removed due to copyright restrictions. It was a schematic diagram of the three different responses of a material to plasma; (1) functionalization (2) coating and (3) etching (modified after a diagram in Rossell 2007) 13

Figure 2.2: Has been removed due to copyright restrictions. It was SEM photomicrographs of polyethylene terephthalate (PET) treated with oxygen plasma for: (a) 1 min; (b) 4 min; (c) 10 min; and (d) 30 min. Note development of fibrils with increasing treatment time (Wohlfart et al. 2010)..17

Figure 2.3: Has been removed due to copyright restrictions. It was SEM photomicrographs of nanopillar structures (used for solar cell applications), fabricated by etching of silicon nitride film using a gas mixture of CF4/O2 at different treatment times: (a) 90 s; (b) 120 s; (c) 150 s; and (d) 180 s (Sahoo et al. 2009) 18

Figure 2.4: Has been removed due to copyright restrictions. It was a schematic diagram of a transverse section of wood showing wood's complete and cut-through cellular structure with voids and fractures in cell walls. Both of these 'flow paths' increase the surface area available for bonding of adhesives/coatings (modified after an illustration in Frihart 2005) 23

Figure 2.5: Discoloration of wood by blue stain fungi: (left) cross section of a stem of blue-stained lodgepole pine (Pinus contorta) showing darkening of sapwood (arrowed); and (right) a stack of lodepole pine wood containing some blue-stained boards (arrowed) 25

Figure 2.6: Has been removed due to copyright restrictions. It was SEM photomicrographs of the fracture surface of air-plasma treated wood-fibre- polypropylene composites (treatment time 30 s): (a) overall fracture surface; (b) magnified view of the identified area (Yuan et al. 2004) 38

Figure 3.1: Sliding microtome and the blade used to cut thin slices from specimens: (a) the blade holder and sample holder with a fixed sample (dotted arrow indicates direction of sectioning); and (b) close-up of a specimen being sectioned 57

Figure 3.2: Schematic diagram of the plasma reactor used to modify wood specimens (courtesy of Anthony Hyde, The Australian National University) 58

Figure 3.3: A glow-discharge water vapor plasma (purple) produced in the reactor chamber of the plasma device under vacuum (~19.99 Pa) with a radio frequency signal of 125 kHz at 150 watts...59

Figure 3.4: SEM photomicrographs of the transverse surfaces of untreated redwood: (a) a transverse plane with two whole annual rings, showing the transition between earlywood and latewood within annual rings and distinct boundaries at the ring border; (b) higher magnification image showing the border between the thinner-walled and larger-lumened earlywood tracheids at the top and thicker-walled latewood tracheids at the bottom; note the presence of inter-tracheid bordered pits in earlywood and latewood and half-bordered cross-field pitting in radial walls of earlywood tracheids; (c) a high magnification image of latewood tracheids; note the thick walls, small pit (arrowed) and also the conspicuous middle lamella at the corners; and (d) a high magnification image of earlywood tracheids; note the thin walls and large inter-tracheid bordered pits 63

Figure 3.5: SEM photomicrographs of transverse surfaces of plasma treated latewood tracheids in redwood: (a) tracheids exposed to plasma for 33 s, note creation of a micro-roughened surface and small cavities in cell walls; (b) tracheids exposed to plasma for 333 s; note further erosion of the secondary cell walls and formation of ridges created by middle lamellae at the surface; (c) tracheids exposed to plasma for 667 s, showing a rough surface with enlarged voids; and (d)

tracheids subjected to plasma for 1333 s, showing pronounced etching of secondary wall; split-screen enlarged images showing middle lamella (arrowed) and thin lamellae radiating from the middle lamella to the tertiary wall layer 64

Figure 3.6: SEM photomicrographs of transverse surfaces of plasma treated earlywood tracheids in redwood: (a) tracheids exposed to plasma for 333 s; (b) higher magnification image of tracheids exposed to plasma for 333 s, showing etching of secondary cell walls. Note the voids in the cell wall; (c) tracheids exposed to plasma for 1333 s; split-screen image showing a higher magnification image of a tracheid, note thinning of tracheids' walls and the greater resistance of the resinous contents of the ray cells to etching; and (d) a high magnification image of tracheids exposed to plasma for 1333 s showing higher resistance of compound middle lamella and cell wall material in the corner of tracheids to etching 65

Figure 3.7: SEM photomicrographs of transverse surfaces of rose gum (*E. grandis*): (a) untreated fibers; and (b) surface exposed to plasma for 1333 s, note extensive etching (thinning) of cell walls and remnants of middle lamellae between fibers 66

Figure 3.8: Light microscopy images of transverse sections of poplar stained with safranin: (a) untreated section showing cross-section of fibers and ray parenchyma and; (b) Cross-section exposed to plasma for 667 s, showing thinning of fiber cell walls and enlargement of lumina of the fibers, note the erosion of ray parenchyma cells 67

Figure 3.9: SEM photomicrographs of transverse surfaces of rose gum: (a) untreated surface showing cross-cut fibers and three vessels occluded with tyloses and (b) surface subjected to plasma for 1333 s showing etching of fibers and removal of tyloses from two vessels.....68

Figure 3.10: SEM photomicrographs of radial longitudinal surfaces of redwood: (a) untreated surface containing earlywood and latewood tracheids oriented in longitudinal direction and parenchyma cells arranged radially in rays; (b) surface exposed to plasma for 667 s showing enlargement of the apertures of bordered pits and etching of cell walls of tracheids and parenchyma cells; (c) surface exposed to plasma for 1333 s, showing extensive etching and removal of all cellular elements at the surface 71

Figure 3.11: SEM photomicrographs of radial longitudinal surfaces of poplar: (a) untreated surface showing fibers and vessel elements, with an alternating arrangement of inter-vessel pits (arrowed left); (b) surface exposed to plasma for 667 s, showing etching of fibers, ray parenchyma and vessel elements; (c) surface exposed to plasma for 1333 s showing severe etching of all element at the surface, note the etching of inter-vessel pits and perforation plates 72

Figure 3.12: SEM photomicrographs of tangential longitudinal surfaces of redwood: (a) untreated surface showing uniseriate rays and bordered pits in tangential walls (arrowed); (b) surface exposed to plasma for 667 s, note etching of cell walls and bordered pits; (c and d) earlywood exposed to plasma for 1333 s, note thinning of ray parenchyma cells in rays, severe etching of cell walls, and contents of ray and longitudinal parenchyma cells remaining at the surface (d) (arrowed) 73

Figure 3.13: Light microscopy images of cross-fields in radial sections of redwood: (a) untreated section, note the presence taxodioid cross-field pitting and resinous deposits in ray parenchyma cells (goldish brown); and (b) sections subjected to plasma for 667 s, showing erosion of pits and cell walls, note presence of resinous material in ray parenchyma cells.....74

Figure 3.14: SEM photomicrographs of radial longitudinal and transverse surfaces of Actinostrobus: (a) untreated earlywood tracheids showing a bordered pit and large warts on the tertiary wall layer; (b) tracheids exposed to plasma for 333 s, note remnants of large warts on tracheid walls; (c) tracheids exposed to plasma for 667 s, note presence of warts on the "pulpy

layer" on tracheids; (d) tracheids exposed to plasma for 1333 s, note heavily etched remnants of cell wall remaining at the wood surface; (e) untreated transverse surface showing warty layers covering cell walls and pit borders and (f) tracheids exposed to plasma for 1333 s showing thinning of cell walls on the surface and remnants of warts inside tracheids 75

Figure 3.15: Radial longitudinal surfaces of redwood before and after plasma treatment: (a) untreated earlywood showing bordered pits in tracheids with bi- and triseriate arrangement of pits, note intact pit membranes; (b) untreated earlywood showing taxodioid cross-field pits, note intact pit membranes; (c) earlywood tracheids exposed to plasma for 667 s, note etching of half-bordered cross-field pit membranes (arrowed left of centre) and etching of the raised border of a bordered pit (arrowed top right); (d) earlywood and latewood (far left) exposed to plasma for 1333 s, note complete degradation of upper cell walls of earlywood tracheids and etching of bordered pits in sub-surface tracheids (arrowed centre); (e) latewood tracheid exposed to plasma for 1333 s showing etching of borders on both sides of bordered pits, note roughening of cell wall, and outer collars of bordered pits remaining at the surface (arrowed left); (f) latewood tracheid exposed to plasma for 1333 s showing etching of cell wall material separating bordered pits (arrowed right) and (g) earlywood tracheids exposed to plasma for 1333 s showing heavily etched tracheid walls, note that in this case the borders of pits resisted etching and are suspended at the surface by a thin web of cell wall material.....77

Figure 3.16: Light microscopy images of radial sections of radiata pine: (a) untreated section showing longitudinal tracheids containing bordered pits, note pit apertures and outer border; (b) section exposed to plasma for 667 s, showing complete or partial (arrowed) removal of bordered pits and intervening cell walls, (c) section exposed to plasma for 1333 s, showing complete removal of cell walls (in radial plane).....78

Figure 3.17: SEM photomicrographs of tangential longitudinal surfaces of redwood; (a) untreated earlywood showing a uniseriate ray (centre) and bordered pits in tangential walls (arrowed left of centre); and (b) earlywood and latewood exposed to plasma for 1333 s, note etching of cell walls (arrowed left of centre) and greater resistance of the outer borders of bordered pits to etching (arrowed right of centre).....79

Figure 3.18: SEM photomicrographs of adjacent vessel elements in poplar; (a) untreated surfaces showing two vessels with the inter-vessel bordered pits and helical thickening on cell walls; split-screen image showing magnified image of pits and (b) surface exposed to plasma for 667 s; split-screen is a higher magnification image of etched inter-vessel bordered pits, and (c) surface exposed to plasma for 1333 s showing severe etching of the alternating inter-vessel pits and their adjacent walls; note the greater resistance of outer borders of the pits and helical thickening to etching.....81

Figure 4.1: Principles of a chromatic confocal profilometer (www.altimet.fr) 87

Figure 4.2: Cross section of a slat of yellow cedar containing normal wood and compression wood (darker color, arrowed) used to provide experimental specimens.....92

Figure 4.3: Method of masking surfaces of cellulose and lignin pellets prior to plasma treatment 93

Figure 4.4: Screen shot of the function within PaperMap software used to extract profiles of cell walls along the delimited length (50 µm). Images show a tangential cell wall and its cross-sectional profiles (right) 95

Figure 4.5: 2-D chromatic confocal profilometry maps of yellow cedar surfaces (RLS) with full-spectral color progression bars: (a) Untreated surface showing six longitudinal tracheids with their protruding tangential cell walls, note the presence of bordered pits with a uniseriate

arrangement; (b) the same surface exposed to plasma for 667 s, note removal of tangential cell walls and etching of bordered pits on radial cell walls 98

Figure 4.6: 3-D topographical images of radial longitudinal surfaces of yellow cedar and their corresponding transverse 2-D profiles: (a) 3D image of untreated specimen showing two adjacent longitudinal tracheids in the centre, note the thickness of raised tangential cell walls and the outlines of biseriate bordered pits in between these cell walls; (b) 2D profile of image 4.6a drawn across the longitudinal tracheids and showing the height and thickness of cell walls at the traverse points; (c) 3D image showing the same area as image 4.6a, after exposure to plasma for 333 s, note the height and thickness of cell walls; and (d) corresponding 2D profile of image 4.6c 99

Figure 4.7: Topographical images of bordered pits at radial longitudinal surface of yellow cedar: (a) untreated earlywood tracheids with a uniseriate arrangements of bordered pits, note presence of pit domes; (b) same earlywood tracheids shown in Fig. 4.7a after exposure to plasma for 333 s showing a rougher surface with partial erosion of pits; and (c) the same earlywood tracheids shown in Fig. 4.7 a-b after exposure to plasma for 667 s showing etching of bordered pits, note the absence of pit domes and greater resistance of the outer collar of the bordered pits to etching 100

Figure 4.8: Topographical images of cell walls on a radial longitudinal surface of yellow cedar before and after plasma treatment: (a) untreated earlywood tracheid showing tangential cell walls and bordered pits; (b) the same earlywood tracheid shown in Fig. 4.8a after exposure to plasma for 333 s, note thinning of cell walls and decreases in height of tangential cell walls in places and (c) the same earlywood tracheid shown in Fig. 4.8a–b after exposure to plasma for 667 s, note pronounced thinning and decreases in height of tangential cell walls and etching of bordered pits and the residual of middle lamella in between tracheids.....101

Figure 4.9: Effect of treatment time on the ratio of cell wall material removed by plasma to their initial volume in yellow cedar and poplar specimens (results are averaged across species and cell walls [radial and tangential]). Error bars are ± standard error of differences of means (from analysis of variance). Non-overlap of these bars indicates that means are significantly different at 5% level (p<0.05).....103

Figure 4.10: Effect of treatment time on the mass losses of yellow cedar and poplar cell walls exposed to plasma (results are averaged across species and cell walls [radial and tangential]). Error bars are ± standard error of differences of means (from analysis of variance). Non-overlap of these bars indicates that means are significantly different at 5% level (p<0.05) 103

Figure 4.11: Effect of wood species and cell wall type on losses of volume of cell walls in specimens exposed to plasma (results are averaged across treatment time). Least significant difference (lsd) bar is based on 95% confidence intervals (from analysis of variance) to estimate the significance of differences between individual means.....104

Figure 4.12: Effect of wood type (normal v. compression wood) of yellow cedar specimens on the ratio of cell wall volume removed to the initial volume as a result of plasma treatment for 667 s. Note the left Y axis represents the transformed data expressed on a logarithmic scale. The right (Y_2) axis expresses data in the natural scale. Error bars are ± standard error of differences of means (from analysis of variance). Non-overlap of these bars indicates that means are significantly different at 5% level (p<0.05).....105

Figure 4.13: SEM photomicrographs of radial longitudinal surfaces of earlywood in normal and compression wood of yellow cedar: (a) normal untreated tracheids showing standing tangential cell walls; (b) earlywood tracheids exposed to plasma for 667 s, note thinning of tangential cell walls and enlargement of bordered pit apertures; (c) untreated earlywood tracheids in

compression wood, note the helical cavities and ribs in S_2L; (d) compression wood tracheids exposed to plasma for 667 s, note widening of the cavities and separation of some of the ribs from the underlying cell wall layers 106

Figure 4.14: SEM photomicrographs of transverse surfaces of compression wood tracheids in the earlywood of yellow cedar: (a) untreated surface; and (b) surface exposed to plasma for 667s...107

Figure 4.15: Topographical images of the surface of cellulose-lignin pellets: (a) untreated surface and (b) pellet surface exposed to plasma for 1333 s.....107

Figure 4.16: SEM and light microscopy images of the surface of cellulose-lignin pellets: (a) untreated surface showing a flat surface with some micro-cracks; (b) surface exposed to plasma for 1333 s showing a micro-roughened surface and differential erosion of the surface; (c) higher magnification image of surface treated for 1333 s; and (d) reflected light microscopy image of the surface of a pellet exposed to plasma for 1333 s, showing a distinct color difference between cellulose and lignin 109

Figure 4.17: Light microscopy images and two and three dimensional images of the surface of cellulose-lignin pellets: (a) reflected light microscopy image showing golden brown (left hand side) and white colored areas (right hand side) indicating the presence of lignin and cellulose, respectively; (b) 2D confocal profilometry map of the same area shown in Fig. 4.17a; and (c) 3D topographical image of the same area in Fig. 4.17a-b showing greater erosion on the right hand side of the image (cellulose) compared to the erosion of lignin on the left hand side 110

Figure 4.18: Profile obtained from a linear scan across masked and unmasked areas in a cellulose pellet exposed to plasma for 1333 s.....111

Figure 4.19: Effect of pellet type (cellulose v. lignin) on the depth of etching of pellets exposed to plasma (results are averaged across plasma treatment times). Error bars are ± standard error of differences of means (from analysis of variance). Non-overlap of these bars indicates that means are significantly different at 5% level ($p<0.05$) 112

Figure 4.20: Effect of plasma treatment time on the depth of etching of pellets exposed to plasma (results are averaged across pellet type). Error bars are ± standard error of differences of means (from analysis of variance). Non-overlap of these bars indicates that means are significantly different at 5% level ($p<0.05$).....112

Figure 4.21: SEM and light microscopy images of the masked (left side) and unmasked (right side) areas of cellulose (a and b) and lignin (c and d) pellets exposed to plasma for 667s: (a) SEM photomicrograph showing the border between the masked (left side) and unmasked surface in a cellulose pellet, note the increased brightness of the area exposed to plasma; (b) reflected light microscopy image of the pellet in Fig. 4.21a showing the boundary between the etched and masked areas, note the darker color of the area exposed to plasma; (c) SEM photomicrograph showing the boundary between the masked (left side) and unmasked surface of a lignin pellet, note the increased lightness of the area exposed to plasma and; (d) reflected light microscopy of the pellet in Fig. 4.21c showing boundary between the etched and masked areas, note the darker brown color of the plasma treated lignin.....113

Figure 5.1: Chromatograph of monosaccharide analysis of plasma treated poplar using HPLC; arabinose (Ara), galactose (Gal), glucose (Glu), xylose (Xyl), mannose (Man) and fucose as an internal standard 125

Figure 5.2: Assignment of the baselines for the calculation of area under peaks in a FTIR spectrum (zoomed spectrum of an untreated poplar specimen) 127

Figure 5.3: Changes in the total lignin (a), acid insoluble lignin (b) and acid soluble lignin (c) of vacuum (control) and plasma treated poplar and lodgepole pine veneers. lsd (least significant difference) bar is based on 95% confidence intervals (from analysis of variance) to estimate the significance of differences between individual means 131

Figure 5.4: Changes in total sugar content of plasma treated poplar and lodgepole pine veneers. lsd (least significant difference) bar is based on 95% confidence intervals (from analysis of variance) to estimate the significance of differences between individual means.....132

Figure 5.5: Effects of species (a) and plasma treatment (b) on arabinose content of wood samples. Error bars are ± standard error of differences of means (from analysis of variance). Non-overlap of these bars indicates that means are significantly different at 5% level (p<0.05) 133

Figure 5.6: The effect of plasma treatment on the sugar content of poplar and lodgepole pine: (a) galactose; (b) mannose; (c) xylose; (d) glucose; and (e) cellulose to total sugar content. lsd (least significant difference) bars based on 95% confidence intervals for plasma x plasma interactions and ± 2x standard errors of the difference (sed) bars for plasma effects derived from analysis of variance 134

Figure 5.7: (a) FTIR spectra of lodgepole pine (from bottom to top: untreated, and plasma treated for 333 s, 667 s, 1000 s and 1333 s). Raw spectra were baseline corrected manually at 3732.31, 3021.03, 2248.56, 1830.05, 1694.48, 1549.36, 1488.26, 1396.60, 1297.31, 1188.47, 923.05, 844.76 and 789.39 cm^{-1}, then the band around 1373 cm^{-1} (a C-H band) was used as an internal standard i.e. its intensity was adjusted to 1.5 and all spectra zeroed at 1900 cm^{-1} in accord with the method used by Tolvaj and Faix (1995); (b) enlarged area of Fig. 5.7a, ranging from around 1800 to 1100 cm^{-1} 137

Figure 5.8: Areas under altered peaks in FTIR spectra of plasma-treated lodgepole pine relative to those of controls 140

Figure 5.9: (a) FTIR spectra of poplar (from bottom to top: untreated, and plasma treated for 333 s, 667 s, 1000 s and 1333 s). Raw spectra were baseline corrected manually at 3700.00, 1900.00, 1540.00, 1484.00, 1400.00, 1295.00, 1188.00, 921.14, 865.00, 800.84 and 651.00 cm^{-1} then the band around 1373 cm^{-1} (a C-H band) was used as an internal standard i.e. its intensity was adjusted to1.5 and all spectra zeroed at 1900 cm^{-1} in accord with the method used by Tolvaj and Faix (1995); (b) enlarged area of Fig. 5.9a, ranging from around 1800 to 1100 cm^{-1} 142

Figure 5.10: Areas under altered peaks in FTIR spectra of plasma-treated poplar relative to those of controls 143

Figure 5.11: (a) An XPS survey spectrum showing the electron intensity (arbitrary units) (vertical) versus binding energy (horizontal) for untreated lodgpole pine with domination of C1s and O1s in the spectrum; (b) high-resolution C1s spectrum of the same sample 144

Figure 6.1: KVS instrument used for contact angle measurements of untreated and plasma treated blue stained wood 160

Figure 6.2: Effect of plasma treatments on contact angle of water droplets on blue-stained lodgepole pine sapwood (Y1 axis is expressed on a logarithmic scale, Y2 axis is back transformed ex to compare results on the natural scale). Error bars are ± standard error of differences of means (from analysis of variance). Non-overlap of these bars indicates that means are significantly different at 5% level (p<0.05).....165

Figure 6.3: Effect of plasma treatments on the absorption of bleach by blue-stained lodgepole pine sapwood. Error bars are ± standard error of differences of means (from analysis of variance). Non-overlap of these bars indicates that means are significantly different at 5% level (p<0.05)...166

Figure 6.4: Effect of plasma treatments on the b* (yellowness) of blue-stained lodgepole pine sapwood. Increasing values for b* indicates the removal of blue discoloration. Error bars are ± standard error of differences of means (from analysis of variance). Non-overlap of these bars indicates that means are significantly different at 5% level (p<0.05) 167

Figure 6.5: Effect of plasma treatments on ΔE (total color change) of blue-stained lodgepole pine sapwood. Error bars are ± standard error of differences of means (from analysis of variance). Non-overlap of these bars indicates that means are significantly different at 5% level (p<0.05) 167

Figure 6.6: Changes in the appearance of blue-stained lodgepole pine sapwood specimens (left column) exposed to plasma for different periods of time (top to bottom) and bleached by sodium hypochlorite (right column), and a sample of unstained lodgepole pine sapwood (bottom of the image) 168

Figure 6.7: Effect of plasma treatments and bleaching on ΔE (total color change) of blue-stained lodgepole pine sapwood. Error bars are ± standard error of differences of means (from analysis of variance). Non-overlap of these bars indicates that means are significantly different at 5% level (p<0.05) 169

Figure 6.8: Effect of plasma treatments on the a* (redness) of bleached blue-stained sapwood; note, dotted line indicates a* of unstained pine sapwood. Error bars are ± standard error of differences of means (from analysis of variance). Non-overlap of these bars indicates that means are significantly different at 5% level (p<0.05) 170

Figure 6.9: Effect of plasma treatments on the b* (yellowness) of bleached blue-stained sapwood; note, dotted line indicates b* of unstained pine sapwood. Error bars are ± standard error of differences of means (from analysis of variance). Non-overlap of these bars indicates that means are significantly different at 5% level (p<0.05) 171

Figure 6.10: Effect of plasma treatments on the L* (lightness) of bleached blue-stained sapwood; note, dotted line indicates L* of unstained pine sapwood. Error bars are ± standard error of differences of means (from analysis of variance). Non-overlap of these bars indicates that means are significantly different at 5% level (p<0.05) 171

Figure 6.11: Transmitted light microscopy images of untreated and plasma-treated blue-stained lodgepole pine sapwood; (a) untreated tangential longitudinal section of untreated wood showing a fungal hypha running along a longitudinal tracheid and penetrating a ray parenchyma cell; (b) tangential longitudinal section exposed to plasma for 333 s, note that the hypha and ray (centre) have been etched by the plasma; (c) untreated radial longitudinal section showing fungal hyphae penetrating into bordered pits; (d) radial longitudinal section exposed to plasma for 333 s, showing etching of cell walls and hyphae, note that hyphae are much lighter as a result of plasma treatment 172

Figure 6.12: SEM photomicrographs of a hyphal mat of *Grosmannia clavigera*, which was grown for 3 weeks (a-d) and lodgepole pine wood (e-f): (a) untreated hyphae showing warty surfaces; (b) hyphae exposed to plasma for 667 s showing degradation of hyphae and exposure of internal hyphal walls; (c) higher magnification image of untreated hyphae showing their tubular shape and presence of globular granules on hyphal walls; (d) higher magnification image of hyphae exposed to plasma for 667 s showing removal (etching) of hyphal walls; and (e and f) radial longitudinal tracheids in the earlywood of lodgepole pine sapwood (R.L.S) before (e) and after exposure to plasma for 667 s (f), note etching of bordered pits by plasma and creation of voids at the surface of tracheids 174

Figure 6.13: Transmission electron photomicrographs of a hypha of *Grosmannia clavigera* from 3-week old mycelium: (a) untreated hypha, note the rough warty layer on the intact wall; (b) a hypha

exposed to plasma for 667 s showing erosion of its wall; (c) untreated hypha with a hollow tubular shape, note the globular granules; (d) hypha exposed to plasma for 667 s showing thinning of the wall and loss of electron density 175

Figure 7.1: Schematic diagram of the cutting pattern used to prepare veneers, samples and specimens from hot-oil modified blue-stained lodgepole pine sapwood blocks.....184

Figure 7.2: Schematic diagram of the cutting pattern used to produce samples, veneer and specimens from blue-stained lodgepole pine sapwood blocks.....185

Figure 7.3: A set of specimens including (from left to right) control; hot-oil/plasma treated; plasma treated; and hot-oil modified (five coatings were applied on delimited areas on each specimen at random; a = Acrylic latex; b = Natural deck oil; c = Natural wood UV plus finish; d = Semitransparent wood finish; e = Premium oil-based deck stain) 189

Figure7.4: Color of blue-stained lodgepole pinewood; before (left) and after (right) hot-oil treatment (220 ºC) for 2h.....193

Figure 7.5: SEM photomicrographs of blue-stained lodgepole pine sapwood surfaces before and after hot-oil and plasma treatments: (a) untreated surface showing earlywood tracheids and uniseriate arrangements of bordered pits; (b) hot-oil modified samples, showing deposition of oil on and in tracheid lumens; (c) hot-oil modified blue-stained wood exposed to plasma for 333 s, note removal of oil and ballooning of membranes through pit apertures; (d and e) hot-oil modified blue-stained wood exposed to plasma for 1333 s showing etching of wood cell walls; and (f) high magnification photograph of a hot-oil modified blue-stained sample exposed to plasma for 1333 s showing almost complete removal of upper cell wall layers and exposure of sub-surface layers, note the greater resistance of bordered pits to etching 194

Figure 7.6: Surface topographical maps of the cell wall around pits in hot-oil modified blue-stained lodgepole pine sapwood before and after plasma treatment; (a) hot-oil modified surface before plasma treatment; (b and c) same surface shown in Fig. 7.6a after exposure to plasma for 333 s and 667 s, respectively. (e and f) showing another bordered pit before (e) and after (f) exposure to plasma for 667 s 195

Figure 7.7: The effect of plasma treatment time on contact angles of water droplets on uncoated hot-oil modified blue-stained lodgepole pine sapwood. Note that Y1 axis is expressed on a logarithmic scale, Y2 axis is back transformed to compare results on the natural scale. Error bars are ± standard error of differences of means (from analysis of variance). Non-overlap of these bars indicates that means are significantly different at 5% level (p<0.05).....197

Figure 7.8: Water uptake of hot-oil modified blue-stained lodgepole pine sapwood finished with different coatings (results are averaged across different plasma treatments). ACL = Acrylic latex paint; PUR = Polyurethane; SNS = Supernatural semi-transparent stain; C123 = Cetol 1 and Cetol 23 semi-transparent stain. Error bars are ± standard error of differences of means (from analysis of variance). Non-overlap of these bars indicates that means are significantly different at 5% level (p<0.05).....198

Figure 7.9: Wet adhesion of different coatings to plasma-treated hot-oil modified blue-stained lodgepole pine sapwood (results are averaged across different plasma treatments). ACL = Acrylic latex paint; PUR = Polyurethane; SNS = Supernatural semi-transparent stain; C123 = Cetol 1 and Cetol 23 semi-transparent stain. Error bars are ± standard error of differences of means (from analysis of variance). Non-overlap of these bars indicates that means are significantly different at 5% level (p<0.05).....199

Figure 7.10: Effect of plasma treatment and coating type on dry adhesion of coatings on hot-oil modified blue-stained lodgepole pine sapwood; ACL = Acrylic latex paint; PUR = Polyurethane; SNS = Supernatural semi-transparent stain; C123 = Cetol 1 and Cetol 23 semi-transparent stain. Least significant difference (lsd) bar is based on 95% confidence intervals (from analysis of variance) to estimate the significance of differences between individual means.....200

Figure 7.11: Appearance of coated samples after exposure to weathering for 18 month; (from left to right) control, hot-oil/plasma treated, plasma treated and hot-oil modified (five different coatings were applied to delimited areas on each specimen at random; a = Acrylic latex; b = Natural deck oil; c = Natural wood UV plus finish; d = Semitransparent wood finish; e = Premium oil-based deck stain).....201

Figure 7.12: Interaction of treatment and coating type on ΔE (total color change) of weathered (18 months) blue-stained lodgepole pine wood; ACL = Acrylic latex; NDO = Natural deck oil; SFS = Semitransparent wood finish; UVP = Natural wood UV plus finish; OBS = Premium oil-based deck stain. Least significant difference (lsd) bar is based on 95% confidence intervals (from analysis of variance) to estimate the significance of differences between individual means.....202

Figure 7.13: Interactions of treatment and coating type on the ratio of G* (surface gloss) of weathered (18 months) blue-stained lodgepole pine wood to that of non weathered wood samples; ACL = Acrylic latex; NDO = Natural deck oil; SFS = Semitransparent wood finish; UVP = Natural wood UV plus finish; OBS = Premium oil-based deck stain. Least significant difference (lsd) bar is based on 95% confidence intervals (from analysis of variance) to estimate the significance of differences between individual means 203

Figure 7.14: Interactions of treatment and coating type on the ratio of water uptake of weathered (18 months) blue-stained lodgepole pine wood to that of non weathered wood samples; ACL = Acrylic latex; NDO = Natural deck oil; SFS = Semitransparent wood finish; UVP = Natural wood UV plus finish; OBS = Premium oil-based deck stain. Least significant difference (lsd) bar is based on 95% confidence intervals (from analysis of variance) to estimate the significance of differences between individual means.....204

Figure 7.15: Effect of hot-oil and plasma treatments on the surface cracking of coated blue-stained lodgepole pine samples exposed to the weather for eighteen months in Vancouver (results are averaged across coating types). Error bars are ± standard error of differences of means (from analysis of variance). Non-overlap of these bars indicates that means are significantly different at 5% level (p<0.05).....205

Figure 7.16: Effect of coating type on surface cracking of hot-oil and plasma modified blue-stained lodgepole pine samples exposed to the weather for eighteen months in Vancouver (results are averaged across treatment type); ACL = Acrylic latex; NDO = Natural deck oil; SFS = Semitransparent wood finish; UVP = Natural wood UV plus finish; OBS = Premium oil-based deck stain. Error bars are ± standard error of differences of means (from analysis of variance). Non-overlap of these bars indicates that means are significantly different at 5% level (p<0.05) 206

Acknowledgements

Professor Philip D. Evans, as a Ph.D. student I acknowledge all your scientific support and guidance throughout my studies at the University of British Columbia; as an international student, however, my greatest appreciation goes to you as a teacher whose energy, enthusiasm, patience and approach to research taught me lifelong lessons.

I would also like to thank Professor Stavros Avramidis and Professor Keith Mitchell for being on my supervisory committee and for their advice and encouragement during committee and informal meetings.

I am very grateful for the financial support of ForValueNet (NSERC), Forest Innovation Investment (through FPInnovations), Rix Family Foundation, and the in-kind support of Canadian Foundation for Innovation and BC Knowledge Development Fund.

I am thankful to the researchers and fellow graduate students in the Wood Surface Science group in the Faculty of Forestry at UBC for creating a highly collaborative environment in a very internationally diverse group. In particular, Dr. Marcos Gonzalez's and Dr. Jahangir Chowdhury's support and advice deserve special thanks. I am very thankful to Ian Cullis and Jonathan Haase, my office mates, who were a great help and comfort to me.

My warmest thanks go to Rebecca Dauwe whose love, empathy, encouragement and support during the past few years have motivated me to take firm steps forward.

My father, mother and brother, your wholehearted love and support have always been with me, upon which I could bridge the farness from home.

Dedication

To my father and all seeking minds…

1 General introduction

1.1 Introduction

The surface properties of wood play an important role when wood is used or processed into different products such as siding, joinery and wood composites (Tshabalala 2005). For example, the surface degradation of wood when it is used outdoors, places wood at a disadvantage compared to other materials (Feist and Hon 1984, Rowell 2005, Evans 2008).

Much effort has been expended in the search for better methods of modifying wood surfaces in preparation for adhesive bonding and the application of coatings (Kamke and Lee 2007). The methods employed have mainly involved physical and chemical pre-treatments (Denes et al. 2005, Hill 2006). A newer surface treatment uses plasma instead of wet chemicals. Plasma consists of an activated gaseous discharge that is capable of modifying the surface of materials prior to application of adhesives or coatings in a direct, non-toxic way without producing large amounts of physical or chemical waste products (Wu 1982, Boenig 1982, Kinloch 1987, Liston 1994, Chu et al. 2002, Jama and Delobel 2007, Lee et al. 2011).

The term plasma was first used in 1927 to describe the "inner region of an electrical discharge in which a significant number of the constituent atoms and /or molecules are electrically charged or ionized" (Boenig 1982). More recently plasma has been defined as "an excited gas which consists of atoms, molecules, ions, free electrons and metastable species" or "simply a mixture of electrons, negatively and positively charged particles, and neutral atoms and molecules" (Kinloch 1987, Inagaki 1996).

Plasmas are capable of rapidly modifying materials and plasma treatment have opened up novel ways of modifying wood based materials, including surface functionalization and coating. For example, plasma treatment with organic gases can rapidly alter the surface energy of solid

wood surfaces without changing bulk properties (Denes and Young 1999, Magalhães and de Souza 2002, Odraskova et al. 2008). This technology is claimed to be a very efficient 'dry' approach that avoids the disadvantages of related wet treatments such as organic solvent extraction (Cho et al. 2001, Denes et al. 2005, Blantocas et al. 2006).

Plasma pre-treatment using inorganic gases can increase the surface permeability of wood, performance of coatings and the fracture strength of glued wood (Sakata et al. 1993, Podgorski et al. 2000, Lukowsky and Hora 2002, Rehn et al. 2003). Ramos (2001) and Evans et al. (2007) found that prolonged exposure to a glow-discharge plasma significantly increased the glue bond strength of difficult-to-glue eucalyptus species. Wolkenhauer et al. (2009) showed that plasma generated from dielectric barrier discharge increased the surface energy of aged wood. Plasma treatments were also effective at increasing the adhesion of varnish to wood and bamboo (Setoyama 1996). Yuan et al. (2004) showed that plasma treatment could significantly improve the static and dynamic mechanical properties of wood-fibre-polypropylene composites. Based on their findings they suggested that increases in surface roughness of plasma-treated wood fibers, which they observed using scanning electron microscopy, led to higher interfacial contact and mechanical interlocking resulting in an overall improvement in mechanical properties.

Very few studies have examined the effect of plasma on the structure and physical and mechanical properties of wood, despite the interest in using plasma to modify wood (Denes et al. 2005). More information is available, however, on how plasma can modify the microstructure and properties of paper. For example, Sapieha et al. (1988) exposed several kinds of paper to plasma, and found that plasma acted like a fine microtome, continuously removing thin layers of cellulose. The rate of etching of cellulose could be controlled by changing parameters, such as gas pressure and composition, and discharge power. Not surprisingly, it has been shown that

chemical changes to cellulose during cold plasma treatment, affects the wettability and the adhesion properties of cellulose (Carlsson and Stroem 1991).

It is clear from studies conducted to date that surface modification of wood by plasma can improve surface energy and bond strength of adhesives and coatings (Denes et al. 2005, Evans et al. 2007, Avramidis et al. 2011a-b). However, there is little fundamental information on the effect of plasma on the microstructure and chemical and physical properties of wood.

1.2 General hypothesis

There is some evidence in the literature, mainly from studies of plasma treatment of paper, that plasma can etch the wood cell wall. The ability of plasma to etch and roughen the surfaces of plastics is well known (Egitto et al. 1990, Oehrlein et al. 2011). Ablation of these materials occurs when plasma reduces the molecular weight of their polymeric constituents and they become volatile enough to be removed by the vacuum pump employed in plasma devices (Boenig 1982). If the substrate consists of a blend or alloy of materials that react differently in plasma, differential ablation of these components can create a micro-roughened surface (Kolluri 2003, Oehrlein et al. 2011). Wood consists of a blend of cellulose, hemicelluloses, and lignin (Sjöström 1981). Therefore it is plausible that the same effect could occur when wood is exposed to plasma.

In this thesis I hypothesize that plasma will etch wood surfaces and produce new cell wall microstructures because of differential ablation of wood's polymeric constituents.

There is some evidence that ionizing rays, predominantly gamma-rays, can alter the physical, mechanical and chemical properties of wood (Tabirih et al. 1977, de Lhoneux et al. 1984). Considering this evidence and the energetic nature of particles in plasma I further hypothesize that differential etching of wood's polymeric components will change the surface

chemistry of wood. I also examine factors affecting the etching of wood by plasma and possible applications of plasma etching for wood processing (see below).

1.3 Outline of study

This thesis consists of eight chapters. Following this introductory chapter, Chapter 2 reviews the literature on plasma and plasma treatments including a brief introduction to the different types and ways of generating plasma and their effects on materials. Relevant literature on wood surface properties and modification, and previous research on the plasma modification of lignocellulosics is also reviewed. Chapter 3 examines the effect of glow-discharge plasma on the microstructure of wood. This chapter focusses on the differential etching of cell walls and cell types found in wood. Chapter 4 examines factors that influence etching of wood cell walls, and uses a new technique (surface confocal profilometry) to quantify the etching of wood and model wood compounds. Chapter 5 examines changes in surface chemistry of plasma treated wood. Chapter 6 tests the ability of plasma alone and in combination with bleaching to remove blue stain from wood colonized by staining fungi. Chapter 7 examines whether plasma can improve the adhesion and outdoor performance of coatings applied to wood that has been thermally modified using hot oil. Finally, Chapter 8 discusses the findings of all experimental chapters, draws general conclusions and makes suggestion for further research needed to fully understand findings arising from the research described in this thesis.

2 Literature review

2.1 Introduction

Wood continues to be used for many applications because of its many excellent material properties (such as a good strength to weight ratio, attractive appearance etc.), however, it also suffers from a number of disadvantages. Wood's dimensional instability in response to changing atmospheric conditions, susceptibility to biological attack and changes in appearance when exposed to weathering, place restrictions on its potential end-uses. The origin of wood's properties can be understood with reference to its structure at the macroscopic, microscopic and molecular levels (Hill 2006). Therefore the chemistry and physical characteristics of wood's components need to be understood to make sensible property changes to wood.

There has recently been renewed interest in changing and improving the properties of wood using chemical modification. This interest has been stimulated by environmental restrictions on the use of wood preservatives such as creosote, pentachlorophenol and chromated copper arsenate (Preston 2000). Wood modification is a process that can be used to improve the material properties of wood, but ideally it should produce a material that can be disposed of without presenting an environmental hazard any greater than that associated with the disposal of the unmodified wood (Preston 2000).

Modification of materials with plasma has become important recently. Plasma treatments provide fast and efficient methods for improving the surface properties of materials, as mentioned in Chapter 1. There are large numbers of publications on modification of polymers with plasma (see reviews by Chu et al. 2002, Oehrlein et al. 2011).

Plasma has been widely used to modify polymers to improve their wettability, adhesion and other surface properties (Inagaki 1996). Plasma modification of wood and other lignocellulosic

materials is seen as being important because it can enhance some critical surface properties. However, there have been relatively few publications on the modification of wood compared with those on the modification of polymers by plasma. Most studies of the plasma modification of wood have been confined to the laboratory, and commercial applications of the technology for wood processing have not been reported in the public literature.

This chapter reviews the literature on plasma and plasma treatments including a brief introduction to the different types and ways of generating plasma and its effects on materials. The review mainly focuses on plasma modification of lignocellulosic materials (wood and paper), but relevant papers on woods' surface properties and modification are also reviewed. Some of these papers provide extensive information on plasma processing, whereas others describe the process in a more cursory manner. This is due, in part, to the high diversity of plasma processes used to modify wood surfaces, and the complexity of the environments in the plasma devices. Furthermore, the main focus of the majority of publications is on the characteristics of the plasma generated surfaces, rather than the plasma process itself (Denes et al. 2005).

2.2 Plasma

2.2.1 Introduction

When blood is cleared of its various corpuscles there remains a transparent liquid, which was named plasma[1] by the Czech medical scientist, Johannes Purkinje (1787-1869). The Nobel Prize winning American chemist Irving Langmuir in 1927 was the first to use the term plasma to describe the inner region of an electrical discharge in which a significant number of the atoms and /or molecules are electrically charged or ionized. Langmuir was reminded of the circulation of red and white corpuscles in the plasma of blood by the way an electrified fluid carries electrons and ions (Tonks 1967, Fitzpatrick 2008).

Recently, more detailed definitions of plasma have appeared in the literature. Kinloch (1987) defined plasma as an exited gas, which consists of atoms, molecules, ions, free electrons and metastable species or simply a mixture of electrons, negatively and positively charged particles, and neutral atoms and molecules. Plasma is also considered to be the fourth state of matter because it is more highly activated than solid, liquid or gaseous states (Inagaki 1996).

In many cases interactions between charged particles and neutral particles are important in determining the behavior and usefulness of a plasma. The type of atoms in a plasma, the ratio of ionized to neutral particles and the particle energies, all result in a broad spectrum of plasma types, characteristics and behaviors. These unique behaviors have resulted in growing number of applications for plasma (Eliezer and Eliezer 2001).

The species in plasma that modify materials are electrons, ions, and radicals. The latter two species are generated by collisions between electrons and gas molecules existing in plasma.

---

[1] From the Greek word which means “moldable substance” or “jelly”

These electrons, ions, and radicals can react with the surface of materials in four ways: (1) implantation reactions of atoms; (2) radical generation; (3) polymer-forming reactions; and (4) plasma etching. The type of reaction that is initiated depends mainly on the plasma gas, the energy level of the plasma and the nature of the polymeric material being modified (Kaplan and Rose 2007). Plasma composed of inorganic gases such as argon, helium, hydrogen, nitrogen, and oxygen often favors implantation of atoms, radical generation and etching reactions, whereas plasma derived from organic gases such as hydrocarbons and alkylsilanes favors to polymer-forming reactions (Inagaki 1996).

2.2.1.1 Plasma types

Plasmas can be classified according to their temperature and pressure. For example, plasma can be classified as equilibrium (hot or thermal) or non-equilibrium (cold or non-thermal/low temperature) plasma. Equilibrium in this context refers to thermal equilibrium among the species present in the plasma. Non-equilibrium plasmas are commonly known as cold plasmas while equilibrium plasmas are known as thermal plasmas (Denes 1997). Equilibrium or thermal plasmas are those in which the temperature is the same for all the species present in the plasma. The energy to ionize and activate the gas comes from thermal heating which can cause the plasma to reach temperatures greater than 10,000 ºC. A well known example of a thermal plasma in nature is the solar corona (Aschwanden 2004). Such plasmas are mainly used in plasma spray, plasma torches, waste destruction and welding applications. On the other hand, non-equilibrium (cold) plasmas, do not have a defining temperature. Nevertheless, in these types of plasmas, electrons have a very high temperature (as hot as 10,000 °C), which allows them to activate other species and produce ionization, excite other species present and cause dissociation of molecules (Kaplan and Rose 2007). Because ions, atoms and molecules cannot exchange heat with

electrons, these species are almost maintained at room temperature. As a result such plasmas are 'cold' (room temperature or sometimes slightly higher), but generally lower than 100 ºC (Rossell 2007).

Non-equilibrium plasmas are typically divided into two types: (1) those generated either under reduced pressure; (2) those generated in air at normal atmospheric pressure. Under reduced pressure, the plasma that is generated is called a glow-discharge plasma, while plasma generated in air at normal atmospheric pressure is called a dielectric barrier or corona discharge plasma (Boenig 1982, Uehara 1999, Kogelschatz 2003).

2.2.1.2 Plasma generation

Plasma can be produced in the laboratory by raising the energy of a gas regardless of the nature of the energy source. Plasmas lose energy to their surroundings through collision and radiation processes and, consequently, energy must be supplied continuously to the system to sustain the discharge (Inagaki 1996). "The easiest way to continuously inject energy into a system is using electrical energy" and for this reason electrical discharges are commonly used to produce most plasmas (Denes and Manolache 2004). Plasma generated by electrical discharge can be classified as either cold or hot, as mentioned above. Examples of naturally occurring plasmas are lightning, and those created during the phenomenon known as Aurora Borealis or Northern Lights (Denes and Manolache 2004). A low temperature plasma generated under reduced pressure is a glow-discharge plasma, as mentioned above.

Three essential requirements are needed to form a glow-discharge plasma (Inagaki 1996). These are: (1) energy source for ionization; (2) a vacuum system for maintaining plasma state; and (3) a reaction chamber. Electrical energy from a direct or alternating current is usually used for ionization of atoms and molecules. Electric power is supplied to atoms and molecules from a

pair of electrodes placed in the reaction chamber in capacitative or inductive coupling modes. The reaction chamber is usually a bell jar or tubular chamber and is invariably made of glass or stainless steel (Inagaki 1996). Different equipment is used to generate plasma in dielectric barrier or corona discharge in air or at atmospheric pressure. A typical corona discharge treatment apparatus consists of a high frequency generator, a high voltage transformer and a treating station assembly (Cramm and Bibee 1982). The high frequency generator converts the available electrical energy into a higher frequency suitable for the treatment, while the transformer increases the available voltage to a level needed to generate plasma and to perform the electronic impedance matching function (Cramm and Bibee 1982, Kinloch 1987). Electrical energy is transmitted to atoms and molecules in the air through metal electrodes which may be insulated with dielectric materials. Occasionally the term "corona" is used only for discharge between bare metal electrodes at atmospheric pressure (Kogelschatz 2003).

2.2.2 Glow-discharge plasma

Under reduced pressure, a glow-discharge plasma is generated. Radio frequency (RF) glow-discharge (RFGD) plasma devices are widely used for the surface modification of polymers because they are able to produce a large volume of stable plasma. RF discharges have been classified into two types depending on the method of coupling the RF power with the load: (1) capacitive coupling and (2) inductive coupling. Both modes can use internal or external electrodes. The external mode uses a discharge tube that is made of glass (quartz or borosilicate glass), which makes it possible to reduce contamination of the plasma by impurities from the electrodes. Hence, this coupling mode is common in RF plasma devices. In general, the RF discharges operate in the 50 kHz–100 MHz range and the pressure during discharge is between 10^{-3} and 100 torr (Boenig 1982, Chu et al. 2002).

Glow-discharge processes that are suitable for surface modification of materials take advantage of energetic electrons, ions, free radicals, and vacuum UV radiation present in the glow-discharges. These species have energies high enough to break even the most stable chemical bonds within substrates (Denes 1997).

2.2.3 Effects of plasma on the surface of materials

From the time when Langmuir first defined plasmas much effort has gone into understanding the plasma state and also to use plasmas to modify materials. The microelectronics industry was one of the first to develop plasma processing technologies. Today many other industries such as the biomedical, automotive, textile and lighting industries are using plasmas to modify the surface of materials (BMBF 2001). Plasma processing technology aims to modify the chemical and physical properties of a surface (Inagaki 1996). Unlike liquid cleaners and etchants, which use only molecular chemistry, plasmas employ molecular, atomic, free radical and metastable species for chemical effects, and electrons and positive ions for kinetic effects (Rawlinson 1999).

Energetic particles in plasma are able to break covalent chemical bonds in organic materials, thus creating free radicals at polymer surfaces. Almost all chemical bonds involved in organic structures can be dissociated in plasma, however, higher energies are usually required for the dissociation of unsaturated linkages and the formation of multiple free radicals. Accordingly, "initial or plasma-generated unsaturated bonds will have a better 'survival rate' under plasma conditions, in comparison to single bonds" (Denes 1997). The reactions of radicals formed in plasma include chain scission, radical transfer, oxidation and recombination on polymer surfaces (Wu 1982).

The effect of a plasma on a given material is determined by the chemistry of the reactions between the surface and the reactive species present in the plasma. At the low energies typically used for plasma treatment, plasma only changes the surface of the material; the effects are confined to a region only several molecules deep and the bulk properties of the substrate are unaffected. However, plasmas also generate electromagnetic radiation, in the form of vacuum UV photons, which can penetrate bulk polymers to depths of 10 to 75 μm depending on their wavelength. UV radiation can also cause chain scission and cross-linking (Egitto 1990, Rawlinson 1999).

Surfaces changes resulting from plasma treatment depend on the composition of the substrate and the gas used. Gases, or mixtures of gases, used for plasma treatment of polymers can include air, nitrogen, argon, oxygen, nitrous oxide, helium, tetrafluoromethane, water vapor, carbon dioxide, methane, or ammonia (Finson et al. 1995). Each gas produces a unique plasma and specific changes to the surface properties of the material being treated. Substitution of molecular moieties at the surface can make polymers either wettable or non-wettable depending on the chemistry of the polymer and the source gases. The specific type of substituted atoms or groups determines the specific surface potential (Finson et al. 1995). For example, argon plasma treatment can induce cross-linking between substrate and polymer, whereas fluorine plasma treatment decreases the surface energy of polymers (Liu et al. 2005). Plasma treatment processes using different gases are optimized by varying the time, power, pressure and gas flow rate to the substrate and the modification of surfaces by plasma has been sub-divided into 3 general types: (1) functionalization or activation; (2) coating or deposition and (3) etching or ablation (Fig. 2.1) (Rossell 2007).

Figure 2.1: Has been removed due to copyright restrictions. It was a schematic diagram of the three different responses of a material to plasma; (1) functionalization (2) coating and (3) etching (modified after a diagram in Rossell 2007)

2.2.3.1 Plasma functionalization (activation)

Plasma functionalization involves plasma species that do not react among themselves, but rather with the substrate surface at determined positions (Rossell 2007). The name also encompasses the process of substituting atoms in the polymer's molecules with chemical groups from the plasma (Kolluri 2003).

Free electrons and metastable particles in plasma are able to break covalent chemical bonds, thus creating free radicals at polymer surfaces (Boenig 1982). When polymers are exposed to plasma, they show ESR (electron spin resonance) signals, indicating the formation of radicals. Such radicals can be formed in a number of ways, for example with hydrogen abstraction from polymer chains by radicals or electrons, and/or C-C bond scission by electron or ion bombardment (Inagaki 1996). These free radicals then undergo additional reactions, depending on the gases present in the plasma or the subsequent exposure of the radicals to gases in the atmosphere. Free radical reactions can create a surface that is very different from that of the starting bulk polymer (Boenig 1982, Steinbruchel et al. 1986).

Implantation reactions during plasma treatment are one of the most important ways in which plasma modifies polymers (Inagaki 1996). The surface energy of the polymer placed in a plasma can be increased very rapidly by plasma-induced oxidation, nitration, hydrolyzation, or amination. The higher surface energy of the polymer surface increases its wettability[2] (Kolluri 2003). For example, gas molecules such as oxygen and nitrogen are activated by plasma; the activated oxygen and nitrogen species interact with polymer surfaces, and functional groups (hydroxyl, carbonyl, amino and amido) are formed. Such implantation reactions lead to large changes in the surface properties of the polymer, for example, hydrophobic polymers can become hydrophilic as a result of the reaction of hydroxyl groups. This type of 'plasma treatment' is frequently used to improve the adhesive properties of polymers (Inagaki 1996). The increase in apparent bonded surface area that results serves to increase the strength of adhesive bonds. This process can also be used to substitute groups at the surface of polymers with ones that facilitate covalent bonding between the polymer substrate and adhesives (Kolluri 2003).

2.2.3.2 Plasma deposition (coating)

When organic gases are used to generate a plasma, polymer-like products are deposited on the surface of all substrates in the reaction chamber. This process is called plasma polymerization, and the product formed as a result of plasma polymerization is called a plasma polymer (Inagaki 1996). The creation and properties of a plasma polymer are strongly dependant on the plasma conditions, e.g., the magnitude of the input RF power to maintain the glow-discharge, the flow rate of the organic gases introduced into the plasma, and the pressure in the reaction chamber (Inagaki 1996). Some chemical deposition processes have long been carried

[2] The ability of a liquid to spread over and penetrate the surface

out in the gaseous or vapor phases. There are a whole family of related processes differing in detail, and collectively referred to as chemical vapor deposition (CVD) techniques (Chapman 1980). Plasma deposition is essentially an extension and enhancement of some of these processes, but a plasma is used to dissociate and activate the reaction gases. The detail of the stoichiometry of the modified surfaces or films is somewhat different for the two methods, but more importantly (at least in the semiconductor industry) the plasma modification process can be accomplished at a lower substrate temperature (Chapman 1980).

2.2.3.3 Plasma etching (ablation)

Etching or ablation involves the removal of material from a substrate. The ability of plasma to etch and roughen the surfaces of metals and plastics is well known and is used to obtain specific patterns at modified surfaces (Egitto et al. 1990).

Etching reactions at the surface of polymers occur when they are exposed to plasma for prolonged periods of time, and the molecular weight of the polymer is reduced (Boenig 1982). Plasma species diffuse into the substrate and react with surface molecules. As a result of this interaction, mono- and multiple-free radical structures, ions of either polarity or molecular fragments with charged functionalities can be generated (Denes 1997). These reactions may produce materials that are volatile enough to be removed from the surface of the substrate by the vacuum pump employed in plasma devices, as mentioned above (Boenig 1982). The intensity of the production of low molecular weight and volatile structures will control the rate of surface etching, which competes with the other reactions occurring at the surface such as plasma polymerization (Flamm and Herb 1989).

The etching rate of a polymer largely depends on the plasma treatment conditions (e.g. discharge gas, pressure, discharge power, temperature and treatment time) and on the polymer's

chemical and physical properties (Wu 1982). Of these parameters the type of gas (etchant) is the most important factor affecting etching. For example, oxygen plasmas are reactive etchants, whereas argon plasmas are not as reactive (Hansen et al. 1965, Taylor and Wolf 1980, Olde Riekerink 2001, Wohlfart et al. 2010).

The chemical structure of polymers has a major influence on the rate of plasma etching. Many studies have examined the relationship between the chemical composition of polymers and their susceptibility to plasma etching. As results of such studies, it has been established that aromatic polymers have lower etching rates than aliphatic polymers. Polymers containing little (or no) oxygen and no halogen (except fluorine) are very resistant to etching in oxygen plasma. Accordingly, polymers containing oxygen functionalities such as ether, carboxylic acid, and ester groups are more susceptible to plasma etching than polyolefins, which have no such substituents. Fluorine and cyano (-C≡N) moieties in polymers enhance etch resistance, due to strong bonding in backbone chains, whereas polymers containing chlorine are rapidly eroded in an oxygen plasma (Reich and Stivala 1971, Yasuda et al. 1973, Taylor and Wolf 1980, Pederson 1982, Gokan et al. 1983, Inagaki et al. 2003, Moss et al. 1986, Moss 1987, Fricke et al. 2011). Consequently, if the substrate consists of a blend or alloy of materials that react differently in plasma, differential etching or ablation of these components can create a micro-roughened surface (Fig. 2.2) (Kolluri 2003, Wohlfart et al. 2010).

Figure 2.2: Has been removed due to copyright restrictions. It was SEM photomicrographs of polyethylene terephthalate (PET) treated with oxygen plasma for: (a) 1 min; (b) 4 min; (c) 10 min; and (d) 30 min. Note development of fibrils with increasing treatment time (Wohlfart et al. 2010)

Weight losses due to etching are restricted to the top-most layers of the polymer, and weight losses below the surface are much smaller or do not occur at all. Therefore, polymers subjected to plasma etching possess similar bulk chemical and physical properties as the parent polymers (Inagaki 1996). Chu et al. (2002) wrote that "the elemental composition, chemical structure, degree of polymerization, and crystallinity of plasma treated substrates are hardly altered and are similar to those of the original polymers". The superficial nature of plasma modification of polymers and the fact that no liquids are used has led to the development of plasma processes for the dry etching of materials (Chu et al. 2002).

Plasma etching is commonly used in the semiconductor industry and has the advantage over earlier etching technologies of being solvent-free, thus producing less waste. The complexity of integrated circuits (ICs) has greatly increased since the demonstration of the first working semiconductor integrated circuit in 1958. Increases in performance of integrated circuits rely on increasing the numbers of memory cells per wafer. Hence, the fabrication of device patterns with smaller dimensions has become more important. Plasma can etch materials at the micro/nano-scale (Fig. 2.3), and plasma etching of silicon nitride was one of the first plasma processes to be used by industry (Boenig 1982, Flamm and Herb 1989, Sahoo et al. 2009).

Figure 2.3: Has been removed due to copyright restrictions. It was SEM photomicrographs of nanopillar structures (used for solar cell applications), fabricated by etching of silicon nitride film using a gas mixture of CF4/O2 at different treatment times: (a) 90 s; (b) 120 s; (c) 150 s; and (d) 180 s (Sahoo et al. 2009)

Plasma etching of polymer surfaces can do the following: (1) alter the adhesion of the polymers; (2) change the materials' mechanical and/or physical properties; (3) change the chemical composition of the material or degrade or dissolve low-molecular weight constituents that migrate to surfaces; (4) relieve residual surface stresses. Plasma etching has been observed in studies of the morphology of surfaces and the internal structure of fibers (Boenig 1982, Egitto et al. 1990).

Plasmas are very effective at removing very thin layers of contaminants from the surface of materials (Lee et al. 1999). Hence, lower energy plasmas are commonly used for plasma cleaning as opposed to plasma etching. Plasma cleaning involves the removal of impurities and contaminants such as hydraulic oils and lubricants from surfaces through the use of plasma created from gaseous species (Belkind et al. 1996). Gases such as argon and oxygen, as well as mixtures such as air, hydrogen/nitrogen and fluorine-containing gas are used. The pressures of the gaseous species are typically below 0.133 Pa (1 torr). The energetic, ionic species react with species on the surface of the item to be cleaned, often producing gaseous products which can be removed by a vacuum system (Ward 1996, Nickerson 1998). The energetic species also clean the surface by colliding with it and 'knocking-off' contaminants from the surface. Prolonged or higher power plasma cleaning etches surfaces, going beyond the 'cleaning' phase (Finson et al. 1995, Kaplan and Rose 2007).

2.3 Wood surface properties and modification

2.3.1 Introduction

The boundary region between two adjacent bulk phases is known as an 'interface' although, when one of the phases is a gas or a vapor, the term 'surface' is commonly used (Aveyard and Haydon 1973). The chemical and physical properties at the surface or interface with another

material are essentially different from those of the bulk of the material (Aveyard and Haydon 1973).

The topic of interfacial science is vast, however, there are some crucial areas that are usually considered in defining a material's surface properties. The properties and reactions at polymer surfaces have been sub-divided into three different categories: (1) interactions occurring at the polymer's surface; (2) chemical composition and chemical reactions occurring at the polymer surface; and (3) surface morphology (Inagaki 1996). Surface tension, wetting and adsorption are probably the most important aspects of surfaces that are relevant to adhesion, dyeability, printing, water and oil repellency, etc. (Barnes and Gentle 2005).

Surface modification of polymers can be used to change surface properties, but any changes are shallow in depth (Liston et al. 1994). Surface modification can include one or a series of operations including cleaning, removal of loose material, and physical and/or chemical modification of a surface to which an adhesive or coating is applied. For example, for adhesive bonding, surface modification tries to increase surface polarity, wettability, and create sites for adhesive bonding. In most cases, the main reasons for surface treatment prior to bonding are to: (1) remove or prevent the later formation of a weak layer at the surface of the substrate; (2) maximize the degree of molecular interaction between the adhesive or primer and the substrate; (3) optimize the adhesion forces that develop across interfaces and therefore ensure sufficient joint strength, initially and during the service life of the bond; and (4) create specific microstructures at the surface of the substrate (Ebnesajjad and Ebnesajjad 2006). Normally, optimum surface energy and structure is achieved by chemical treatments. The chemical composition and the morphology of the surface are altered so that the surface energy of the substrate is maximized for adhesion. Chemical treatments also increase the chances that

hydrogen, dipole, van der Waals, ionic, and/or covalent bonding can form at the interface between the substrate and adhesive. Mechanical abrasion is another simple means of surface preparation that generates less waste than chemical treatments. Mechanical abrasion works by creating a clean surface and increasing the contact area between the substrate and adhesive. During the ordinary gluing of objects, these methods may not be needed since optimal adhesion is not always necessary. When a strong adhesive bond is required, the minimum surface preparation required is cleaning and removal of dirt and grease from contact surfaces (Ebnesajjad and Ebnesajjad 2006). Alternatives to the aforementioned treatments (with similar surface changes) include plasma, corona, and flame treatment methods. These methods act in similar ways to chemical treatments with less generation of hazardous wastes (Boenig 1982, Ebnesajjad and Ebnesajjad 2006).

2.3.2 Wood surfaces

Wood is a porous, cellular, and anisotropic substrate. The anisotropic properties of wood arise because its cells (fibers) are much longer than they are wide and cellulose chains are oriented parallel to the fiber direction. There are also large differences between wood species in their chemistry and morphology. Therefore a simple model for wood surfaces is not sensible (Frihart 2005).

The surface properties of wood can be divided into two major groups: physical or chemical. Physical properties include morphology, roughness, smoothness, specific surface area and permeability. Chemical properties include elemental and molecular, or functional group composition. Together these properties determine the thermodynamic characteristics of wood surfaces, such as surface free energy and surface acid-base acceptor and donor number (Tshabalala 2005). The surface properties of wood play an important role when wood is used or

processed into different products such as siding, joinery and wood composites. Thus, for example, the quality and durability of a wood coating are determined by the surface properties of the wood and the coating. The same is true for wood composites, as the efficiency of stress transfer from the glue to the wood's components is strongly influenced by the surface properties of both the wood and adhesive (Tshabalala 2005).

Wood's surface physical and chemical properties vary depending on how the surface is prepared, and what type of wood is being processed. Initial operations in wood processing, like sawing, alter surface quality (smoothness or roughness/fuzziness, burn marks, etc) and control orientation of annual rings at the surface. Drying can create defects like staining, checking, case-hardening, etc, (Kollmann and Côté 1968). Different secondary surface preparation techniques like sanding or planing can also create defects at wood surfaces. For example, abrasive planing can create crushed and fractured cells at surfaces. Because of their thinner cell walls earlywood tracheids in softwoods and vessels in hardwoods are more prone to crushing and this leads to rougher surfaces when crushed cells spring back (Stewart and Crist 1982, Murmanis et al. 1986). However, even with good surface preparation, the natural microstructure of wood influences surface properties. For example, earlywood cells with their thinner walls should be easier to bond because their lumens are more accessible to adhesives. The sapwood of a species is generally easier to bond than heartwood because it has a lower extractive content than heartwood. Juvenile, compression, and tension wood all have different microstructures compared to mature wood, which can influence adhesive/coating bonding (River et al. 1991, Frihart 2005). The resin ducts in softwoods are especially rich in extractives. Voids in vessel elements, tracheids, ray cells and resin canals or fractures created during sanding or planing increase the surface area and provide regions where better penetration and interlocking of adhesives can

occur (Fig. 2.4) (Frihart 2005). On the other hand, air entrapped in voids can weaken the interface between adhesive/coating and the wood surface (Young et al. 1985, Frihart 2005).

Figure 2.4: Has been removed due to copyright restrictions. It was a schematic diagram of a transverse section of wood showing wood's complete and cut-through cellular structure with voids and fractures in cell walls. Both of these 'flow paths' increase the surface area available for bonding of adhesives/coatings (modified after an illustration in Frihart 2005)

The chemical composition of wood affects the surface properties of wood. Cellulose is the main chemical component of the wood cell wall, but it may not be the main component at wood surfaces. It has been suggested that hemicellulose is the main chemical component of wood that hydrogen bonds with water because hemicelluloses are more accessible than cellulose (River et al. 1991). However, there are other factors that influence the surface characteristics of wood. Variable percentages of lignin, hemicelluloses, cellulose and extractives are present at wood surfaces depending on how the wood is cut, ie, transverse, tangential or radial. Cutting may expose the middle lamella, which is rich in lignin or the secondary wall which has a lower concentration of lignin (Young et al. 1985). The chemical composite of ray cells is different to that of longitudinally oriented elements, and variable percentages of ray cells at wood surfaces can influence the chemical composition of wood surfaces (Saka 2001). Migration of hydrophobic extractives to wood surfaces during drying can result in poor wettability. Acidity or reactivity of extractives, molecular reorientation of the surface functional groups, and closure of

wood cell micro-pores affect adhesive adsorption into the wood (Denes et al. 2005). Exposure to air and light (aging) can cause surface oxidation, and dust and fatty acids can be deposited at wood surfaces from the atmosphere (Young et al. 1985).

Most often, wood has been used because of its pleasant color as well as its warmth, hardness, strength and low cost. The color of wood depends on how its chemical components interact with light (Hon and Minemura 2001). Wood absorbs and reflects light and these interactions produce colors that range from almost white, as in holly (*Ilex aquifolium* L.), to almost black in the heartwood of African ebony (*Diospyros crassiflora* Hiern.). The color of wood conveys feelings of natural gentleness (Hon and Minemura 2001). When light is focused on the surface of wood, one component is reflected directly and the other part is absorbed. The light that is not absorbed is emitted through scattering, reflection, and transmission. The human eye recognizes the unabsorbed light as the wood's color (Hon and Minemura 2001). Cellulose and hemicelluloses do not absorb visible light, and native lignin that is isolated with minimum chemical or physical changes is pale yellow. Extractives which make up only a few percent by weight of wood's mass, greatly influence wood's color, as well as its fragrance, and durability. Hence, extractives greatly influence the properties and processing of wood (Fengel and Wegener 1984, Williams 1999). The color of wood can also change as a result of chemical reactions that take place between extractives and enzymes present in freshly cut wood or due to exposure of wood to light (Yeo et al. 2003). Exposure of wood surfaces to a combination of solar radiation (UV and visible light), moisture and heat, windblown particles, atmospheric pollutants and certain microorganisms, influences the color, surface chemistry and roughness of wood (Evans 2008). These changes are collectively called weathering. They do not affect wood's strength properties, but greatly change the surface properties of wood (Evans 2008).

The color of green (freshly felled) wood can be altered by microorganisms that grow on the surface of wood. This discoloration is due to the pigmentation of fungal hyphae or the reaction of wood to compounds secreted by microorganisms (Hon and Minemura 2001). For example, blue stain is caused by fungi that colonize sapwood. These fungi contain melanin and are therefore dark brown in color (Schmidt and Czeschlik 2006). The fungi in the wood appear blue or grey to the naked eye although they are brown when viewed under the microscope. This visible blue/grey discoloration reduces the value of wood for appearance and some structural applications (Fig. 2.5). Therefore, depending on its final use, wood is often treated to prevent fungal staining and improve its surface properties for different applications.

Figure 2.5: Discoloration of wood by blue stain fungi: (left) cross section of a stem of blue-stained lodgepole pine (Pinus contorta) showing darkening of sapwood (arrowed); and (right) a stack of lodepole pine wood containing some blue-stained boards (arrowed)

2.3.3 Modification of wood surfaces

Chemical modification of wood seeks to improve the properties in which wood is deficient without compromising those that give it its appeal (Kiguchi 1996).

Bulk chemical modification of wood is a very effective means of improving wood's properties such as dimensional stability or durability. In general, such modification is achieved under heterogeneous conditions, involving solid-liquid reactions. However, modification of

wood is not straight-forward because it is difficult to ensure that the reagent is evenly dispersed throughout the wood, and also to remove all of the reagent and by-products at the end of the reactions (Hill 2006). The reactions generally require an excess of chemical reagent, and the efficiency of the reactions are comparatively low. Furthermore, the reactions usually require high temperatures and corrosion resistant reactors. In contrast, if the reaction is confined to the surface of the substrate, then accessibility of the reagent to the wood is better and subsequent clean-up of the modified wood is more easily accomplished (Kiguchi 1996, Hill 2006).

Some types of wood modification techniques are cleaner and more easily accomplished. However, even wood modified using such techniques may require further modification to improve their surface properties. For example, thermal modification reduces the hygroscopicity of wood and imparts other desirable characteristics such as increased dimensional stability and natural durability (Militz 2008). Exposing wood to high temperatures, however, darkens wood and may reduce some mechanical properties particularly toughness, abrasion resistance, and cleavage strength, but also (to a lesser extent) modulus of rupture (MOR), shear strength and hardness (Militz 2008). Heat treating wood can reduce the surface wettability of wood which adversely affects adhesion of paints and coatings (Podgorski et al. 2000, Hakkou et al. 2005).

These are many properties demanded of wood surfaces depending on how and where they are used. These include weathering resistance, hardness, water resistance, water repellency, wettability for adhesives or coatings, and so on (Kiguchi 1996). Papers on surface treatments to improve adhesion first appeared in the literature in 1939 (Tischer 1939). Since then, surface modification of wood has been used to improve the ultraviolet stability of wood, to change the surface energy of wood (to reduce wetting by water, and/or improve compatibility with coatings or matrix material), and to improve bonding between wood surfaces (Hill 2006).

2.3.3.1 Mechanical treatments

Mechanical treatment of wood prior to gluing or coating removes old or contaminated surface layers from wood and increases wood's surface area, which leads to better adhesion of glues or coatings (de Moura and Hernández 2005). Planing and sanding are the most common methods for mechanically improving the surface properties of wood (Murmanis et al. 1983, Hernández and Cool 2008, Cool and Hernández 2011). Planing of wood exposes fresh surfaces and removes contaminants such as extractives that interfere with gluing. Vessel elements, tracheids and other cells when cut provide additional surface area and regions for penetration and interlocking of adhesives and coatings (Young et al. 1985, Hernández and Cool 2008, Cool and Hernández 2011). However, planing may have a negative effect on glue bond strength. For example, air may be trapped in freshly exposed cells, which can create voids within glue lines thereby reducing glue line strength, as mentioned above. Such entrapped air creates interfacial discontinuities, which focus stresses that can cause premature failure of glue laminated wood when load is applied (Williams 1999). In contrast, sanding, unlike abrasive planing causes less surface damage to wood. Machine sanding, if backed up by a soft roll, felt pad or air bag, allows abrasive grits to ride up and over material that cannot be cut or scraped away, thereby avoiding compression of cells (Murmanis et al. 1986). Sanding increases the interfacial surface area of wood which promotes better glue bond strength (de Moura and Hernández 2005). However, sanding with abrasive papers of any grit size does not always guarantee good glue bond strength particularly if the abrasive deposits small wood particles or dust at the wood surface, or creates weak boundary layers (Murmanis et al. 1983, Murmanis et al. 1986, de Moura and Hernández 2006). The effectiveness of sanding depends upon the grit (abrasive) size of sandpaper that is used to prepare the wood. Belfas et al. (1993) investigated the effect of sanding with a range of

abrasive papers from coarse (80 grit) through to very fine (12,000 grit) on the wettability and shear strength of regrowth karri (*Eucalyptus diversicolor* F. Muell.) and jarrah (*Eucalyptus marginata* ex Sm.) wood. They found that sanding with coarser sandpaper (80 grit) gave the largest improvement in both wettability and dry and wet shear strength (Belfas et al. 1993).

The surface structure of wood can be altered more dramatically by incising which is a well-established technique to mechanically perforate the surface of refractory wood species prior to pressure impregnation with wood preservatives (Keith and Chauret 1988). Different perforation systems using needles, drills, slit discs, lasers, and water jets have been used, however, visible marks on the wood surface and strength losses resulting from incising are considered to be disadvantageous for certain wood products (Kass 1975, Keith and Chauret 1988, Winandy and Morell 1998).

Because wood surface preparation is a critical factor in obtaining satisfactory performance from coatings and glues, and taking into account the limitation of the chemical and physical pre-treatments examined to date, there is scope for the development of additional surface treatments.

2.3.3.2 Biological treatments

Controlled applications of microbial decomposition are biotechnological methods that can be used to modify wood and improve its permeability. These methods mainly employ bacteria, enzymes or fungi for treating wood (Mai et al. 2004).

Bacteria increase the permeability of wood when logs are stored in water for long periods of time (Fogarty 1973, Kobayashi et al. 1998). The bacteria degrade wood's pit membranes. Substances encrusting cell lumina and pit chambers are also partly removed. These changes are responsible for the improved permeability and drying characteristics of 'ponded wood' (Kobayashi et al. 1998). However, increases in permeability occur slowly and property changes

are not always homogeneous, which has restricted the wide-spread commercialization of ponding (Lehringer et al. 2009).

Enzymes have been used for the surface activation of wood particles, to form binderless composites (Hill 2006). Enzymatic surface modification can be achieved by oxidative and/or hydrolytic systems (Kenealy et al. 2006). Enzyme catalyzed bonding of wood can be achieved either by activation of lignin, or by surface activation of wood particles with chemicals or enzymes (Kenealy et al. 2006). Felby et al. (1997) studied the free radicals formed in European beech (*Fagus sylvatica* L.) wood during laccase-catalyzed oxidation. ESR spectroscopy indicated the presence of at least 2 radical species in the suspension liquid. These radicals were phenoxy radicals located in solubilized or colloidal lignin. It was suggested that wood fibers were modified by direct laccase oxidation of the surface, as well as by modification processes involving colloidal lignin fragments in a cyclic phenol/phenoxy reaction pathway (Felby et al. 1997). Kharazipour et al. (1997) found that laccase treatment produced a highly oxidized lignin surface with a high content of carboxylic groups. From their results, they suggested utilizing the bonding strength of enzymatically activated lignin for the production of wood composites. Recently Goswami et al. (2008) found that enzymatic modification could plasticize wood cell walls. They used a multicomponent enzyme (Cellulose Onozuka R-10 from *Trichoderma viride*) with activity on cellulose and xylan. Treatment of isolated fibers with this enzyme reduced the ultimate stress of the fibers. They accounted for this observation by suggesting that modification of amorphous cellulose chains at the surface of the microfibrils may have loosened contact between cellulose fibrils and the pliant matrix. As a result, cellulose fibrils in enzyme-treated wood were able to glide after a critical stress was exceeded, making the modified wood more

elastic. They suggested that such behavior from wood veneers would be desirable in composites with complicated geometries (Goswami et al. 2008).

Enzymes such as pectinases, cellulases, and hemicellulases can partially degrade pit membranes and increase the permeability of Norway spruce (*Picea abies* L. Karst.) heartwood and sapwood (Militz 1993). Some enzymatic treatment systems have been commercialized and additional systems are being developed (Kenealy et al. 2006). However, there are also drawbacks to these enzymatic treatments (like ponding). For example, several weeks of incubation is needed to increase permeability to the desired level, and localized differences in enzyme activity lead to variation in the permeability of the processed material. Furthermore, the introduction of enzymes or bacteria into dried wood is difficult because aspirated pits restrict the penetration of microbial suspensions or enzymatic solutions into wood (Militz 1993, Lehringer et al. 2009).

In contrast to isolated enzymes, fungal hyphae are able to transport their specific enzymes deep into the wood substrate during colonization (Scheffer 1973). The hyphae largely follow the nutrient-rich parenchyma cells and rays, and grow from there into the adjacent tracheids primarily through simple or bordered pits or even by creating bore holes in cell walls (Scheffer 1973, Schwarze et al. 2006, Schmidt and Czeschlik 2006). During the first period of substrate colonization, the secreted enzymes alter the chemical structure of the pit membranes and selectively degrade them (Schwarze and Landmesser 2000). This function of fungi has been used to improve the permeability of both sapwood and heartwood, with almost no negative effects on the strength properties of softwoods (Schwarze et al. 2006). However, this application of fungi for increasing wood permeability, which is termed “bioincising”, hasn’t been scaled up to the industrial level, due to inability to control fungal activity and some undesired side effects of fungal growth such as surface discoloration (Lehringer et al. 2009).

2.3.3.3 Chemical treatments

Wood is photodegraded when used outdoors because "lignin strongly absorbs ultraviolet light and this leads to radical-induced depolymerization of lignin and cellulose" (Derbyshire and Miller 1981, Evans et al. 1996). Clear finishes perform badly on wood during exterior exposure due to photodegradation of the underlying wood substrate (Derbyshire and Miller 1981). Hence, chemical pretreatments which photostabilize wood surfaces can prolong the life of coatings (Evans et al 1992). Chemical modification of wood surfaces has been used to improve the UV stability of wood (Evans et al. 1996). For example, treatment of wood surfaces with dilute aqueous solutions of hexavalent chromium compounds is effective at restricting the photodegradation of wood during natural weathering and enhancing the performance of clear coatings and stains. However, as pointed out by Evans et al. (1992) "chromium trioxide produces a brown coloration initially, which slowly changes to green, which some customers don't like". Furthermore, health concerns about the use of hexavalent chromium has discouraged commercial development of chromium trioxide as a photoprotective pre-treatment underneath clear coatings (Evans et al. 1992).

Kiguchi and Evans (1998) examined grafting of a UV absorber to wood surfaces to improve wood's photostability. They concluded that grafting of a UV absorber to wood was a promising means of protecting wood surfaces from photodegradation. They pointed out that the treatment was "as effective as chromium trioxide in restricting losses in veneer mass during weathering and superior to chromium trioxide in terms of its effects on tensile strength". Furthermore, color changes arising from treatment were smaller for grafted wood compared to wood treated with chromium trioxide.

Changes to the surface wettability of wood can be obtained by chemical modification, for example by acetylation, but this is not the primary aim of such modification (Chang and Chang 2001).

Wood surfaces can also be modified to improve glue bonding. Many of the adhesive system currently in use are derived from non-renewable petrochemical resources, and concerns about the decline and increasing cost of these resources are driving research efforts to develop adhesives derived from renewable materials. As an alternative, research is also examining ways of directly bonding wood surfaces without the use of an adhesive. Chemical modification of wood surfaces can be employed to provide active sites to allow for self-bonding directly, or to allow for covalent bonding between wood surfaces via an intermediate reagent (Kiguchi 1996).

Several approaches have been used to chemically modify wood to improve adhesive bonding as follows: (1) altering the surface energy of wood to improve compatibility with low-energy materials such as polyolefins; (2) reaction of the wood surface with a functionalized coupling agent to improve compatibility with low energy materials; (3) bonding of reagents to wood surfaces in order to thermoplasticize the surface for self-bonding; (4) bonding of reagents to wood surfaces to provide the appropriate functionality for bonding sites; and (5) activation of the wood surface using chemicals, for example Fenton's systems, to generate surface free radicals (Hill 2006).

Adhesive bonding to wood can be affected by the presence of extractives at wood surfaces (Kiguchi 1996). Extractives create weak boundary layers and hence oily woods, such as teak (*Tectona grandis* L.) are difficult to bond unless extractives are removed from the surfaces to be bonded. Treatment of wood with a mixture of ethanol and benzene can remove extractives and improve surface wettability (Kiguchi 1996). Sodium hydroxide treatment also improves the

wetting properties of wood, and increases glue-bond strength (Young et al. 1985). Aqueous alkaline solutions reduce surface tension, remove extractives, and increase the ability of adhesives to dissolve extractives at wood surfaces. For example, Yoshimoto et al. (1972) observed that sodium hydroxide in four different concentrations (1, 0.5, 0.25 and 0.125 %) dissolved and removed pit membranes especially tori without modifying cell walls and pit borders when applied to two conifer species, sugi (*Cryptomeria japonica* D. Don) and kuromatso (*Pinus thunbergii* Parl.).

Fungal stains can be removed by bleaching the surface of wood to restore the value of blue-stained wood for appearance-grade markets (Ross et al. 1998). For example, a solution of alkaline peroxide (3%) removed blue stain from the surface of ponderosa pine (*Pinus ponderosa* Laws.). The most effective treatment involved treating samples at 60 ºC for one hour (Lee et al. 1995). This technique was reasonably efficient at removing the blue stain and restoring the wood's original color, but because samples were dipped in a hot solution the treatment cannot be classified as a surface treatment. More recently, Evans et al. (2007) screened a range of bleaching agents to determine the most effective ones at removing blue stain from lodgepole pine (*Pinus contorta* Dougl. ex Loud.), and they also optimized treatment parameters for one of the treatments. They found a sodium hypochlorite treatment was the best one at removing blue stain. This treatment was most effective when the solution was sprayed on the wood surface at room temperature (20 °C) at a high concentration of 10.5 % (Evans et al. 2007).

2.3.3.4 High energy treatments

Many different technologies have been developed to modify wood, but in the past there was less economic or environmental reasons to commercialize such technologies. Today growing environmental and legislative pressure has made wood modification technologies more

commercially attractive. For example, several processes for modifying wood have been commercialized in Europe in the past ten years. Continued advances in process development and environmental legislation may see the commercialization of these technologies in other parts of the world (BMBF 2001, Hill 2006).

High energy radiation can produce significant changes in the molecular structure of polymers and wood (Mater 1957). Some attempts were made in the past to use high energy radiation (e.g. gamma rays) to modify the properties of wood, for example hygroscopicity. High doses of ionizing radiation rapidly alter the properties of wood and paper because the radiation depolymerizes cellulose and reduces its crystallinity, which makes the cellulose water soluble (Mater 1957, de Lhoneux et al. 1984). It was shown that exposure to gamma radiation affected hemicelluloses more than cellulose in wood. In comparison lignin was even less affected (Seifert 1964). These changes do not occur at low levels of radiation (Aoki et al 1977). Lignin in wood may also be degraded and partially solubilized by high-energy radiation (Seifert 1964, Skvortsov 1990). Hachihama et al. (1960) exposed Japanese red pine (*Pinus densiflora* Sieb. & Zucc.) to high doses of gamma irradiation and reported that such treatment significantly decreased the holocellulose contents of irradiated wood and made the lignin extractable with ethanol and dioxane. However, their measurement of the native lignin (Brauns' lignin) content showed only small changes between irradiated and non-irradiated samples. Based on their observations they suggested that changes in the behavior of lignin in irradiated wood were caused mainly by carbohydrate degradation and the cleavage of lignin/carbohydrate linkages (Hachihama et al. 1960). Smith and Mixer (1959) concluded that aromatic compounds (lignin and other extractives) in redwood (*Sequoia sempervirens* (D. Don) End.) protected the cellulose and hemicellulose from deleterious effects of radiation. Accordingly, Flachowsky et al. (1990)

reported significant degradation of hemicellulose and cellulose and less degradation of lignin as a result of exposure of spruce wood (*Picea* sp.) to various doses of gamma rays.

Gamma radiation also alters the microstructure of wood. For example, Antoine et al. (1971) found that irradiation of Norway spruce (*Picea abies* (L) Karst) with gamma rays in air with doses of up to 655 Mrad caused longitudinal and transverse micro-cracks to develop in cell walls. As a result the irradiated wood became more friable. Bamber and Sangster (1977) observed that gamma radiation reduced the thickness of tracheid walls in hoop pine (*Araucaria cunninghamii* D. Don) and a Mexican pine (*Pinus pseudostrobus* Lindl.). The torus and margo in the bordered pits of tracheids and the walls of parenchyma cells were destroyed by radiation (Bamber and Sangster 1977). They observed that the form of tracheids was not lost upon irradiation and suggested that the resistance of lignin to gamma radiation was responsible for this observation.

Changes to wood's microstructure as a result of irradiation are accompanied by losses in the mechanical properties of wood. For example, Aoki et al. (1977) found that gamma radiation decreased the tensile, bending and compressive strengths of hinoki (*Chamacyparis obtusa* Endl.). Antoine et al (1971) found some differences in the chemical composition of irradiated and untreated samples suggesting that cellulose and lignin were degraded by gamma radiation. They suggested that an increase in carboxyl groups in gamma radiated wood was responsible for the lower pH of irradiated surfaces. Tabirih et al. (1977) studied anatomical changes in white oak (*Quercus alba* L.) wood upon exposure to gamma radiation. They observed that exposure to gamma radiation reduced cell wall thickness. Decreases in cell wall thickness were related to radiation dose and they noted that at high doses of radiation the earlywood was heavily degraded. Chemical analyses of irradiated wood samples indicated that decreases in cell wall

thickness were related to cellulose degradation (Tabirih et al. 1977). These changes were accompanied by an increase in extractives content, while the holocellulose content of the wood decreased, as expected. The lignin content (percentage) of the irradiated wood appeared to remain constant (Tabirih et al. 1977).

de Lhoneux et al. (1984) studied the effect of gamma radiation on the ultrastructure of Douglas-fir (*Pseudotsuga menziesii* (Mirb) Franco) (heartwood) and yellow-poplar (*Liriodendron tulipifera* L.). They found that gamma irradiation degraded cell walls, particularly those areas that were rich in cellulose. Accordingly, in both species, the middle lamella was more resistant to degradation than the secondary wall. They also noted that the S_3 layer in the secondary wall of Douglas-fir and the warty layer in yellow-poplar were more resistant to degradation than the other secondary wall layers. More recently Khan et al. (2006) studied the effect of UV and gamma radiation on the surface properties of plywood coated with an epoxy acrylate. They found that a UV radiation pretreatment increased the pendulum hardness, adhesion strength, surface hardness and percent gloss of the coated plywood. The physical properties of the coating on plywood decreased when high levels of gamma radiation were used as a pretreatment. Unfortunately the authors didn't provide any explanation for their findings.

2.4 Plasma modification of wood

2.4.1 Introduction

Cold plasma processes are an attractive way of modifying wood. Firstly, they are simple dry procedures that allow the implantation of a wide range of functional groups onto surfaces, as mentioned above. They permit the creation of specific surface characteristics via the control of treatment parameters, such as gas flow rate, pressure, power, and treatment time. Finally,

modifications resulting from cold plasma treatment are confined to the outermost layers of substrates, leaving the bulk properties of the material intact (Denes and Young 1999).

The surface modification of wood and the introduction of specific groups onto the surface of lignocellulosics (e.g. fibers, powder, wood wafers) is traditionally achieved using an excess of liquid reagent. Following modification, the removal of unreacted compounds adds extra time and increases the cost of the procedures. These problems can be eliminated using cold plasma techniques. For example, clear coatings can be deposited directly on wood surfaces using an RF-plasma (Denes and Young 1999, Denes et al. 2005).

2.4.2 Plasma modification and wood composites

Increasing concern for the environment has given impetus to research on the substitution of synthetic fibers, in composites with wood fibers (Nayak 1999, Lee et al. 2011). However, the addition of wood fibers to polymers often does not produce the desired property improvements because of incompatibility between the hydrophilic wood fibers and the hydrophobic matrix (polymer), and also weak interfacial adhesion between fibers and the matrix (Lee et al. 2011). Poor dispersion of wood fiber in the polymer matrices due to strong fibre-fibre interactions resulting from strong intermolecular hydrogen bonding also prevents natural fiber reinforced composites from achieving desired properties (Kazayawoko et al. 1999). Various methods have been used to overcome these problems including electrical discharge modification of fibers prior to mixing them with polymers (Bledzki et al. 1998). For example, the effect of corona plasma treatment of wood and polymer surfaces on the tensile properties of a wood-polymer composite was investigated by Dong et al. (1993). They found that the treatment increased the strength properties of the composite and improved the ductility of composites containing 15 to 30% of modified fiber. Belgacem et al. (1994) examined the effect of corona treatment on the

mechanical properties of cellulose-fiber/polypropylene composites. The cellulose fibers and polypropylene were modified with plasma for different periods of time. The tensile properties of composites made from combinations of treated or untreated cellulose fibers and polypropylene were subsequently measured. Belgacem et al. (1994) found that plasma treatment of the cellulose fibers alone, or both the fibers and the polypropylene improved the properties of the composites. They also found a positive effect of treatment time on the properties of the composites.

Yuan et al. (2004) used argon and air-plasma treatments to modify the surface of wood fibers and improve their compatibility with polypropylene. The tensile strength, and tensile and storage moduli of the composite sheets increased to some extent after plasma treatment. Scanning electron microscopy of fracture surfaces of tested composites suggested that plasma treatment improved interfacial bonding between wood fibers and polypropylene (Fig. 2.6). X-ray photoelectron spectroscopy (XPS) showed that plasma treatment increased the oxygen/carbon ratios of wood fibers (Yuan et al. 2004).

Figure 2.6: Has been removed due to copyright restrictions. It was SEM photomicrographs of the fracture surface of air-plasma treated wood-fibre- polypropylene composites (treatment time 30 s): (a) overall fracture surface; (b) magnified view of the identified area (Yuan et al. 2004)

Zanini et al. (2005) evaluated the effects of cold argon plasma modification on the type and amount of radicals formed on Kraft and chemithermomechanical pulp fibers. Interestingly, they

found that phenoxy radicals generated in lignin on plasma treated fibers formed intermonomeric bonds and rebuilt the lignin's original structure (which was destroyed by pulping). These results suggest that plasma treatment could be used for the auto-adhesion of wood. Mahlberg et al. (1999) used atomic force microscopy (AFM) to examine the effect of oxygen plasma treatment on the surface morphology of polypropylene, Kraft pulp, filter paper and wood. They observed the formation of nodular structures on both polypropylene and lignocellulosics surfaces after plasma treatment. The diameter of the nodules increased with treatment time. The overall roughness of the surfaces, however, decreased with treatment time. These phenomena were most apparent for treated polypropylene surfaces. They suggested that such features were probably caused by different physical and chemical processes (e.g., etching, sublimation of new constituents formed, and/or rearrangement of the chemically altered surface) (Mahlberg et al. 1999). Adhesion between polypropylene and lignocellulosic materials was slightly improved by the plasma treatment (Mahlberg et al. 1999). Gassan and Gutowski (2000) used corona discharge treatment to improve the mechanical properties of jute-fibre/epoxy composites. They found that exposure of single jute fibers to plasma significantly increased surface free energy due to an increase in the fibers' surface polarity. The effect of corona treatment increased with increasing corona energy and resulted in an improvement (15%) in storage modulus of fibers. Gassan and Gutowski (2000), however, reported that corona treatment did not affect the modulus of elasticity of the fibers and changes in mechanical properties were subtle when jute yarns were exposed to the corona plasma.

Plasma treatments can also modify the surface chemistry and energy of paper. It is assumed that changes are confined to the outermost layers, without the paper's bulk properties being affected. Various plasmas including those formed from oxygen, nitrogen, inert gases (e.g.

argon), fluorinated hydrocarbons, organic silicon compounds and their mixtures can modify the surface properties of paper (Tan et al. 2001, Navarro et al. 2003, Vaswani et al. 2005).

The effect of a dielectric-barrier discharge treatment on the properties of bleached chemical and unbleached mechanical pulp fibers was investigated by Vander Wielen et al. (2005). Changes at fiber surfaces were investigated by AFM, inverse gas chromatography (IGC), contact angle evaluation, determination of water retention value and zero-span tensile strength tests. These techniques revealed that at low plasma energy levels the plasma treatment increased the surface energy, carboxylic acid content, roughness and the coefficient of friction of the fibers. The increased surface energy of paper at low levels of plasma energy was thought to be due to increased oxidation, as suggested by increases in surface acids and cleaning of fiber surfaces (suggested by AFM images). At higher plasma energy levels, however, the fibers became smoother and surface energy of fibers was similar to that of untreated fibers. These results were explained by greater degradation/removal of polysaccharides, in accord with decreases in zero-span tensile strength of treated paper.

Tan et al. (2001) demonstrated that plasma-assisted deposition of hexamethyldisilazane (HMDS) was an efficient method for making paper surfaces hydrophobic, while still maintaining its porous structure. The coating of HMDS was resistant to strong bases and acids, as well as to indoor ultraviolet light.

Recently there has been interest in plasma modification of paper to improve printability. Schuman et al. (2005) studied the effect of plasma treatment on the printing and barrier properties of dispersion-coated (containing wax) paperboard. Good printability was noted after the paperboard was plasma treated and the barrier properties of the paperboard were preserved. Pykonen and Lahti (2008) examined offset print quality of nitrogen/helium plasma-treated

papers. Pigment coated and surface-sized papers were treated with plasma, and the effects of the treatment on the surface energy, surface chemistry and morphology of the papers were evaluated. Plasma treatment increased the surface energy of the paper as expected, and the O/C ratio of the paper increased. SEM images revealed that high energy plasma treatment could change the structure of the paper. An evaluation of the printing properties of the plasma treated paper revealed that the treatment influenced both ink and water absorption properties and caused ink to set faster.

2.4.3 Plasma treatment of solid wood

Plasmas have been used for a long time to alter the surface chemistry (surface oxidation) and physical properties of polymers, as mentioned above. Many excellent reviews are available on this subject (Liston et al. 1994, Inagaki 1996, Chu et al. 2002, Oehrlein et al. 2011). However, the attention given to plasma modification of lignocellulosics (wood and paper) has been quite one-sided. Most of the studies conducted to-date have focused on the plasma modification of cellulose and its derivatives. Relatively few studies have examined the effects of plasma on the chemical and physical properties of solid wood. Hence, there is a lack of information on the properties of plasma-modified wood surfaces (Chen and Zavarin 1990, Wolkenhauer et al. 2007). Nevertheless, it is clear from the studies conducted to-date that plasma treatments can increase the surface energy of wood and alter the bond strength of adhesives and coatings (Denes et al. 2005).

2.4.3.1 Effect on chemical properties

Furuno et al. (1990) first treated hinoki and buna (*Fagus crenata* Blume.) wood with corona plasma. They followed the formation of aldehyde groups in the plasma treated samples using

reduction with $NaBH_4$ solution and Schiff's staining method in combination with infrared spectroscopy. Lipska-Quinn (1994) examined the chemical changes at the surface of white fir (*Abies concolor* (Gordon) Lindley ex Hildebrand) treated with air, CO_2 or NH_3 plasmas. Plasma treated samples were extracted with 10% aqueous NaOH solution and were examined using X-ray photoelectron spectroscopy (XPS). XPS revealed that plasma treatment caused the formation of carbonyl, carboxyl and NH_3^+ or R-(C=O)-NH_2 (for ammonia plasma) at wood surfaces. Plasmas formed from air or carbon dioxide oxidized the wood surface causing an increase in the O/C ratios of treated surfaces. Treatment with ammonia plasma had the opposite effect (Lipska-Quinn 1994).

Sakata et al. (1993) found that corona plasma treated wood had increased affinity for Schiff's reagent. This observation suggested that the treatment increased the aldehyde content at the wood surface, in accord with the findings of Furuno et al. (1990). They isolated hemicellulose, lignin and alcohol benzene extractives from modified wood and tested their aldehyde content. The level of aldehydes in cellulose, hemicellulose and lignin was only slightly higher than that in unmodified wood. On the other hand, the aldehyde level of the alcoholic-benzene extracts increased significantly. Therefore they concluded that corona plasma treatment mainly altered the chemical composition of extractives at the surface of wood. Recently Avramidis et al. (2009) analyzed plasma treated beech, oak, spruce and Oregon pine [Douglas-fir (*Pseudotsuga menzeiesii* (Mirb) Franco)] and measured changes in the physical and chemical properties of treated surfaces. XPS was used to analyze the chemical composition of plasma treated and untreated beech. As expected, they found a higher total surface energy for plasma treated surfaces. XPS revealed a higher O/C ratio for plasma treated beech due to an increase in C-O and O-C=C groups, which accounted for the higher surface polarity of plasma treated wood.

2.4.3.2 Effects of plasma on wood structure and physical properties

A few studies have examined the effects of plasma treatments on the structure and physical properties of wood. Chen and Zavarin (1990) showed that a radio frequency plasma could increase the permeability of Douglas-fir wood. Improvements to the permeability of the treated wood appeared to be due to destruction of aspirated pits. Chen and Zavarin (1990) noted that cell walls of tracheids were damaged by plasma treatments. Lipska-Quinn (1994) used scanning electron microscopy to examine the effect of plasma treatment on the morphology of white fir. After air plasma treatment, wood cells became distorted (swollen) and pits were degraded. These findings accord with those of Chen and Zavarin (1990). Furuno et al. (1990) examined changes in the morphology of hinoki and buna wood after corona discharge treatment. They found that tracheid walls in hinoki and vessels walls in buna appeared to be brittle and fragile after treatment. Damaged cell walls were easily degraded when treated wood was soaked in water. Enlargement of bordered and cross-field pits also occurred during treatment.

Uehara et al. (1993) found that corona discharge plasma treatment caused degradation of Japanese beech (*F. crenata*) wood meal. Degraded cell walls peeled off when treated wood meal was washed in water, an observation which accords with that of Furuno et al. (1990).

Ramos (2001) found that prolonged (high energy) water-vapor plasma treatments could increase glue bond strength of high density eucalypts. The treatments also caused permanent losses in weight of thin sections and removed (etched) vestures from inter-vessel pits. These findings partly accord with those of Setoyama (1996) who observed that plasma reduced the weight of wood and cellulose samples.

2.4.4 Processing of solid wood with plasma

Plasma treatments, e.g. low pressure plasma, corona or dielectric barrier discharge plasmas, have been used for a long time to improve wettability, printability and adhesive properties of polymers. Not surprisingly there has been interest in examining whether plasma treatments can have the same beneficial effects on the properties and processing of wood (Wolkenhauer et al. 2007).

2.4.4.1 Glue bonding

Removal of surface contaminants generally increases glue bond strength because it allows the adhesive to interlock with the substrate surface rather than with a weak boundary layer (Kolluri 2003). Increasing the surface energy of a material above the surface tension of the adhesive makes it possible for the adhesive to wet the entire surface of the polymer substrate (Ebnesajjad and Ebnesajjad 2006). Plasmas can remove surface contaminants and increase the surface energy of materials, and these effects are thought to be responsible, in part, for their positive effects on the adhesive properties of polymers (Kolluri 2003). Another factor that contributes to improved adhesion of plasma modified surfaces is an increase in surface area of the polymer as a result of ablation and micro-roughening (Schultz and Nardin 1999). The increase in the apparent surface area of contact serves to increase the strength of adhesive bonds (Schultz and Nardin 1999). Finally, modification of the surface chemistry of a material can facilitate covalent bonding between the adhesive and substrate, further enhancing adhesion (Kolluri 2003).

There have been very few studies that have looked at the ability of plasma to improve the gluing properties of wood, despite the use of plasma treatment to improve the adhesion of polymers. More studies have looked at the effect of plasma on the surface wettability of wood,

and have assumed that improved wettability will increase the adhesive strength of glues and coatings to wood (Chen and Zavarin 1990, Podgorski et al. 2000, Custódio et al. 2009).

Sakata et al. (1993) used a corona discharge plasma treatment to modify the properties of various resinous wood species. The treatment was able to reduce the contact angle of urea formaldehyde (UF) resin droplets on wood veneers, as expected. A UF and poly-vinyl acetate emulsion at a ratio of 1:2 was used to glue plasma treated samples. Tensile strength perpendicular to the surface of the joint increased rapidly as a result of a mild corona plasma treatment. Uehara and Jodai (1987) were also able to improve the wettability of wood using a corona discharge treatment, in accord with finding of Sakata et al. (1993). They also found that their treatment increased the strength of wood joints glued with a UF resin.

Rehn and Viöl (2003) showed that plasma treatment could improve the fracture strength of glued pine (*Pinus* sp.) wood by 68%. Untreated wood mainly (65%) failed at the interface between glue and wood. In contrast, following plasma treatment, more failure occurred in the wood, indicating better adhesive bonding.

Ramos (2001) and Evans et al. (2007) examined the effect of plasma treatment on glue-bond strength of the following four difficult-to-glue eucalyptus species: blackbutt (*Eucalyptus pilularis* Smith); Gympie messmate (*E. cloeziana* F. Muell); rose gum (*E. grandis* W. Hill ex Maiden) and spotted gum (*Corymbia maculata* Hook. formerly *E. maculata*). Prolonged plasma treatment at high energy levels improved both the dry and wet shear strength of glue bonds in all four species.

Rehn et al. (2003) also examined the effect of plasma treatment on glue bond strength of robinia (*Robina pseudoacacia* L.), oak (*Quercus* sp) and teak (*Tectona grandis* L.) wood. Samples were plasma treated, coated with lacquer and pressed together. The lacquer was used as

the glue. The wood samples were soaked in water for 2 days before fracture strength tests. Their results showed that plasma treatment increased the fracture strength of glued robinia and oak wood, but it had little effect on the glue bond strength of teak.

More recently, Huang et al. (2011) examined the effect of atmospheric plasma treatment on the wettability and glue bond strength of poplar (*Populus* sp.) veneers. They exposed air-dried, oven-dried and over oven-dried poplar veneers to plasma and measured the contact angle of glycerin and UF resin droplets on treated surfaces. As expected, they found that plasma treatment reduced the contact angle of glue droplets on all treated surfaces, however, their treatment only improved the glue bond (shear) strength of the over oven-dried samples. The authors did not provide any explanation for this observation.

Avramidis et al. (2011a) examined the effect of atmospheric plasma on the curing of poly vinyl acetate (PVAc) used to glue maple (*Acer pseudoplanatus* L.), oak (*Quercus* sp.), European beech and teak veneers. They measured the time-dependent shear bond strength of the glued samples. They found a significant improvement in curing and adhesion properties of PVAc for plasma treated samples. They ascribed this finding to the faster water penetration from the glue into the wood. In related research, Avramidis et al. (2011b) exposed wax treated European beech to plasma and measured the surface wettability and adhesion of PVAc to the treated wood. As expected, they found an increase in wettability and adhesion strength of PVAc as a result of plasma treatment. Nevertheless, Avramidis and coworkers did not come to a firm conclusion based on their observations and they indicated that "further studies are needed to confirm the increased adhesion of adhesives and paints after plasma treatment, and other testing methods are necessary in order to obtain comparable and quantitative results" (Avramidis et al. 2011b).

2.4.4.2 Coating

Wood is often finished with various protective and decorative/protective coatings (Bulian and Graystone 2009). As pointed out by Frihart (2005) 'despite the apparent simplicity of this, there are great difficulties in obtaining uniform adsorption, strong adhesion and long-lasting performance from coatings on wood". The performance of coatings on wood can be improved by roughening wood surfaces, making them more permeable and removing extractives that interfere with the bonding of the coating or its penetration into the wood (Bulian and Graystone 2009). Various chemical or biological pre-treatments have been used to change the surface properties of wood and improve coating performance. Not surprisingly, there has been interest in using plasma treatments to do the same (Denes et al. 2005). For example, Podgorski et al. (2000) examined the outdoor-performance of a solvent-based (alkyd resin) and a water-based coating (acrylic resin) on plasma treated Scots pine (*Pinus sylvestris* L.) and lauan (*Shorea* sp.). Some samples of lauan wood had been heat-treated at 230°C for 60 minutes prior to plasma treatment. The adhesion tests, however, did not suggest improvement in the coatings' resistance to weathering, even though the plasma treatments increased the ability of the coatings to wet wood surfaces.

Plasma treatments have been used to cure or directly deposit surface coatings on wood. For example, Matsui et al. (1992) treated Japanese cedar (*Cryptomeria japonica* D. Don) wood with tetrafluoromethane (CF_4) plasma and was able to generate oil- and water-repellent wood surfaces without changing the appearance and tactile properties of the wood. XPS of the plasma treated surfaces indicated the presence of fluorine-containing functional groups including CF, CF_2, and CF_3, in addition to newly added oxygen atoms.

Denes and Young (1999) coated wood with polydimethylsiloxane (PDMSO) which contained various UV stabilizers, absorbers or reflectors. An oxygen plasma was then used to polymerize the coating. Coated samples were exposed to accelerated weathering. The plasma-cured coatings performed well during accelerated weathering and the coating significantly improved the weathering resistance of the wood. In related research, Denes et al. (1999) coated southern yellow pine (*Pinus palustris* Mill.) using hexamethyldisiloxane (HMDSO)-RF plasma treatments. X-ray photoelectron spectroscopy and attenuated total reflectance Fourier transform infrared (ATR-FTIR) spectroscopy revealed the presence of macromolecular layers of Si bonded to plasma treated wood surfaces. Molecular fragmentation analysis of the coating indicated that it was highly cross-linked. Denes et al. (1999) stressed that short treatment times were sufficient to coat the wood and that the RF power had a significant effect both on the plasma induced surface chemistry and on the properties of the resulting coatings. Wood surfaces coated with Si exhibited very high contact angles of about 120˚ following plasma treatments. The cross-linked nature of the coatings and the complete coating of wood surfaces explained the hydrophobicity of the plasma modified wood.

Podgorski et al. (2001) optimized plasma conditions (e.g. gas flow, power, treatment time) for the deposition of polymers derived from fluorine and silicone (in gaseous and liquid phase) at the surface of Scots pine. They suggested that both fluorine and silicone, particularly when present in liquids, were suitable monomers for plasma-coating of wood. Their evaluation of plasma treated surfaces, however, was only based on contact angle measurement and no additional techniques were used to evaluate the properties of the coated surfaces.

Bente et al. (2004) employed dielectric barrier discharges using ethane, methane and silane/N_2 for plasma modification of Norway spruce wood. All of these treatments made the

wood hydrophobic especially the silane treatment. Atomic force microscopy showed that plasma treatment made wood surfaces rougher and this was thought to contribute to the increased hydrophobicity of modified surfaces.

Magalhães and de Souza (2002) coated Caribbean pine (*Pinus caribaea* Morelet var. *hondurensis*) wood with materials generated from ethylene, acetylene, vinyl acetate, or butane-1 plasmas. The properties of the coated wood varied depending on the parent gas used to generate the plasma. The ethylene and acetylene plasmas generated highly hydrophobic surfaces, but the most hydrophobic surfaces (Θ = 140˚) were obtained using a butane-1 plasma. Lukowsky and Hora (2002) compared the ability of different plasma treatments to improve the performance of exterior coatings on Scots pine sapwood. They claimed that plasma treatments increased the wet adhesion of coatings, which was thought to be related to the increased surface energy of treated wood. However, they did not provide any explanation for their findings, and the reliability of the adhesion test used in their research seems questionable.

The effect of a dielectric barrier discharge plasma on the surface properties of sawn, planed or polished pine wood (*Pinus* sp.) has also been investigated (Rehn and Viöl 2003). An atmospheric air plasma was more effective at increasing the wettability of wood surfaces than helium, nitrogen, or argon plasmas. Plasma treatment for only 1 to 20 seconds could make wood surfaces hydrophilic, or increase surface absorption 22 fold. Rehn and Viöl (2003) also showed that plasma treatment in methane or acetylene could make wood surfaces hydrophobic. For example, after plasma treatment for 1 minute in an Ar:CH_4=80:20 gas mixture at atmospheric pressure, the absorption of water by wood was 32 times lower than that of the untreated control.

Blanchard et al. (2009) treated sugar maple (*Acer saccharum* Marsh.) with plasma derived from different gases (N_2, H_2, O_2, and Ar) or their mixtures. They found that treatments improved

the adhesion of a waterborne UV-curable polyurethane/polyacrylate resin to the treated sugar maple wood. Improvements in adhesion were explained by changes in surface energy (lower contact angle) and increases in penetration depth of coatings on plasma treated surfaces.

More recently, Pabelina et al. (2011) used plasma treatment to deposit flame retardants on wood. They applied solutions of boric acid, phosphoric acid and "commercially-available flame retardant (CFR)" to plywood using different methods including direct application (spraying), vacuum vapor deposition and cold plasma deposition. They evaluated the efficiency of these application techniques using thermogravimetric analysis (TGA) of the treated plywoods. They found that samples treated by vacuum vapor deposition were the most thermally stable. However, the phosphoric acid plasma treated samples had the best thermal stability and flame retardant properties. Pabelina et al. (2011) did not provide any information on the type of wood used in this test and they suggested that additional experimentation was needed to confirm their findings and explore whether the treatments could be used by industry.

2.5 Overview

It is clear from this review that modification of wood by plasma can improve surface energy and bond strength of adhesives and coatings. However, little information is available on the effect of plasma on the structure and chemical and physical properties of wood (Denes et al. 2005, Mertens et al. 2006, Wolkenhauer et al. 2007).

Plasma etching has been used extensively to modify the mechanical and physical properties of polymers and change their wettability and adhesion properties (Egitto et al. 1996). Ablation of polymers occurs when plasma reduces the molecular weight of their chemical constituents and they become volatile enough to be removed by the vacuum pump employed in plasma devices (Boenig 1982). If the substrate consists of a blend or alloy of materials that react differently in

plasma, differential ablation of these components can create a microroughened surface (Kolluri 2003). Wood consists of a blend of cellulose, hemicelluloses, and lignin (Sjöström 1981). Therefore it is plausible that the same effect could be produced at the surface of wood, as suggested in Chapter 1.

Evidence of plasma etching of wood can be found in a few studies (Chen and Zavarin 1990, Lipska-Quinn 1994, Setoyama 1996, Ramos 2001, Evans et al. 2007). The relevant observations include distortion of cell walls, creation pulpy cell wall layers and removal (etching) of vestures from inter-vessel pits. However, the existing knowledge on the ability of plasma to etch wood and its constituents is very limited.

This review has identified a number of important gaps in our knowledge of the plasma etching of wood. This thesis seeks to enlarge our knowledge of the plasma etching of wood and close the most important knowledge gaps in the experimental Chapters that follow:

Chapter 3; here I hypothesize that there will be differential etching of wood cell walls because of variation in the susceptibility of their polymeric constituents to degradation by plasma.

Chapter 4; here I use confocal profilometry to accurately quantify plasma etching of wood cell walls and further examine how the etching of wood is affected by treatment time (plasma energy) and wood's chemical composition.

Chapter 5; here I hypothesize that chemical changes will be more pronounced in the holocellulose (cellulose and hemicellulose) component of wood than lignin and examine chemical changes at wood surfaces that occur as a result of plasma treatment.

Chapter 6; here I hypothesize that plasma will etch and remove the chitin from hyphae of fungi in blue-stained lodgepole pine and plasma treatment will increase the ability of hypochlorite bleach to remove blue stain from blue-stained wood.

Chapter 7; here I hypothesize that plasma will be able to break down and etch away vegetable oil deposited at the surface of blue-stained wood that has been thermally modified using hot oil and examine changes in wood properties such as wettability and the adhesion and performance of coatings.

3 Effects of plasma etching on the microstructure of wood[3]

3.1 Introduction

Plasmas created from organic gases have been used to create hydrophobic wood surfaces (Matsui et al. 1992, Denes and Young 1999, Podgorski et al. 2001, Magalhães and de Souza 2002, Bente et al. 2004, Avramidis et al. 2009). Conversely, plasmas created from inorganic gases have been used to increase the surface energy of wood to make it easier to glue (Uehara and Jodai 1987, Chen and Zavarin 1990, Sakata et al. 1993, Mahlberg et al. 1999, Podgorski et al. 2000, Ramos 2001, Rehn and Viöl 2003, Mertens et al. 2006). Plasma is also able to etch materials, but there has been relatively little research on the etching of wood by plasma. The etching of wood by plasma was first noted by Chen (1989) and subsequent research has shown that plasma can remove membranes and vestures from bordered pits in softwoods and hardwoods, respectively, enlarge bordered and cross-field pits and create a 'pulpy layer' on tracheid walls (Chen and Zavarin 1990, Furuno et al. 1990, Lipska Quinn 1994, Ramos 2001).

Etching of materials by plasma occurs because electrons and other reactive species within the plasma have sufficient energy to break even the most stable chemical bonds (Denes et al. 2005). Hence, prolonged exposure to plasma can reduce the molecular weight of a polymer until it volatilizes from the surface of the substrate (Boenig 1982). The etching of polymers by plasma is strongly dependent on the chemical composition of the material as well as the energy of the plasma (Kolluri 2003). For example, aromatic polymers are more resistant to plasma etching

[3]Parts of this chapter have been published and the original publication is available at www.springerlink.com. Jamali, A. and Evans, P.D. Etching of wood surfaces by glow discharge plasma. Wood Science and Technology. Volume 45, Issue 1 (2011), pages 169-182.

than aliphatic polymers (Pederson 1982; Egitto et al. 1990). Hence, if a material consists of a blend of polymers that react differently in plasma, then differential etching of the polymer can occur (Kolluri 2003). Wood is a blend of aromatic (lignin) and aliphatic polymers (cellulose and hemicelluloses), and it is reasonable to assume that differential etching of wood will occur when it is exposed to plasma.

In this Chapter, I hypothesize that there will be differential etching of wood cell walls because of variation in the susceptibility of their polymeric constituents to degradation by plasma. To test this hypothesis, wood was exposed for different periods of time to a glow-discharge plasma generated from water vapor. Both scanning electron microscopy (SEM) and light microscopy were used to examine the etching of different cell types and wall layers in wood exposed to plasma.

3.2 Materials and methods

3.2.1 Wood samples and specimen preparation

Straight grained samples of different dimensions, but free of macroscopic defects such as knots were obtained from different softwood and hardwood species in the wood collection of the Forest Science Center at the University of British Columbia (Table 3.1).

Table 3.1: Wood species treated with glow-discharge plasma and examined using scanning electron microscopy or light microscopy

Type	Species	Scientific name	Family
Softwood	Redwood	*Sequoia sempervirens* (D. Don) End.	Taxodiaceae
	Actinostrobus	*Actinostrobus arenarius* (Gardner)	Cupressaceae
	Yellow cedar	*Chamaecyparis nootkatensis* (D. Don) Spach	Cupressaceae
	Radiata pine	*Pinus radiata* D. Don	Pinaceae
	Hoop pine	*Araucaria cunninghamii* Aiton ex D. Don	Araucariaceae
Hardwood	Hybrid poplar	*Populus* sp.	Salicaceae
	Rose gum	*Eucalyptus grandis* W. Hill ex Maiden	Myrtaceae

Two different types of specimens measuring 5 x 5 x 5 mm^3 and 10 x 10 x 10 mm^3 for scanning electron and light microscopy, respectively, were cut from the wood samples using a RYOBI® BS 902 band saw and razor blades. These wood samples were generally cut from the sapwood rather than from the heartwood of the selected species. Sapwood was preferred, because anatomical features in sapwood are not obscured by extractives and also because sapwood is from the outer more mature part of the tree, and hence the risk of inadvertent

inclusion of juvenile wood in the samples is reduced (Heady 1997). Specimens were vacuum (80 kPa) impregnated with distilled water and left to soak in water for 3 days.

Small water-saturated blocks (5 x 5 x 5 mm^3) were clamped in a small vice located beneath the stage of a low power binocular microscope, with the face to be cut (radial longitudinal, tangential longitudinal or transverse) protruding from the jaws of the vice.

Each specimen was viewed at x 10 magnification and a sharp single-edged razor blade (Stainless Steel Injector Blades, type 71990) was used to manually slice thin (20 to 30 µm) sections from the radial longitudinal, tangential longitudinal or transverse faces of specimens until clean, undamaged surfaces were obtained. For radial longitudinal (RLS) and tangential longitudinal surfaces (TLS) the cut was always made parallel to the longitudinal axis of the wood, since, as pointed out by Heady (1997) 'cutting at an angle across tracheids or fibers caused chaffing of the cut edge'. The final surface was prepared by slicing only one thin section off the exposed surface using a new blade or a portion of the blade that was not previously used, in order to minimize distortion caused by the blade (previously observed by Heady and Evans 2000). Specimens were then conditioned at 20 ± 1˚C and 65 ± 5% r.h. for 3 days. These specimens were used for scanning electron microscopy.

Small blocks (10 x 10 x 10 mm^3) were used to cut thin slices (25 µm thick) for light microscopy using a microtome (Spencer Lens Co. Buffalo, USA) (Fig. 3.1). One block from the species of interest was clamped firmly in the fixed sample holder of the microtome with the required face (radial longitudinal, tangential longitudinal or transverse) facing uppermost. A disposable stainless steel blade (Type S35, Feather Safety Razor Co., Japan) in a blade-holder was used to cut thin slices (~25 µm) from the surface of the block. During cutting the blade was oriented at an angle of ~30º to the specimen. A drop of distilled water was placed on the cutting

surface prior to each cut and a small clean paint brush was used to support the sections when they were being cut and to prevent them from folding or disintegrating (Fig. 3.1). Each section was removed from the brush by dipping the end of the brush containing the section in a small Petri dish (55 x 17 mm (dia x h)) containing distilled water. Several sections were obtained from each surface of interest, but only the higher quality ones (free of folds or crumbling) were transferred from the Petri dish into another dish and air dried. These sections were plasma treated and examined using light microscopy (see below).

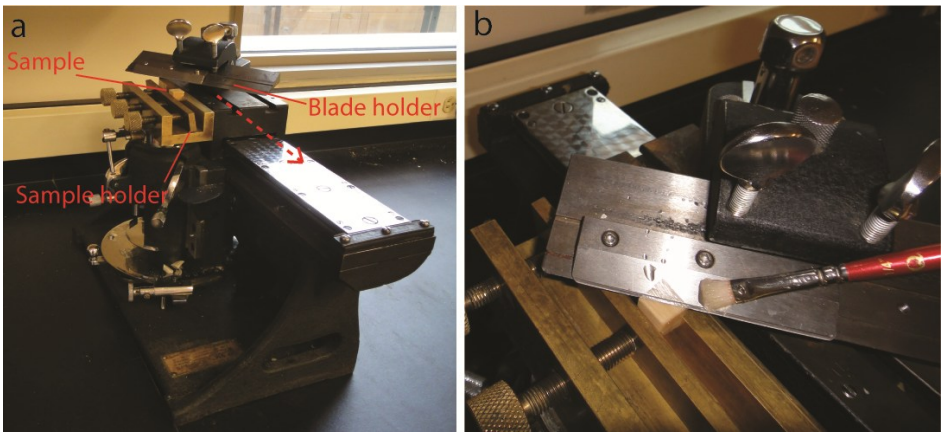

Figure 3.1: Sliding microtome and the blade used to cut thin slices from specimens: (a) the blade holder and sample holder with a fixed sample (dotted arrow indicates direction of sectioning); and (b) close-up of a specimen being sectioned

3.2.2 Plasma treatments

Wood specimens were modified in a plasma reactor that was designed to treat silicon wafers and clean atomic force microscopy tips to produce high energy surfaces (Fig. 3.2). One specimen was placed in the glass chamber of the plasma reactor at a time, and a vacuum of 19.998 +/- 1.33 Pa was drawn using a rotary oil vacuum pump. The pressure in the chamber was monitored using a differential pressure gauge (MKS Baratron). A metering valve was opened to allow water vapor from a small glass reservoir into the chamber and the vacuum (19.998 +/- 1.33 Pa) was redrawn (Fig. 3.2). A high voltage radio frequency signal (1 kV at 125 kHz) produced from

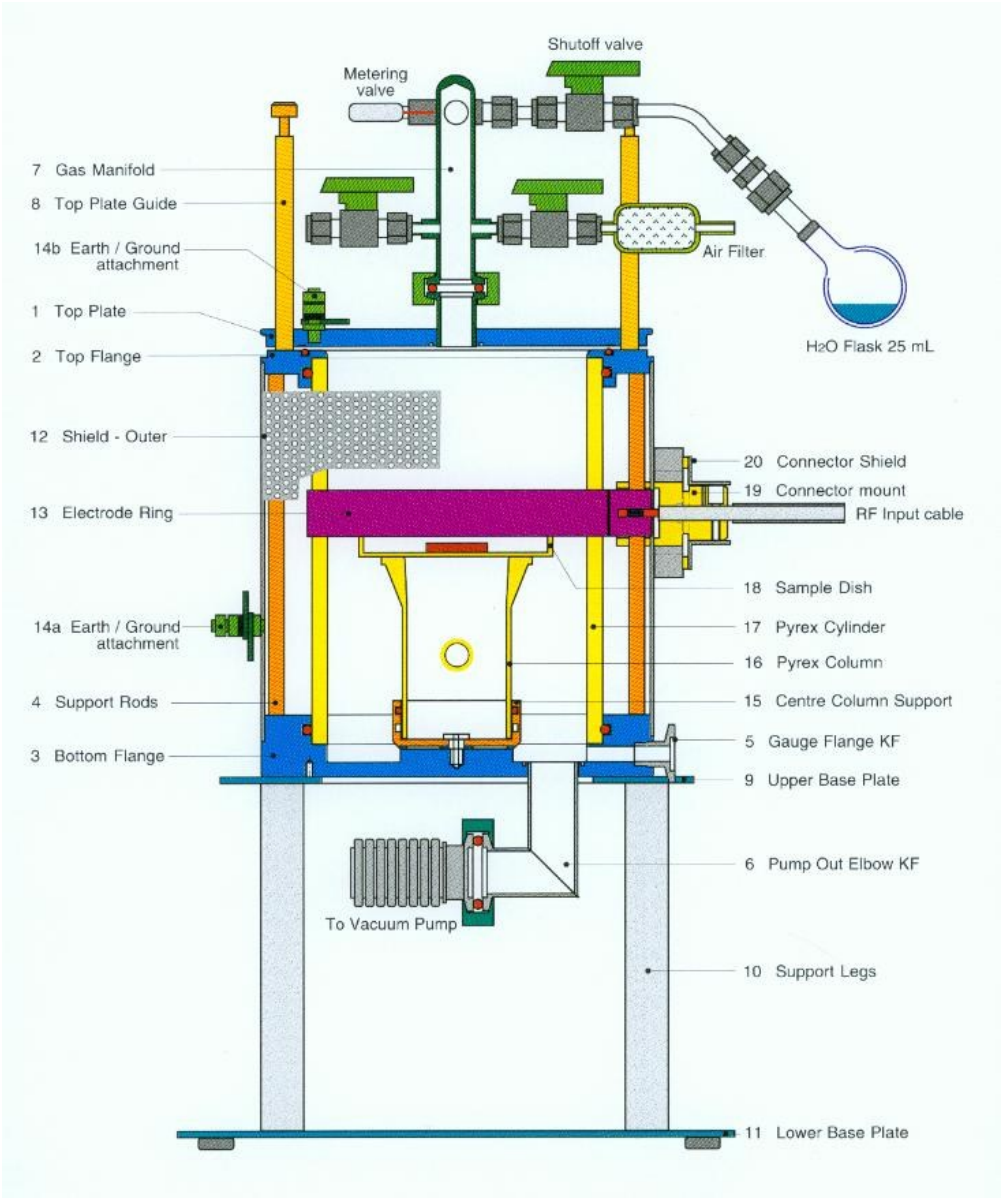

Figure 3.2: Schematic diagram of the plasma reactor used to modify wood specimens (courtesy of Anthony Hyde, The Australian National University)

a high voltage radio-frequency generator (ENI HPG-2) was capacitively coupled through a ring electrode (diameter 150 mm) on the exterior of the chamber into the low pressure interior of the reactor chamber by grounding all internal stainless steel components (Fig. 3.2). The power output of the R.F generator to the chamber was adjusted to the desired level (150 W). The duration of treatment varied from 33 to 1333 s and was measured using a digital timer. After

treatment the R.F. power was tuned to zero and a neoprene diaphragm valve connecting the chamber to the vacuum pump was closed. The chamber was vented to atmosphere and samples were removed from the chamber, taking care to avoid touching and contaminating the surface of interest.

Figure 3.3 shows a glow-discharge plasma produced in the plasma device that was used to treat wood specimens.

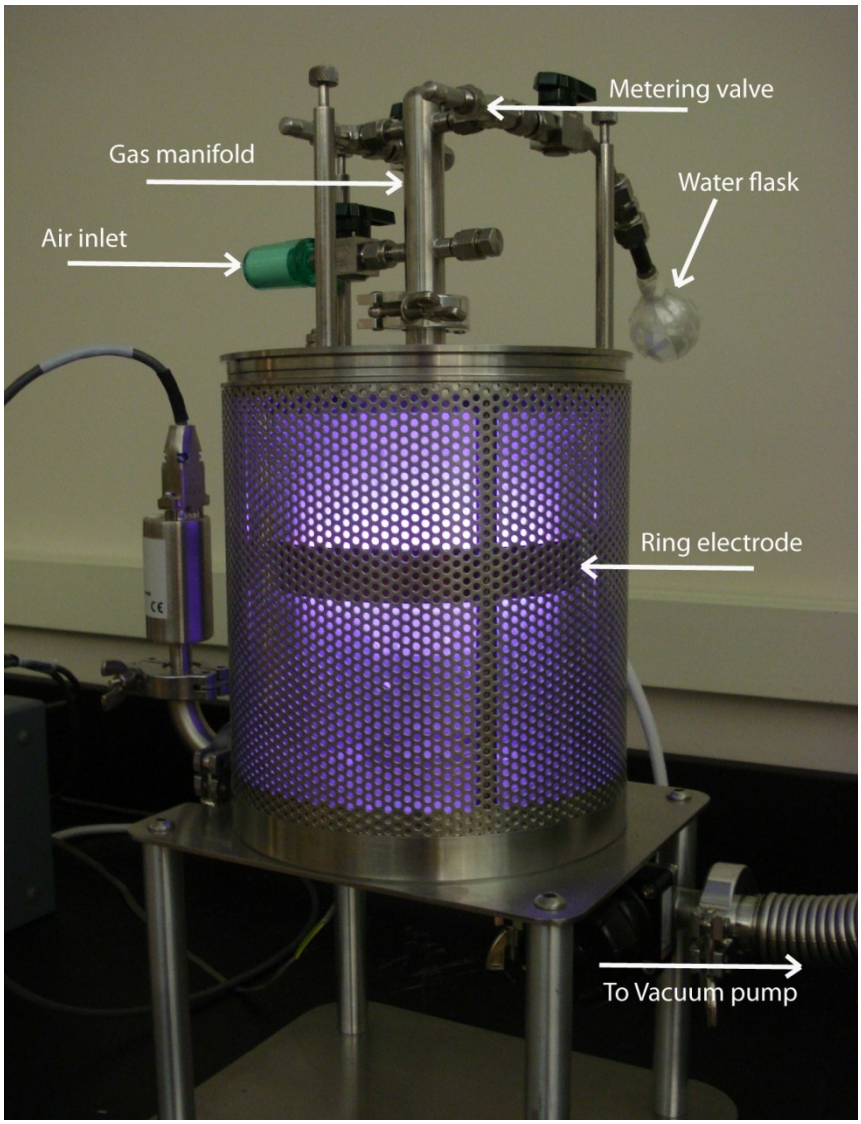

Figure 3.3: A glow-discharge water vapor plasma (purple) produced in the reactor chamber of the plasma device under vacuum (~19.99 Pa) with a radio frequency signal of 125 kHz at 150 watts

3.2.3 Scanning electron microscopy

Plasma modified and unmodified specimens were dried over silica granules in a vacuum desiccator for 24 h at 22ºC. Dried samples were then glued to 12 mm-diameter aluminum mounting stubs using Nylon nail polish as an adhesive. Up to three specimens were mounted on individual stubs. All SEM specimens were identified by an abbreviated identification code by labeling the underside of each stub. They were then coated with a 8 nm layer of gold using a sputter coater (Nanotech SEMPrep II) and examined using either a variable pressure scanning electron microscope (Hitachi S-2600N, VPSEM) or a field emission scanning electron microscope (Hitachi S-4700, FESEM). The accelerating voltages used by the VPSEM and FESEM were 7 to 15 kV and 1 to 5 kV, respectively. Secondary electron images of plasma modified and unmodified specimens were obtained from the microscopes and saved as TIFF files.

3.2.4 Light microscopy

Untreated and plasma-treated thin sections (see above) were placed on glass slides measuring 76 x 26 x 1 mm^3 (Matsunami Glass Ind. Ltd. Japan), and covered with ~ 1 mL of distilled water. A cover-slip measuring 22 x 40 x 0.20 mm^3 (Fisher Finest Premium Cover Glass, Fisher Scientific, Pittsburgh, USA) was placed over each section and they were examined using a light microscope (Carl Zeiss, Germany). For a better visualization of pale-colored wood samples, sections were stained with safranin. Staining involved placing sections in a clean small Petri dish (55 x 17 mm (dia x h)) containing fresh ethanol (industrial grade) to dehydrate the sections. The sections then were transferred into a beaker (20 mL) containing a saturated solution of safranin (BDH Chemical Ltd, England) in ethanol. The beaker was sealed with Parafilm® and stored in the laboratory for 3 days. The stained sections were then thoroughly

rinsed with ethanol and transferred to a Petri dish (150 x 15 mm (dia x h)) containing toluene (industrial grade) under a fume hood. After clearing in toluene for 30 min., sections were mounted on glass slides as follows. A drop of DPX (dibutyl phthalate xylene) mountant (Fluka Analytical, Germany) was placed on a warm glass slide. Then each section was laid on the droplet of DPX, and a warm cover-slip was gradually lowered on the section from a tilted position and immediately pressed against the slide. A dissecting needle was used to gently tamp the cover-slip down on the slide trying to remove any air bubbles between the section and the cover-slip. DPX-mounted sections were left overnight on a warm hot plate in a fume hood. Digital photographs of the sections were taken at magnifications of x4 to x40 using a high resolution digital camera (Olympus DP71, Japan) attached to a Carl Zeiss (Germany) microscope and saved as bitmap files.

3.3 Results

The following section describes the changes in the microstructure of wood in different planes (i.e. TS, RLS and TLS) as a result of plasma treatment. Most of the observations are on redwood, but there are others for different softwoods and hardwoods to illustrate the effects of plasma on different anatomical features of wood. Appendix 1 contains a more extensive collection of SEM and light microscopy images of untreated and plasma treated wood samples.

3.3.1 Effect of plasma on microstructure of wood cell walls

Plasma was able to etch wood cell walls. Comparison of surface microstructure and wood cell walls of untreated and plasma treated samples clearly show etching of cell walls in different planes. Figure 3.4 shows untreated transverse surfaces (cross-section) of redwood. Thin-walled earlywood tracheids and thicker-walled latewood tracheids with smaller lumina can be seen in

this figure (Fig. 3.4a-b). The middle lamellae can be seen in the higher magnification images (Fig. 3.4c-d).

Plasma treatment eroded redwood's cell walls, and prolonged exposure to plasma created voids and cavities in cell walls. However, different regions of the cell wall were more resistant to etching than others. Differential etching of wood cell walls can be seen in Figure 3.5a–d.

The photographs in Fig. 3.5a–d show cross-sections of latewood tracheids in redwood exposed to plasma for short (33 s) and long (1333 s) periods of time. Exposure of wood surfaces to plasma for a short period of time (33 s) created small holes in the cell walls of latewood tracheids (Fig. 3.5a). The walls of latewood tracheids exposed to plasma for longer periods of time (333 and 667 s) contained larger radially and tangentially oriented voids where cell wall substance appeared to have been preferentially etched (Fig. 3.5b-c). In cell walls exposed to plasma for prolonged periods of time (1333 s) the voids were even larger and separated by thin bridges of wall material that radiated from the middle lamella to the tertiary wall layer (Fig. 3.5d and see arrowed insets). These thin lamellae appeared to be more resistant to etching than the intervening cell wall material.

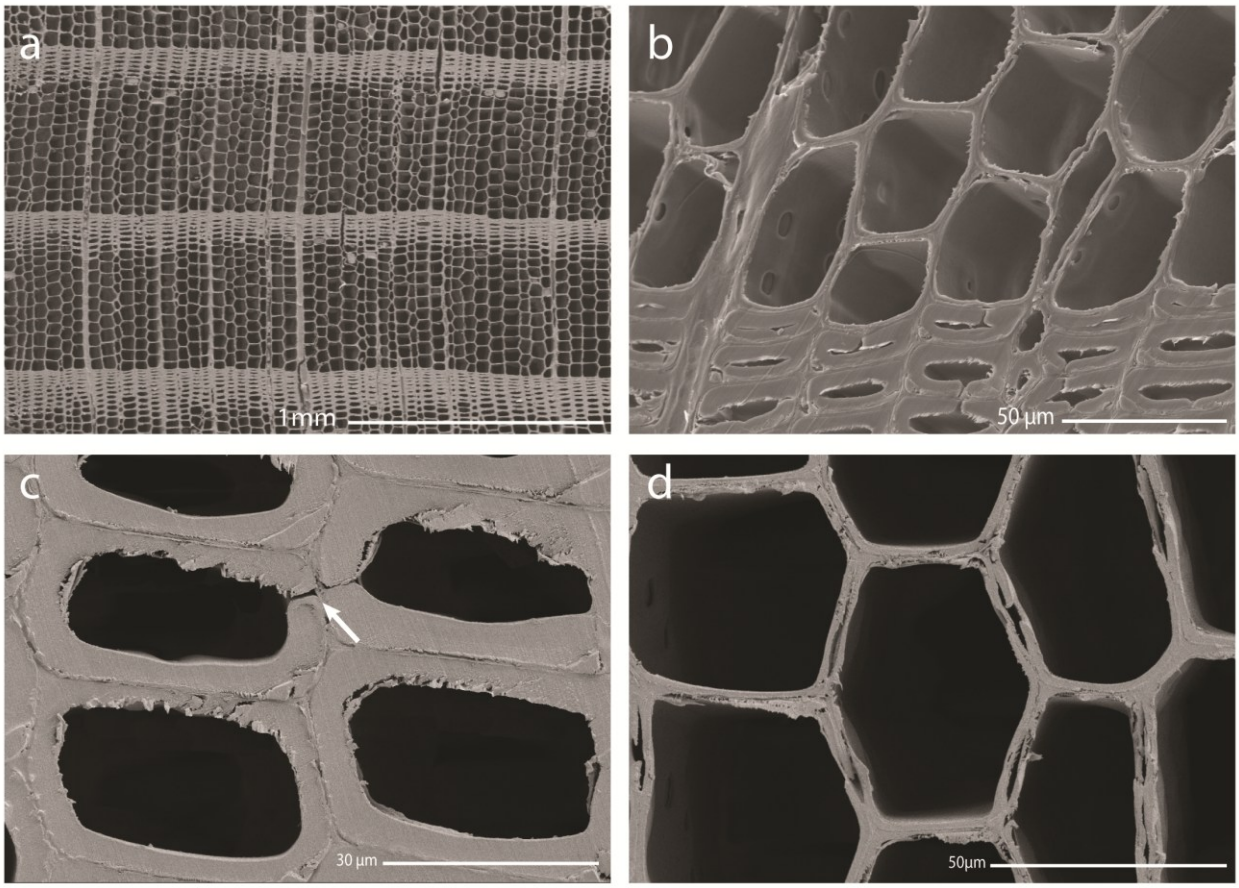

Figure 3.4: SEM photomicrographs of the transverse surfaces of untreated redwood: (a) a transverse plane with two whole annual rings, showing the transition between earlywood and latewood within annual rings and distinct boundaries at the ring border; (b) higher magnification image showing the border between the thinner-walled and larger-lumened earlywood tracheids at the top and thicker-walled latewood tracheids at the bottom; note the presence of inter-tracheid bordered pits in earlywood and latewood and half-bordered cross-field pitting in radial walls of earlywood tracheids; (c) a high magnification image of latewood tracheids; note the thick walls, small pit (arrowed) and also the conspicuous middle lamella at the corners; and (d) a high magnification image of earlywood tracheids; note the thin walls and large inter-tracheid bordered pits

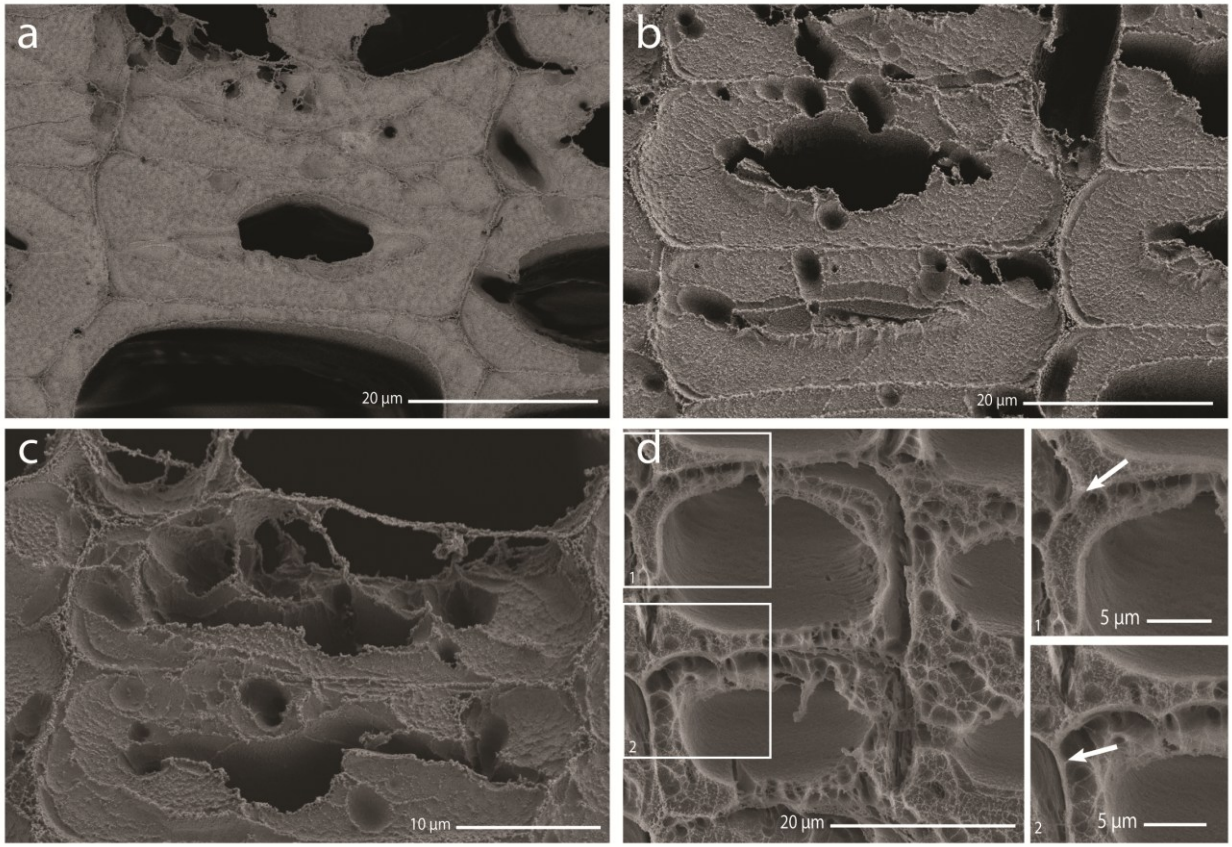

Figure 3.5: SEM photomicrographs of transverse surfaces of plasma treated latewood tracheids in redwood: (a) tracheids exposed to plasma for 33 s, note creation of a micro-roughened surface and small cavities in cell walls; (b) tracheids exposed to plasma for 333 s; note further erosion of the secondary cell walls and formation of ridges created by middle lamellae at the surface; (c) tracheids exposed to plasma for 667 s, showing a rough surface with enlarged voids; and (d) tracheids subjected to plasma for 1333 s, showing pronounced etching of secondary wall; split-screen enlarged images showing middle lamella (arrowed) and thin lamellae radiating from the middle lamella to the tertiary wall layer

Etching of earlywood cell walls was more difficult to see because the cell walls are much thinner. Fig. 3.6 (a and b) shows erosion of earlywood cell walls. The middle lamellae appear to be more resistant to erosion than the secondary wall (Fig. 3.6b), and there are voids in the secondary walls that are separated by thin lamellae, in accord with observation of the etching of latewood tracheids (above). Prolonged plasma treatment caused earlywood cell walls to become thinner (Fig. 3.6c-d). Such thinning of cell walls was pronounced in samples exposed to plasma for 1333 s (Fig. 3.6d). The resinous contents of ray cells, however, appeared to be resistant to etching (arrowed in Fig. 3.6c).

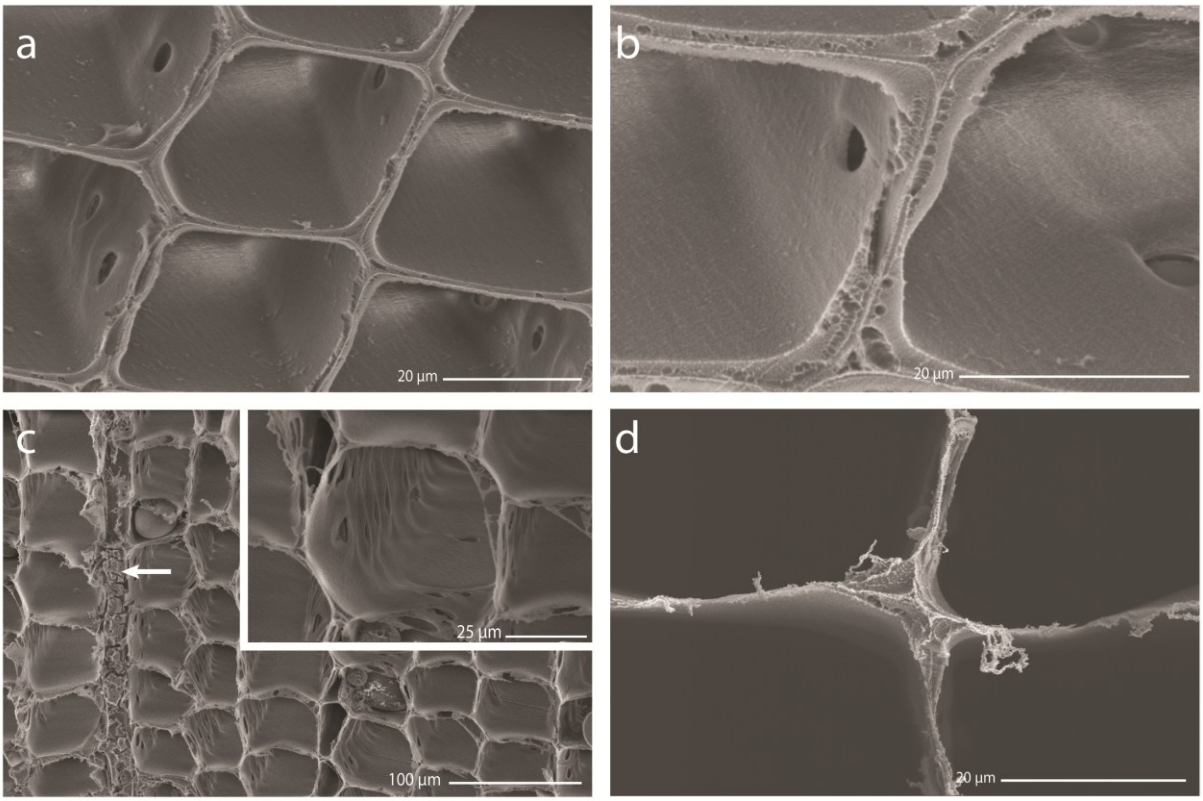

Figure 3.6: SEM photomicrographs of transverse surfaces of plasma treated earlywood tracheids in redwood: (a) tracheids exposed to plasma for 333 s; (b) higher magnification image of tracheids exposed to plasma for 333 s, showing etching of secondary cell walls. Note the voids in the cell wall; (c) tracheids exposed to plasma for 1333 s; split-screen image showing a higher magnification image of a tracheid, note thinning of tracheids' walls and the greater resistance of the resinous contents of the ray cells to etching; and (d) a high magnification image of tracheids exposed to plasma for 1333 s showing higher resistance of compound middle lamella and cell wall material in the corner of tracheids to etching

Hardwood species mainly contain fibers, vessel elements and parenchyma cells (Fengel and Wegener 1984). Fibers, vessels and parenchyma cell walls were etched by plasma and became thinner (Fig. 3.7 - 3.9). Etching of secondary walls and creation of voids on the transverse surface of fibers in hardwood species occurred as a result of plasma treatment (in accord with observations of the etching of tracheids walls in redwood, above). Figure 3.7 shows SEM images of untreated and plasma-treated (1333 s) fibers in rose gum. The middle lamellae and the cell wall layer adjacent to the lumen appeared to be more resistant to etching then the intervening secondary wall (Fig. 3.7b).

The thinning of cell walls and increases in size of lumina were conspicuous in cross-sections of plasma-treated poplar viewed under the light microscope (Fig. 3.8).

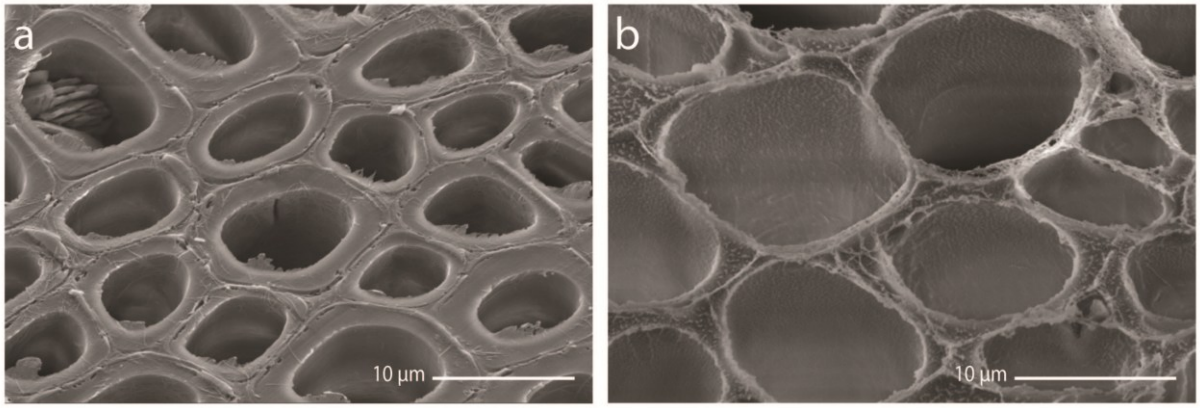

Figure 3.7: SEM photomicrographs of transverse surfaces of rose gum (*E. grandis*): (a) untreated fibers; and (b) surface exposed to plasma for 1333 s, note extensive etching (thinning) of cell walls and remnants of middle lamellae between fibers

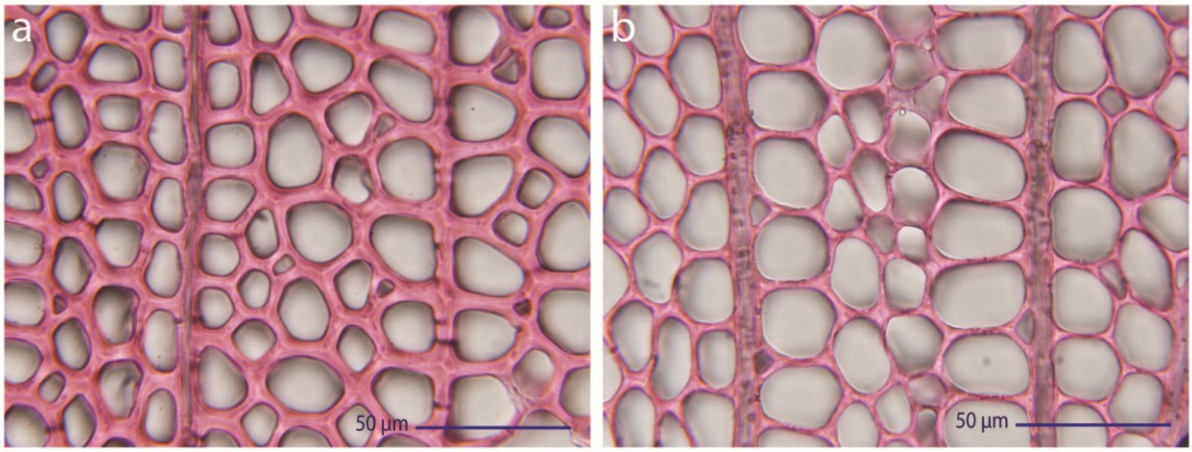

Figure 3.8: Light microscopy images of transverse sections of poplar stained with safranin: (a) untreated section showing cross-section of fibers and ray parenchyma and; (b) Cross-section exposed to plasma for 667 s, showing thinning of fiber cell walls and enlargement of lumina of the fibers, note the erosion of ray parenchyma cells

Rose gum vessels contained tyloses, which are a common feature of eucalyptus and many other hardwood species (Foster 1967, Sachs et al. 1970) (Fig. 3.9a). Tyloses were etched from vessels during prolonged plasma treatments (Fig. 3.9b). Figure 3.9b also shows the erosion and thinning of fibers and vessel element walls.

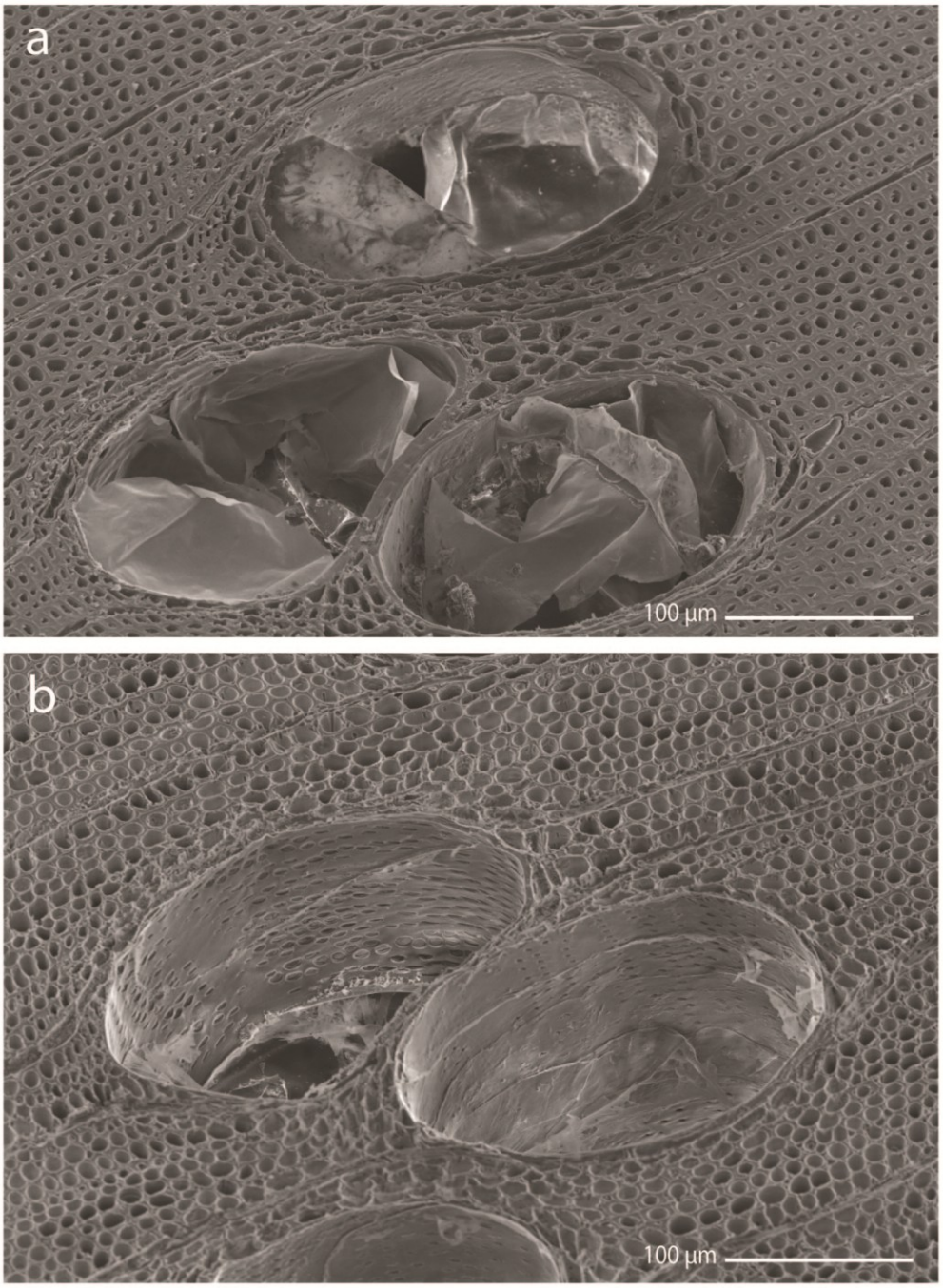

Figure 3.9: SEM photomicrographs of transverse surfaces of rose gum: (a) untreated surface showing cross-cut fibers and three vessels occluded with tyloses and (b) surface subjected to plasma for 1333 s showing etching of fibers and removal of tyloses from two vessels

Changes to the microstructure of wood as a result of plasma treatment were also obvious in radial and tangential longitudinal surfaces. Plasma created large voids at these surfaces by eroding pits. Microstructural changes became more pronounced with increasing exposure to plasma and there was complete removal of cell walls from the surface of specimens exposed to plasma for prolonged periods of time. Figure 3.10a, shows an untreated radial surface in redwood (Fig. 3.10a) and surfaces exposed to plasma for 667 s (Fig. 3.10b) and 1333 s (Fig. 3.10c). Exposure to plasma etched and opened-up pits creating voids in cell walls. Both tracheid and parenchyma cell walls were etched by plasma, but the resinous content of the latter were less affected by exposure to plasma (Fig. 3.10b). Longer exposure to plasma (1333 s) etched away the uppermost layer of cell walls (Fig. 3.10c).

Figure 3.11 shows SEM images of radial surfaces of poplar before (Fig. 3.11a) and after plasma treatment for 667 s (Fig. 3.11b) and 1333 s (Fig. 3.11c). Fibers, vessel elements and parenchyma cells can be seen in Figure 3.11. The etching of wood cell walls in poplar (Fig. 3.11), however, differed from that of redwood, because of the presence of different cell types. Fibers in poplar contain pits that are smaller in numbers and size compared to the pits in tracheids of softwoods. Etching of inter-fiber pits in poplar created small holes in cell walls compared to the larger voids created by etching of bordered pits in redwood (compare Fig. 3.10 and 3.11). On the other hand etching of vessel elements and their inter-vessel pitting created more numerous voids (Fig. 3.11). Nevertheless, prolonged plasma treatment etched and opened up most of the inter-fiber, inter-vessel and vessel-parenchyma pits and removed cell walls from the uppermost layer of wood, in accord with my observations of the etching of softwood (Fig. 3.11c). Vessel elements in poplar contained helical thickening. This was also eroded by plasma, but helical thickening was more resistant to etching than the underlying cell wall (Figure 3.11b and c).

Etching of tangential longitudinal surfaces by plasma increased with treatment time (Fig. 3.12). The walls of ray parenchyma cells in rays in redwood were eroded by plasma (Fig. 3.12). Figure 3.12 also shows that the contents of vertical parenchyma cells and ray parenchyma cells were relatively resistant to etching (arrowed in Fig. 3.12 c and d).

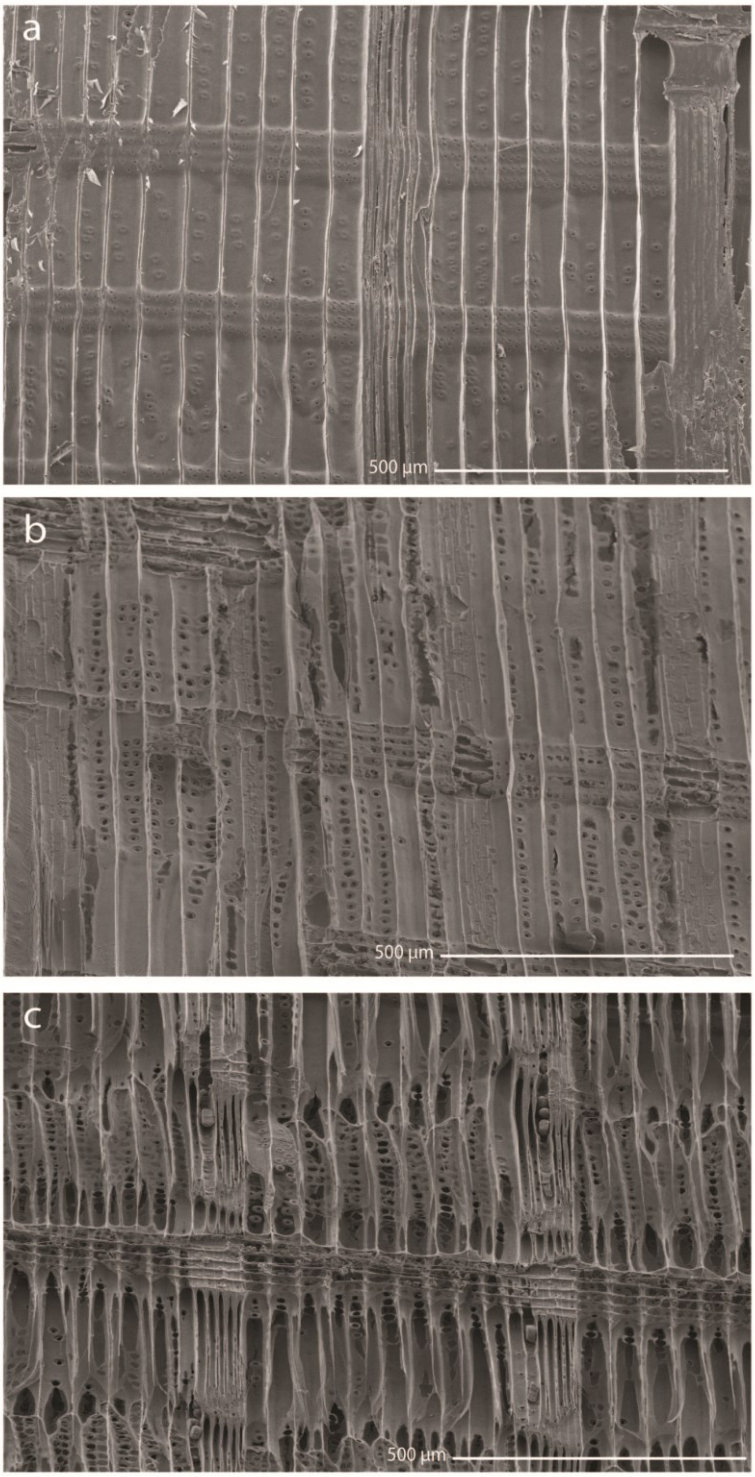

Figure 3.10: SEM photomicrographs of radial longitudinal surfaces of redwood: (a) untreated surface containing earlywood and latewood tracheids oriented in longitudinal direction and parenchyma cells arranged radially in rays; (b) surface exposed to plasma for 667 s showing enlargement of the apertures of bordered pits and etching of cell walls of tracheids and parenchyma cells; (c) surface exposed to plasma for 1333 s, showing extensive etching and removal of all cellular elements at the surface

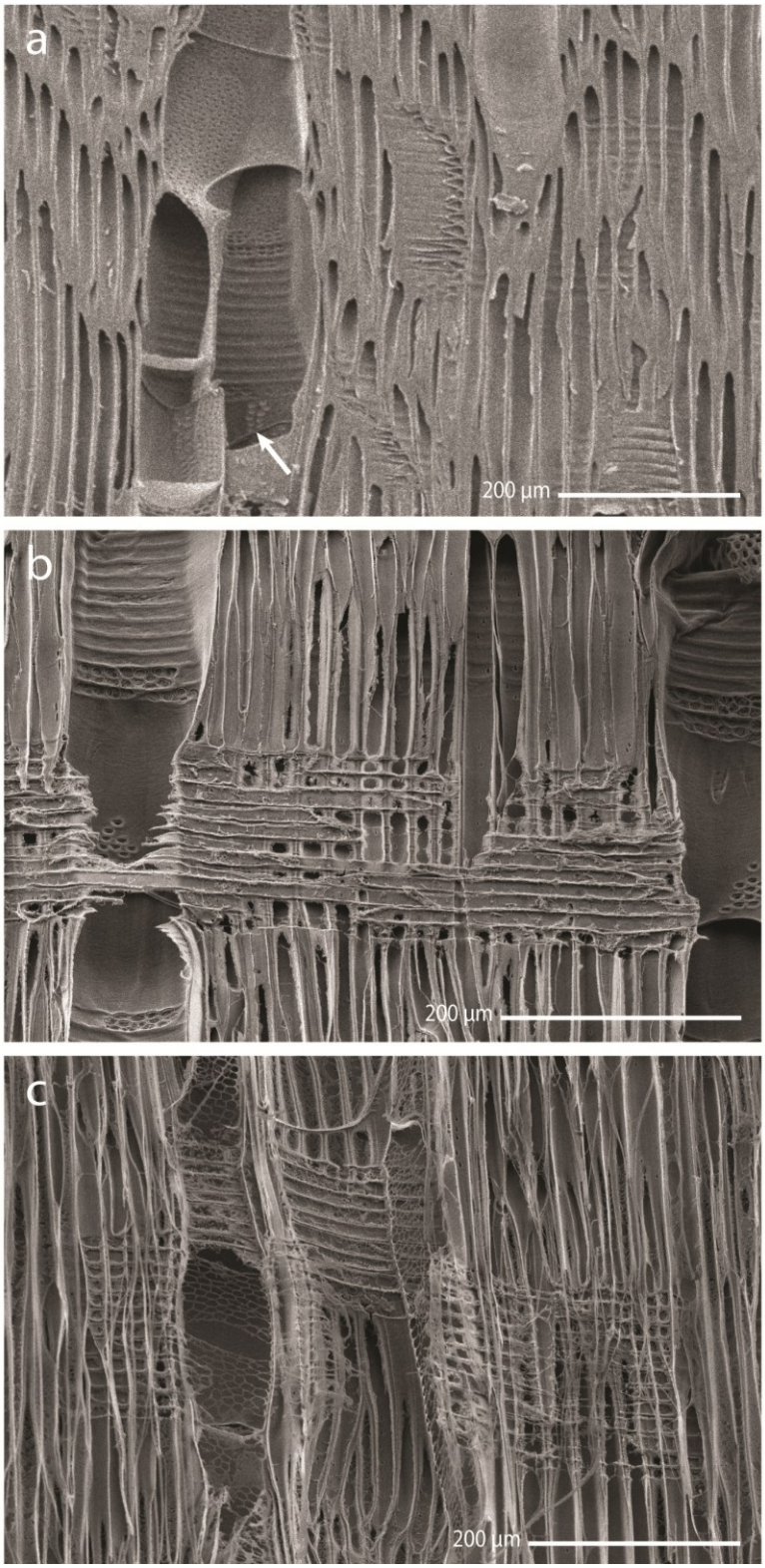

Figure 3.11: SEM photomicrographs of radial longitudinal surfaces of poplar: (a) untreated surface showing fibers and vessel elements, with an alternating arrangement of inter-vessel pits (arrowed left); (b) surface exposed to plasma for 667 s, showing etching of fibers, ray parenchyma and vessel elements; (c) surface exposed to plasma for 1333 s showing severe etching of all element at the surface, note the etching of inter-vessel pits and perforation plates

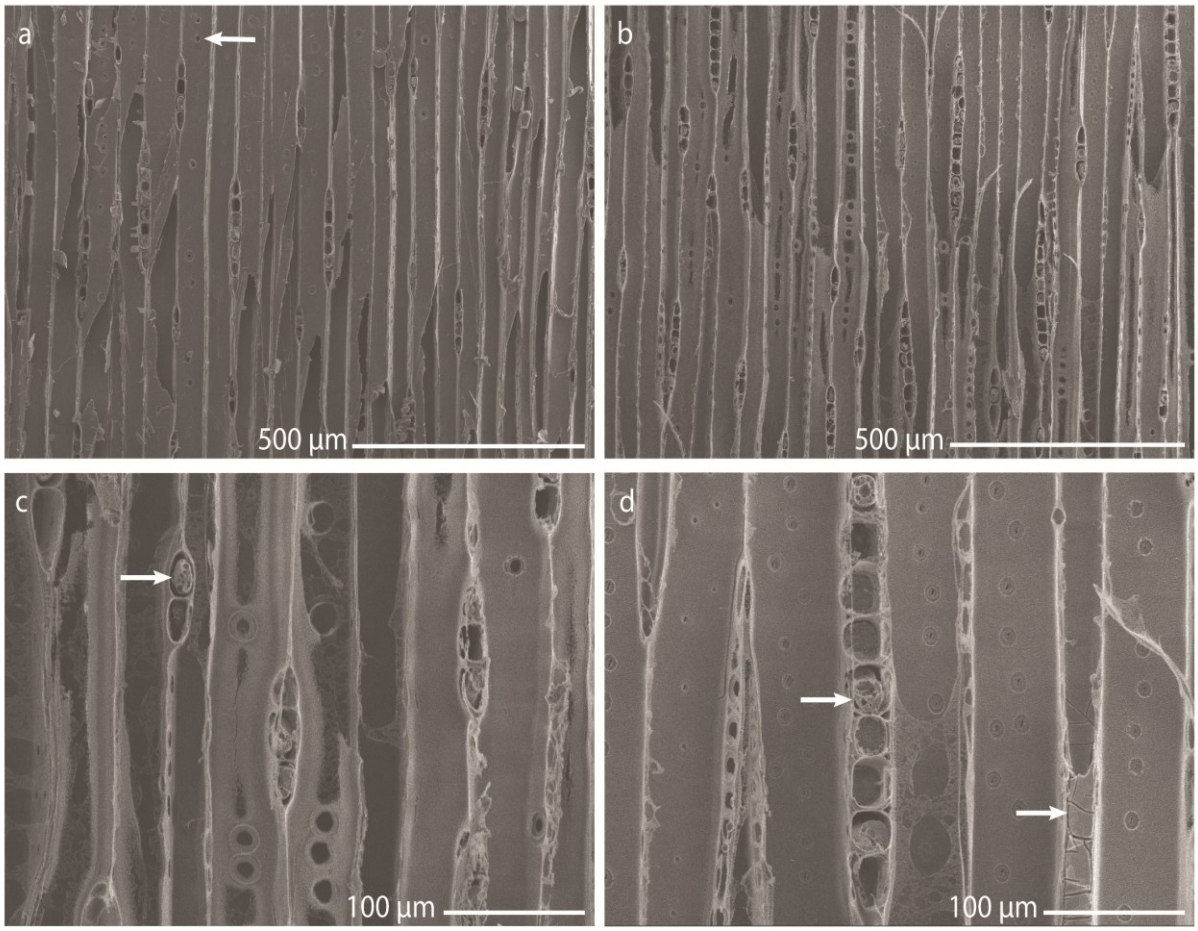

Figure 3.12: SEM photomicrographs of tangential longitudinal surfaces of redwood: (a) untreated surface showing uniseriate rays and bordered pits in tangential walls (arrowed); (b) surface exposed to plasma for 667 s, note etching of cell walls and bordered pits; (c and d) earlywood exposed to plasma for 1333 s, note thinning of ray parenchyma cells in rays, severe etching of cell walls, and contents of ray and longitudinal parenchyma cells remaining at the surface (d) (arrowed)

The presence of 'resin' in ray parenchyma cells was more noticeable in photographs obtained with the light microscope (Fig. 3.13a). Resin was still present in ray parenchyma cells after plasma treatment, but the deposits were smaller (Fig. 3.13b). Taxodioid cross-field pits in redwood were also more obvious under the light microscope. Plasma degraded the borders of the taxodioid cross-field pits, and enlargement of these pits sometimes created large voids in the cross-fields (top left in Fig. 3.13b).

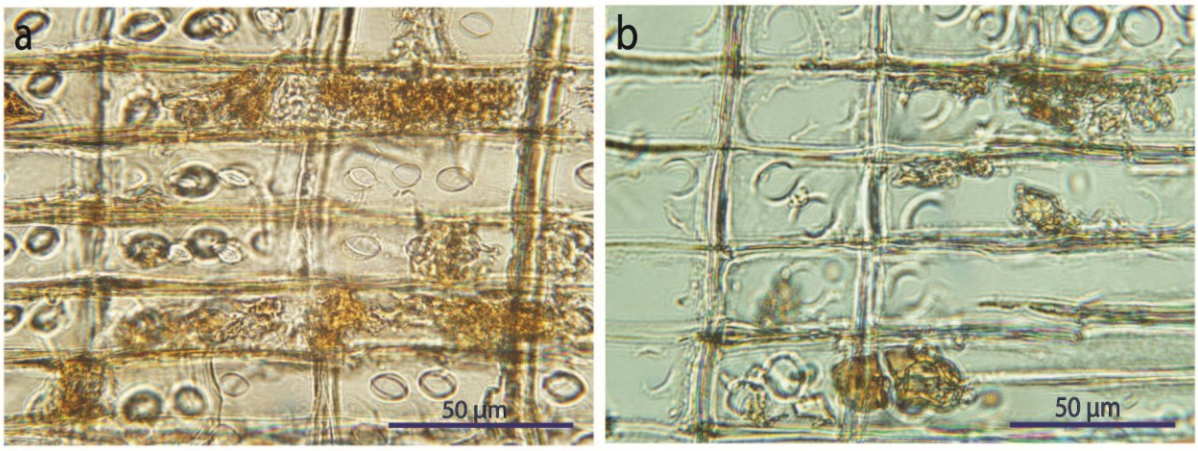

Figure 3.13: Light microscopy images of cross-fields in radial sections of redwood: (a) untreated section, note the presence taxodioid cross-field pitting and resinous deposits in ray parenchyma cells (goldish brown); and (b) sections subjected to plasma for 667 s, showing erosion of pits and cell walls, note presence of resinous material in ray parenchyma cells

Observations of the plasma etching of the warty layer were made on *Actinostrobus arenarius*. This species has a very prominent warty layer with large warts (Heady and Evans 2005) (Fig. 3.14a and e). Plasma treatment caused the warts in *A. arenarius* to become smaller and less distinct. Figure 3.14c shows remnants of the warts on the walls of tracheids exposed to plasma for 667 s. Warts, however, were completely etched from walls in specimens exposed to plasma for 1333 s (Fig. 3.14d).

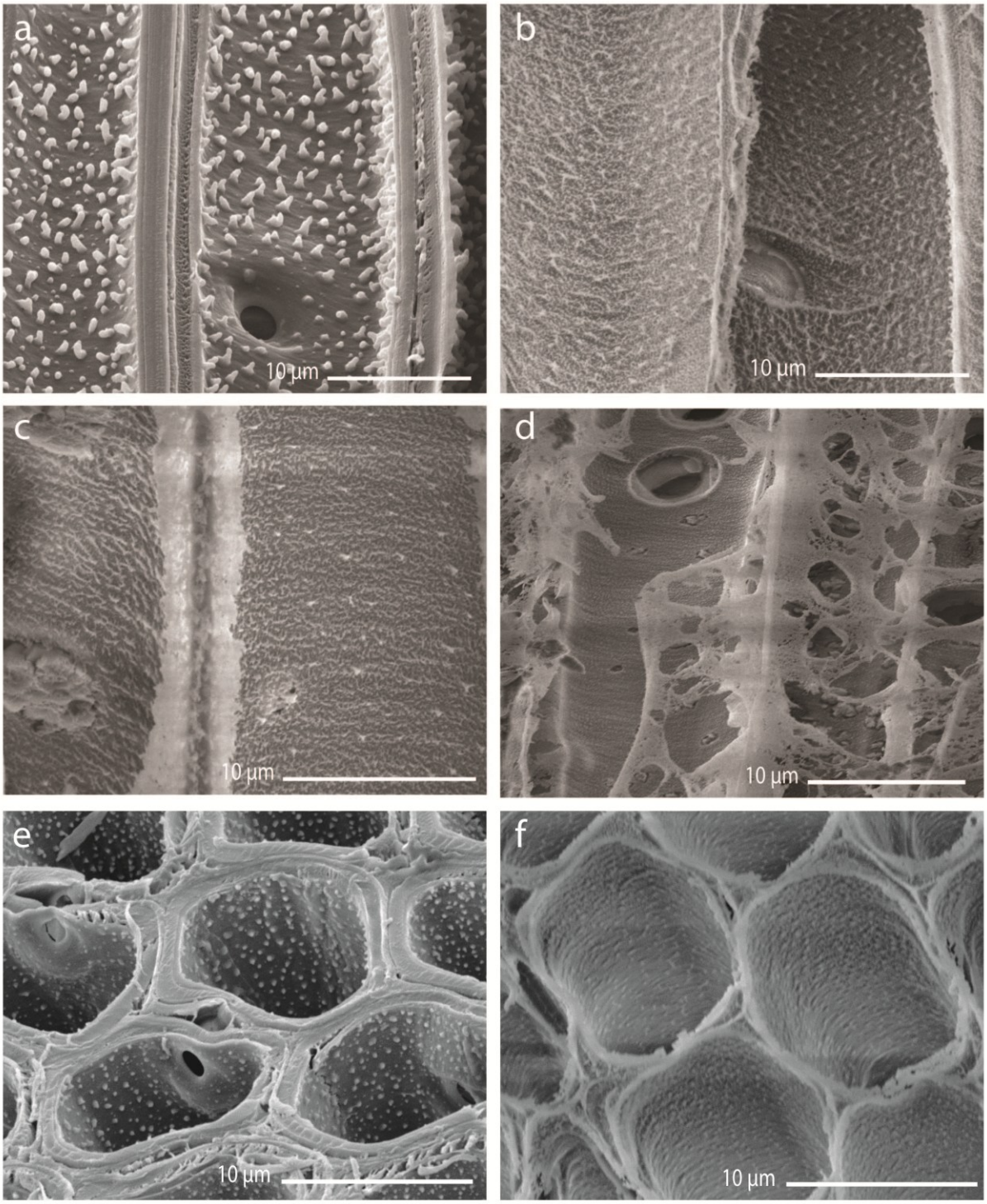

Figure 3.14: SEM photomicrographs of radial longitudinal and transverse surfaces of Actinostrobus: (a) untreated earlywood tracheids showing a bordered pit and large warts on the tertiary wall layer; (b) tracheids exposed to plasma for 333 s, note remnants of large warts on tracheid walls; (c) tracheids exposed to plasma for 667 s, note presence of warts on the "pulpy layer" on tracheids; (d) tracheids exposed to plasma for 1333 s, note heavily etched remnants of cell wall remaining at the wood surface; (e) untreated transverse surface showing warty layers covering cell walls and pit borders and (f) tracheids exposed to plasma for 1333 s showing thinning of cell walls on the surface and remnants of warts inside tracheids

3.3.2 Effect of plasma etching on the microstructure of pits

Etching of wood cell walls by plasma began with the etching and enlargement of pits. The etching of bordered and half-bordered pit-pairs in redwood (Fig. 3.15a and b) commenced with loss of their membranes, and this created voids in the cell wall that were the same size as the apertures of the pits (Fig. 3.15c). Subsequently, micro-roughening of cell walls and erosion of raised pit borders at the surface of specimens occurred (arrowed in Fig. 3.15c–d). The pit borders on the undersides of tracheids were then etched creating large voids in cell walls (Fig. 3.15e). These voids were often separated by collars of cell wall material at the outer margins of the pits that appeared to be more resistant to etching than the surrounding cell wall (Fig. 3.15e). The cell wall material separating bordered pits was also etched and removed (arrowed in Fig. 3.15f). Occasionally, etching of cell wall material separating bordered pits occurred faster than the etching of the pits themselves and in such cases only a thin web of cell wall material remained in which the bordered pits were suspended (Fig. 3.15g). Erosion of bordered pits and creation of voids in the cell walls of the softwood, radiata pine were also obvious when plasma treated sections were viewed under the light microscope (Fig. 3.16).

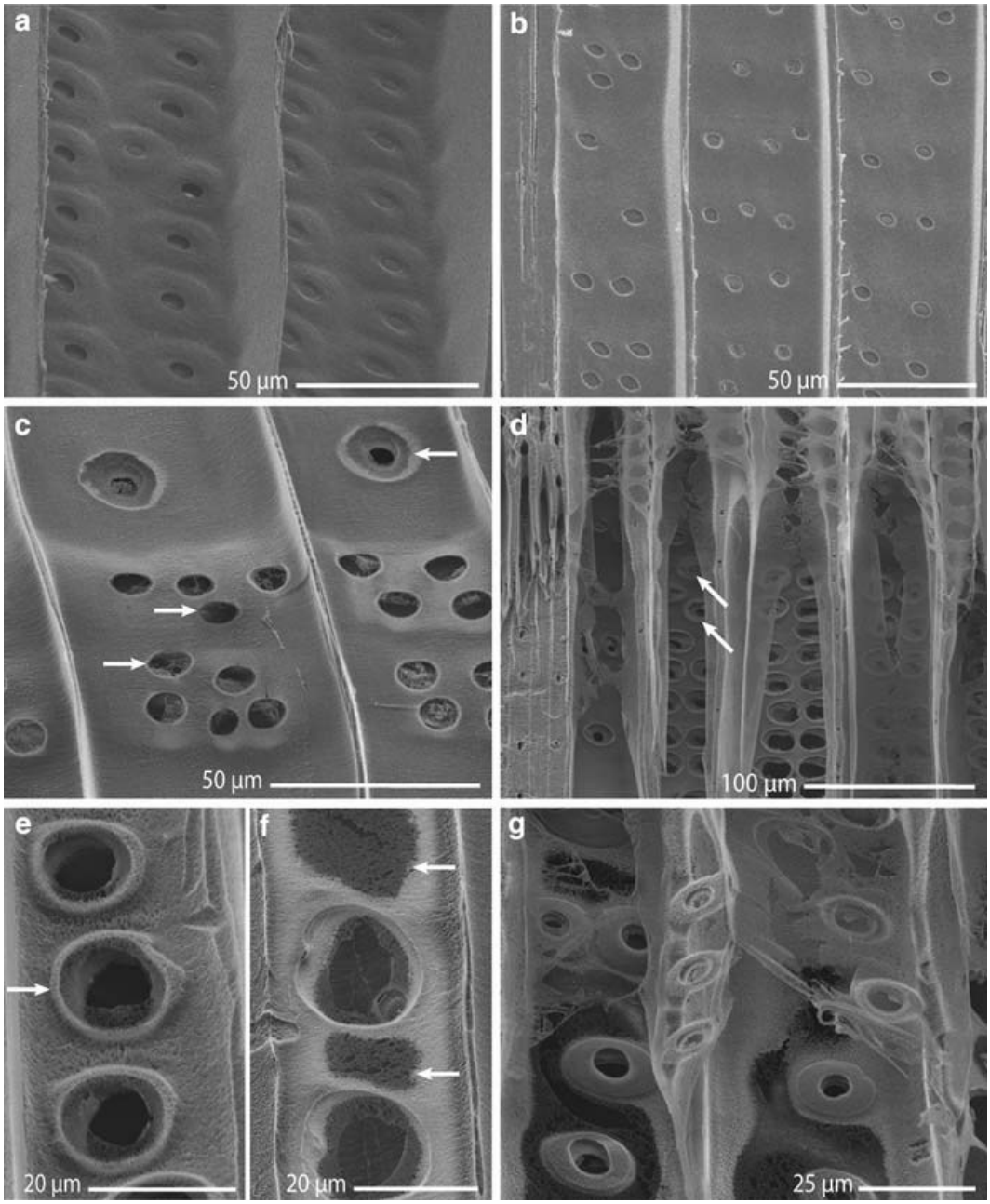

Figure 3.15: Radial longitudinal surfaces of redwood before and after plasma treatment: (a) untreated earlywood showing bordered pits in tracheids with bi- and triseriate arrangement of pits, note intact pit membranes; (b) untreated earlywood showing taxodioid cross-field pits, note intact pit membranes; (c) earlywood tracheids exposed to plasma for 667 s, note etching of half-bordered cross-field pit membranes (arrowed left of centre) and etching of the raised border of a bordered pit (arrowed top right); (d) earlywood and latewood (far left) exposed to plasma for 1333 s, note complete degradation of upper cell walls of earlywood tracheids and etching of bordered pits in sub-surface tracheids (arrowed centre); (e) latewood tracheid exposed to plasma for 1333 s showing etching of borders on both sides of bordered pits, note roughening of cell wall, and outer collars of bordered pits remaining at the surface (arrowed left); (f) latewood tracheid exposed to plasma for 1333 s showing etching of cell wall material separating bordered pits (arrowed right) and (g) earlywood tracheids exposed to plasma for 1333 s showing heavily etched tracheid walls, note that in this case the borders of pits resisted etching and are suspended at the surface by a thin web of cell wall material

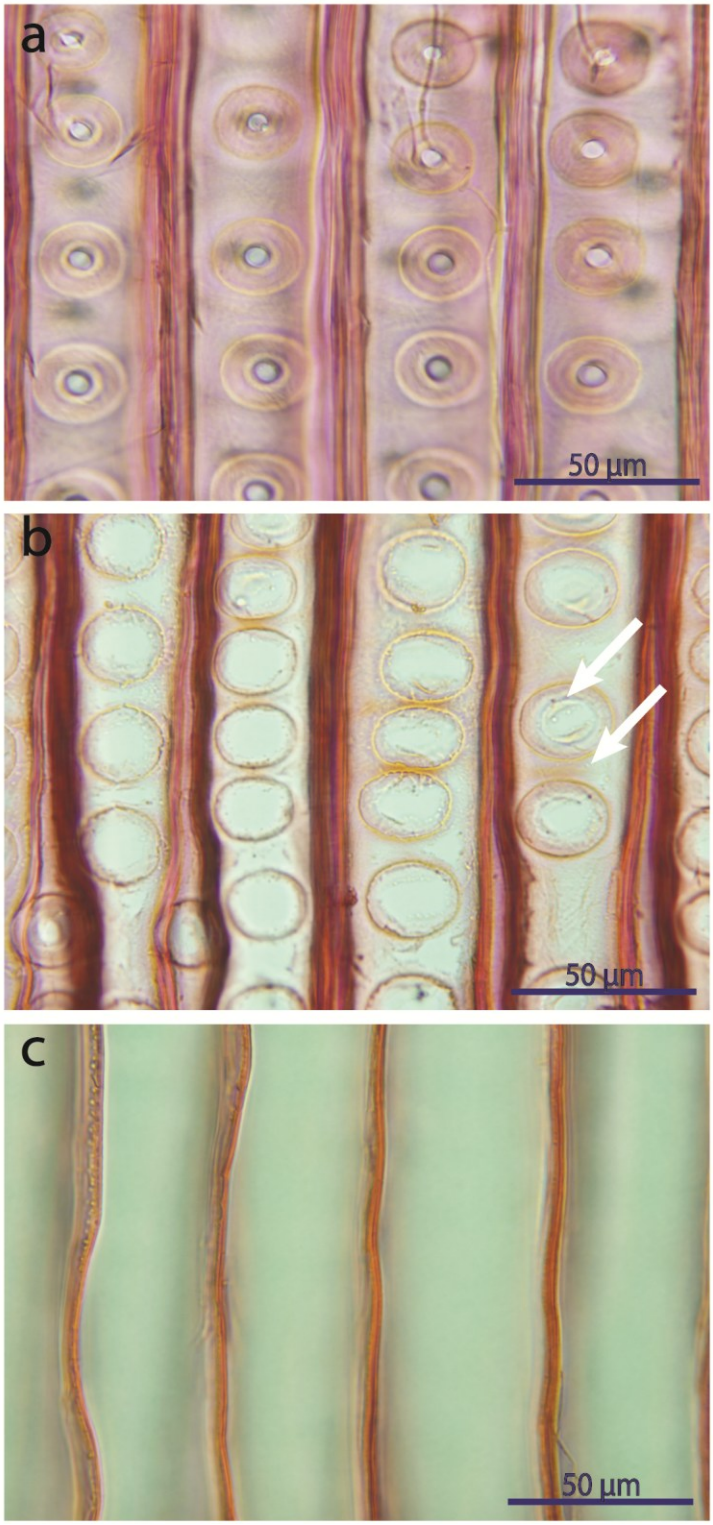

Figure 3.16: Light microscopy images of radial sections of radiata pine: (a) untreated section showing longitudinal tracheids containing bordered pits, note pit apertures and outer border; (b) section exposed to plasma for 667 s, showing complete or partial (arrowed) removal of bordered pits and intervening cell walls, (c) section exposed to plasma for 1333 s, showing complete removal of cell walls (in radial plane)

The latewood tracheids of redwood also contain small bordered pits that can be observed in tangential longitudinal sections. The apertures of these bordered pits and the cell wall material separating the pits were etched by plasma, but the outer border of the pits was more resistant to etching, in accord with observations of the etching of bordered pits in radial longitudinal sections (Fig. 3.17).

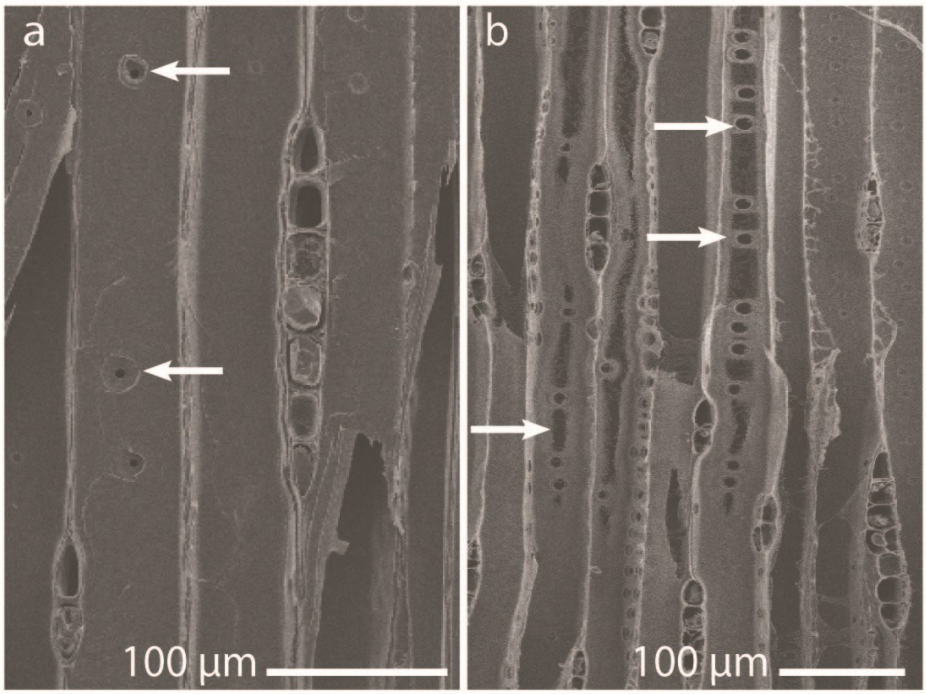

Figure 3.17: SEM photomicrographs of tangential longitudinal surfaces of redwood; (a) untreated earlywood showing a uniseriate ray (centre) and bordered pits in tangential walls (arrowed left of centre); and (b) earlywood and latewood exposed to plasma for 1333 s, note etching of cell walls (arrowed left of centre) and greater resistance of the outer borders of bordered pits to etching (arrowed right of centre)

Inter-vessel pits between adjacent vessels in hardwoods resemble softwood inter-tracheid bordered pits (Fengel 1966, Schmid and Machado 1968), but the pit membrane lacks a torus and margo. Inter-vessel pits in poplar were etched by plasma. Etching commenced with the erosion of pit borders and this created voids in the cell walls of plasma treated samples (Fig. 3.18b). Further etching of the alternating inter-vessel pits and their adjacent walls, which was observed in samples exposed to plasma for 1333s, created honeycomb-like structure at the surface of plasma treated wood. These structures were produced because the outer borders of the pits were more resistant to etching than the adjacent cell wall material in accord with observations of the etching of bordered pits in redwood (Fig. 3.18c). Figure 3.18b-c also shows that helical thickening in lumina of the vessel elements were resistant to etching.

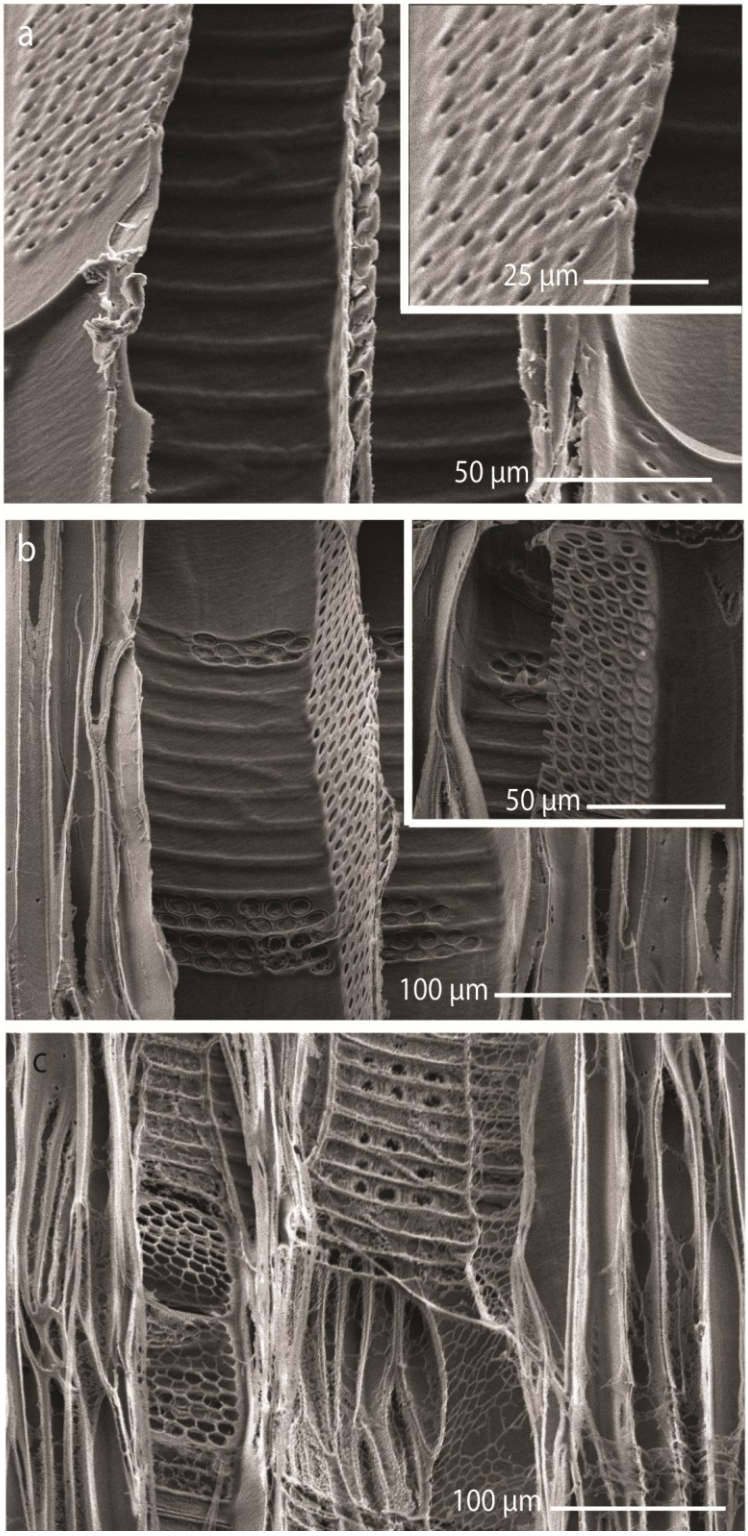

Figure 3.18: SEM photomicrographs of adjacent vessel elements in poplar; (a) untreated surfaces showing two vessels with the inter-vessel bordered pits and helical thickening on cell walls; split-screen image showing magnified image of pits and (b) surface exposed to plasma for 667 s; split-screen is a higher magnification image of etched inter-vessel bordered pits, and (c) surface exposed to plasma for 1333 s showing severe etching of the alternating inter-vessel pits and their adjacent walls; note the greater resistance of outer borders of the pits and helical thickening to etching

3.4 Discussion

In the introduction to this chapter, I hypothesized that plasma would modify the surface microstructure of wood and cause differential etching of wood cell walls. My results showed that plasma etches wood cell walls and the degree of etching appeared to be related to the length of time that samples were exposed to plasma. The finding that the middle lamella, which contains a high concentration of lignin, was more resistant to etching than the secondary wall supports my hypothesis that there would be differential etching of cell walls (Fergus et al. 1969). This observation tends to suggest that lignin is less susceptible to etching by plasma than cellulose, in accord with observations of the greater resistance of aromatic polymers to plasma etching compared to aliphatic polymers (Pederson 1982, Egitto et al. 1990). The increased resistance of lignin to plasma etching may also explain my observations of differential etching within individual S_2 layer of the cell wall layers. For example, prolonged exposure of redwood to plasma created voids in the secondary wall, which were separated by thin lamellae. This pattern of physical degradation resembles that created by acid hydrolysis of wood cell walls and also decay by fungi belonging to the Ascomycetes and Fungi Imperfecti, which degrade cellulose faster than lignin (Parham and Côté 1971, Worrall et al. 1997).

Cell wall layers of pit borders in redwood were generally etched more easily by plasma than surrounding wall layers. This observation may be related to the fact that they are thinner towards the pit aperture than the surrounding secondary cell walls, and may be etched on both sides by plasma. A similar explanation could account for the rapid etching of pit membranes. The very outer border of the bordered pits in redwood and radiata pine and inter-vessel pits in poplar, however, appeared to be more resistant to etching than the adjacent cell wall. The cell wall of softwoods in this region is locally thickened and contains crystalline cellulose microfibrils that

are oriented around the pit and packed closely together (Donaldson and Frankland 2004). Crystalline components of semi-crystalline polymers are more resistant to plasma etching than more amorphous components (Warner et al. 1975). Accordingly, it is possible that the increased resistance of outer borders of softwood pits to plasma etching can be accounted for by their increased thickness and high concentration of crystalline cellulose microfibrils. Alternatively, the increased resistance of the outer pit border to plasma etching may be due to its higher lignin content and the extension of the lignin-rich middle lamella into this region of the cell wall as suggested by histochemical studies of the structure of bordered pits in softwoods (Jutte and Spit 1963, Parham and Côté 1971). The higher lignin content of this part of the cell wall in bordered pits of radiata pine accounted for its higher resistant to degradation by soft rot fungi and erosion bacteria according to Singh (1997).

The higher resistance of warts on the cell walls of *A. arenarius* to plasma etching may also be related to their chemical composition. Baird et al. (1974) showed that warts are mostly composed of lignin-like material and suggested that the lignin in the warty layer is even more concentrated and condensed than the lignin in the rest of the cell wall. The warty layer and also the middle lamella are more resistant than the secondary cell wall layers to degradation by brown rot fungi (Liese 1965). Brown rot fungi preferentially degrade cellulose and hemicellulose and only modify lignin (Liese 1965, Liese 1970). This pattern of degradation of wood cell walls by brown rot and the pattern observed here further support my suggestion that lignin is less susceptible to degradation by plasma than other constituents of the cell wall.

My observations of the plasma etching of wood cell walls also show some similarities with the degradation of wood cell walls by gamma radiation (de Lhoneux et al. 1984; Tabirih et al. 1977). These studies showed that lignin-rich cell wall layers, including the warty layer, middle

lamellae and outer pit borders were more resistant to degradation by gamma radiation than other cell wall layers (de Lhoneux et al. 1984). Gamma irradiation also caused wood cell walls to become thinner, as was observed here (Tabirih et al. 1977).

My observations of etching of pit membranes, pit borders, tyloses and helical thickening also indicate that the anatomical structure of the cell wall influences the rate of plasma etching. Most of the thin cell wall features such as pit membranes, and tyloses were rapidly etched and removed from the uppermost surface of wood that was exposed to plasma. Tyloses are sac-like intrusions into the lumen of vessels or ray parenchyma. Tyloses' walls are composed of lignin, cellulose, and hemicelluloses, but unlike normal wood cell walls, their microfibrils are not organized, but randomly oriented (Foster 1967, Sachs et al. 1970). This aspect of the structure of tyloses and their large surface area may also have contributed to their rapid removal from vessels by plasma treatment, as opposed to the outer borders of pits or helical thickening that are composed of highly oriented and closely packed cellulose microfibrils and were more resistant to plasma etching (Timell 1978, Nair 1987).

Plasma etching finds practical applications in the semiconductor industry as mentioned in Chapter 2 (Boenig 1982, Sahoo et al. 2009). There are no related applications of plasma etching for wood processing, but the ability of plasma to etch pit membranes and borders suggests one possible application. Prolonged plasma treatment increases the penetration of phenol formaldehyde adhesive into high-density eucalypt species resulting in improved adhesive bond strength (Ramos 2001, Evans et al. 2007). Plasma etching treatments might have similar beneficial effects on coating penetration and performance in softwoods, in accord with observations of the effect of bacterial etching of bordered pit membranes on coating penetration (Singh et al. 1998). Hence, it is possible that plasma treatments might be employed to etch wood

surfaces prior to coating or gluing to improve the penetration and performance of coatings and adhesives, particularly in impermeable wood substrates. For practical reasons, it would be beneficial to quantify the etching rate of wood surfaces based on their chemical composition and plasma treatment parameters. This would allow plasma treatments to be optimized for different wood species to produce a tailored-surface for specific applications. Experiments in the next chapter will aim to quantify the etching of wood cell walls and their polymeric constituents.

3.5 Conclusions

Glow-discharge plasma was able to etch and completely remove cell walls at the surface of softwoods and hardwoods. Therefore, I conclude that all of wood's cell wall polymers can be degraded by plasma even though cell wall layers that are rich in lignin were etched more slowly than other parts of the cell wall. Plasma initially created voids in cell walls of softwood by etching pit membranes and then pit borders and intervening cell wall material. The creation of these large voids allowed etching of sub-surface layers to occur. Therefore, it is concluded that plasma can etch sub-surface cells if the plasma can penetrate wood's porous microstructure.

Plasma etching of wood cell walls resembles the physical degradation of wood caused by gamma radiation. Etching of wood cell walls was more pronounced if samples were exposed to plasma for longer periods of time. Therefore I conclude that etching of wood cell walls is strongly influenced by plasma energy applied to wood samples and to a lesser extent by the morphology and chemical composition of wood cell walls. However, further experiments described in the following chapters of this thesis, will shed greater light on the factors influencing the rate of etching of wood and chemical changes occurring at wood surfaces exposed to plasma.

4 Quantification of etching of wood and its polymeric components using confocal profilometry[4]

4.1 Introduction

When polymers are exposed to plasma their surfaces are etched and the polymers lose weight (Inagaki 1996). Etching of polymers has been investigated using scanning electron microscopy (Egitto et al. 1990, Kiihamäki and Franssila 1999). The same technique has been used to examine the etching of wood fibers and composites (Yuan et al. 2004, Vander Wielen et al. 2006). My observations of the etching of wood cell walls by plasma (Chapter 3) suggested that etching was affected by a number of different factors including plasma treatment time and chemical composition of cell wall layers. However, no attempt was made to quantify the influence of such factors on the etching of wood cell walls.

The etching of polymers by plasma has been quantified by measuring weight losses using sensitive gravimetric balances (Taylor and Wolf 1980, Egitto et al. 1990). However, weight losses occurring as a result of plasma treatment are difficult to measure because impurities and water from the atmosphere can affect sample weights (Taylor and Wolf 1980, Egitto et al. 1990). Weight loss measurements have also been used to assess the surface degradation of thin wood veneers exposed to the weather (Evans 1988), but care also has to be taken to ensure that veneer weights are not affected by absorption of moisture from the atmosphere. An alternative method that has been used to measure the degradation of wood exposed to weathering is to measure the erosion of exposed wood using optical microscopy (Black and Mraz 1974, Feist and Mraz 1978,

---

[4]Parts of this chapter have been published and the original publication is available at www.springerlink.com. Jamali, A. and Evans, P.D. Etching of wood surfaces by glow discharge plasma. Wood Science and Technology. Volume 45, Issue 1 (2011), pages 169-182.

Sell and Feist 1986, Arnold et al. 1991 Williams et al. 2001), or laser scanning profilometry (Arnold et al. 1992). More recently optical confocal profilometry has been used to quantify the erosion of wood exposed to weathering (Liu 2011). The same technique has been used to precisely measure the erosion of metals, ceramics and dental enamel with a resolution of 20 nm and an accuracy of ± 300 nm (Wilken et al. 2003, Theocharopoulos et al. 2010). Optical confocal profilometry operates as follows. White light passes through a lens with chromatic aberration and is split into different components (Fig. 4.1). Light with a wavelength (λ_m) is focused on a point at the surface of the material and reflected back. A detection device transforms the reflected light signal into an electrical signal that is then recorded by a computer. The central wavelength of this monochromatic light corresponds to the exact height of the measured point. By electromechanically regulating the object's surface in the x and y directions, the 3D topography of the scanned surface can be reconstructed with a resolution of 2 nm in the z (height) direction. The spatial resolution in the x–y direction is 0.5 µm (Li et al. 2006, ALTIMET 2007).

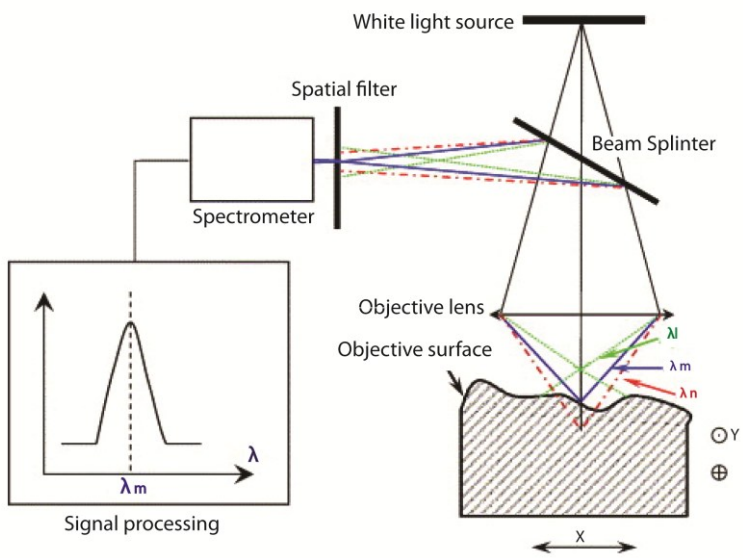

Figure 4.1: Principles of a chromatic confocal profilometer (www.altimet.fr)

Confocal profilometry can provide information on the surface topography of a material without the need for any special surface preparation. Thus a confocal profilometer can be used to map the topography of an area before and after treatment.

In this chapter, I use confocal profilometry to accurately quantify plasma etching of wood cell walls and further examine how the etching of wood is affected by treatment time (plasma energy) and wood's chemical composition. I expand observations made in Chapter 3 to include highly lignified compression wood and compressed pellets containing cellulose and/or lignin. The use of these materials allowed me to test the hypothesis suggested by my results in Chapter 3 that lignin is more resistant to plasma etching than cellulose.

4.2 Materials and methods

4.2.1 Experimental design and statistical analysis

Three experiments are described in this Chapter. The first examined the effect of wood species (poplar or yellow cedar), length of time samples were exposed to plasma and cell wall type (radial or tangential) on etching of wood cell walls. This experiment used the ability of confocal profilometry to accurately measure small changes in the surface topography of samples to quantify the erosion of wood cell walls exposed to plasma. A second experiment examined differences in the etching of wood cell walls in 'normal wood' and compression wood. The third and final experiment compared the etching of cellulose and lignin pellets, exposed to plasma for different periods of time.

For the first experiment a factorial split-split plot design was used to examine the effects of three fixed factors on the erosion of wood cell walls during plasma treatment: wood species (poplar or yellow cedar); (2) cell wall type (radial or tangential); and (3) treatment time (0 s [vacuum], 33 s, 333 s, 667 s, and 1333 s). Eight pieces of yellow cedar and poplar wood (four

from each species) provided replication at the higher level. Each piece was cut into two samples that were randomly allocated to 'cell wall type' (radial or tangential). Each of these samples then was cut into five specimens, which were randomly allocated to the different plasma treatment times or the control (vacuum). A total of 160 surface scans were performed (2 species [yellow cedar or poplar] x 2 surface types [radial longitudinal or tangential longitudinal] x 5 treatments x 4 specimens x 2 [pre- and post-plasma treatment scanning]). Analysis of variance was used to examine the effects of wood species, cell wall type, plasma treatment time and random factors on ratio of loss of cell wall volume to initial volume, and also mass loss of cell wall.

For the second experiment a randomized complete block design with one fixed factor was used to examine the effect of wood type (highly lignified compression wood or normal wood) on the erosion of cell walls by plasma. Twelve pieces of wood (experimental blocks) containing compression and normal wood were used to provide replication at the higher level. Two specimens (compression or normal wood, one of each type) were cut from each block and used for subsequent experimentation. A total of 48 surface scans were performed (12 blocks x 2 wood types [compression or normal wood] x 2 [pre- and post-plasma treatment scanning]). Analysis of variance was used to examine the effect of wood type (highly lignified compression wood v. normally lignified) on ratio of loss of cell wall volume to initial volume for plasma treated samples.

For the third experiment a completely randomized design was used to examine the effects of two fixed factors (pellet type [cellulose v. lignin] and treatment time) on the etching of pellets. Thirty pellets were made from cellulose and lignin (15 of each type) and randomly assigned to different treatment times. A total of 60 linear scans were performed on 30 pellets and the average depth of etching obtained from each of the 2-scans on each pellet was used as the response

variable (2 pellet types [cellulose or lignin] x 3 plasma treatments x 5 specimens). Analysis of variance was used to examine the effects of pellet type and treatment time on the etching of pellets.

All statistical computation was performed using the professional statistical program Genstat v. 12 (VSN International 2009). Before the final analysis, diagnostic checks were performed to determine whether data conformed to the underlying assumptions of analysis of variance, ie, normality with constant variance and, as result of such tests, data for volume of cell wall material etched by plasma in the second experiment (compression v. normal wood) were transformed into natural logarithms. Significant results ($p<0.05$) are presented in graphs, which contain error bars (+/- standard error of differences of means, derived from the analysis of variance) that can be used to compare differences between individual means. Appendix 2 contains all of the results of the statistical analysis of data for this Chapter, including the results of the diagnostic tests used to determine whether data conformed to the underlying assumptions of analysis of variance.

4.2.2 Wood samples

4.2.2.1 Normal wood

Pieces of yellow cedar and hybrid poplar wood with different dimensions, but free of macroscopic defects such as knots, were obtained from UBC's wood collection. These pieces were cut into samples measuring 10 (tangential) x 10 (radial) x 60 (longitudinal) mm^3 using a small band saw (as above, Chapter 3, part 3.2.1). Specimens measuring 10 x 10 x 3 mm^3 were cut from these wood samples. Clean undamaged radial and tangential longitudinal surfaces were prepared from these specimens as described in Chapter 3 (part 3.2.1).

4.2.2.2 Compression wood

Compression wood is formed on the lower side of leaning trunks or branches of gymnosperms (softwoods). Compression wood "was first described in 1860 by the German botanist Karl Gustav Sanio" (Timell 1980). Tracheids in compression wood are chemically and morphologically different from 'normal' wood cells. In transverse section, tracheids are rounded with intercellular spaces between cells, and the secondary wall consists of an S_1 and modified S_2 layer. This modified S_2 layer is thicker than the corresponding layer in normal earlywood cells and contains helical cavities (Timell 1986). The modified S_2 layer also has a high concentration of lignin, and its lignin contains a greater concentration of p-hydroxyphenylpropane units than lignin from normal wood (Côté et al. 1966, Morohoshi and Sakakibara 1971, Yasuda and Sakakibara 1975).

In this Chapter I compared the etching of compression wood with that of normal wood as mentioned above. A piece of yellow cedar wood measuring 60 (tangential) x 120 (radial) x 200 (longitudinal) mm^3 and containing both compression wood and normal wood was selected from a block of yellow cedar in the Centre for Advanced Wood Processing at UBC. This piece was cross-cut using a band saw to produce 12 cross-sectional slats , each 10 mm thick (Fig. 4.2). Small blocks measuring 10 x 10 x 10 mm^3 and containing compression wood or normal wood were cut from the slats. Thin sections were cut from the blocks using a microtome and observed under a light microscope to confirm the presence of compression wood. Then each block was clamped in a vice and viewed under a binocular microscope and smooth radial surfaces of these blocks were prepared as described in Chapter 3 (part 3.2.1). An area of earlywood was marked using a sharp razor blade. This area was scanned using confocal profilometry both before and after plasma treatment.

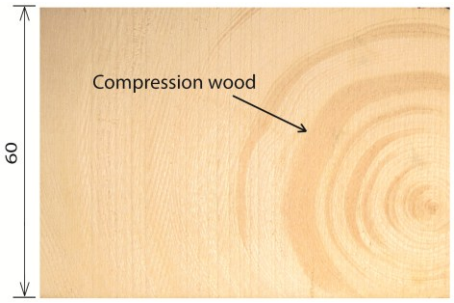

Figure 4.2: Cross section of a slat of yellow cedar containing normal wood and compression wood (darker color, arrowed) used to provide experimental specimens

Additional samples from normal and reaction wood were cut from the slats and ground using a Wiley mill to pass a 40-mesh screen. The lignin content (acid soluble and insoluble) of these samples was measured, as described in Chapter 5 (part 5.2.2).

4.2.3 Preparation of cellulose/lignin pellets

Pure, binder-free microgranular cellulose powder (Whatman CC 41 from Whatman Bio Systems Ltd., Maidstone, Kent, England), and powdered cellulolytic enzyme lignin (CEL) isolated from steam-pretreated lodgepole pine (Nakagame et al. 2010) were dried for 24 hours at 60°C and then allowed to cool at room temperature in a desiccator over silica granules. Dried and cooled cellulose or lignin powder (~ 200 mg) were placed in a hydraulic press (ICL, International Crystal Laboratories, USA) and pressed at 68.94 x 10^3 kPa (10000 psi) for 3 min. to produce a 12 mm diameter pellet. Dry cellulose (1) and lignin (1) were also mixed together using a bench mixer (Vortex, Fisher Scientific) to form a homogeneous blend and pressed into pellets. All pellets were kept in a desiccator over silica granules until they were needed.

To help measure the erosion rate of cellulose and lignin exposed to plasma, part of each pellet was masked. Small glass cover-slips (Matsunami Glass Ind. Ltd. Japan) measuring 18 x 18 mm^2 (0.25 mm thick) were used to mask half of each pellets' surfaces (Fig. 4.3). Each cover-slip

was plasma treated (333 s) to clean their surfaces and edges, and to minimize any effects that etching of their surfaces might have on the etching of cellulose and lignin pellets.

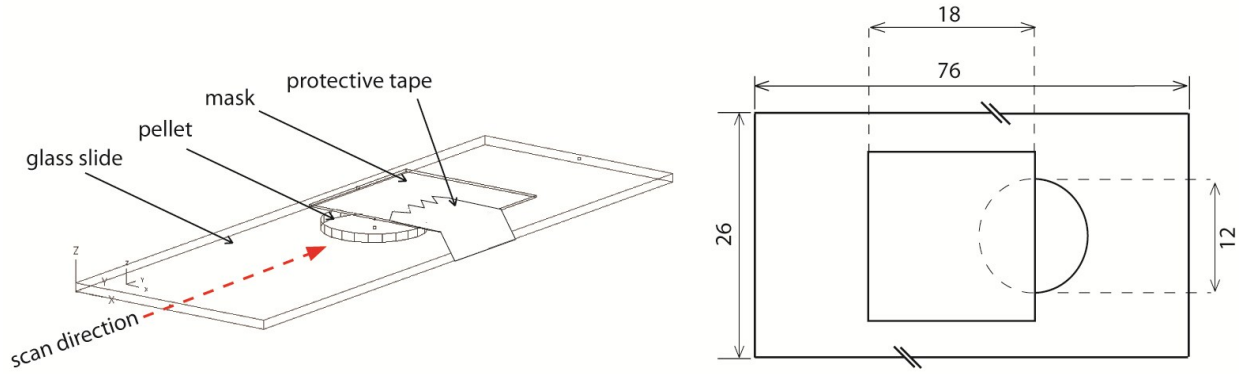

Figure 4.3: Method of masking surfaces of cellulose and lignin pellets prior to plasma treatment

The pellet and its mask were placed on a pre-cleaned glass microscope slide measuring 76 x 26 x 1 mm^3 (Matsunami Glass Ind. Ltd. Japan) and masking tape (18 mm (w), 3M all-purpose masking tape) was used to secure the cover slip to the pellet and the glass slide (Fig. 4.3).

4.2.4 Plasma treatments

Wood samples and cellulose and lignin pellets were plasma treated, as described in Chapter 3 (part 3.2.2). Yellow cedar and poplar wood samples were plasma treated from 33 s to 1333 s. Samples exposed to vacuum acted as controls. Cellulose/lignin pellets were exposed to plasma from 333 s to 1333 s. Compression and normal wood samples were plasma treated for 667 s.

4.2.5 Surface confocal profilometry and data acquisition

4.2.5.1 Profilometry of wood samples

A white-light non-contact confocal profilometer (Altisurf500 ®, ALTIMET, France) was used to measure the height of samples before and after plasma treatment.

Wood specimens were marked to delimit an area (0.5 x 0.5 mm^2) on surfaces of interest (radial or tangential) measuring by placing specimens under a low power binocular microscope and cutting small perpendicular grooves in the surfaces using a sharp razor blade. Marked specimens were placed on the x-y stage of the profilometer and the topography of the marked area was imaged at high resolution using the following measurement parameters: spacing between measurement points 0.5 x 0.5 µm; resolution=1001 x 1001; scan speed=100 µm/second and measurement range in the z-direction was from 10 nm to 300 µm. The software PaperMap (v. 3.2.0) was used to produce high-resolution topographic images of wood surfaces and cell walls before and after plasma treatment. Using the same software the volume of the cell wall was measured before plasma treatment using an average of all the available profile area (i.e. an interval of 0.5 µm) of the cell wall within a delimited length (50 µm) on the surface. The x and y coordinates of the analyzed cell wall within the marked area was recorded. Figure 4.4 shows a screen shot of the function used to obtain the profile of a cell wall. The marked area was re-scanned after plasma treatment and the position of the pre-measured cell wall was located using the recorded coordinates on the surface. The volume of the cell wall was measured as above and the loss volume due to treatment (plasma or vacuum) was calculated. The erosion of wood cell walls during plasma treatment was also expressed as the mass loss of wood. Mass losses were calculated based on the density of wood cell walls (1.53 g/cm^3) (Kellogg et al. 1969) and the calculated volume loss as follows: Mass loss = 1.53×10^{-6} ($\mu g/\mu m^3$) x removed volume (μm^3).

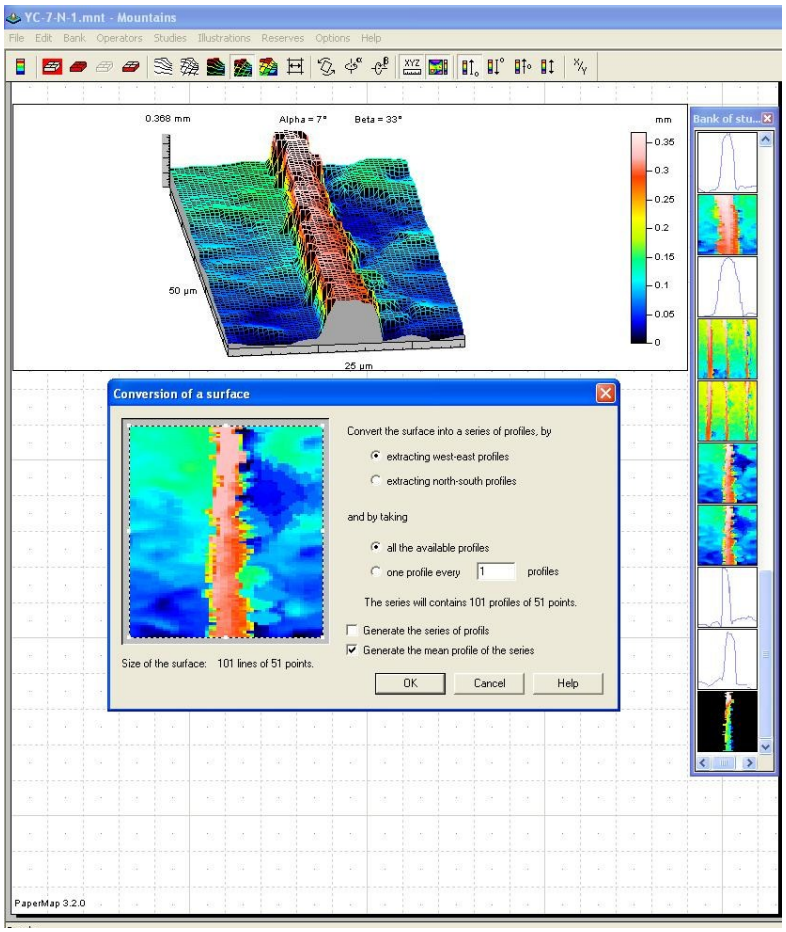

Figure 4.4: Screen shot of the function within PaperMap software used to extract profiles of cell walls along the delimited length (50 µm). Images show a tangential cell wall and its cross-sectional profiles (right)

4.2.5.2 Profilometry of cellulose and lignin pellets

The surfaces of the cellulose/lignin pellets were scanned before and after plasma treatment using confocal profilometry using the same parameters described above. The software Papermap was used to produce topographical images and calculate the following roughness parameters of the pellets surface before and after plasma treatment (ALTIMET 2007):

S_a = arithmetic mean of the deviations from the mean

S_q = quadratic mean of the deviations from the mean (computes the efficient value for the amplitudes of the surface)

S_t = total height of the surface (distance between the highest peak and the deepest hole)

Pure cellulose or lignin pellets that had been plasma treated for different periods of times were scanned to obtain linear profiles across the masked and unmasked areas. Two scans, 1 mm apart, were made across the center of each pellet. The length of each scan was 4 mm, with half of this length on the border of the masked area. The spacing between measurement points was 0.5 μm. Each linear profile was carefully examined using the PaperMap software to define the border between the masked and unmasked areas. All data points in each profile were exported to Excel 2007 (Microsoft Corporation 2006). The average height for the masked and unmasked areas of each profile was calculated and the depth of etching was measured by subtracting the height of the unmasked part of each sample from that of the masked part. The average depth of etching was calculated from the two scans performed on each sample.

A dark signal acquisition or calibration was performed on the profilometer at regular intervals during the experiments. This calibration recorded the value of the intrinsic noise in the optical sensor and subtracted it from the sensor's measurements. The origin of the axes on the sliding stage was also calibrated regularly to obtain a precise origin for each axis (x, y and z).

4.2.6 Light and scanning electron microscopy

Scanning electron microscopy and light microscopy were used to examine the surface of wood and cellulose and lignin pellets exposed to plasma and supplement observations from surface confocal profilometry.

Wood and cellulose and lignin pellets (plasma treated and untreated controls) were coated with 5 nm of gold using a sputter coater (Nanotech SEMPrep II) and viewed using a Cambridge Instrument S360 scanning electron microscope operating at an accelerating voltage of 5kV.

Reflected light microscopy was also used to image the surface of plasma treated pellets (cellulose and lignin). Digital photographs of the surfaces of interest were taken at magnifications of

x4 to x40 using a high resolution digital camera attached to a Carl Zeiss microscope and saved as bitmap files (as above). Cellulose is white and lignin is a tan/brown color. Therefore light microscope images could be used to locate the area of the pellets that contained cellulose or lignin and compare etching of plasma treated cellulose and lignin in the masked and unmasked areas of the pellets.

4.3 Results

4.3.1 Use of white light confocal profilometry to image the surface structure of wood

White light profilometry was able to image the microscopic structure of wood surfaces and detect changes in microstructure due to plasma treatments. Changes at wood surfaces were followed by mapping the wood's microstructure and surface topography before and after plasma treatments (Fig. 4.5), as mentioned above. Topographical maps depict surface height in 2-D using colors that correspond to different heights. Changes at the surface as a result of plasma treatment can be followed by comparing the colors on the two images with reference to the associated color scale (Fig. 4.5).

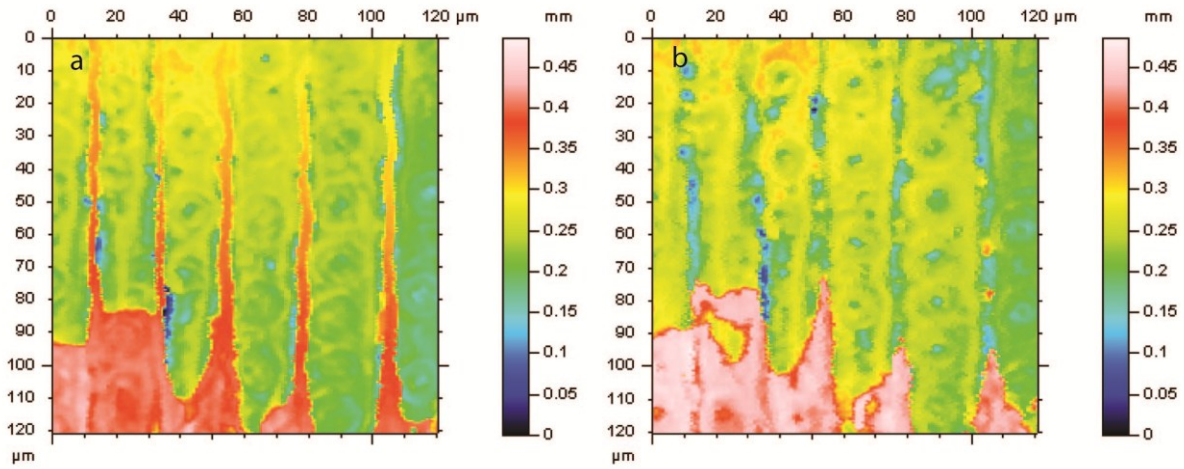

Figure 4.5: 2-D chromatic confocal profilometry maps of yellow cedar surfaces (RLS) with full-spectral color progression bars: (a) Untreated surface showing six longitudinal tracheids with their protruding tangential cell walls, note the presence of bordered pits with a uniseriate arrangement; (b) the same surface exposed to plasma for 667 s, note removal of tangential cell walls and etching of bordered pits on radial cell walls

The three-dimensional (3D) images of plasma treated and untreated surfaces provide both visual and numerical information on the surface etching of wood (Fig. 4.6).

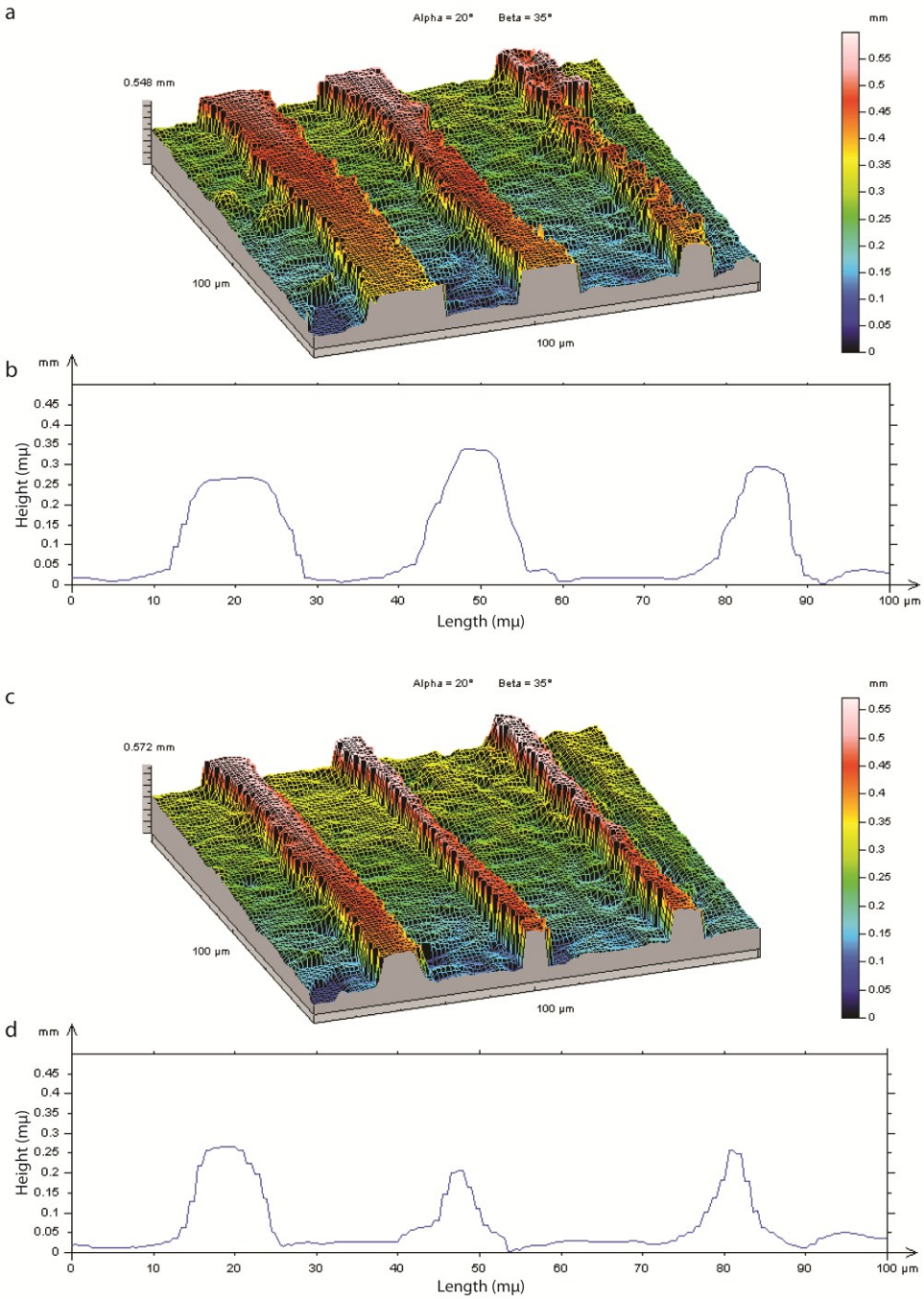

Figure 4.6: 3-D topographical images of radial longitudinal surfaces of yellow cedar and their corresponding transverse 2-D profiles: (a) 3D image of untreated specimen showing two adjacent longitudinal tracheids in the centre, note the thickness of raised tangential cell walls and the outlines of biseriate bordered pits in between these cell walls; (b) 2D profile of image 4.6a drawn across the longitudinal tracheids and showing the height and thickness of cell walls at the traverse points; (c) 3D image showing the same area as image 4.6a, after exposure to plasma for 333 s, note the height and thickness of cell walls; and (d) corresponding 2D profile of image 4.6c

Figure 4.6 shows topographic images of cell walls in a radial longitudinal surface of yellow cedar before and after 333 s of plasma treatment. This figure also shows the 2-D line profiles of these images (drawn across the centre of the images). Plasma treatment caused cell walls to become thinner, and reduced their height (Fig. 4.6).

Confocal profilometry confirmed some aspects of the etching of wood surfaces that were observed using scanning electron microscopy in Chapter 3. The outer borders of the bordered pits were less affected by plasma (Fig. 4.7a-c), than the pit dome as observed previously. Furthermore the middle lamella appeared to be more resistance to etching than the secondary wall (Fig. 4.8)

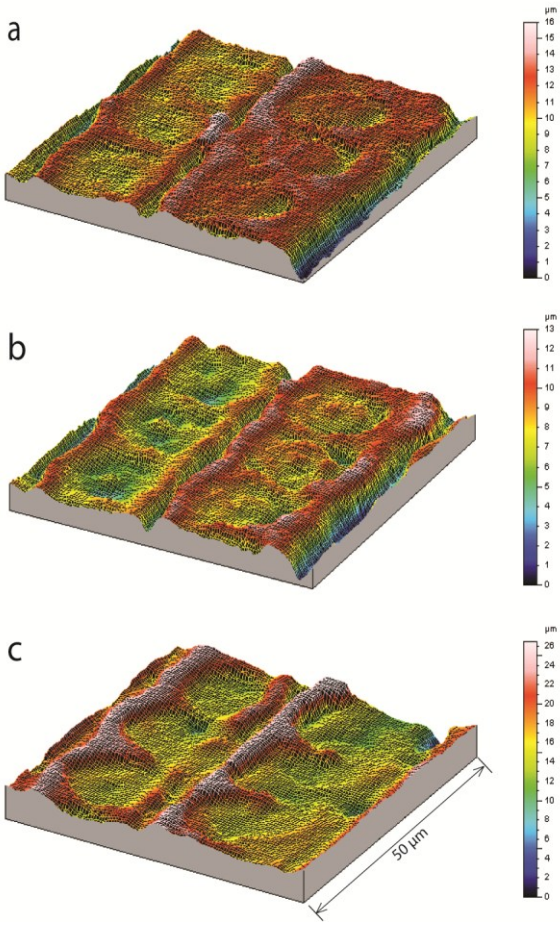

Figure 4.7: Topographical images of bordered pits at radial longitudinal surface of yellow cedar: (a) untreated earlywood tracheids with a uniseriate arrangements of bordered pits, note presence of pit domes; (b) same earlywood tracheids shown in Fig. 4.7a after exposure to plasma for 333 s showing a rougher surface with partial erosion of pits; and (c) the same earlywood tracheids shown in Fig. 4.7 a-b after exposure to plasma for 667 s showing etching of bordered pits, note the absence of pit domes and greater resistance of the outer collar of the bordered pits to etching

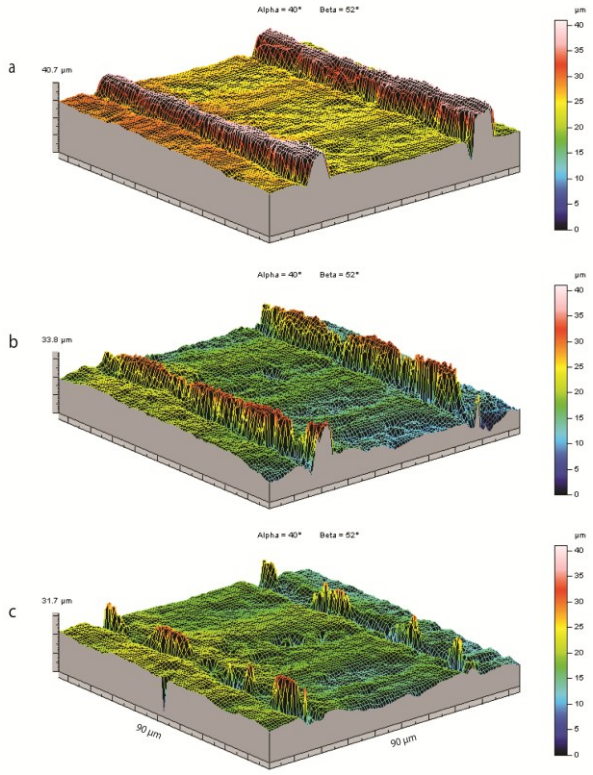

Figure 4.8: Topographical images of cell walls on a radial longitudinal surface of yellow cedar before and after plasma treatment: (a) untreated earlywood tracheid showing tangential cell walls and bordered pits; (b) the same earlywood tracheid shown in Fig. 4.8a after exposure to plasma for 333 s, note thinning of cell walls and decreases in height of tangential cell walls in places and (c) the same earlywood tracheid shown in Fig. 4.8a–b after exposure to plasma for 667 s, note pronounced thinning and decreases in height of tangential cell walls and etching of bordered pits and the residual of middle lamella in between tracheids

Figure 4.8 shows three dimensional topographic maps of a radial longitudinal surface before and after plasma treatment. Figure 4.8a shows the cell walls of a tracheid before plasma treatment. In between these cell walls, the outlines of bordered pits with a biseriate arrangment can be seen. Figure 4.8b and 4.8c show the same area of the cell wall after plasma treatment for 333, 667 seconds, respectively. Plasma treatment caused cell walls to become thinner towards the middle of the cell walls, and cell walls also decreased in height. Cell walls and bordered pits were heavily etched in tracheids subjected to plasma treatment for 667 s (Fig. 4.8c), although the middle lamella of cell walls showed greater resistance to etching.

4.3.2 Quantification of plasma etching of radial and tangential cell walls of yellow cedar and poplar

Table 4.1 summarizes the results of the analysis of variance of the effects of wood species, cell wall type, and plasma treatment time on the volume and mass losses of cell walls after plasma treatment.

Table 4.1: Summary of the statistical significance of species type, cell wall type and plasma treatment time on ratio of cell wall removed during plasma to their initial volume and mass losses of the cell walls

Experimental factor	P-values associated with the two response variables	
	Ratio of cell wall removed to the initial cell wall volume	Mass loss
Species (S)	0.721	0.989
Cell wall (C)	0.159	0.419
Treatment (T)	<0.001	<0.001
S x C	0.050	0.265
S x T	0.123	0.320
C x T	0.569	0.660
S x C x T	0.638	0.848

Plasma treatment reduced the volume of cell walls and analysis of variance revealed a very highly significant ($p<0.001$) effect of treatment time on the ratio of volume of cell wall removed during plasma treatment to that present before treatment. There was also a highly significant ($p<0.001$) effect of treatment time on mass losses of cell wall material. However, volume and weight losses of cell walls resulting from 33 seconds exposure to plasma (33 s) were not significantly different ($p>0.05$) from those of the control (only exposed to vacuum). The effect of treatment time on losses of volume and mass of cell wall material from specimens exposed to plasma are shown in Figs. 4.9, and 4.10, respectively.

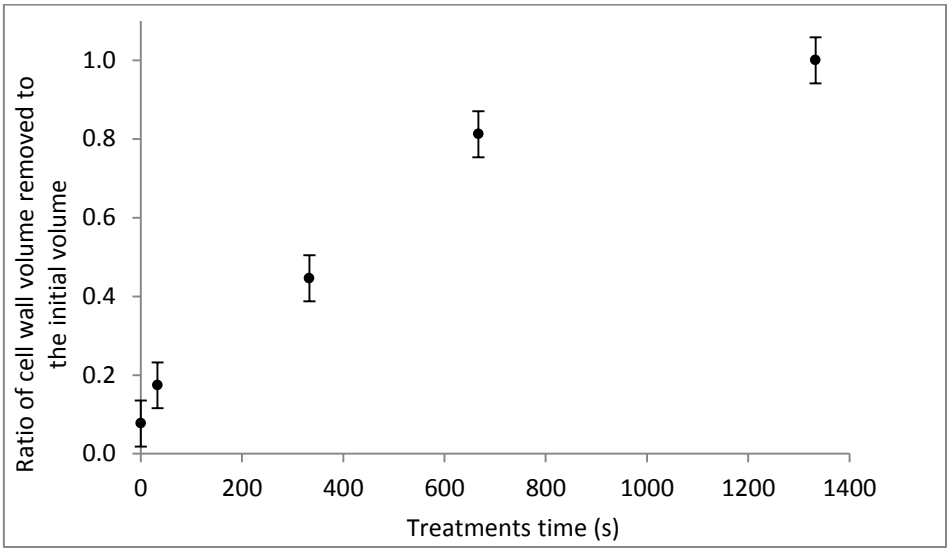

Figure 4.9: Effect of treatment time on the ratio of cell wall material removed by plasma to their initial volume in yellow cedar and poplar specimens (results are averaged across species and cell walls [radial and tangential]). Error bars are ± standard error of differences of means (from analysis of variance). Non-overlap of these bars indicates that means are significantly different at 5% level (p<0.05)

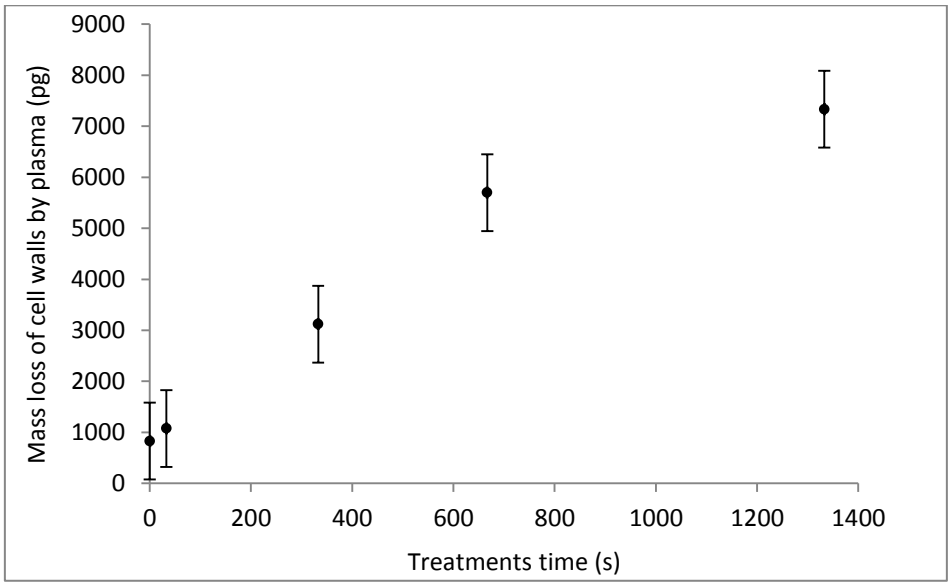

Figure 4.10: Effect of treatment time on the mass losses of yellow cedar and poplar cell walls exposed to plasma (results are averaged across species and cell walls [radial and tangential]). Error bars are ± standard error of differences of means (from analysis of variance). Non-overlap of these bars indicates that means are significantly different at 5% level (p<0.05)

The effect of species type (yellow cedar v. poplar) or wall type (radial v. tangential) on volume and mass losses of cell wall material from specimens exposed to plasma were not statistically significant (p>0.05) (Table 4.1). However, there was a significant effect (p = 0.05) of species and cell wall type on losses of volume of cell walls in specimens exposed to plasma (Table 4.1). This interaction occurred because etching of tangential cell walls (in RLS) was greater than that in radial cell walls (in TLS) in poplar, whereas in yellow cedar the difference between the etching of cell wall types was not significant, although radial cell walls were etched more than tangential cell walls (Fig. 4.11).

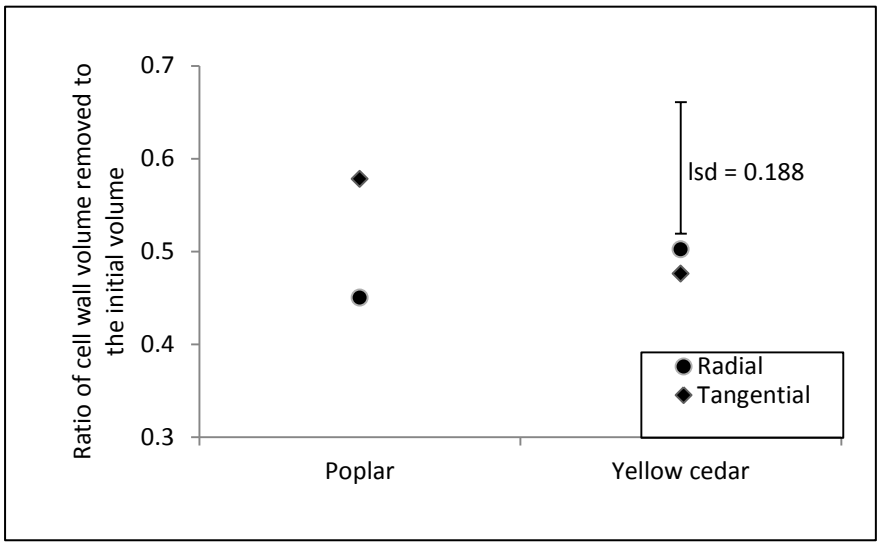

Figure 4.11: Effect of wood species and cell wall type on losses of volume of cell walls in specimens exposed to plasma (results are averaged across treatment time). Least significant difference (lsd) bar is based on 95% confidence intervals (from analysis of variance) to estimate the significance of differences between individual means

4.3.3 Etching of compression wood

The lignin content of compression wood (40.1 %) was significantly higher than that of 'normal wood' (32.8 %), as expected.

3D surface mapping (as above) was used to quantify the etching of cell walls in normal wood and compression wood of yellow cedar. Analysis of variance indicated a very significant

effect ($p < 0.001$) of wood type (compression v. normal wood) on the ratio of cell wall removed during plasma treatment to the initial cell wall volume. The volume of cell wall removed from the surface of compression wood was significantly ($p<0.05$) smaller than that removed from normal wood. Figure 4.12 shows the ratio of cell wall volume removed to the initial volume for normal wood and compression wood exposed to plasma for 667 s.

Scanning electron microscopy shows the etching of compression and normal wood. Helical cavities and ribs were distinctive features of the cell wall of compression wood as others have observed (Timell 1986). The cell walls of normal wood became thinner as a result of plasma treatment and the apertures of bordered pits became larger (Fig. 4.13a-b). The cell walls of compression wood also became thinner as a result of plasma treatment (Fig. 4.13c-d), but thinning of cell walls was less pronounced than that of normal wood. The helical cavities in compression wood were bigger after plasma treatment and the ribs in the S_2L layer sometimes detached from the underlying cell wall (Fig. 4.13d).

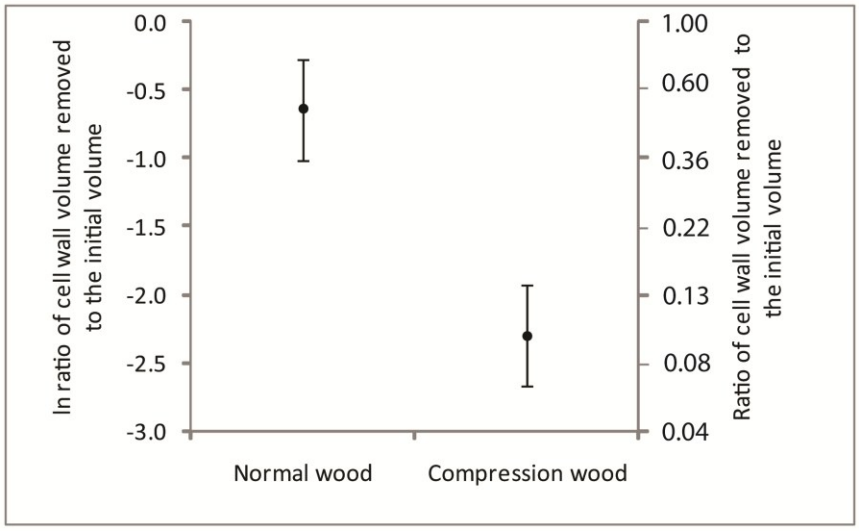

Figure 4.12: Effect of wood type (normal v. compression wood) of yellow cedar specimens on the ratio of cell wall volume removed to the initial volume as a result of plasma treatment for 667 s. Note the left Y axis represents the transformed data expressed on a logarithmic scale. The right (Y_2) axis expresses data in the natural scale. Error bars are ± standard error of differences of means (from analysis of variance). Non-overlap of these bars indicates that means are significantly different at 5% level ($p<0.05$)

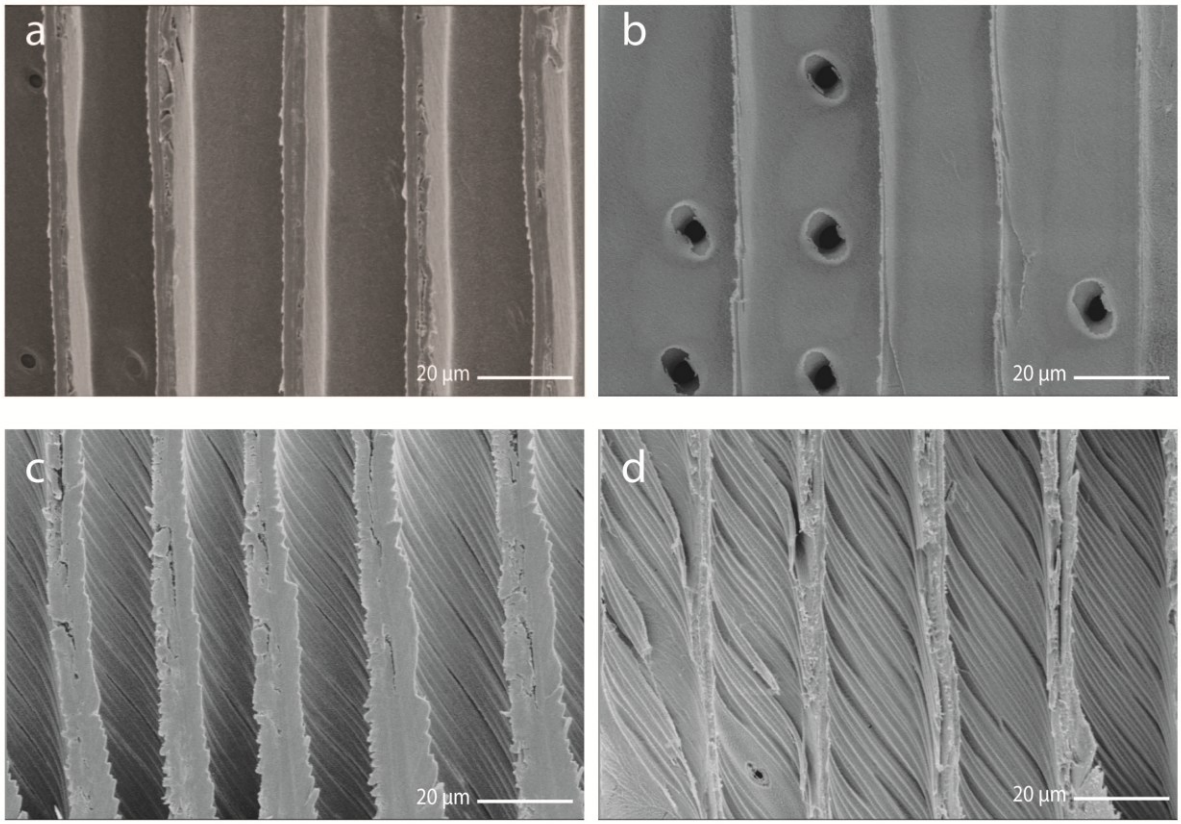

Figure 4.13: SEM photomicrographs of radial longitudinal surfaces of earlywood in normal and compression wood of yellow cedar: (a) normal untreated tracheids showing standing tangential cell walls; (b) earlywood tracheids exposed to plasma for 667 s, note thinning of tangential cell walls and enlargement of bordered pit apertures; (c) untreated earlywood tracheids in compression wood, note the helical cavities and ribs in S_2L; (d) compression wood tracheids exposed to plasma for 667 s, note widening of the cavities and separation of some of the ribs from the underlying cell wall layers

SEM observations of transverse surfaces of compression wood confirmed that thinning of wood cell walls occurred as a result of plasma treatment. They also revealed that the middle lamella is more resistant to etching by plasma, as was also observed for normal wood (Fig. 4.14). Etching of the highly lignified S_2L layer appears to be less than that of secondary wall in normal wood, but the S_2L layer in compression wood was often detached from the adjacent wall layers in plasma treated samples (Fig. 4.14b).

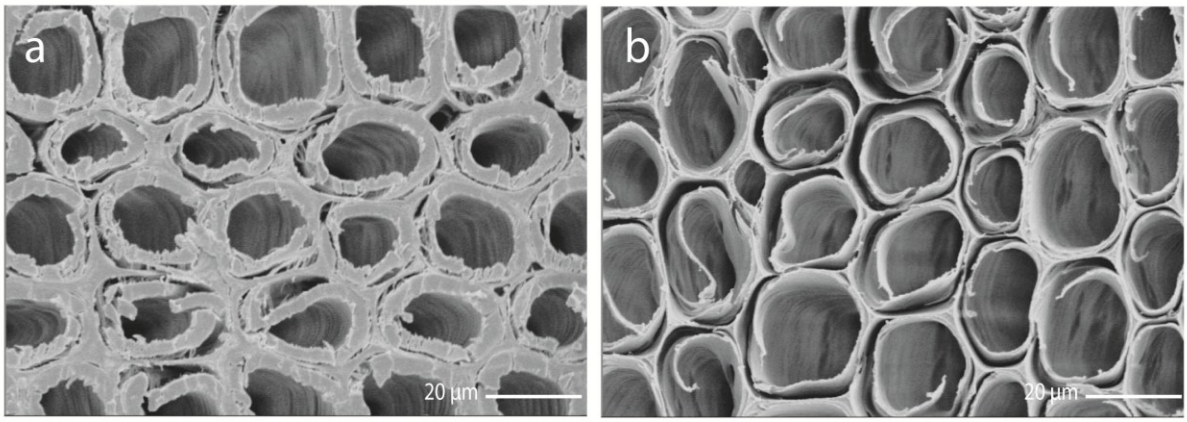

Figure 4.14: SEM photomicrographs of transverse surfaces of compression wood tracheids in the earlywood of yellow cedar: (a) untreated surface; and (b) surface exposed to plasma for 667s

4.3.4 Etching of cellulose and lignin pellets

Plasma treatment made the surface of cellulose/lignin pellets rougher. Figure 4.15 shows small islands within the pellets that were less eroded than the surrounding material.

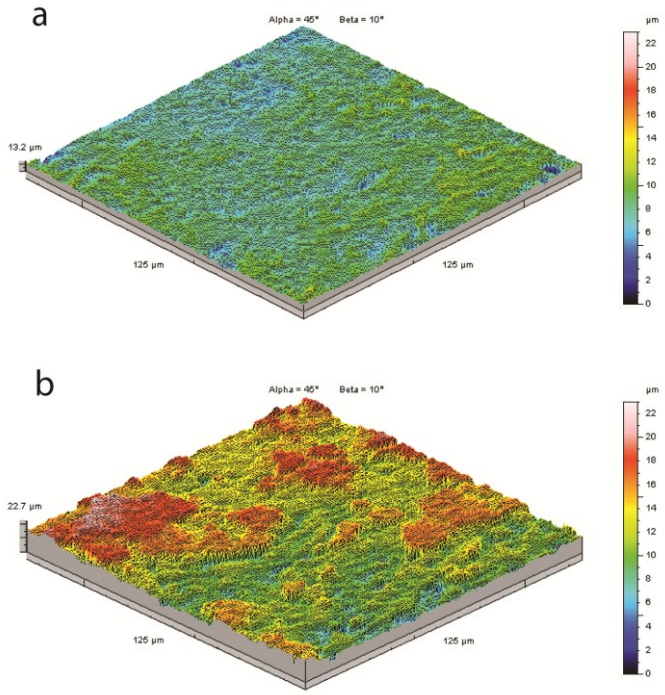

Figure 4.15: Topographical images of the surface of cellulose-lignin pellets: (a) untreated surface and (b) pellet surface exposed to plasma for 1333 s

Table 4.2 shows the surface roughness parameters for the lignin/cellulose pellets before and after plasma treatment. Comparison of roughness parameters (S_a [arithmetic mean of the deviations from the mean], S_q [quadratic mean of the deviations from the mean] and S_t [total height of the surface]) of plasma treated and untreated pellets indicates that the surface of pellets became rougher as a result of plasma treatment.

Table 4.2: Roughness parameters (S_a, S_q and S_t) of lignin/cellulose pellet surface before and after exposure to plasma for 667 s

Roughness parameters	Treatment	
	Untreated	Plasma treated
S_a	0.819	2.54
S_q	1.08	3.02
St	13.20	22.70

Scanning electron microscopy confirmed that plasma treatment made the surface of pellets rougher (Fig. 4.16a-c), and light microscopy revealed that increased roughness of the surface of plasma-treated pellets was due to greater etching of cellulose (white) compared to lignin (brown) (Fig. 4.16d).

Because cellulose and lignin in pellets could be differentiated by their color it was possible to match 2D light microscopy images with 3D topographical maps obtained using surface profilometry (Fig. 4.17). Comparison of these images provides strong evidence that lignin is less susceptible to etching than cellulose and reveals that increases in roughness of the surface of pellets as a result of plasma treatment were due to differential etching of cellulose and lignin (Fig. 4.17).

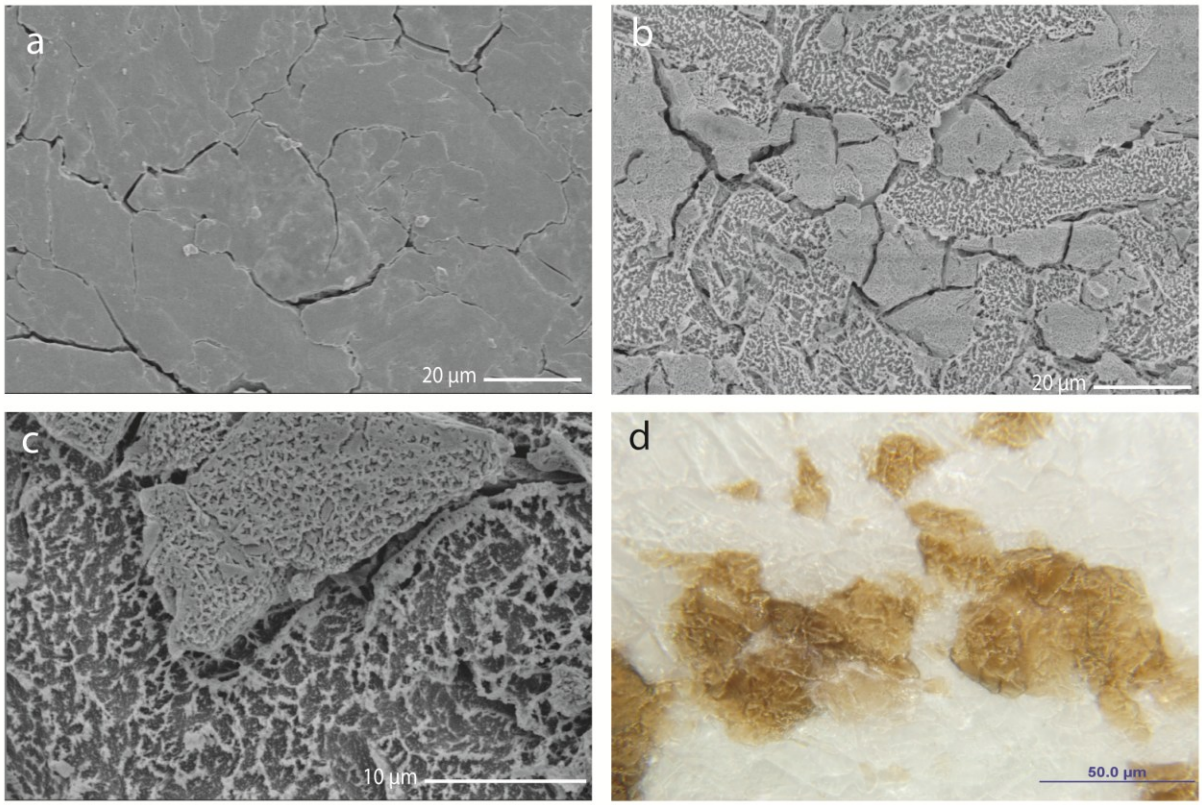

Figure 4.16: SEM and light microscopy images of the surface of cellulose-lignin pellets: (a) untreated surface showing a flat surface with some micro-cracks; (b) surface exposed to plasma for 1333 s showing a micro-roughened surface and differential erosion of the surface; (c) higher magnification image of surface treated for 1333 s; and (d) reflected light microscopy image of the surface of a pellet exposed to plasma for 1333 s, showing a distinct color difference between cellulose and lignin

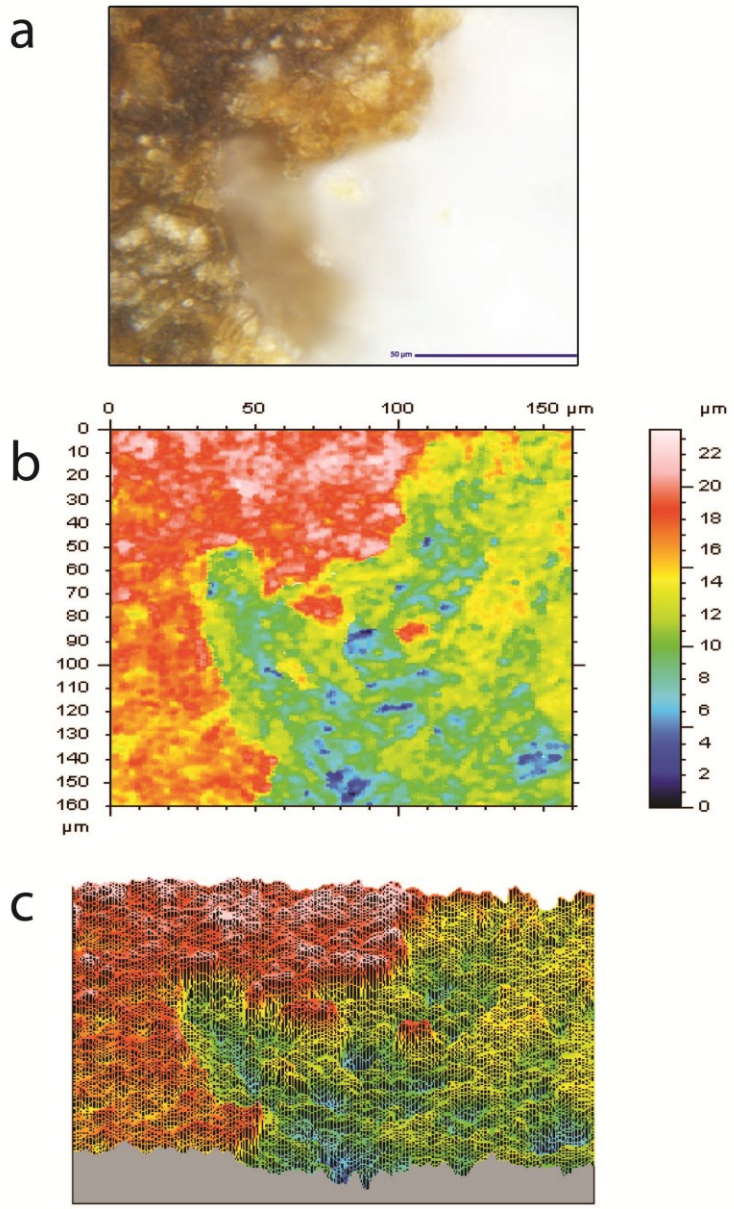

Figure 4.17: Light microscopy images and two and three dimensional images of the surface of cellulose-lignin pellets: (a) reflected light microscopy image showing golden brown (left hand side) and white colored areas (right hand side) indicating the presence of lignin and cellulose, respectively; (b) 2D confocal profilometry map of the same area shown in Fig. 4.17a; and (c) 3D topographical image of the same area in Fig. 4.17a-b showing greater erosion on the right hand side of the image (cellulose) compared to the erosion of lignin on the left hand side

The etching of cellulose and lignin were quantified using surface profilometry of separate cellulose and lignin pellets. Linear profiles across the masked and unmasked areas of the plasma treated cellulose and lignin pellets, both showed a step at the boundary between the masked and unmasked area, as expected. Such a step is shown in Figure 4.18. This figure shows a profile across masked and unmasked areas in a cellulose pellet exposed to plasma for 1333 s.

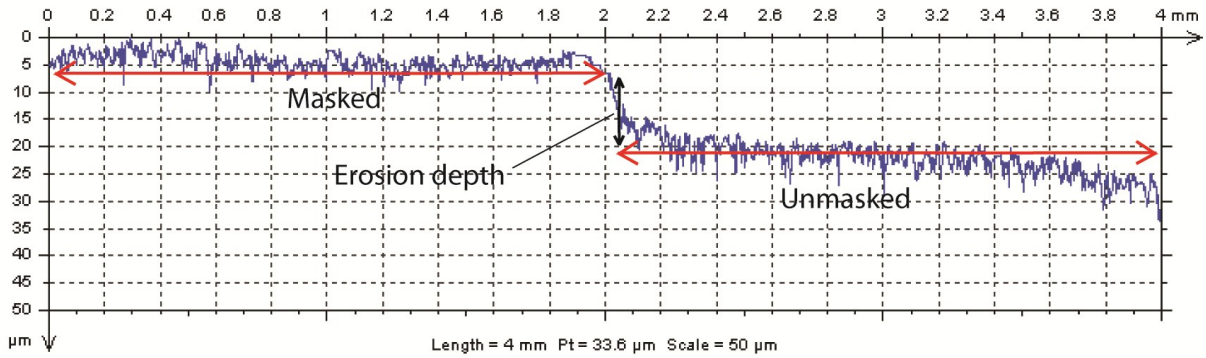

Figure 4.18: Profile obtained from a linear scan across masked and unmasked areas in a cellulose pellet exposed to plasma for 1333 s

Analysis of variance of step-height data revealed a very highly significant effect ($p<0.001$) of pellet type (cellulose and lignin) and plasma treatment time ($p<0.001$) on the depth of etching of pellets. The depth of etching was significantly greater for cellulose pellets compared to lignin pellets (Fig. 4.19). The depth of etching of both cellulose and lignin pellets was positively correlated with the length of time pellets were exposed to plasma (Fig. 4.20). However, there was no significant ($p>0.05$) interaction of pellet type and treatment time on depth of etching of pellets.

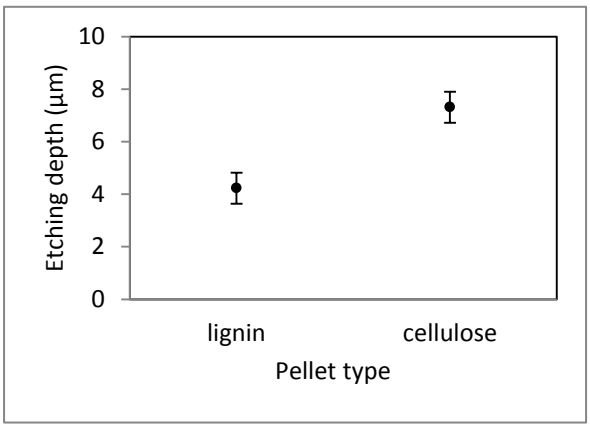

Figure 4.19: Effect of pellet type (cellulose v. lignin) on the depth of etching of pellets exposed to plasma (results are averaged across plasma treatment times). Error bars are ± standard error of differences of means (from analysis of variance). Non-overlap of these bars indicates that means are significantly different at 5% level (p<0.05)

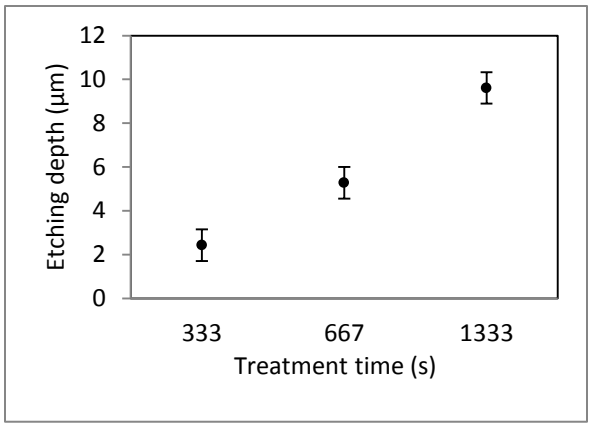

Figure 4.20: Effect of plasma treatment time on the depth of etching of pellets exposed to plasma (results are averaged across pellet type). Error bars are ± standard error of differences of means (from analysis of variance). Non-overlap of these bars indicates that means are significantly different at 5% level (p<0.05)

There were differences in the structure and color of cellulose and lignin in the masked and unmasked areas after pellets were exposed to plasma. The surface of unmasked areas in cellulose pellets became rougher and darker (Fig. 4.21a and 4.21b). The surface of unmasked areas in lignin pellets exposed to plasma developed cracks that gave the exposed area of the pellets the appearance of dry 'cracked' mud. Lignin exposed to plasma was also darker than unexposed lignin that had been protected by the glass mask and masking tape (Fig. 4.21c and 4.21d).

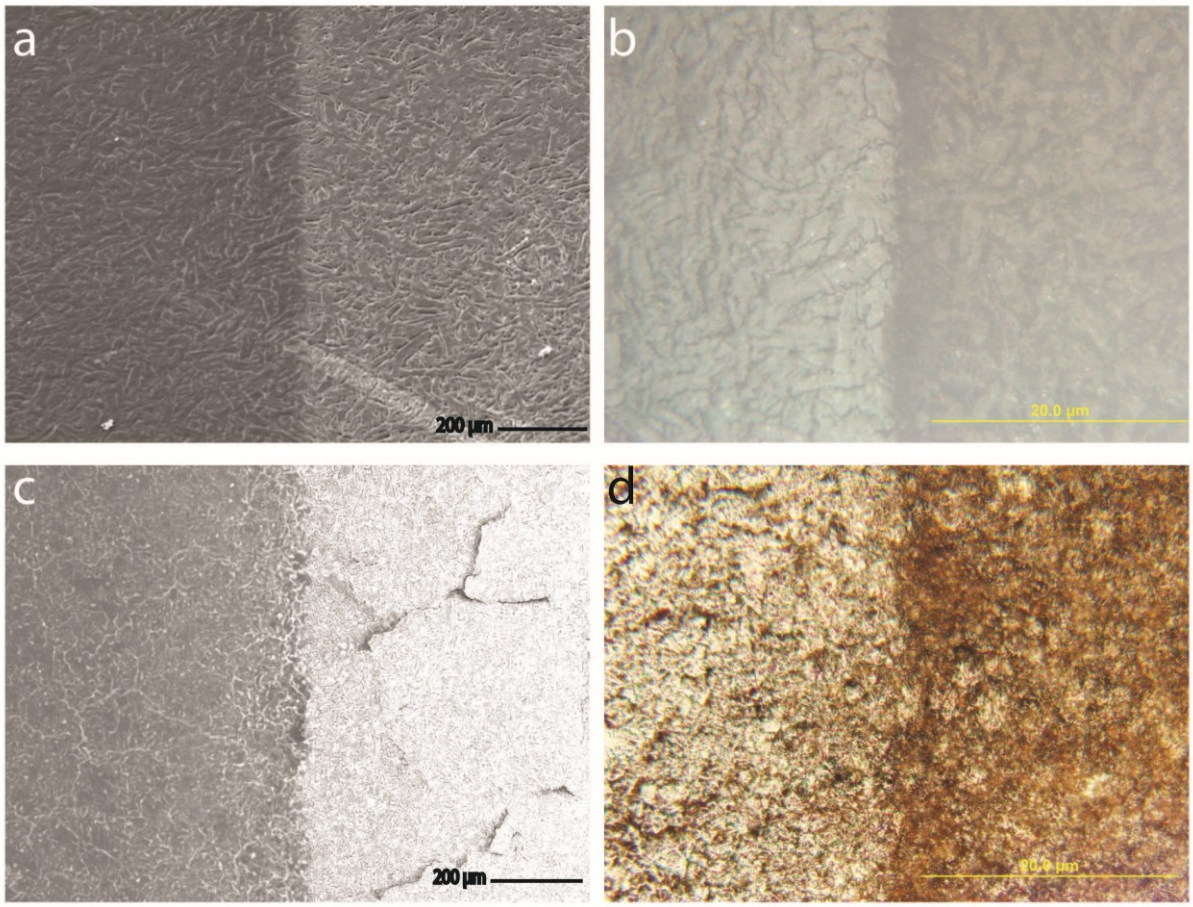

Figure 4.21: SEM and light microscopy images of the masked (left side) and unmasked (right side) areas of cellulose (a and b) and lignin (c and d) pellets exposed to plasma for 667s: (a) SEM photomicrograph showing the border between the masked (left side) and unmasked surface in a cellulose pellet, note the increased brightness of the area exposed to plasma; (b) reflected light microscopy image of the pellet in Fig. 4.21a showing the boundary between the etched and masked areas, note the darker color of the area exposed to plasma; (c) SEM photomicrograph showing the boundary between the masked (left side) and unmasked surface of a lignin pellet, note the increased lightness of the area exposed to plasma and; (d) reflected light microscopy of the pellet in Fig. 4.21c showing boundary between the etched and masked areas, note the darker brown color of the plasma treated lignin

4.4 Discussion

Confocal profilometry was clearly able to detect changes to the wood's microstructure caused by plasma. It was also able to quantify the etching of wood cell walls. There was a strong relationship between treatment time, and hence plasma energy applied to samples, and volume and mass of cell wall material etched by plasma. These findings accord with observation in Chapter 3 and also the results of previous studies of the plasma etching of polymers. These studies found a positive relationship between etching of polymers and the time they were exposed to plasma, despite differences in the intrinsic susceptibility of the various polymers to plasma etching (Yasuda et al. 1973, Pederson 1982, Gokan et al. 1983, Kogoma and Turban 1986, Sadova and Pankratova 2009, Inagaki et al. 2003, Fricke et al. 2011). There was no significant difference in the etching of different cell walls (i.e. radial v. tangential) and wood species (i.e. poplar and yellow cedar), but there was a significant ($p = 0.05$) interaction of species and cell type on volume of cell wall material removed by plasma. It is possible that milder plasma treatment might reveal further differences in the susceptibility of different cell walls to etching by plasma.

Confocal profilometry confirmed observation in Chapter 3 that the middle lamella and also the outer border of bordered pits are more resistant to plasma etching than other parts of the cell wall. The former observation led to my hypothesis that lignin is more resistant to plasma etching than cellulose. The higher lignin content of compression wood in softwoods is one of its defining features (Parham and Côté 1971, Timell 1982), and I first tested my hypothesis by examining plasma etching of cell walls in compression wood with that of cell walls in normal wood. Chemical analysis of the compression wood exposed to plasma confirmed that it had a higher lignin content than 'normal wood'. Confocal profilometry showed that cell walls in compression

wood were significantly more resistant to plasma etching than cell walls in normal wood. The higher lignin content of cell walls in compression wood may explain this finding. Lignin in compression wood is more highly condensed than the lignin in normal wood, which might also explain why it was more resistant to plasma etching (Morohoshi and Sakakibara 1971, Yasuda and Sakakibara 1975). The structure of compression wood is also different to that of normal wood, and presence of helical cavities in the S_2 layer of compression wood in particular influenced etching of cell walls. Widening of these helical cavities occurred when compression wood was exposed to plasma. These cavities are not lignified and the ribs are accessible on both sides to plasma. These features may explain why the ribs delaminated from the underlying cell wall layer.

I performed another experiment to test my hypothesis that lignin is more resistant to plasma etching than cellulose. This experiment used profilometry in combination with light and scanning electron microscopy to examine the etching of cellulose and lignin in compressed pellets. 3D topographical images obtained using profilometry and reflected light microscopy of the pellets surfaces was used to identify cellulose and lignin in pellets. Comparison of images obtained using these two techniques revealed that plasma caused more severe erosion of areas of pellets that were composed of cellulose and less erosion of areas composed of lignin.

The differential erosion of cellulose and lignin pellets exposed to plasma was quantified using profilometry. Analysis of the depth of erosion of unmasked areas of cellulose and lignin pellets exposed to plasma revealed greater etching of cellulose compared to lignin. This finding is supported by a study of the rate of decomposition of cellulose and lignin exposed to microwave plasma (Kobayashi et al. 2006). Kobayashi and co-workers showed greater weight losses for cellulose compared to lignin during plasma treatment (Kobayashi et al. 2006). My

observation of greater etching of cellulose compared to lignin accords with my observation in Chapter 3 that cell wall layers that contained higher concentrations of lignin were the most resistant cell wall layers to plasma etching.

Lignin is also reported to be less affected by gamma radiation than cellulose (Seifert 1964, Flachowsky et al. 1990). Accordingly as mentioned in Chapter 3, studies of the morphology of wood exposed to gamma radiation have shown that cell wall layers that are rich in lignin are more resistant to degradation than other parts of the cell wall (de Lhoneux et al. 1984). The greater resistance of lignin to plasma etching compared to cellulose may be explained by its polymeric structure. Lignin is a heterogeneous polymer with an aromatic backbone (Sakakibara 1980). Aromatic polymers are more resistant to plasma etching compared to aliphatic polymers (Taylor and Wolf 1980, Inagaki et al. 2003). The presence of strong backbone and backbone-side chain bonds also increase the resistance of a polymer to plasma etching (Taylor and Wolf 1980). In the case of reaction wood, its higher content of phenyl and phenylcoumaran inter-unit bonds, and greater frequency of carbon-carbon bonds may contribute to the increased resistance of its lignin to plasma etching (Yasuda and Sakakibara 1975).

One unexpected finding was that exposure to plasma made lignin darker. This may be due to the oxidation of lignin. Oxidation of lignin causes lignin to change color (Falkehag et al. 1966, Polcin et al. 1969, Fleury and Rapson 1969), and plasma treatment of lignin in oxygen containing atmospheres has the capacity to oxidize lignin (Toriz et al. 2000, Klarhofer, et al. 2010). Similarly, changes in color of plasma treated cellulose may be due to its degradation and oxidation because plasma treatment has been shown to oxidize both cellulose and cellulosic fibers (Kan and Yuen 2009, Calvimontes et al. 2011). Oxidized celluloses are often yellow or yellowish brown due to the formation of carbonyl groups (Timar-Balazsy and Eastop 1998). The

brighter color of plasma treated cellulose and lignin in SEM photomicrographs could be due to "charging" artifacts caused by imperfect coating of rougher, plasma-treated surfaces (Shaffner and Van Veld 1971).

4.5 Conclusions

The aims of this chapter were to quantify the plasma etching of wood cell walls using white light confocal profilometry and test the hypothesis that lignin is more resistant to plasma etching than cellulose. Confocal profilometry was able to quantify the erosion of cell walls in normal wood and compression wood exposed to plasma. As a result I was able to examine the effects of plasma treatment time and cell wall composition on plasma etching. Minimal surface preparation of samples was required when using confocal profilometry to assess the erosion of wood cell walls by plasma. Therefore I conclude that confocal profilometry is able to assess the erosion of wood cell walls by plasma, and possibly other physical, chemical and biological agencies that are capable of degrading wood cell walls.

I tested my hypothesis that lignin is more resistant to plasma etching than cellulose by using confocal profilometry to quantify the erosion of cell walls containing different levels of lignin (compression v. normal wood) and also pure cellulose and lignin in pellets exposed to plasma. There was less etching of cell walls in lignin rich compression wood than that of cell walls in normal wood. Furthermore lignin in pellets exposed to plasma was more resistant to etching than cellulose in pellets. Therefore I conclude that lignin is more resistant to etching by plasma than cellulose.

The method I developed to quantify plasma etching of cell walls using confocal profilometry should create opportunities in future to more closely examine the kinetics of plasma etching and how it is affected by different factors including etchant gas and plasma power. Other

possible applications of the technique include: (1) 3-D imaging and quantification of the dimensions of anatomical features in wood such as bordered pits and helical thickening; (2) quantifying the erosion of untreated and treated cell walls in wood exposed to UV radiation or weathering; (3) assessing surface quality and erosion of paper (both treated and untreated).

5 Effects of plasma etching on chemical composition of wood

5.1 Introduction

In Chapters 3 and 4 I examined the ability of plasma to etch wood surfaces. Plasma etched wood surfaces and produced new microstructures. Changes in surface structure, however, depended on both plasma treatment time and the ultra-structure of wood cell walls. I found evidence that areas of cell walls that are rich in lignin were more resistant to etching. Conversely cellulose rich regions of the cell wall were more susceptible to etching. These observations of the relative susceptibilities of lignin and cellulose to plasma etching were confirmed by experimentation on cellulose and lignin models (Chapter 4). The literature on the plasma modification of wood and paper was reviewed in Chapter 2. One study by Vander Wielen et al. (2005) on the effects of plasma on pulp fibers suggested that lignin was less susceptible to etching than cellulose. Studies of the chemical changes occurring at the surface of plasma treated wood, however, have not confirmed this suggestion although there is stronger chemical evidence that lignin is less susceptible to degradation by gamma radiation than cellulose and hemicellulose (Hachihama et al. 1960, Seifert 1964, Tabirih et al. 1977, de Lhoneux et al. 1984, Flachowsky et al. 1990).

Plasma interacts with polymers causing bond scission and free radical formation on polymeric chains, like gamma radiation (Inagaki 1996), and my results in Chapters 3 and 4, as well as previous studies of the effect of plasma on the morphology of wood and paper fibers suggest that lignin in wood will be more resistant to etching than cellulose. In this Chapter I use wet chemical techniques, Fourier transform infra-red spectroscopy (FTIR) and X-ray photoelectron spectroscopy (XPS) to examine chemical changes at wood surfaces that occur as a

result of plasma treatment. I hypothesize that chemical changes will be more pronounced in the holocellulose (cellulose and hemicellulose) component of wood than lignin.

5.2 Materials and methods

5.2.1 Experimental design and statistical analysis

A randomized experimental design was used to examine the effects of two fixed factors (i.e. plasma treatment and wood species) on the acid insoluble (Klason) lignin, soluble lignin and structural carbohydrates in wood. A total of 200 veneers were cut from poplar and lodgepole pine wood blocks (see below). Veneers from each species were subdivided into batches of five veneers (20 batches per species). Data from the chemical analysis of each batch (replicate) was used as the response variable (2 species [poplar or lodgepole pine] x 2 treatments [vacuum/control or plasma] x 10 batches). Analysis of variance was used to examine the effects of species type and plasma treatment on the response variables (see below). Statistical computation was performed using Genstat v. 12 (VSN International 2009). Before the final analysis, diagnostic checks were performed to determine whether data conformed to the underlying assumptions of analysis of variance, ie, normality with constant variance. Significant results ($p<0.05$) are presented in graphs, which contains LSD bars or ± SED bars that can be used to compare differences between means. Appendix 3 contains all of the results of the statistical analysis of data for this Chapter.

FTIR and XPS were used to detect changes in the surface chemistry of wood following plasma treatments (see below).

5.2.2 Wood samples

All chemical analyses were conducted on poplar and lodgpole pine sapwood. These species were chosen to examine differences (if any) in the responses of softwood and hardwood to plasma treatment (Fengel and Wegener 1984). Wood was obtained from the Centre for Advanced Wood Processing at UBC and kept in a constant climate room at 20 ± 1˚C and 65 ± 5% r.h. for one week. Wood samples measuring 80 (longitudinal) x 15 (radial) x 15 (tangential) mm^3 were cut from the sapwood of each species. Before samples were converted to the final dimensions needed for different chemical analysis (see below), they were extracted with cold and hot water using the methods described by Browning (1967). Water extraction was chosen in preference to extraction with organic solvent because many organic solvent cannot be completely removed from wood by drying, and they affect the chemical properties of wood (Ashton 1974). For example, cellulose containing nonpolar solvent is highly reactive and can be easily acetylated (Richter et al. 1957).

5.2.3 Wet chemical analysis

5.2.3.1 Veneer preparation and treatment

The effect of plasma treatment on the acid insoluble and soluble lignin and structural carbohydrates in wood was examined using treated and untreated wood veneers. Veneers measuring 80 mm (long) x 15 mm (wide) x ~ 40 µm (thick) were cut from the radial longitudinal surfaces of extracted lodgepole pine and poplar wood blocks as described by Evans (1988). One hundred veneers from each species were produced and subdivided into batches of five veneers. Each batch of veneers was air-dried for 72 h, weighed and oven dried for 24 h at 60°C. Each batch of veneers was placed in a vacuum desiccator over silica gel to cool down and then re-weighed. These batches then were randomly assigned to either plasma treatment (667 s) or the

control (exposed to vacuum for 667 s). The method used to plasma-treat veneers was the same as that described in Chapter 3 (part 3.2.2). After treatment, each batch of veneers was dipped in a separate glass beaker containing 50 mL of nanopure sterilized water at 70°C for 15 seconds. The veneers were then placed on glass backing plates for 72 h to allow them veneers to air dry. The aqueous extract from veneers was frozen and stored prior to chemical analysis (see below).

Batches of veneers were also dried in an oven at 60°C for 24 hours and their acid insoluble lignin (Klason lignin), soluble lignin and structural carbohydrate contents were measured as follows.

5.2.3.2 Acid insoluble (Klason) lignin

The acid insoluble (Klason) lignin content of veneers was analyzed using methods described in Tappi standard (T 222 om-88, 1991) with some modifications. Each batch of veneers was cut into small pieces using a pair of scissors that had been cleaned with acetone. Approximately 200 mg of veneers (treated and the vacuum/control) were hydrolyzed in 3 mL of 72% H_2SO_4 for 2 h at 25°C with intermittent stirring. Then the strong acid solution was diluted to 3% and samples were transferred to 150 mL bottles. Each bottle was sealed with a rubber stopper and an aluminum crimp-top was placed on top of the bottles. The bottles were then autoclaved at 121°C for 1 h. After this secondary hydrolysis, the bottles were cooled at room temperature for 3 h and the hydrolyzate from each bottle was filtered through separate pre-weighed medium coarse sintered glass crucibles. Approximately 10 mL of the hydrolyzate was drawn from the filtrate using a graduated glass pipette for analysis of acid-soluble lignin and monosaccharides (see below). The lignin residue in each crucible then was washed with 30 mL nanopure water. Each crucible was dried at 105±3 ºC overnight, cooled in a desiccator and re-weighed to the nearest

0.1 mg. The acid-insoluble lignin was calculated as a percentage of the initial oven-dry weight of the sample (Tappi, T 222 om-88, 1991). No correction for ash content was made.

5.2.3.3 Acid soluble lignin

Acid soluble lignin (ASL) is measured to account for the solubilization of smaller lignin fragments that do not condense in the acid fraction during hydrolysis (Browning 1967). The ASL content was measured in the retained acidic filtrate from the Klason lignin determination (see above). A 1 mL aliquot of each filtrate was analyzed at 205 nm wavelength using a UV/visible spectrophotometer (Varian Cary 50 BIO, USA) against a blank reference solution of 3% H_2SO_4. Samples were diluted as required with 3% H_2SO_4 to give an absorbance of between 0.2 and 0.7 in accord with TAPPI standard (Tappi, UM 250, 1991). The amount of soluble lignin in each aliquot was determined using Beer's Law with an absorptivity constant of 110 L g^{-1} cm^{-1} (Tappi, UM 250, 1991).

5.2.3.4 High performance liquid chromatography

High performance liquid chromatography (HPLC) was used to analyze the carbohydrate composition of plasma-treated wood and controls according to Tappi standard (T 249 cm-00, 2000). The filtrate from the Klason lignin determination (~ 10 mL) for each sample was frozen and kept in a freezer before HPLC analysis. Frozen samples were defrosted overnight in a fridge and aliquots (20 μL) from each sample were passed through separate 0.45 μm nylon syringe filters (Chromatographic Specialties Inc., Canada). Monosaccharides were determined using a DX-2500 HPLC system (Dionex, Sunnyvale, CA, USA) equipped with an AS3500 autosampler, a GP50 gradient pump, an anion-exchange column (Dionex CarboPac PA1), and an ED40 electrochemical detector. The column was eluted with deionized water at a flow rate of 1

mL/min. Optimization of baseline stability and detector sensitivity was achieved by post-column addition of 0.2 M NaOH. The column was reconditioned using 1 M NaOH after each analysis. Standard solutions were prepared from arabinose, galactose, glucose, xylose and mannose in the approximate proportions found in wood and used to quantify the monosaccharides in samples (Tappi, T 249 cm-00, 2000). Sugar standards were dissolved in nanopure water and subjected to primary and secondary hydrolysis as was performed for the determination of Klason lignin (above). Integrated areas on chromatographs were quantified after baseline correction against standard solutions at different concentrations using fucose as an internal standard (Tappi, T 249 cm-00, 2000). An example of a chromatograph obtained from a single analysis of one poplar specimen is shown in Figure 5.1.

Sugar concentrations in samples were determined using regression equations from calibration curves that were derived from external standards. From monosaccharide composition, and based on several assumptions on the glucose associated with hemicelluloses in hardwoods and softwoods, the cellulose content was calculated using the algorithms of Janson (1970), and is presented as the ratio of glucose to total carbohydrates.

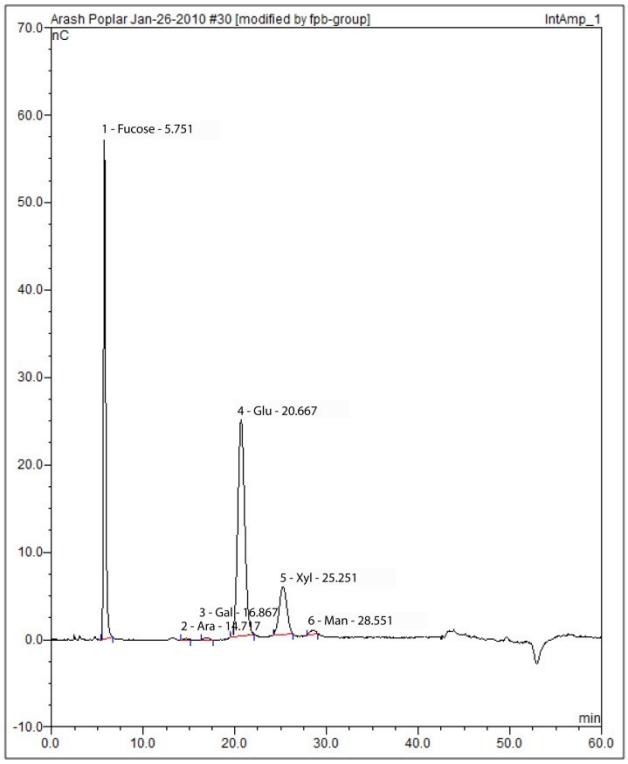

Figure 5.1: Chromatograph of monosaccharide analysis of plasma treated poplar using HPLC; arabinose (Ara), galactose (Gal), glucose (Glu), xylose (Xyl), mannose (Man) and fucose as an internal standard

5.2.3.5 Analysis of aqueous extract

The hot aqueous extracts resulting from dipping of untreated/vacuum and plasma treated veneers in nanopure water were cooled in glass beakers at room temperature. The extract in each beaker (50 mL) was transferred to a 50 mL plastic falcon tube and frozen at -80 °C in a Forma Scientific freezer. Frozen samples were freeze-dried in freeze-dry flasks attached to a bench top freeze-dryer (LABCONCO, MO, USA) operating at 0.016 mbar and -50°C until all the frozen liquid was sublimed. The residue was brought to a hydrolysis reaction volume of 20 mL by adding nanopure water. The monomer/oligomer content of each solution was analyzed using the method of Sluiter et al. (2006). Samples (300 µL) were drawn from the liquid before hydrolysis, for determination of monomeric sugar in the liquid. Preliminary tests did not detect any

monomeric sugars in the liquid before the hydrolysis. Therefore samples were hydrolyzed in a 3% solution of sulfuric acid to convert oligomeric carbohydrates to their corresponding monomeric sugars. Phenolics and sugar content of hydrolyzed volume (20 mL) were measured after filtering hydrolyzates through 0.45µm nylon syringe filters, as described above.

5.2.4 Fourier transform infra-red spectroscopy (FTIR)

FTIR spectra were obtained using a spectrometer (Perkin Elmer Spectrum One, Waltham, MA, USA) by direct reflectance ATR-IR on small wood samples.

Poplar and lodgepole pine sapwood blocks measuring 10 (longitudinal) x 10 (radial) x 3 (tangential) mm^3 were cut from the wood blocks described above (part 5.2.2) and their radial surfaces were microtomed. These samples were air dried for 72 hours and then kept in a vacuum desiccator over silica gel for 72 h. IR spectra of radial surfaces were obtained using a single bounce attenuated total reflectance accessory (PikeMiracle, PIKE Technologies, WI, USA) attached to a spectrometer, after background spectra were obtained. These small blocks were plasma treated as described previously (Chapter 3, part 3.2.2) and the spectra of the plasma treated surfaces were obtained in the same places on the surfaces where initial (untreated) spectra were collected. The crystal of the ATR head was pressed on samples because the amount of infrared absorption when using the ATR technique is dependent on close contact between the sample and the prism (crystal) (Kuo et al. 1988, Stenius and Vuorinen 1999). Accordingly, the force applied to the sample against the crystal was kept the same for the collection of all spectra.

Each spectrum was obtained by accumulating 32 scans over the range 4,000–600 cm^{-1} at a spectral resolution of 4 cm^{-1}. The baseline of each spectrum was manually corrected over the full abscissa range, normalized (internal standard band) and then zeroed as described by Faix (1992). To quantify the area under individual peaks, a baseline was constructed by connecting the lowest

data points on either sides of the peak (Fig. 5.2). Baselines were used as references to calculate the area under each peak as described by Tolvaj and Faix (1995). Quantification of peak areas used Spectrum software (v 5.3.1) on a PC attached to the spectrometer.

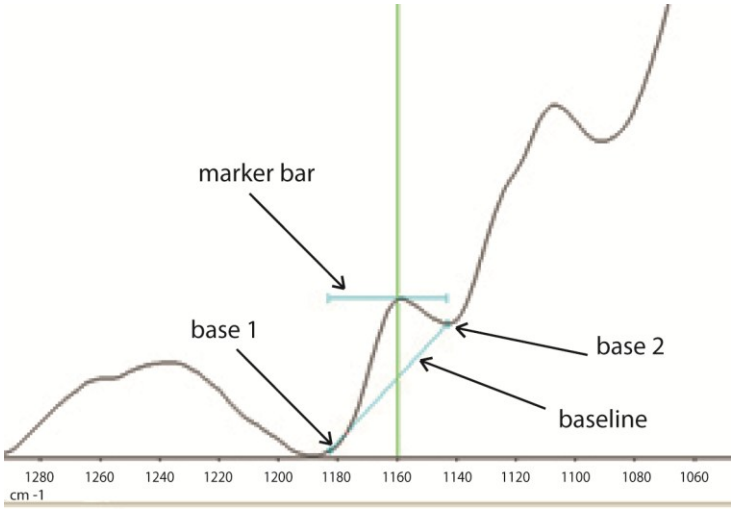

Figure 5.2: Assignment of the baselines for the calculation of area under peaks in a FTIR spectrum (zoomed spectrum of an untreated poplar specimen)

Changes in the areas under peaks for treated samples are expressed relative to those of the controls. Peak area values for functional groups associated with lignin are expressed as a ratio of carbohydrate peaks to provide information on changes in the composition of the main structural components relative to each other as described by Rodrigues et al. (1998).

5.2.5 X-ray photoelectron spectroscopy (XPS)

One wood block measuring 40 (longitudinal) x 15 (radial) x 15 (tangential) mm^3 was cut from each wood species (i.e. extracted poplar and lodgepole pine blocks, see above). Four veneers with a thickness of ~ 50 µm were cut from the radial longitudinal surfaces of each wood block using fresh disposable stainless steel blades and a microtome. Veneers were air-dried for 24 h to a moisture content of 8 percent and then stored in a vacuum desiccator over silica gel.

Care was taken during the preparation and storage of samples to minimize surface contamination of veneers.

Veneers were assigned to different plasma treatments, and treated as described in Chapter 3 (part 3.2.2). Vacuum treated veneers acted as a control. After treatment, samples were removed from the chamber of the plasma device, taking care to avoid touching and contaminating their upper surfaces. Veneers were directly transferred into clean glass vials.

X-ray photoelectron spectra of veneers' surface were obtained in the Advanced Materials and Process Engineering Laboratory (AMPEL) at UBC using an XPS (LEYBOLD MAX 200, Germany) with a base pressure of 1 x 10^{-9} mbar with an AlK alpha source. X-ray take-off angle was 90 degrees and the emitted photo-electrons were collected from a 4 x 7 mm^2 area of the surface of each sample. Initial (survey) spectra were recorded in 0.8 eV steps and the analyzer pass energy was 192 eV. High-resolution narrow-scan spectra were measured for C1s core levels in 0.1 eV steps at a 48 eV pass energy.

From the relative size of the oxygen and carbon peaks, from initial XPS spectra of samples (with subtraction of the Shirley background) the ratio of oxygen atoms to carbon atoms on the surface of wooden veneers was determined, using the method of Suranyi et al. (1980).

Detailed chemical-bond analysis of carbon was performed by curve fitting of the C1s peak area with a least squares method using the XPSPEAK software (version 4.1) from Kwok (2000). Peak synthesis was performed using mixed Gaussian and Lorentzian functions with a nonlinear baseline (Shirley). For peak fitting, further restrictions were chosen, namely an identical full width at half maximum (FWHM) for each class of carbon (i.e. 1.1 eV) and the same curve form (Gaussian-Lorentzian product function). According to the classification of carbon atoms in wood reported by Dorris et al. (1978) and Sinn et al. (2001) the C1s peak is deconvoluted into four

sub-peaks. The fractional areas of each class of carbon i.e. (C1, C2, C3 and C4) to the sum of these areas are equal to the fractions of surface carbon atoms corresponding to each chemical class. The binding energy of C1 was referenced to 284.6 eV and the energy-shift between the classes of carbon was fixed as follows: C2=C1+1.5 eV, C3=C1+2.8 eV, C4= C1+3.75 eV (Sinn et al. 2001, Inari et al. 2006).

5.3 Results

5.3.1 Wet chemical analysis

The statistical analyses of the effects of plasma treatment on the chemical composition of lodgepole pine and poplar are summarized in Table 5.1. Analyses of variance revealed significant effects of plasma treatment and wood species (main factors) and also interactions between them on the chemical composition of wood. Statistically significant interaction between two factors occurs when the effect of one experimental factor (e.g. plasma) on the response variable (e.g. lignin, sugars) depends on the value of another factor (e.g. wood species) (Kutner et al. 2005). In other words, the test of an interaction reveals whether or not the effect of one factor is the same for each level of the other factor on the measured variable. In the following sections I discuss the effects of and interaction between plasma treatment and wood species on wood's chemical composition.

Table 5.1: The effects of and interactions between experimental factors on chemical constituents of lodgepole pine and poplar wood samples

Experimental Factors	Response variables									
	Lignin			Sugars						
	T.Lig	**AIL**	**ASL**	**T.Sug**	**Ara**	**Gal**	**Glu**	**Xyl**	**Man**	**Cell/T.Sug**
Species (S)	NS	***	***	*	***	***	NS	***	***	***
Treatment (T)	***	***	***	***	***	***	***	***	***	***
T x S	***	***	***	**	NS	***	NS	***	*	**

=p<0.05; **=p<0.01; ***=p<0.001; NS=not significant (p>0.05)
T.Lig, total lignin content; AIL, acid insoluble lignin; ASL, acid soluble lignin; T.Sug, total sugar content; Ara, arabinose; Gal, galactose; Glu, glucose; Xyl, xylose; Man, mannose; Cell/T.Sug, ratio of cellulose to total sugar content

5.3.1.1 Lignin content

There were significant effects of plasma treatment and plasma x species interaction on lignin content of wood (Table 5.1). The effects of plasma treatment and species type on percentages of the total lignin, acid insoluble lignin (AIL), acid soluble lignin (ASL) content of wood are shown in Figure 5.3.

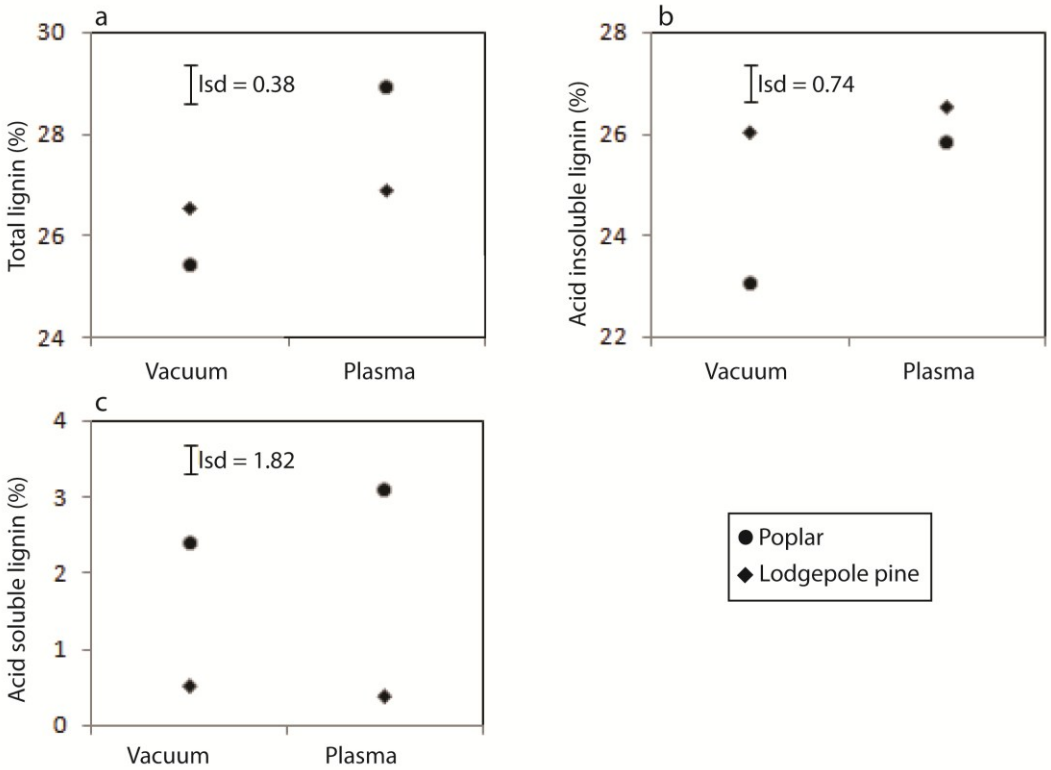

Figure 5.3: Changes in the total lignin (a), acid insoluble lignin (b) and acid soluble lignin (c) of vacuum (control) and plasma treated poplar and lodgepole pine veneers. lsd (least significant difference) bar is based on 95% confidence intervals (from analysis of variance) to estimate the significance of differences between individual means

The total lignin content of plasma treated poplar and lodgepole pine samples were higher than those of the controls. However, the difference was only significant for plasma treated poplar samples, which accounts for the significant interaction ($p<0.001$) of plasma treatment and species type on lignin content (Fig. 5.3a). The same trend was observed for the acid insoluble lignin content of plasma treated and untreated poplar and lodgepole pine samples (Fig. 5.3b).

There was also a significant ($p<0.001$) interaction of plasma treatment and species on acid soluble lignin (ASL) content because plasma treatment increased the ASL content of poplar and lowered that of lodgepole pine (Fig. 5.3c).

5.3.1.2 Sugar content

The total sugar content of plasma treated wood was significantly lower than that of the control. Analysis of variance revealed an interaction between plasma treatment and species. As can be seen in Figure 5.4 the reduction of total sugar content as a result of plasma treatment was more pronounced in poplar compared to lodgepole pine. This effect accounts for the significant ($p<0.01$) interaction of species and plasma treatment on total sugar content.

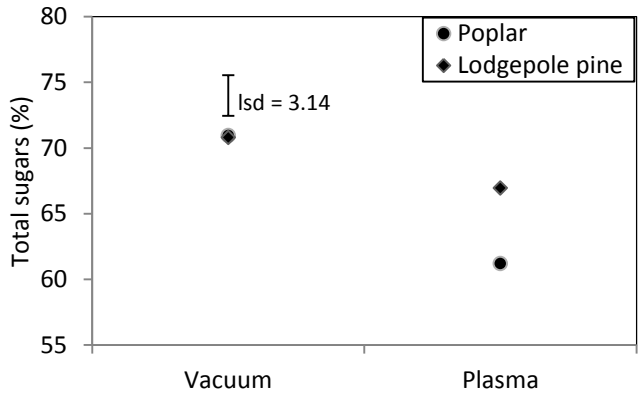

Figure 5.4: Changes in total sugar content of plasma treated poplar and lodgepole pine veneers. lsd (least significant difference) bar is based on 95% confidence intervals (from analysis of variance) to estimate the significance of differences between individual means

Analysis of variance of individual monosaccharides in treated wood and controls revealed that plasma treatment had highly significant effects ($p<0.001$) on all of the different sugars. There were also significant effects of species and interactions of species and plasma treatment on the levels of individual sugars in wood (Table 5.1).

The level of arabinose in wood was significantly affected by plasma treatment and species. Figure 5.5 shows the effects of species and plasma treatment on the percentage of arabinose in wood samples. The amount of arabinose was significantly higher ($p<0.05$) in lodgepole pine compared to poplar and decreased significantly ($p<0.05$) in both poplar and lodgepole pine as a result of plasma treatment (Fig. 5.5a-b).

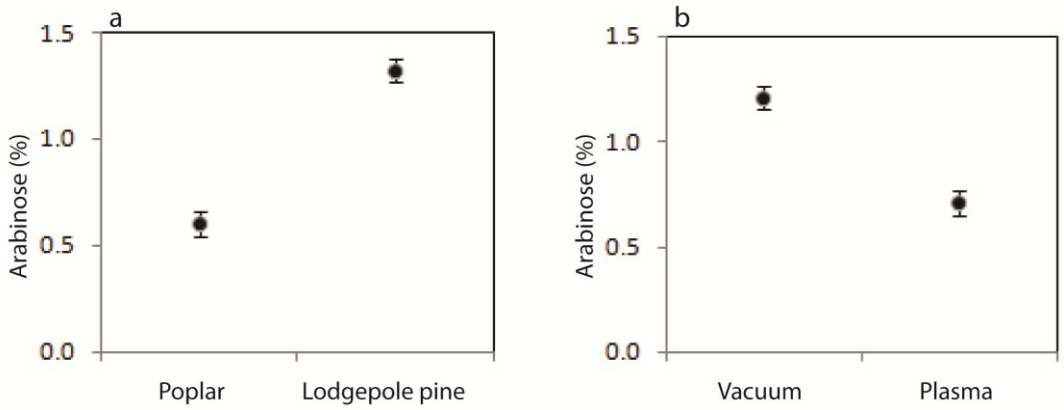

Figure 5.5: Effects of species (a) and plasma treatment (b) on arabinose content of wood samples. Error bars are ± standard error of differences of means (from analysis of variance). Non-overlap of these bars indicates that means are significantly different at 5% level ($p<0.05$)

Figure 5.6 shows the effects of and interaction between plasma treatment and species on the levels of galactose, glucose, xylose and mannose in wood samples. A highly significant treatment effect occurred and there was also a highly significant species x treatment interaction ($p<0.001$) on the galactose content of samples. Plasma treatment reduced the amount of galactose in poplar and lodgepole pine. The interaction of species with plasma treatment occurred because the reduction of galactose in poplar as a result of plasma treatment was greater than that in lodgepole pine (Fig. 5.6a). A similar interaction ($p<0.05$) occurred between plasma and species on the mannose content of wood samples (Fig. 5.6b). A highly significant ($p<0.001$) plasma treatment and species interaction was also observed for xylose. Plasma treatment reduced

the xylose content of poplar to a greater extent than that of lodgepole pine (Fig. 5.6c). Plasma treatment had a highly significant ($p<0.001$) effect on the glucose content of wood samples.

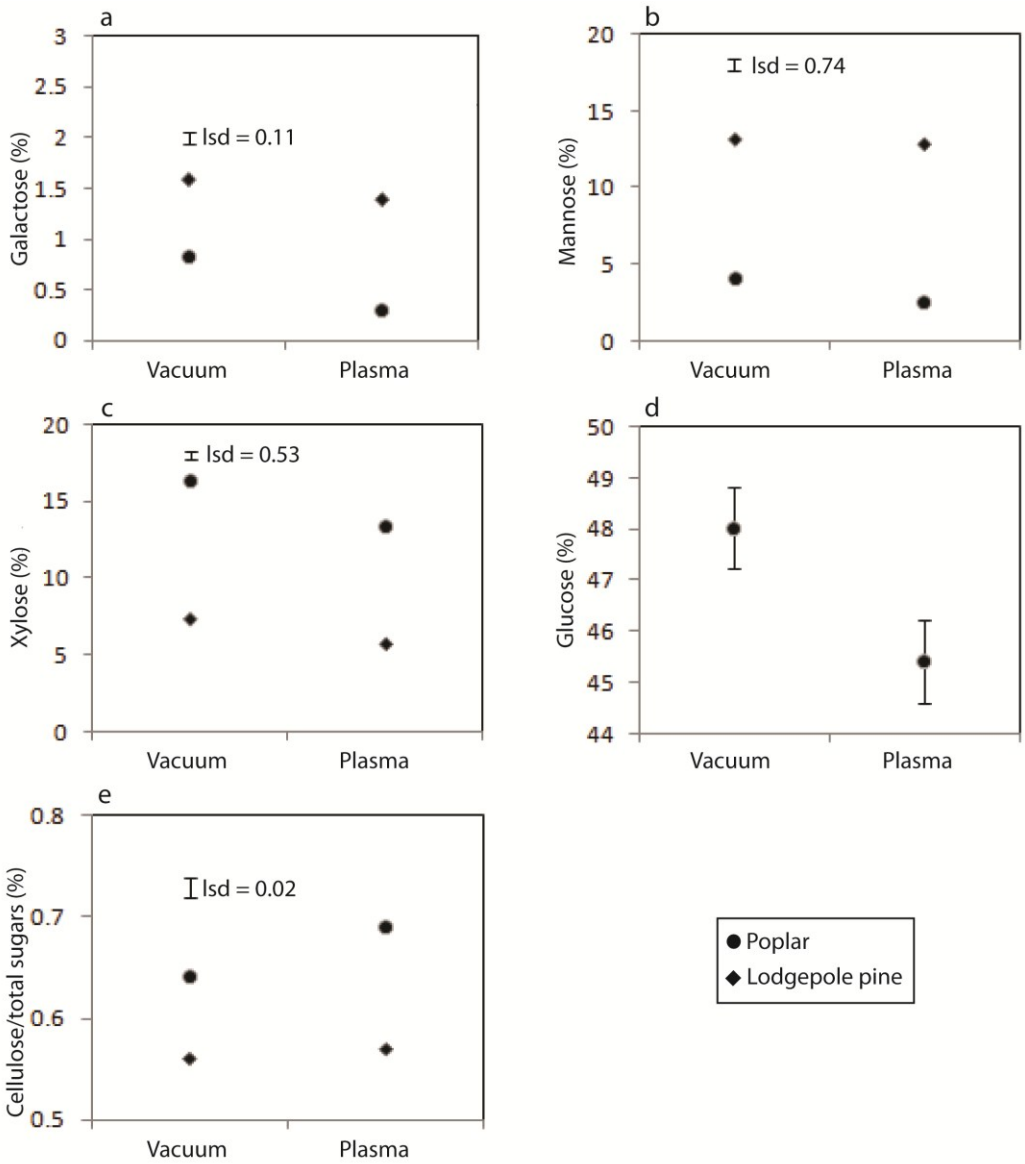

Figure 5.6: The effect of plasma treatment on the sugar content of poplar and lodgepole pine: (a) galactose; (b) mannose; (c) xylose; (d) glucose; and (e) cellulose to total sugar content. lsd (least significant difference) bars based on 95% confidence intervals for plasma x plasma interactions and ± 2x standard errors of the difference (sed) bars for plasma effects derived from analysis of variance

The glucose content of plasma-treated samples was lower than that of the control. However, there was no significant effect of species type or a treatment x species interaction on the glucose

content of wood (Fig. 5.6d). Nevertheless, the results for the ratio of calculated cellulose to total sugar content showed a significant treatment x species interaction (Fig 5.6e). The ratio of cellulose to total sugar content increased in plasma treated samples indicating greater loss of hemicelluloses compared to cellulose, which was more pronounced in poplar compared to lodgepole pine (Fig. 5.6e).

5.3.1.3 Chemical composition of aqueous extracts

Chemical analyses of hot water extracts revealed the presence of small amount of sugars and phenolic compounds in the extracts of both treated and control samples. Table 5.2 summarizes the amount of 'phenolics' and sugars detected in the aqueous extract of plasma treated and untreated veneers.

Table 5.2: Dry mass of phenolics and sugars in aqueous extract of plasma treated and untreated poplar and lodgepole pine wood veneers

Compound	Mass (mg)			
	Poplar		Lodgepole pine	
	Control	Plasma	Control	Plasma
Phenolics	0.25	0.55	0.51	1.06
Sugars	0.00	0.018	0.012	0.053

The amount of phenolics in hot water extracted plasma treated poplar and lodgepole pine were 0.55 and 1.06 mg respectively, substantially greater than 0.25 and 0.51 mg found in the aqueous extract of the untreated (control) veneers. Analysis of aqueous extracts using HPLC revealed higher level of sugars in the aqueous extract of plasma treated veneers (poplar and lodgepole pine). Small amounts of glucose and arabinose were detected in both the control and plasma treated samples (not shown). Glucose and arabinose were found in small amounts, 0.004 mg and 0.007 mg respectively, in the aqueous extract of untreated lodgepole pine. Arabinose

was not detected in the aqueous extract of plasma treated pine, but the level of glucose was much higher (0.053 mg). Traces of these sugars were detected in the aqueous extract of plasma treated poplar samples whereas none were present in the aqueous extract from the untreated poplar controls.

5.3.2 FTIR analysis

It was difficult to discern pronounced changes in the FTIR spectra of pine and poplar veneers as a result of plasma treatment, possibly because chemical changes were confined to the wood surface, and were masked by spectral features of the underlying wood (Fengel and Wegener 1984, Toriz et al 2005). Nevertheless, changes in several bands were evident particularly when samples were treated with plasma for longer periods of time. Furthermore, even slight differences in infrared spectra such as relative heights of adjacent bands or the presence of weak shoulders are evidence of changes in chemical composition of lignocellulosics as pointed out by Hergert (1971).

There were some subtle changes in the FTIR spectra of poplar and lodgepole pine wood as a result of plasma treatment (Fig. 5.7 and 5.9). One of the changes observed in the spectra of lodgepole pine (Fig. 5.7), was a reduction in the strong broad band, from 3100 to 3600 cm^{-1} which is due to OH stretching vibration as a result of intermolecular hydrogen bonding in cellulose (Baeza and Freer 2001). There were also some subtle changes in the region from around 1800 to 1000 cm^{-1}, where there are several discrete, sharp or broad absorptions bands. Spectra in this region follow the same general pattern as a result of plasma treatment. There was a decrease in the band at 1640 cm^{-1} (H–O–H angle vibration of water molecule) as a result of plasma treatment (Baeza and Freer 2001, Haxaire et al. 2002).

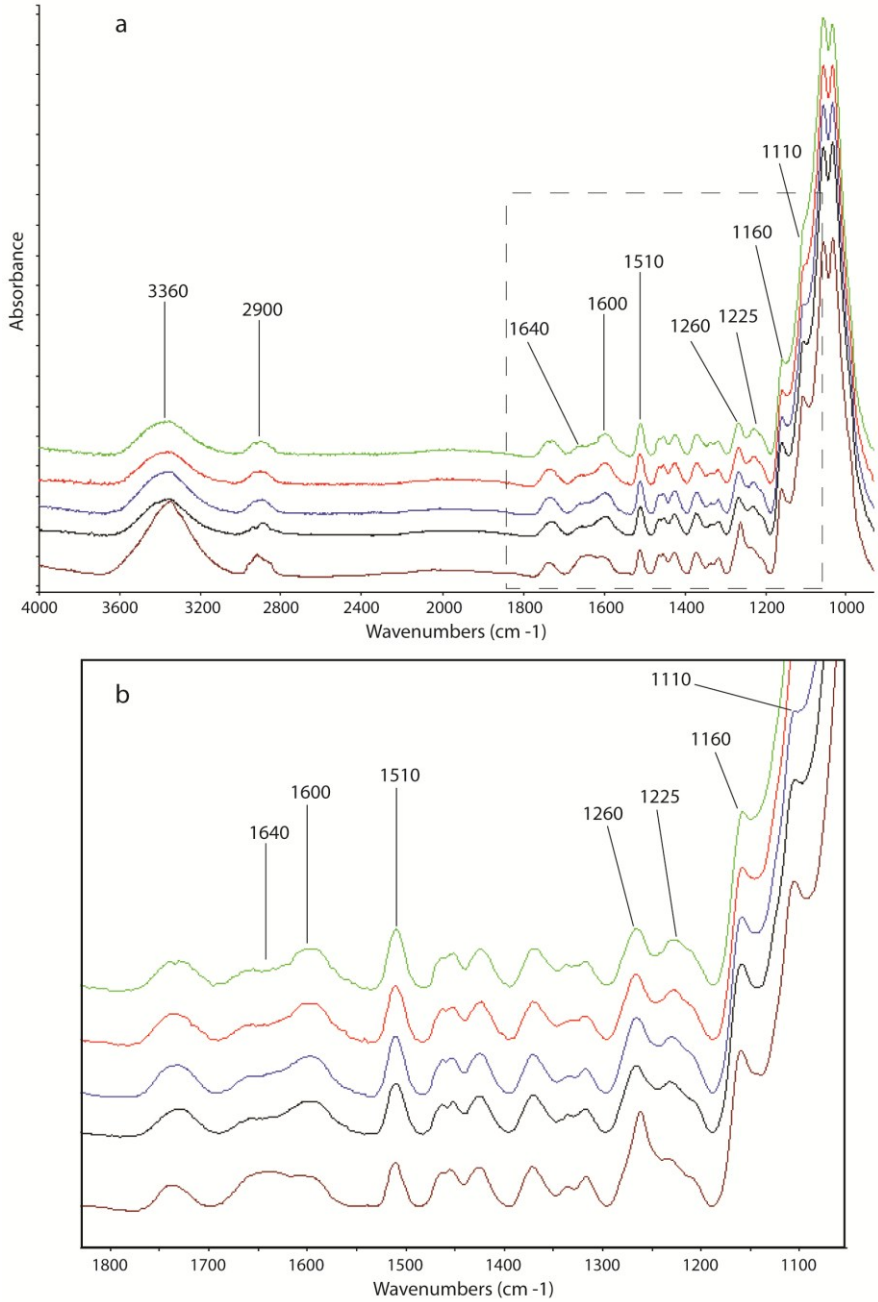

Figure 5.7: (a) FTIR spectra of lodgepole pine (from bottom to top: untreated, and plasma treated for 333 s, 667 s, 1000 s and 1333 s). Raw spectra were baseline corrected manually at 3732.31, 3021.03, 2248.56, 1830.05, 1694.48, 1549.36, 1488.26, 1396.60, 1297.31, 1188.47, 923.05, 844.76 and 789.39 cm^{-1}, then the band around 1373 cm^{-1} (a C-H band) was used as an internal standard i.e. its intensity was adjusted to 1.5 and all spectra zeroed at 1900 cm^{-1} in accord with the method used by Tolvaj and Faix (1995); (b) enlarged area of Fig. 5.7a, ranging from around 1800 to 1100 cm^{-1}

Changes in several bands became more evident as a result of more prolonged plasma treatment. For example, in the spectra of lodgepole pine the bands occurring around 1600 cm^{-1} and 1510 cm^{-1} became clearer and more intense. These two bands are largely due to aromatic skeleton vibration in lignin, but the peak at 1600 cm^{-1} also has a contribution from C=O stretching (Harrington et al. 1964, Hergert 1971, Grandmaison et al. 1987, Pandey and Khali 1998, Baeza and Freer 2001).

A shoulder around the band at 1225 cm^{-1}, which was not pronounced in control spectra, developed in plasma treated lodgepole pine and increased with treatment time. Peaks in the region of 1225 cm^{-1} have been assigned to =C-O stretching vibration of phenolic hydroxyl group and C-C, C-O and C=O stretch in lignin (Durie et al. 1960, Baeza and Freer 2001, Pandey and Pitman 2004). The neighboring band at 1260 cm^{-1}, that showed a slight decrease in height after plasma treatment, has been assigned to guaiacyl ring breathing and C-O linkage in guaiacyl aromatic methoxyl group in lignin (Harrington 1964, Sarkanen et al. 1967, Hergert 1971, Ehrhardt 1984).

Peaks at around 1160 and 1110 cm^{-1} decreased with increasing plasma treatment time. These bands are related to cellulose and hemicelluloses for which the band at 1110 cm^{-1} and 1160 cm^{-1} have been assigned to O-H and C-O-C asymmetric stretching vibration, respectively (Durie et al. 1960, Harrington 1964, Kuo et al. 1988, Faix and Böttcher 1992, Pandey and Theagarajan 1997, Olsson and Salmén 2004).

Plasma treatment caused small irregular changes at a band centered around 2900 cm^{-1}, which is related to the polysaccharides in wood. In the spectra of control samples this band had two shoulders at 2850 cm^{-1} and 2960 cm^{-1}, which have been assigned to CH_2 symmetric and anti-symmetric stretching in cellulose, respectively (Baeza and Freer 2001).

The variations in the IR spectra of the samples as a result of plasma treatment are summarized in Figure 5.8. This figure plots the areas under the peaks of treated wood relative to those of the control. Peaks relevant to carbohydrates decreased significantly after treatment for 333s and then stayed relatively constant except for the peak at 1110 cm^{-1}, which continued to decrease with increasing plasma treatment time. The peak at 1160 cm^{-1} showed smaller decreases as a result of plasma treatment. Peaks relevant to lignin increased as a result of plasma treatment except for peak at 1260 cm^{-1}. The ratios of the lignin/carbohydrate peak areas for untreated controls and plasma treated samples are shown in Table 5.3. The lignin/carbohydrate ratio of samples increased as a result of increases in plasma treatment time (Table 5.3).

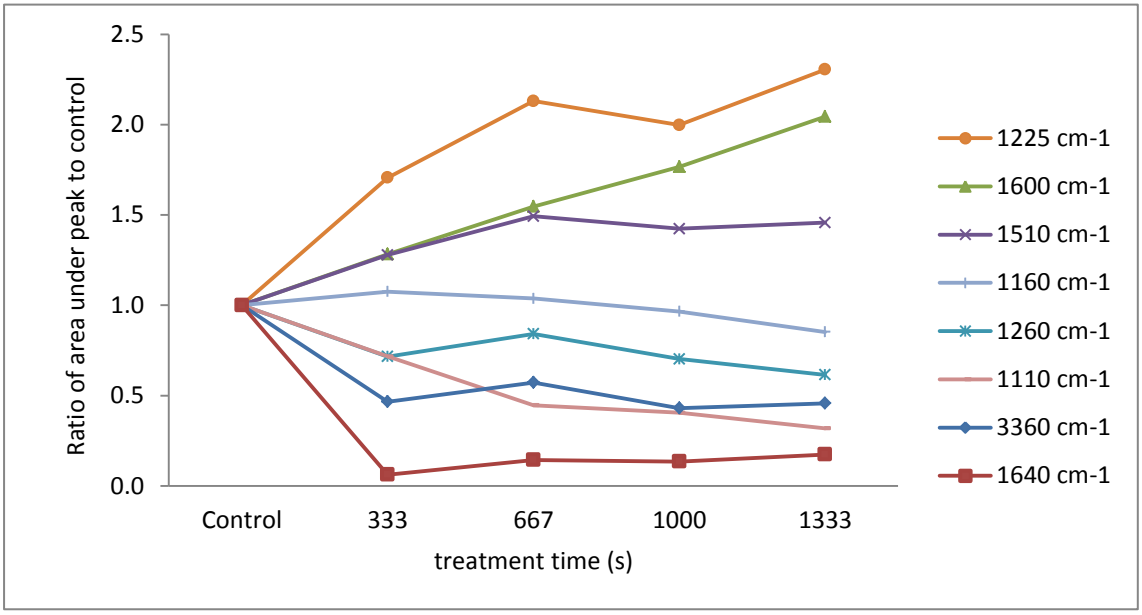

Figure 5.8: Areas under altered peaks in FTIR spectra of plasma-treated lodgepole pine relative to those of controls

Table 5.3: Ratios of the bands associated with lignin and carbohydrates in FTIR spectra of lodgepole pine

Treatment times (s)	Area under peak (A. cm^{-1})			Relative area under aromatic skeleton variation peaks against those in carbohydrate	
	Lignin peak	Carbohydrate peaks			
	1510	1160	1110	1510/1160	1510/1110
0 (Control)	29.01	57.66	33.73	0.50	0.86
333	37.08	62.01	24.19	0.60	1.53
667	43.30	59.84	15.06	0.72	2.87
1000	41.30	55.69	13.68	0.74	3.02
1333	42.27	49.18	10.77	0.86	3.92

Changes in peaks in the spectra of poplar wood caused by plasma treatments are similar to those described above for lodgepole pine wood. However, several bands appeared at slightly lower or higher wavenumbers, and were less distinct than those in spectra of lodgepole pine (Fig. 5.9).

The peak at 1510 cm^{-1} in lodgepole pine due to aromatic skeleton vibration in lignin, appeared at 1505 cm^{-1} in poplar. The peak at 1600 cm^{-1} in lodgepole pine (aromatic skeleton vibration in lignin and C=O stretching) appeared at 1595 cm^{-1} in poplar and was sharper and more distinct, but it was less affected by plasma treatment. The sharp peak around 1260 cm^{-1} in lodgepole pine (guaiacyl units) was not observed in poplar, however, the increase in the intensity of the peak at 1230 cm^{-1} (assigned at 1225 cm^{-1} for lodgepole pine) was more pronounced in poplar. The decrease in the intensity of the peak at 1160 cm^{-1} as a result of plasma-treatment of poplar only occurred in samples exposed to plasma for a prolonged period of time (1333 s). The peak at 1110 cm^{-1} in lodgepole pine, appeared at 1105 cm^{-1} in poplar and its reduction as a result of plasma treatment was less pronounced than that observed in lodgepole pine. Figure 5.10 plots the areas of the peaks for plasma treated poplar wood relative to those of the control. This graph shows an increase in lignin relevant peaks (i.e. 1225, 1600 and 1510 cm^{-1}) and decreases in bands related to carbohydrates. However, compared to lodgepole pine, the reduction in the carbohydrate peaks (i.e. 1105, 1160 and 3360 cm^{-1}) is smaller in poplar.

Table 5.4 shows the area under typical lignin and carbohydrate peaks in FTIR spectra of poplar. The ratio of lignin/carbohydrate peaks increased in poplar as a result of plasma treatment in accord with the changes in lodgepole pine (Table 5.4).

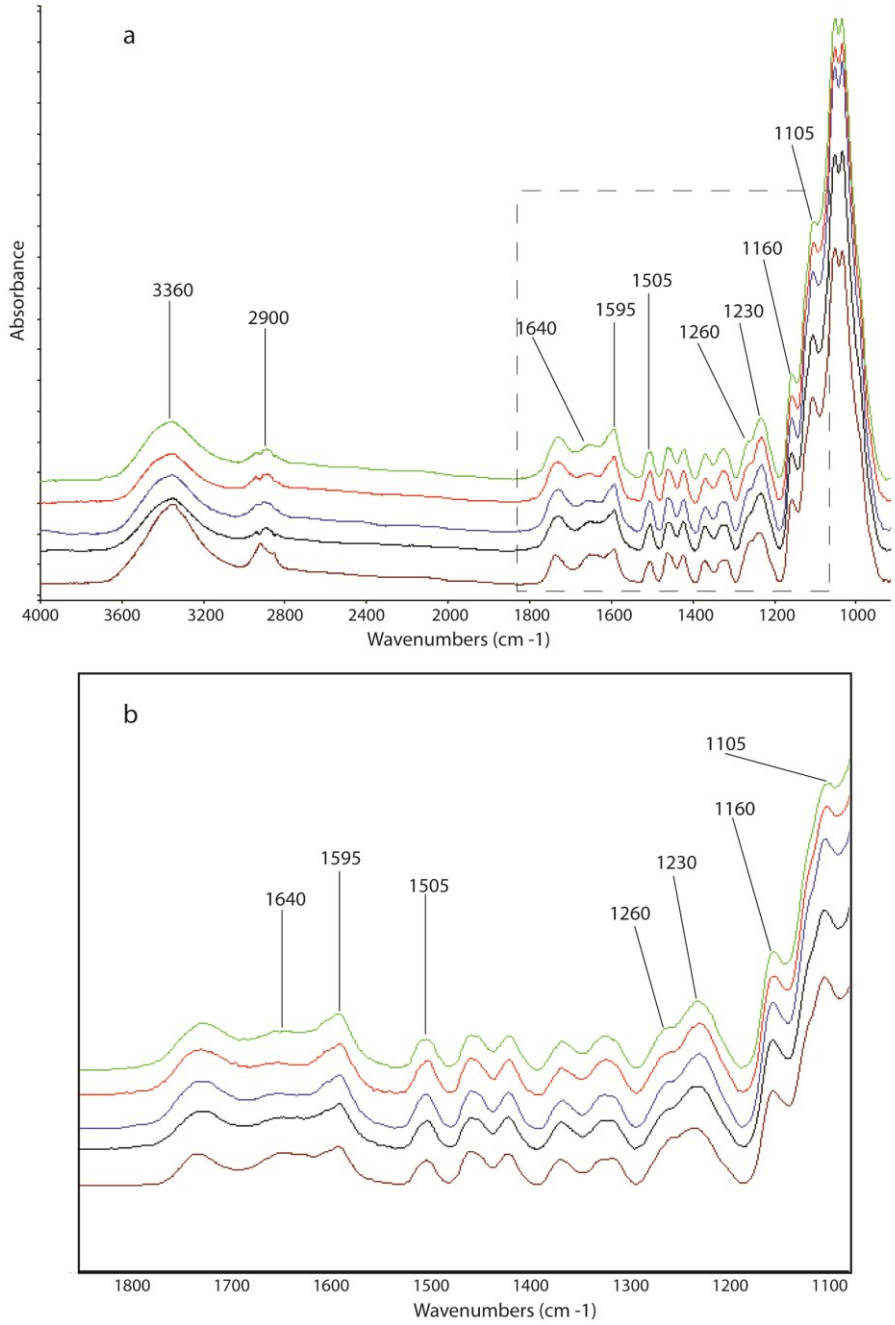

Figure 5.9: (a) FTIR spectra of poplar (from bottom to top: untreated, and plasma treated for 333 s, 667 s, 1000 s and 1333 s). Raw spectra were baseline corrected manually at 3700.00, 1900.00, 1540.00, 1484.00, 1400.00, 1295.00, 1188.00, 921.14, 865.00, 800.84 and 651.00 cm^{-1} then the band around 1373 cm^{-1} (a C-H band) was used as an internal standard i.e. its intensity was adjusted to1.5 and all spectra zeroed at 1900 cm^{-1} in accord with the method used by Tolvaj and Faix (1995); (b) enlarged area of Fig. 5.9a, ranging from around 1800 to 1100 cm^{-1}

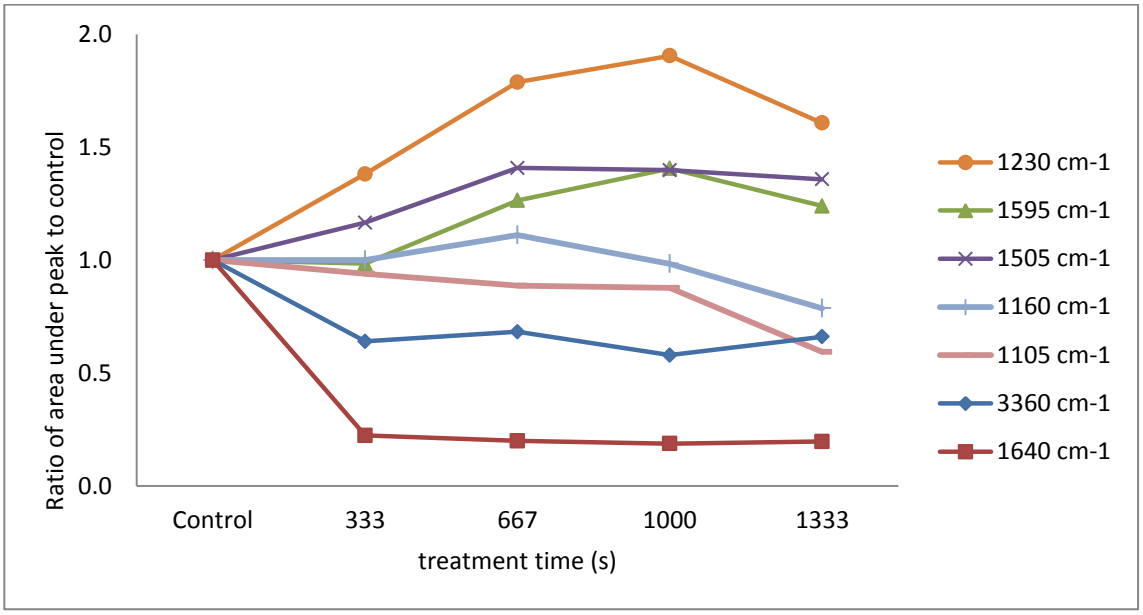

Figure 5.10: Areas under altered peaks in FTIR spectra of plasma-treated poplar relative to those of controls

Table 5.4: Ratios of the bands associated with lignin and carbohydrates in FTIR spectra of poplar

Treatment times (s)	Area under peak (A. cm^{-1})			Relative area under aromatic skeleton variation peaks against those in carbohydrate	
	Lignin peak	Carbohydrate peaks			
	1505	1160	1105	1505/1160	1505/1105
0 (Control)	28.75	50.70	27.11	0.57	1.06
333	33.53	50.75	25.46	0.66	1.32
667	40.49	56.33	24.05	0.72	1.68
1000	40.20	49.87	23.78	0.81	1.69
1333	39.04	39.90	16.09	0.98	2.43

5.3.3 XPS analysis

The XPS spectra of wood samples were dominated by carbon (1s) and oxygen (1s) peaks, which are the elements that make up the main constituents of wood (Young et al. 1982). The XPS survey spectrum of an untreated lodgepole pine sample is shown in Figure 5.11a. The ratio of atomic concentration of oxygen to carbon is shown in Table 5.5. Plasma treatments increased the oxygen/carbon ratio at the surface of both poplar and lodgepole pine.

According to classification of carbon atoms in wood (Dorris et al. 1978), the C (1s) peak in XPS spectra (Fig. 5.11b) consists of four classes of carbon atoms: (1) C1 of carbons corresponds to unoxidized carbon atoms, bonded only by carbon or hydrogen bonds; (2) C2 class corresponds to carbon atoms bonded to a single noncarbonyl oxygen; (3) C3 class of carbon is bonded to a carbonyl or two noncarbonyl oxygen; and C4 class of carbon atoms is bonded to a carbonyl and a noncarbonyl oxygen (Dorris et al. 1978).

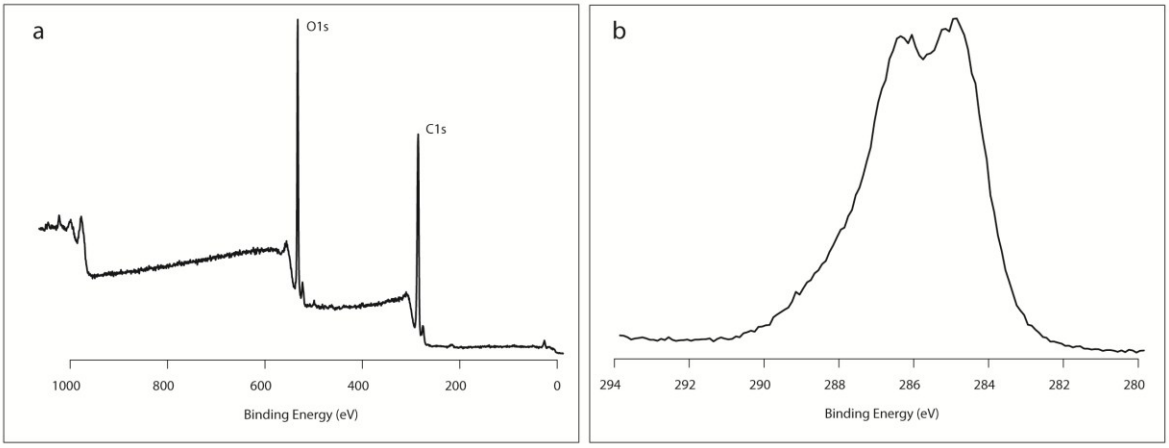

Figure 5.11: (a) An XPS survey spectrum showing the electron intensity (arbitrary units) (vertical) versus binding energy (horizontal) for untreated lodgpole pine with domination of C1s and O1s in the spectrum; (b) high-resolution C1s spectrum of the same sample

The most pronounced carbon (C1s) peaks for both wood species were C1 and C2 (Table 5.5), however, poplar showed lower C1 and higher C2 content in untreated samples compared to those in untreated lodgepole pine. C1 carbon atoms represent 56.23% and 37.99% of the carbon atoms at the surface of untreated lodgepole pine and poplar specimens, respectively (Table 5.5).

Table 5.5: O/C ratio and fractional area percent of C1s components for untreated and plasma-treated lodgepole pine and poplar wood specimens

Sample		O/C	C1%	C2%	C3%	C4%
Lp pine*	Control	0.40	56.23	29.01	10.98	3.78
	333 s	0.55	33.06	38.52	16.06	12.36
	667 s	0.59	32.52	40.25	15.49	11.74
	1333 s	0.55	34.12	39.94	14.27	11.67
Poplar	Control	0.38	37.99	39.92	18.63	3.46
	333 s	0.65	36.74	39.02	15.22	9.02
	667 s	0.45	40.66	39.72	12.53	7.09
	1333 s	0.68	33.63	41.98	16.38	8.01

* *Lp pine = lodgepole pine*

The contribution of C1 carbon in lodgepole pine samples significantly decreased as a result of plasma treatments. Increases in plasma treatment time caused oxygen containing carbon atoms (i.e. C2, C3 and C4 peaks) to increase suggesting oxidation and /or alteration of carbon-carbon and carbon-hydrogen structures in lodgepole pine (Table 5.5). Untreated poplar samples showed higher values for oxidized carbons compared to those in untreated lodgepole pine, however plasma treatment of poplar only increased C4 significantly. Plasma treatment also caused a decrease in C3 and slightly modified the amount of C2 in poplar (Table 5.5).

5.4 Discussion

5.4.1 Hypothesis

Based on my observations of the morphology of plasma treated wood surfaces and etching of lignin and cellulose models (Chapters 3 and 4, respectively), I hypothesized that plasma would alter wood's surface chemical composition. Furthermore, I anticipated that there would be greater degradation of wood's carbohydrates than lignin. The results of wet chemical analyses favorably support my hypothesis. Spectroscopy (i.e. FTIR and XPS) also indicated changes in surface chemistry of plasma treated wood. Plasma treatment is known to modify the surfaces of polymers (Wu 1982), but radical formation, bond cleavage and the degradation rate of individual polymers in a blend of polymers may differ depending on their molecular structures (Moss 1987, Reich and Stivala 1971). Consequently, to fully interpret my results one should take into account the detection range and limitations of the techniques used to analyze the chemical changes occurring at plasma modified wood surfaces. In this section I discuss my findings on the changes in surface chemistry of lodgepole pine and poplar samples due to plasma treatment and the extent to which they support my hypothesis.

Wet chemical analysis of wood veneers showed that the lignin content of wood was significantly influenced by plasma treatment and wood species. Plasma treatment increased the total and acid insoluble lignin content of wood as hypothesized, however, this increase was greater in poplar compared to that in lodgepole pine. Plasma treatment also increased the acid soluble lignin content of poplar, but, it had the opposite effect on the acid soluble lignin content of lodgepole pine. On the other hand, plasma treatment reduced the amount of total sugars in both species as hypothesized. Analysis of individual sugars in wood revealed that plasma reduced the levels of all the analyzed sugars in wood, however, there were interactions between

plasma treatment and species on the levels of individual sugars. These interactions occurred for galactose, mannose and xylose content because these sugars were reduced to a greater extent in poplar compared to lodgepole pine. FTIR analysis of plasma treated wood surfaces revealed that the areas under the peaks assigned to lignin increased relative to those in the control. Changes became more pronounced with increasing treatment time. Plasma treatment altered the ratio of lignin to carbohydrates peaks in poplar and lodgepole pine. The ratios of lignin associated bands to those of carbohydrates were higher in samples subjected to plasma treatment for prolonged periods of time. These observations accord with my findings of higher lignin and reduced sugar content of plasma treated wood. XPS analysis showed a general increase in oxygen to carbon ratio in plasma treated samples suggesting oxidation of wood surfaces as a result of plasma treatment. XPS results also support my hypothesis that plasma alters the surface chemistry of wood. FTIR and XPS spectroscopy revealed a relationship between chemical changes at wood surfaces and plasma treatment time, in accord with findings for the effects of plasma treatment time on the surface microstructure of wood.

The bands at 1600 cm^{-1} and 1510 cm^{-1} in the FTIR spectra of lodgepole pine (1595 cm^{-1} and 1505 cm^{-1} in poplar) are due to the stretching modes of lignin (aromatic skeleton vibration). These bands disappear as a result of wood delignification (Harrington et al. 1964). Hence, increases in the intensity of these bands indicate a higher lignin content at plasma treated surfaces. Furthermore, syringyl units in hardwood lignin absorb at 1230 cm^{-1} and guaiacyl units in softwood lignin absorb near 1230 cm^{-1} and 1268 cm^{-1} (Sarkanen et al. 1967). Hardwood lignin also contains guaiacyl moieties, however, the absorption band at 1268 cm^{-1} is suppressed by a strong absorption at 1230 cm^{-1} (Kuo et al. 1988). Accordingly, the development of a band at around 1230 cm^{-1} (labeled at 1225 cm^{-1}) in lodgepole pine and the increase in its intensity in

the spectra of plasma treated poplar samples, indicates an increase in surface lignin content. There was also some evidence of modification of lignin by plasma treatment. In the FTIR spectra of plasma treated samples there was a small decrease in the peak around 1260 cm^{-1} which is assigned to the C-O linkage of methoxyl group on guaiacyl aromatic ring (Harrington 1964, Sarkanen et al. 1967, Hergert 1971). A change to this lignin related band suggests a similarity between the effect of plasma and gamma radiation on the chemical composition of wood because demethoxylation of lignin is reported to occur during the radiolysis of wood (Seifert 1964). XPS spectra showed that C1 and C3 carbon peaks were changed as a result of plasma treatment. At wood surfaces, C1 and C3 peaks are mainly attributed to lignin (Gray 1978). In poplar both C1 and C3 carbon decreased at plasma treated surfaces which could indicate oxidation of lignin, however, this decrease only occurred for the C1 carbon in lodgepole pine and the C3 carbon increased in lodgepole pine. These XPS observations may appear inconsistent with the findings of increased lignin content of plasma treated wood that were obtained by wet chemistry or FTIR spectroscopy. This inconsistency may be due to the fact that changes detected by XPS are limited to the very upper surface of the wood rather than surface and sub-surface layers. On the other hand, it is clear from previous studies that lignin can be oxidized in oxygen-plasma environments (Toriz et al. 2000, Klarhofer et al. 2010). Oxidation of lignin in weathered and UV irradiated yellow poplar (*Liriodendron tulipifera* L.) wood also caused a reduction in the C1 carbon peak of XPS spectra (Gray 1978, Hon 1984). Accordingly, partial oxidation/degradation of lignin along with other wood constituents at the surface of plasma modified wood may account for the reduction of C1 carbon peak and higher phenolics found in aqueous extract of plasma treated samples compared to those of the control. The presence of an oxidized lignin fraction might also account for the increase in the peak at 1600 cm^{-1} in FTIR spectra of plasma

treated samples, since the ring stretch vibration related to quinone formation has been assigned to the peak at 1600 cm^{-1} (Kimura et al. 1994). The aqueous extract from plasma treated veneers contained only traces of sugars (mainly glucose), but phenolics were present in the extract, as mentioned above. Sugar analysis of the plasma treated veneers also showed lower carbohydrate content in plasma treated samples in both species. Thus it is conceivable that during plasma treatment the cellulose and hemicelluloses were degraded and removed before lignin. Hence, when plasma modified veneers were dipped in water, a degraded lignin fraction was leached into the water.

The small amount of glucose in the aqueous extract of plasma modified veneers probably arises more from the degradation of hemicelluloses rather than cellulose because hemicelluloses are more susceptible to oxidation and hydrolysis than cellulose (Fengel and Wegener 1984). For example, Kotilainen et al. (2001) found that monosaccharides associated with hemicelluloses (arabinose, galactose, mannose and xylose) were more readily degraded by heat than glucose (from cellulose), and they concluded that this was an indication of the greater susceptibility of hemicelluloses to degradation compared to cellulose. My results suggest that hemicelluloses were more susceptible to degradation by plasma than cellulose. This may be a result of their amorphous nature and lower molecular weights compared to cellulose (Goldstein 1991). Amorphous polymers without strong polymeric backbones exhibited greater degradation in oxygen-containing plasma compared to polymers that contained a strong backbone and aromatic rings (Taylor and Wolf 1980, Moss et al. 1986, Moss 1987). Overall my results indicated that the steady increase in relative mass proportion of lignin was accompanied by a simultaneous decrease in the relative mass proportion of carbohydrates during plasma treatment in poplar and to a lesser extent lodgepole pine. Lower losses of sugars during plasma treatment of lodgepole

pine compared to poplar could be due to the higher initial lignin content of lodgepole pine and the ability of lignin to reduce degradation of hemicellulose as observed in gamma irradiated redwood (Smith and Mixer 1959), or alternatively to the higher susceptibility of hemicelluloses in hardwoods to oxidation compared to hemicelluloses in softwoods (Sawabe et al. 1968).

The increase in the soluble portion of the total lignin content of poplar as a result of plasma treatment could be accounted for the solubilization of smaller fragments of lignin that do not condense in the acid fraction during hydrolysis (Browning 1967). Lignin solubilization involves both the breaking of lignin-carbohydrate bonds and lignin depolymerization reactions (Fengel and Wegener 1984). Lignin in wood occurs as a natural complex bonded to hemicelluloses, thus degradation of hemicelluloses is also linked to increase the soluble fraction of lignin (Azuma 1989). Cleavage of lignin/carbohydrate linkages in gamma irradiated wood was also suggested as a reason for increases in soluble lignin observed in irradiated wood (Hachihama et al. 1960). On the other hand, degradation of carbohydrates exposed to plasma or heat treatments was claimed to lead to the formation of unsaturated nonvolatile material which is UV-detectable, and this effect could contribute to the increase in acid soluble lignin content of wood as a result of plasma treatment (Hua et al. 1997, Denes and Young 1998, Zaman et al. 2000).

5.4.2 Relationship of findings to other studies

The aforementioned effects on plasma on lignin and carbohydrate content of wood can be compared with those occurring during the degradation of wood by brown rot fungi. These fungi preferentially degrade cellulose and hemicellulose and only modify lignin (Liese et al. 1970, Worrall et al. 1997). For example, changes in FTIR spectra of plasma treated lodgepole pine and poplar show similarities with spectra of Scots pine and European beech wood decayed by a brown rot fungus. Decay of these species by the brown rot fungus *Coniophora puteana*

((Schumacher) Karsten) is accompanied by increases in relative intensities of the absorption bands due to lignin at around 1560, 1510 and 1230 (Pandey and Pitman 2003, 2004). Degradation of polysaccharides in wood attacked by C. *puteana*, caused a reduction in the intensity of the band at around 1160 cm^{-1} (Pandey and Pitman 2004). A similar effect could account for the diminution of the bands around 1160, 1110 cm^{-1} in plasma treated wood here. Furthermore, Weiland and Guyonnet (2003) observed an increase in the intensity of the band at 1230 cm^{-1} in maritime pine wood (*Pinus pinaster* Ait.) degraded by the brown rot fungus (*Poria placenta*), as was observed for plasma treated wood here.

As mentioned above, I observed that oxygen-containing carbon atoms in XPS spectra of plasma treated veneers increased as a result of plasma treatment. Similar observations were made in studies of air and oxygen plasma treatment of mechanical pulp, greaseproof papers, corrugated medium and surfaces of white fir wood (Suranyi et al. 1980, Yuan et al. 2004, Lipska-Quinn 1994, Carlsson and Stroem 1991). Another study found a diminution of non-oxidized carbon atoms (C1) during corona treatment of cellulosic fibers, particularly after intense treatments (Belgacem et al. 1995). Such a change was thought to result from surface oxidation and formation of new carbon oxygen bonds (Belgacem et al. 1995). Nevertheless, changes observed with XPS can be affected by wood's chemical composition, which complicates interpretation of data. For example, the higher C1 carbon peak in untreated lodgepole pine and its greater reduction as a result of plasma treatments compared to those in poplar could result from the higher initial lignin content of lodgepole pine. The presence of extractives or contaminants at wood surfaces can also give rise to a C1 carbon peak (Johansson et al. 1999). For example, previous studies found that extraction of southern yellow pine,

ponderosa pine and Douglas-fir wood caused a decrease in the C1 carbon peak and an increase in the C2 carbon peaks in XPS spectra of wood surfaces (Ruddick et al. 1992, Denes et al. 1999).

My results also indicate similarities between the effects of plasma treatment and gamma irradiation on the chemical composition of wood. Both plasma and gamma radiation can cause bond scission and radical formation in polymer chains (Inagaki 1996, Myers Jr. 1973). The radicals produced in wood following exposure to plasma may be similar to those produced by exposure to high energy radiation. However, further reactions of the radicals depend on the chemical structure of the material (Inagaki 1996, Myers Jr. 1973). The effects of plasma on the chemical composition of wood are probably milder than those of gamma radiation because of the low energy level of electrons, ions and activated species in plasma compared to the active species in gamma radiation (Denes et al. 2004). Furthermore, modification of materials by plasma is restricted to the surface and therefore the bulk of the polymer is largely unaffected unlike wood exposed to gamma radiation (Boenig 1982). From this viewpoint, the degradation cause by plasma exposure is distinct from that caused by gamma radiation.

5.4.3 Limitations

The methods I used to examine chemical changes occurring at wood surface as a result of plasma treatment have some limitations. It was difficult to use FTIR spectroscopy to detect some chemical changes occurring at plasma modified wood surfaces because some of the different wood components have overlapping IR absorption bands. Furthermore, subtle changes in the FTIR spectra of plasma treated surfaces could not be directly linked to degradation of individual wood polymer. Change in spectra alone cannot be used as an absolute measure of chemical changes occurring at wood surfaces because of natural variation in the chemical composition of wood (Stenius and Vuorinen 1999). This problem was minimized here by collecting IR spectra

from the same area before and after exposure to plasma. As a result it was possible to see that changes in FTIR spectra due to plasma treatment were largely due to degradation of polysaccharides and also to increases in the concentration of lignin at treated surfaces. Another limitation of FTIR spectroscopy is that changes in the bands at particular wavenumbers can be interpreted differently. For example, generation of hydroxyl, carbonyl, and carboxyl groups in air-plasma treated lignin model (organosolv lignin) were detected using a variety of analytical techniques (XPS, UPS and MIES), which provided evidence for the oxidation of lignin according to Klarhofer et al. (2010). On the other hand, loss of hydroxyl groups and the formation of double bonds between carbon and oxygen in plasma treated glucose and cellobiose provides evidence for degradation of cellulose (Klarhofer et al. 2010). Reduction in the band at 3360 cm^{-1} which is assigned to OH stretching vibration in cellulose (due to intermolecular hydrogen bonding) was reported for FTIR spectra of ancient paper treated with oxygen plasma (Baeza and Freer 2001, Laguardia et al. 2005). I also observed a reduction in this band, which may indicate the degradation of cellulose. On the other hand, a reduction in the band at 3360 cm^{-1} can occur due to loss of OH groups following dehydration (Grandmaison et al. 1987, Tolvaj and Faix 1995). My observation of the disappearance of the small peak around 1640 cm^{-1}, which is associated with adsorbed moisture (Olsson and Salmén 2004) in FTIR spectra of plasma treated samples, strengthens the possibility that water loss occurs during plasma treatment. This conclusion is supported by the findings of Yildiz and Gümüşkaya (2007) who observed decreases in the band around 1640 cm^{-1} in thermally modified and also friction-welded wood (Delmotte et al. 2008). Nevertheless there is some ambiguity in this conclusion.

XPS analysis of plasma treated surfaces also had limitations. XPS of processed materials (such as plasma treated surfaces) especially those consisting of carbon and oxygen species (e.g.

wood), can be affected by surface contamination (Johansson et al 1999). In order to minimize the effects of surface contamination on XPS spectra, veneers were handled carefully and stored in clean containers. However, XPS spectra were collected from separate specimens exposed to plasma for different period of time. Because of this, comparison of XPS spectra from treated and untreated veneers is not as accurate as it could have been if spectra were collected from the same sample before and after exposure to plasma.

5.5 Conclusions

In the introduction to this chapter I hypothesized that plasma would alter wood's surface chemistry and cause greater degradation of carbohydrate than lignin. My results supported this hypothesis. Wet chemical analysis showed lower sugar content and proportionally higher lignin content in wood veneers treated with plasma. I found evidence that hemicelluloses were more susceptible to degradation than cellulose. My results also showed that chemical changes in wood induced by plasma treatment were influenced by wood species. Results from FTIR and XPS analysis of plasma treated wood provided evidence of an increased concentration of lignin at treated surfaces. Data obtained from these techniques also suggested that plasma modified and degraded lignin in addition to carbohydrates. Overall, I conclude that plasma degrades the principal polymeric constituents of wood. Carbohydrates in wood are more susceptible to degradation than lignin. Hence, the concentration of lignin at plasma treated surfaces is greater than that at untreated surfaces. This conclusion accords with observations in Chapters 3 and 4 on the resistance of lignin-rich middle lamella in wood to plasma etching and the greater resistance of lignin pellets to plasma etching compared to cellulose pellets. I also conclude that the hemicelluloses and lignin in the hardwood poplar are more susceptible to degradation by plasma than the hemicelluloses and lignin in the softwood lodgepole pine.

Based on abovementioned results, I also conclude that plasma produces chemical changes in wood that are similar to those reported in the literature for wood decayed by brown rot or subjected to gamma radiation.

6 Plasma etching and bleaching to remove blue-stain from lodgepole pine

6.1 Introduction

Blue-stain is an undesirable discoloration of wood caused by fungi belonging to Ascomycota (Fleet et al. 2001). Blue-stain fungi can cause a dark stain throughout sapwood because their hyphae are highly pigmented and penetrate deep into the wood's microstructure (via rays) (Lee et al. 1995, Fleet et al. 2001). Blue-stain can reduce the value of the wood in many appearance applications and some structural applications (Byrne et al. 2006, Schmidt and Czeschlik 2006). There is currently a great deal of blue-stained lodgepole pine lumber being manufactured in British Columbia because of a large infestation of pine forests by the mountain pine beetle (*Dendroctonus ponderosae* Hopkins) and associated ophiostomatoid fungi that cause blue stain (Whitney and Farris 1970, Stirling and Morris 2009).

Several studies have shown that the original color of blue-stained wood can be partially restored by bleaching the stain from affected wood surfaces. For example, Lee et al. (1995) reported that alkaline peroxide bleaching could remove some of the blue stain from ponderosa pine. Evans et al. (2007) found that a sodium hypochlorite bleach was effective at removing the blue-color from blue stained lodgepole pine. None of these bleaching techniques were able to completely remove the blue stain. Therefore, other techniques have been used to increase the effectiveness of bleaches at removing blue stain from wood. For example, Stirling and Morris (2009) examined the effect of short periods of UV exposure on the ability of sodium hypochlorite to remove blue-stain from lodgepole pine. They found that 10 minutes of intense light exposure following bleaching increased the removal of the blue stain.

Bleaching agents change the color of materials through electrophilic or nucleophilic reactions (Hihara et al. 2000). The blue-black color of blue stain fungi is due to the presence of small globules of melanin in hyphal walls (Zink and Fengel 1989). Another important constituent of hyphal walls is chitin. Chitin, like cellulose, is a fibrous polysaccharide, but it differs from cellulose because the C2 hydroxyl group in glucose is replaced by an acetamide function (Muzzarelli and Muzzarelli 1998, Voet et al. 1998). Polysaccharides such as cellulose and chitin can be modified using plasma treatments as an alternative to conventional modification techniques to obtain desirable polymeric properties, as mentioned above (Denes and Young 1998). For example, plasma can increase the porosity of wood and open up the bordered pits (Chen and Zavarin 1990, Jamali and Evans 2011). Cellulosic fibers can also be etched by plasma, and plasma treated fibers have higher surface area and greater porosity compared to untreated ones (Sapieha et al. 1988, Yuan et al. 2004). Accordingly, plasma treatments can increase the permeability of materials, including wood (Chen and Zavarin 1990, Johansson and Masouka 1999, Steen et al. 2002). In the case of blue stained wood it is conceivable that increases in the porosity of fungal hyphae as a result of plasma treatment could increase the accessibility of the bleach to the melanin that is responsible for the discoloration of blue stained wood. Increases in the permeability of wood as a result of plasma treatment might also allow bleach to remove blue stain from deeper within affected wood.

Hence I hypothesize here that plasma will etch and remove the chitin from hyphae of fungi in blue-stained lodgepole pine and plasma treatment will increase the ability of hypochlorite bleach to remove blue stain from blue-stained wood.

6.2 Materials and methods

6.2.1 Experimental design and statistical analysis

A randomized complete block design with one fixed factor (plasma treatment) at six levels (0 (vacuum), 33 s, 333 s, 666 s, 1000 s and 1333 s) was used to examine the effect of plasma treatment on the properties of blue-stained wood before and after bleaching. Six specimens were cut from each of twelve different boards. Analysis of variance was used to examine the effect of fixed and random factors (i.e. plasma treatments, boards) on the following response variables; contact angle, absorption of bleach, changes in color parameters (L*, a* and b*) and color difference (ΔE). Statistical computation was performed using Genstat v. 12 (VSN International 2009). Before the final analysis, diagnostic checks were performed to determine whether data conformed to the underlying assumptions of analysis of variance, i.e., normality with constant variance and, as a result of such tests, data for contact angle measurements were transformed into natural logarithms + 1 before analysis. Significant results ($p<0.05$) are presented in graphs which contain error bars (± standard error of differences of means) that can be used to compare differences between individual means. Appendix 4 contains all of the results of the statistical analysis of data for this Chapter.

6.2.2 Wood samples

Twelve lodgepole pine boards measuring 89 (tangential) x 38 (radial) x 2430 (longitudinal) mm^3 with their growth rings oriented tangentially to their wide faces were purchased from Home Depot in Richmond, British Columbia. Each board contained blue-stained sapwood. A block measuring 89 (tangential) x 38 (radial) x 200 (longitudinal) mm^3 was cut from each of these boards and six specimens measuring 20 (tangential) x 40 (longitudinal) x 3 (radial) mm^3 were cut from the sapwood of each of the blocks. Specimens were conditioned in a constant climate

room at 20 ±1 ºC and 65 ± 5% r.h. for 72 h, and allocated to the different plasma treatments from 33 to 1333 seconds including the control that was exposed to a vacuum.

6.2.3 Contact angle

Contact angle measurements are widely used to determine the surface energy of wood and changes in its wettability that occur as a result of plasma treatment (Podgorski et al. 2002). The effects of plasma treatments on the contact angle of a water droplet applied to the surface of blue-stained pine was assessed as follows. A 5 µL droplet of distilled water was placed on the wood surface before treatment using a syringe, after adjusting the needle of the syringe so that it produced a sessile drop (Podgorski et al. 2001). The static contact angle of the droplet on the sample was measured using a KSV CAM 101 instrument (KSV Instruments Ltd., Finland). The instrument includes a camera, an adjustable sample stage and a red (LED) background light (Fig. 6.1). Images of the droplet were captured for the first 20 second after the droplet was placed on the wood surface. Initially, for the first second, images were captured every 16 milliseconds (62 time frames). Thereafter, images were recorded every second. The tenth frame was used to calculate the contact angle that the water droplet made with the wood surface. The contact angles were calculated by baseline adjustment and curve fitting of the captured drop profile to the theoretical shape predicted by the Young–Laplace equation using instrument software (CAM 200, KSV Instruments 2007). Left and right contact angles were averaged to obtain a mean contact angle for each test. The contact angle was measured on three different locations for each specimen. The same locations on the surface were used to assess the contact angle after plasma treatment.

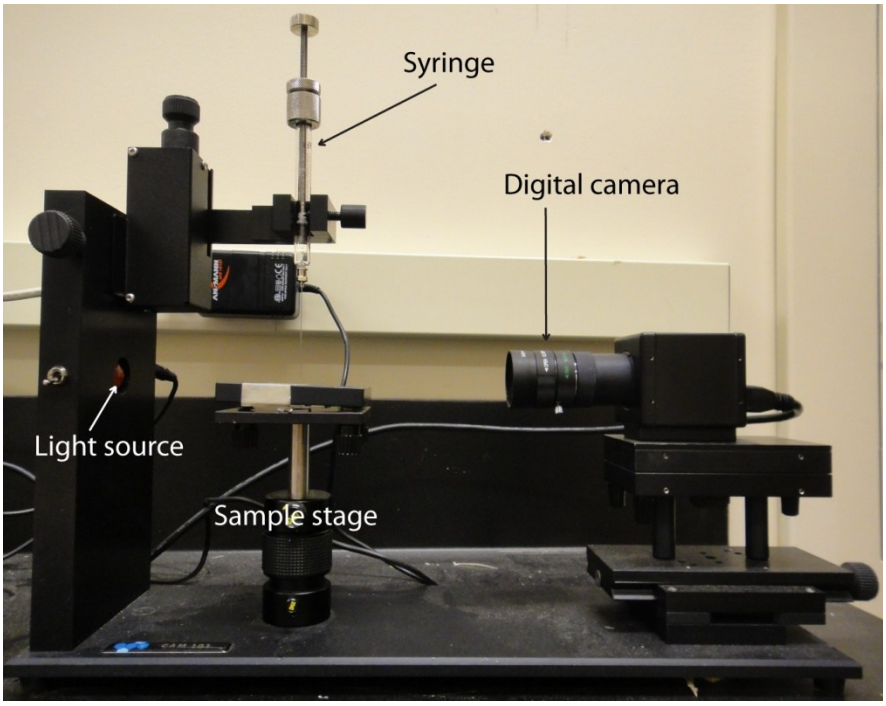

Figure 6.1: KVS instrument used for contact angle measurements of untreated and plasma treated blue stained wood

6.2.4 Bleaching

Plasma and vacuum-treated samples were weighed and then dipped in a fresh aqueous solution (50 mL) of 12% w/v sodium hypochlorite (Advance 12A, Canada) for 30 seconds. Treated samples were blotted with paper towels to remove excess bleach from wood surfaces. Samples were reweighed, and after 10 min they were sprayed with 20 mL of distilled water. Samples were air-dried in the laboratory for 24 hours and then conditioned for one week before measuring their color.

6.2.5 Color measurement

The color of the plasma treated and plasma treated and bleached samples was measured with a portable spectrophotometer (Minolta CM-2600d) and is expressed using CIE Lab color coordinates (CIE 1976). This system uses three parameters to express the color of materials: L*

(lightness on a scale of 0 [black] to 100 [white]), a* (+60 [red] to -60 [green]) and b* (+60 [yellow] to -60 [blue]).

The color of the blue stained wood was measured after they were conditioned, and remeasured immediately after plasma treatment. The color of bleached samples was measured after they were air dried and conditioned (as described above). The color was measured on three locations for each sample. A template was used to ensure that color measurements were made on exactly the same area before and after each treatment. The total color change, ΔE was calculated from CIE Lab parameters. ΔE is expressed as a distance between two points in the color coordinate system using the equation for the total color difference $\Delta E = (\Delta L^{*2} + \Delta a^{*2} + \Delta b^{*2})^{1/2}$, according to ASTM (ASTM D224, 2010),

where:

ΔL^* is the difference in lightness = $L^* - L^*_{initial}$

Δa^* is the difference in a* coordinate = $a^* - a^*_{initial}$

Δb^* is the difference in b* coordinate = $b^* - b^*_{initial}$

6.2.5.1 Light microscopy

Wood blocks measuring 30 (longitudinal) x 20 (tangential) x 20 (radial) mm^3 were cut from conditioned blue-stained lodgepole pine specimens. Both untreated and plasma treated blocks were vacuum (80 kPa) impregnated with water and then soaked in water for 3 days. Sections (25 µm thick) were cut from the radial and tangential surfaces of the blocks using a sledge microtome and disposable blade and holder, as described in Chapter 3. Untreated and plasma treated sections were placed on glass slides, and covered with ~ 1 mL of distilled water. A cover-

slip was placed over each section and the slides were examined using a light microscope (Carl Zeiss, Germany). Digital photographs of the sections at different magnifications (x4 to x40) were taken using a high resolution digital camera (Olympus DP71, Japan), and saved as bitmap files. Wood sections were also stained with safranin as in Chapter 3 (part 3.2.4), and examined using light microscopy, as above.

6.2.5.2 Hyphae collection and analyses

The fungus *Grosmannia clavigera* is the most common pathogenic fungus associated with mountain pine beetle infested lodgepole pine wood (Plattner 2008). Therefore, *G. clavigera* was chosen as the test fungus to study the effect of plasma on the morphology of fungal hyphae. Fungal cultures of *G. clavigera* were obtained from the Immunity Laboratory in the Forest Science Centre at UBC. The fungus was sub-cultured from mycelial margins on new malt extract agar plates. A layer of cellophane film was placed on the agar in each plate before the culture was added to the plates. This layer of cellophane film made it easier to collect hyphae from the plates. Several cultures were prepared by placing a 5 mm diameter agar plug in separate 150 x 15 mm (dia x h) Petri dishes. These Petri dishes were sealed using cellophane and stored for three weeks. Hyphae were collected from the top of the cellophane film using a sterilized micro spatula. These hyphae were placed in small vials containing 20 mL of sterilized nanopure water and agitated with a bench mixer (Vortex, Fisher Scientific) at 3000 rpm for 15 min. to obtain a homogeneous mix of hyphae and water. Each hyphal mix was then transferred into separate small glass Petri dishes (55 x 17 mm (dia x h)) and left in a fume hood for 48 hours to allow the water to evaporate. The Petri dishes were then placed in the plasma reactor and exposed to plasma for 667 s or to a vacuum for the same period of time. Petri dishes were removed from the reactor and hyphae were remixed with 20 mL of nanopure water. A droplet of treated and

untreated hyphal suspensions were each spread on separate aluminium stubs and air-dried for 48 hours. Stubs were coated with ~4 nm of gold using a sputter coater (Nanotech SEMPrep II) and examined using a variable pressure scanning electron microscope (Hitachi S-2600N, VPSEM) with an accelerating voltage of 5 kV. Secondary electron images of plasma modified and unmodified specimens were obtained from the microscope and saved as TIFF files.

Separate hyphae were collected from the treated and untreated hyphal suspensions using tweezers with the aid of a light microscope. Isolated hyphae were placed on a 200 mesh copper grid containing polyvinyl resin (Formvar ®) and a coating of carbon. These samples were examined and imaged using a transmission electron microscope (Hitachi H-7600 TEM) at an accelerating voltage of 80 kV. Images were saved as TIFF files.

6.3 Results

6.3.1 Effect of plasma on contact angle and color of blue-stained wood before and after bleaching

Table 6.1 summarizes the results of the statistical analyses of plasma treatment on wettability, bleach uptake and color of plasma treated and plasma treated and bleached blue-stained wood.

Analyses of variance showed that the contact angles of water droplets on the surface of plasma treated wood were significantly ($p<0.001$) lower than those of vacuum treated wood, as expected (Table 6.1).

Table 6.1: Summary of the results of analyses of variance of the effects plasma treatment on response variables: contact angle, bleach uptake and CIE Lab color parameters

Experimental Factor	**Response variable**					
	Contact angle (°)	Bleach absorption (%)	Color parameters			
			ΔE	a*	b*	L*
Plasma	***	n/a	***	NS	***	NS
Plasma followed-by bleaching	n/a	***	**	**	**	*

**** = p<0.05; ** = p<0.01; *** = p<0.001; NS = not significant (p>0.05); n/a = not applicable***

Figure 6.2 shows the effect of plasma treatment on the surface wettability (contact angle) of blue stained wood. The contact angles of water droplets on plasma treated samples were significantly lower than those of water droplets on the vacuum-treated controls. There was no difference in the contact angles of water droplets applied to wood surfaces exposed to plasma for different periods of time, except the contact angles of droplets on samples treated with plasma for 33 s were significantly ($p<0.05$) higher than those of droplets on surface exposed to plasma for periods of time greater than 333 seconds (Fig. 6.2).

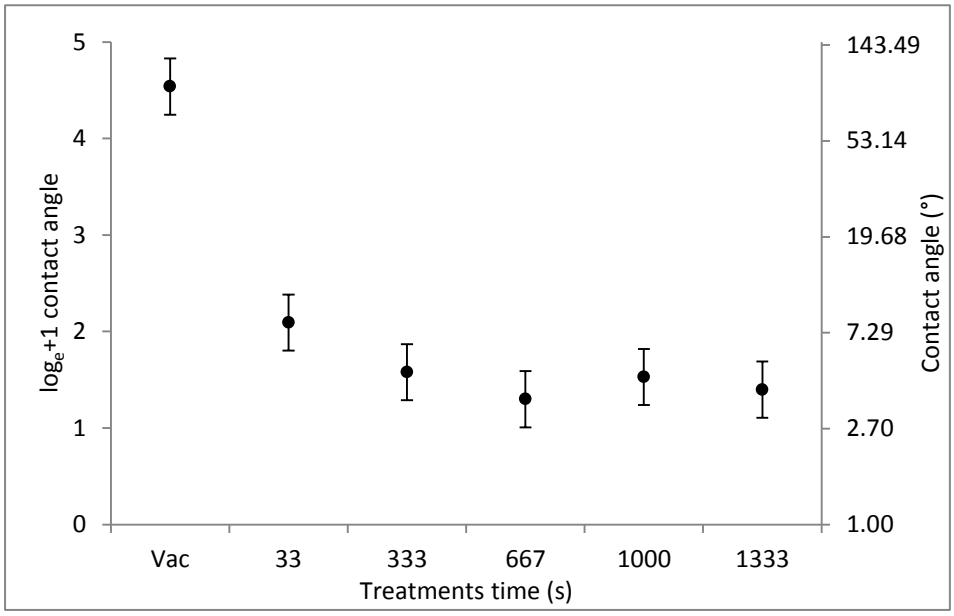

Figure 6.2: Effect of plasma treatments on contact angle of water droplets on blue-stained lodgepole pine sapwood (Y1 axis is expressed on a logarithmic scale, Y2 axis is back transformed e^x to compare results on the natural scale). Error bars are ± standard error of differences of means (from analysis of variance). Non-overlap of these bars indicates that means are significantly different at 5% level ($p<0.05$)

There was a significant ($p<0.001$) effect of plasma treatment on the absorption of bleach by blue-stained wood. Figure 6.3 shows changes in absorption of bleach by blue-stained wood as a result of plasma treatment. Plasma treatments for longer than 33 s significantly increased the bleach uptake by wood compared to that of untreated control. The absorption of bleach was positively correlated with duration of plasma treatment, up to 667 s, but thereafter for 1000 and 1333 s there was a slight (insignificant, $p>0.05$) decrease in the absorption of bleach by plasma-treated blue-stained wood (Fig. 6.3).

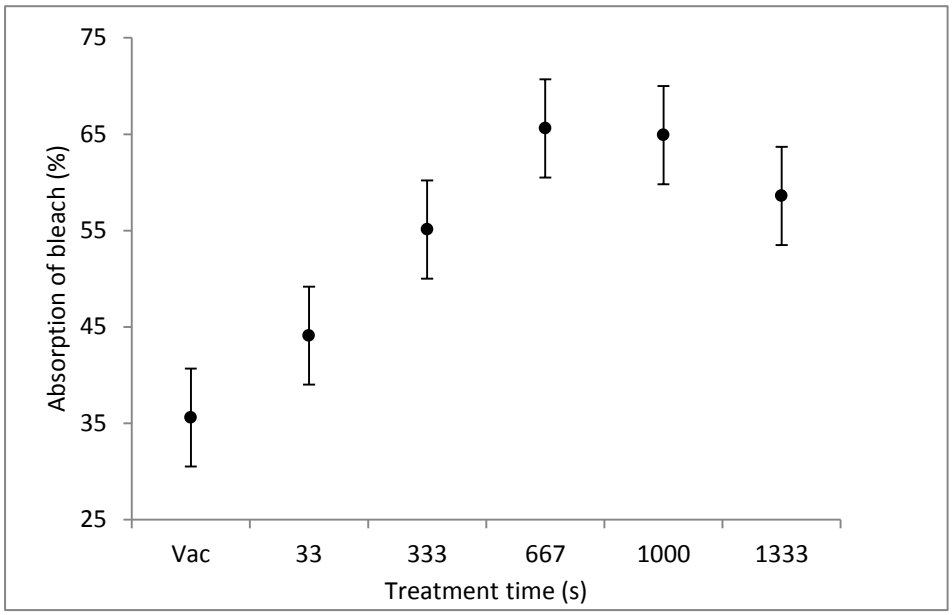

Figure 6.3: Effect of plasma treatments on the absorption of bleach by blue-stained lodgepole pine sapwood. Error bars are ± standard error of differences of means (from analysis of variance). Non-overlap of these bars indicates that means are significantly different at 5% level ($p<0.05$)

Plasma treatment alone without bleaching removed the blue color from blue-stained wood. Hence, plasma treatment had a significant effect on b* (yellowness) of blue-stained lodgepole pine, but there was no significant effect of plasma treatment on the L* and a* parameters. Increases in yellowness (b*) of the samples (i.e. decrease in blueness) were positively correlated with the length of time blue-stained samples were exposed to plasma. However increases in b* of plasma treated samples were only significantly greater ($p<0.05$) than that of the control for samples that were exposed to plasma for 1000 s or 1333 s (Fig. 6.4).

The effect of plasma treatment on the color difference of blue-stained wood (ΔE) was also statistically significant ($p<0.01$) (Table 6.1). Figure 6.5 shows total color difference of the blue-stained wood subjected to the different plasma treatments. This figure shows that ΔE of blue-stained wood treated with plasma for 1000 s or 1333 s were significantly greater than that of the vacuum treated control.

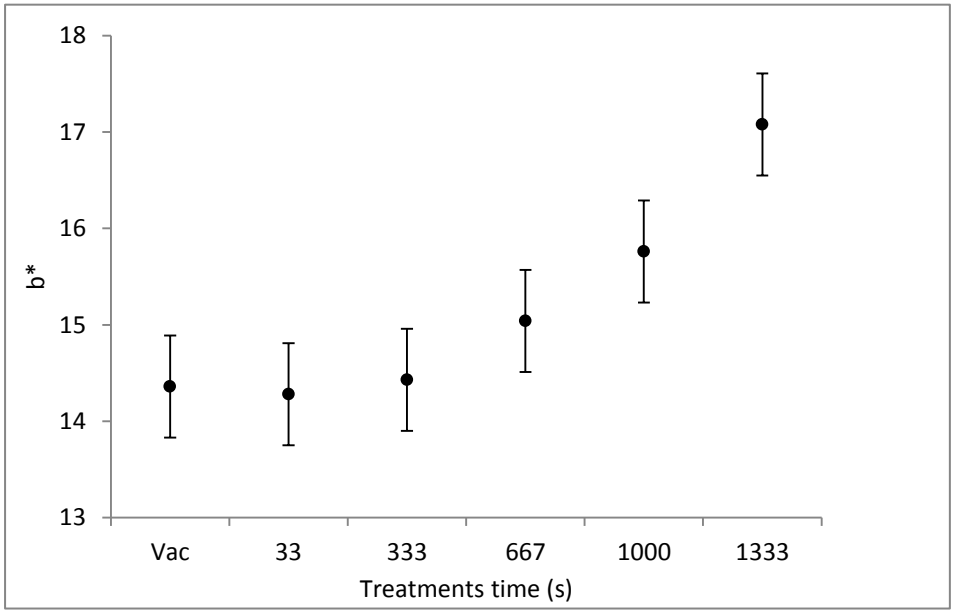

Figure 6.4: Effect of plasma treatments on the b* (yellowness) of blue-stained lodgepole pine sapwood. Increasing values for b* indicates the removal of blue discoloration. Error bars are ± standard error of differences of means (from analysis of variance). Non-overlap of these bars indicates that means are significantly different at 5% level (p<0.05)

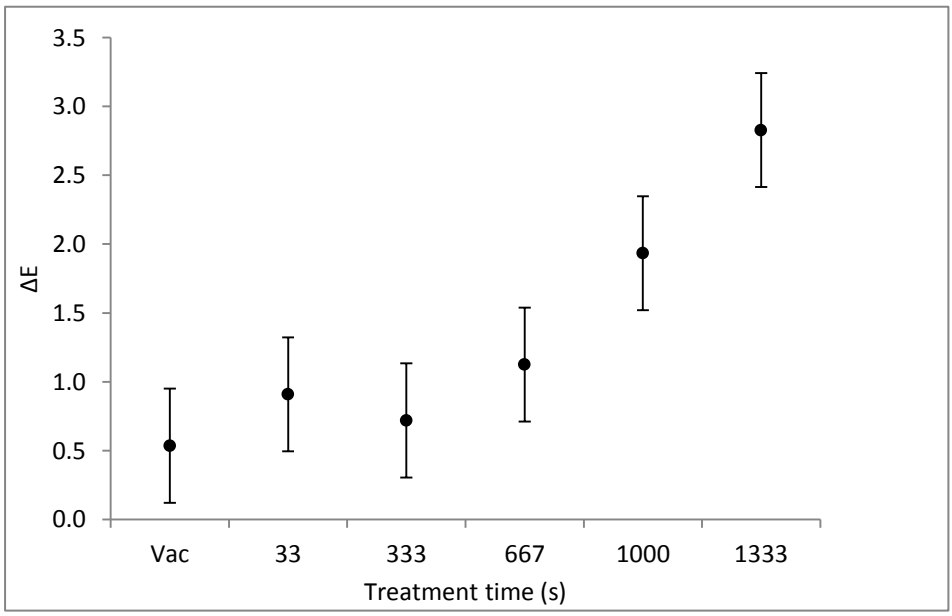

Figure 6.5: Effect of plasma treatments on ΔE (total color change) of blue-stained lodgepole pine sapwood. Error bars are ± standard error of differences of means (from analysis of variance). Non-overlap of these bars indicates that means are significantly different at 5% level (p<0.05)

The appearance of blue-stained wood after plasma pretreatment and bleaching was different from vacuum treated samples. The color of the samples exposed to plasma for 667 s and longer, and then bleached was comparable to that of unstained wood (Fig. 6.6).

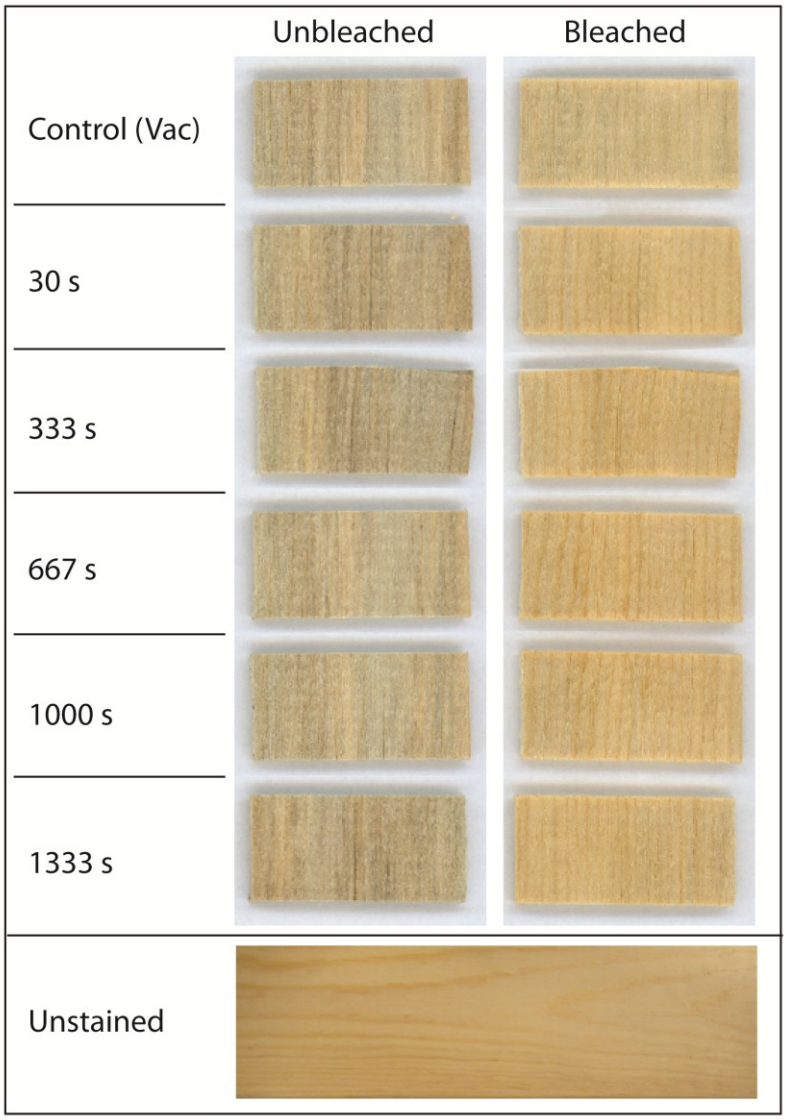

Figure 6.6: Changes in the appearance of blue-stained lodgepole pine sapwood specimens (left column) exposed to plasma for different periods of time (top to bottom) and bleached by sodium hypochlorite (right column), and a sample of unstained lodgepole pine sapwood (bottom of the image)

The combination of plasma treatment and bleaching had a significant effect ($p<0.01$) on total color change (ΔE) of blue-stained samples (Fig. 6.7). Figure 6.7 shows that ΔE was higher for the plasma treated and bleached samples compared to those that had only been exposed to vacuum. The greatest total color difference occurred for samples that were pre-treated with plasma for 667 s and 1000 s. Shorter or longer periods of exposure to plasma had smaller effects. However, the error bars of the means for plasma pre-treated samples overlap indicating that differences in their ΔE values are not statistically significant ($p>0.05$) (Fig. 6.7). To further examine the relationship between plasma pre-treatment and bleaching, changes in the individual color parameter (a*, b* and L*) of blue-stained samples were analyzed.

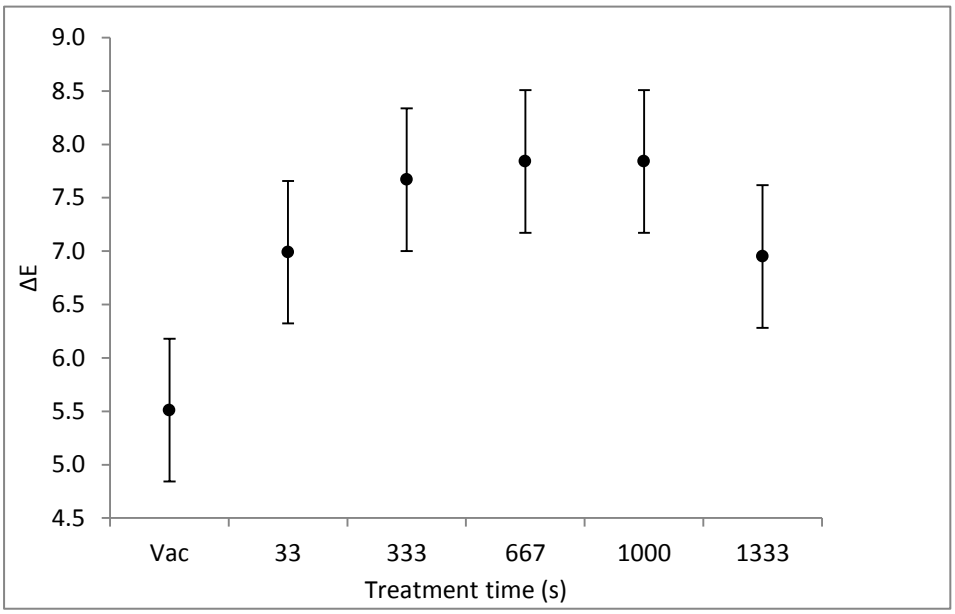

Figure 6.7: Effect of plasma treatments and bleaching on ΔE (total color change) of blue-stained lodgepole pine sapwood. Error bars are ± standard error of differences of means (from analysis of variance). Non-overlap of these bars indicates that means are significantly different at 5% level ($p<0.05$)

Plasma pre-treatment increased the redness (a*) and yellowness (b*), and slightly decreased the lightness (L*) of bleached samples. Figure 6.8 shows the effect of plasma pre-treatment time on the redness of bleached samples. The redness of pre-treated samples after bleaching was

significantly ($p<0.05$) higher than that of the vacuum treated bleached control (Fig. 6.8). The redness of samples increased with plasma pre-treatment time up to 333 s, then stayed constant, before declining in samples that had been pre-treated with plasma for 1333 s. However, differences in redness of plasma pre-treated samples were not statistically significant ($p>0.05$).

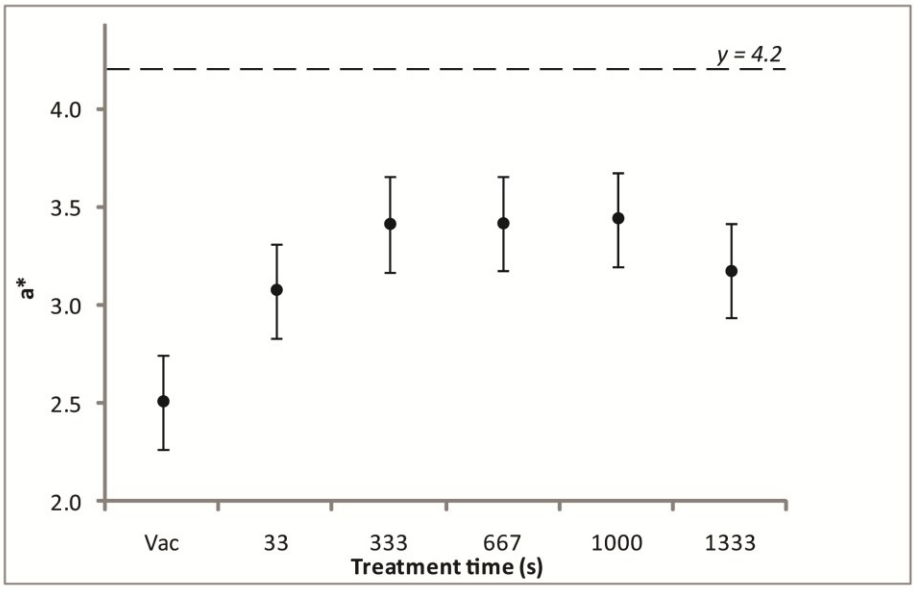

Figure 6.8: Effect of plasma treatments on the a* (redness) of bleached blue-stained sapwood; note, dotted line indicates a* of unstained pine sapwood. Error bars are ± standard error of differences of means (from analysis of variance). Non-overlap of these bars indicates that means are significantly different at 5% level ($p<0.05$)

The yellowness (b*) of bleached lodgepole pine was also significantly ($p<0.05$) higher in samples that were pre-treated with plasma compared to the vacuum pre-treated control (Fig. 6.9). Increase in b* was greatest in samples pre-treated with plasma for 333 s. Longer treatment times slightly ($p>0.05$) reduced b* with the lowest values for samples pre-treated for 1333 s in accord with the observation made for a*.

Plasma pre-treatment caused the lightness of bleached samples to decrease (Fig. 6.10). Decreases in lightness were statistically significant ($p<0.05$) in samples pre-treated with plasma

for longer than 33 s. There was no significant differences (p>0.05) in the lightness of samples pre-treated with plasma for longer periods of time (>333 s) (Fig. 6.10).

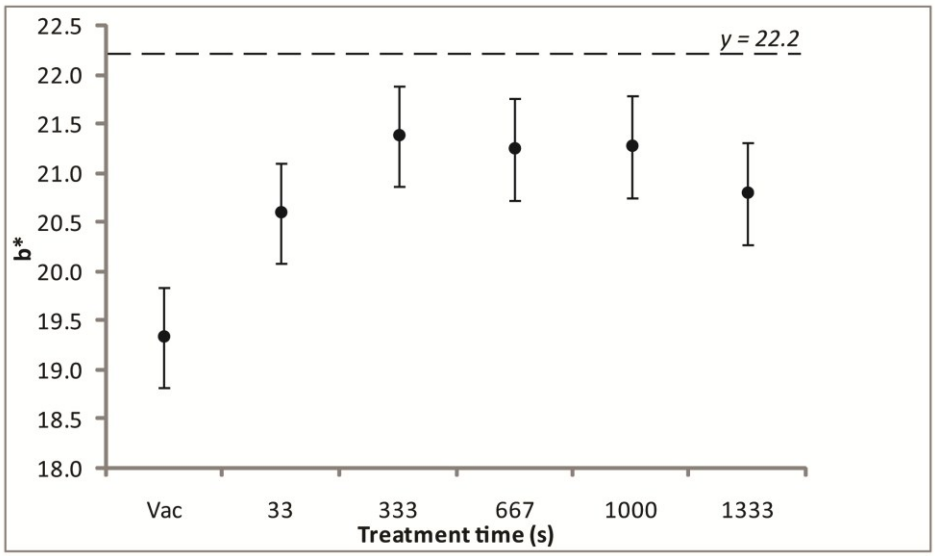

Figure 6.9: Effect of plasma treatments on the b* (yellowness) of bleached blue-stained sapwood; note, dotted line indicates b* of unstained pine sapwood. Error bars are ± standard error of differences of means (from analysis of variance). Non-overlap of these bars indicates that means are significantly different at 5% level (p<0.05)

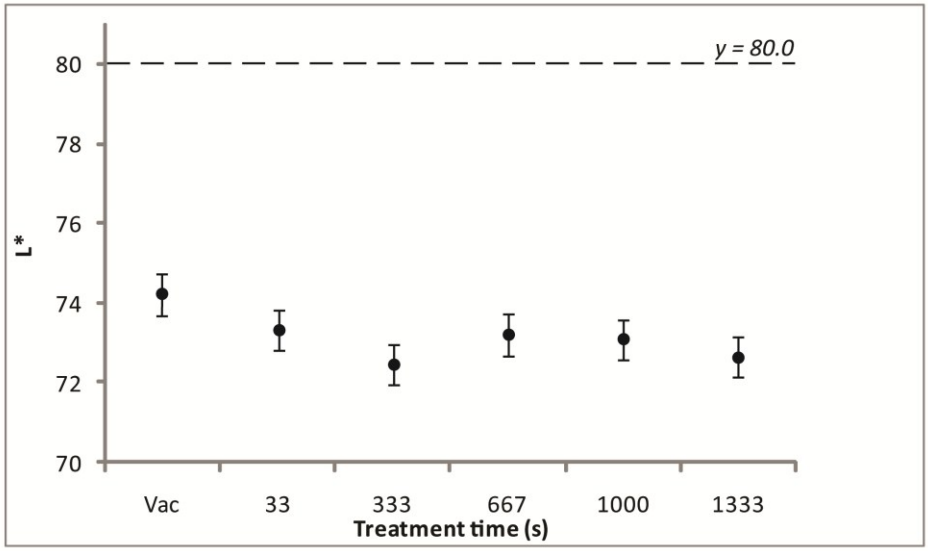

Figure 6.10: Effect of plasma treatments on the L* (lightness) of bleached blue-stained sapwood; note, dotted line indicates L* of unstained pine sapwood. Error bars are ± standard error of differences of means (from analysis of variance). Non-overlap of these bars indicates that means are significantly different at 5% level (p<0.05)

6.3.2 Effect of plasma treatment on the structure of fungal hyphae

Fungal hyphae were visible under the light microscope in both radial and tangential sections of blue-stained lodgepole pine sapwood, particularly when sections were stained with safranin (Fig. 6.11a and b).

Etching of wood cell walls by plasma was noticeable in both tangential and radial sections. Hyphae within tracheids were also etched by plasma, but the remnants of hyphae remained in plasma treated wood cells (Fig. 6.11c and d).The remnants of hyphae, however, appeared to be lighter in color compared to those in the untreated control.

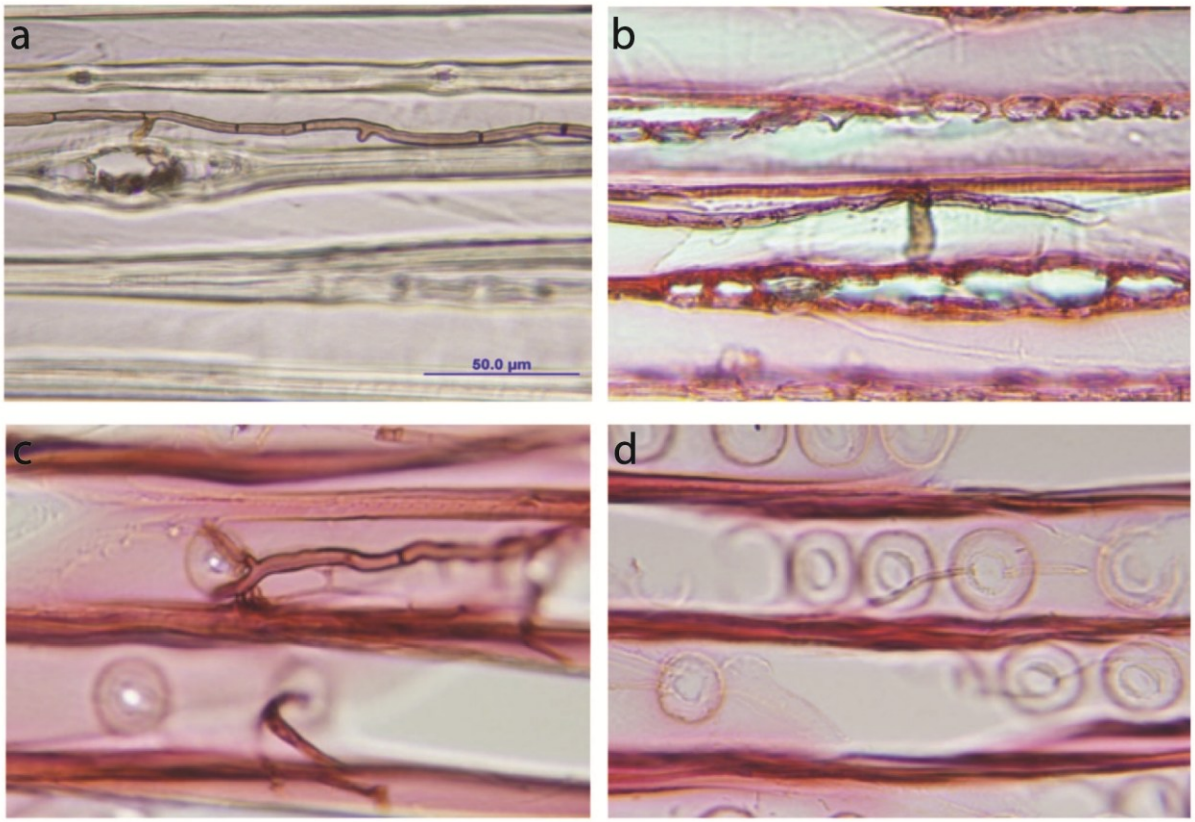

Figure 6.11: Transmitted light microscopy images of untreated and plasma-treated blue-stained lodgepole pine sapwood; (a) untreated tangential longitudinal section of untreated wood showing a fungal hypha running along a longitudinal tracheid and penetrating a ray parenchyma cell; (b) tangential longitudinal section exposed to plasma for 333 s, note that the hypha and ray (centre) have been etched by the plasma; (c) untreated radial longitudinal section showing fungal hyphae penetrating into bordered pits; (d) radial longitudinal section exposed to plasma for 333 s, showing etching of cell walls and hyphae, note that hyphae are much lighter as a result of plasma treatment

Scanning electron microscopy images of a hyphal mat before and after plasma treatment are shown in Figure 6.12. Untreated hyphae have a rough warty surface and are rectangular in cross-section (Fig. 12a). Plasma removed the walls of hyphae and opened up the hyphal tubes (compare Fig. 6.12a and b). The plasma degraded the hyphal mat to a depth of a few hyphae's thicknesses, and removed small fragments and debris from the surfaces of the mat. The density of the warts on the hyphae's wall appeared to be lower in plasma treated hyphae (compare Fig. 6.12a with 6.12b). Scanning electron microscopy of lodgepole pine wood also showed the etching of bordered pits and creation of voids in the cell walls of the tracheids in sapwood (Fig. 6.12e-f).

Further information on the ultrastructure of plasma treated and untreated hyphal walls was obtained using transmission electron microscopy (TEM). High magnification transmission electron microscopy images showed that untreated hyphae had a tubular shape and their surfaces were rough and covered in warts, in accord with the observation made with SEM (above). A high concentration of warts (granules) was present on the intact walls of untreated hyphae (Fig. 6.13a-b). Thinning and erosion of cell walls of hyphae occurred as a result of plasma treatments (Fig. 6.13b). Occasionally, plasma removed the granules from the cell walls of hyphae (Fig. 6.13d).

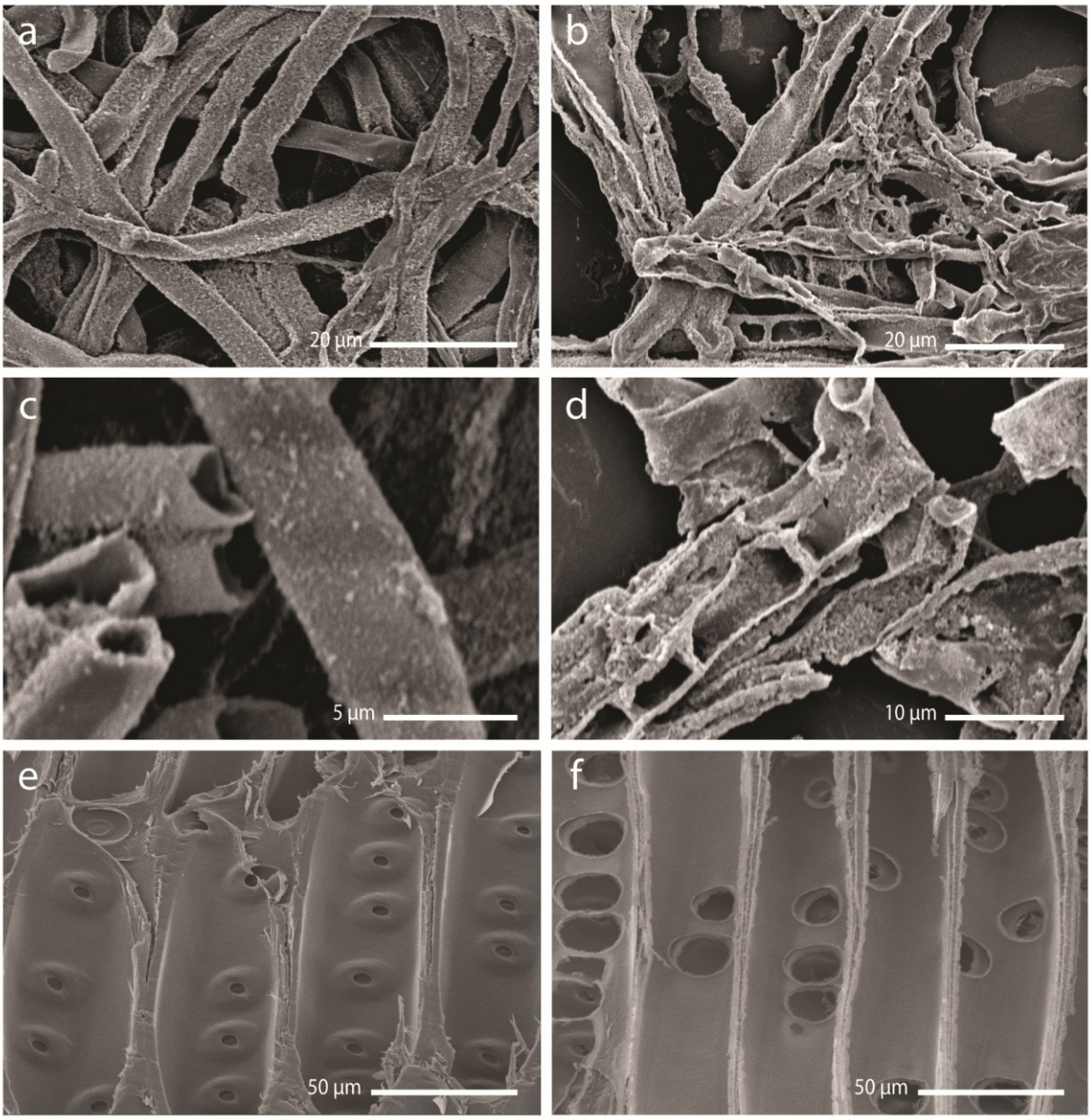

Figure 6.12: SEM photomicrographs of a hyphal mat of *Grosmannia clavigera*, which was grown for 3 weeks (a-d) and lodgepole pine wood (e-f): (a) untreated hyphae showing warty surfaces; (b) hyphae exposed to plasma for 667 s showing degradation of hyphae and exposure of internal hyphal walls; (c) higher magnification image of untreated hyphae showing their tubular shape and presence of globular granules on hyphal walls; (d) higher magnification image of hyphae exposed to plasma for 667 s showing removal (etching) of hyphal walls; and (e and f) radial longitudinal tracheids in the earlywood of lodgepole pine sapwood (R.L.S) before (e) and after exposure to plasma for 667 s (f), note etching of bordered pits by plasma and creation of voids at the surface of tracheids

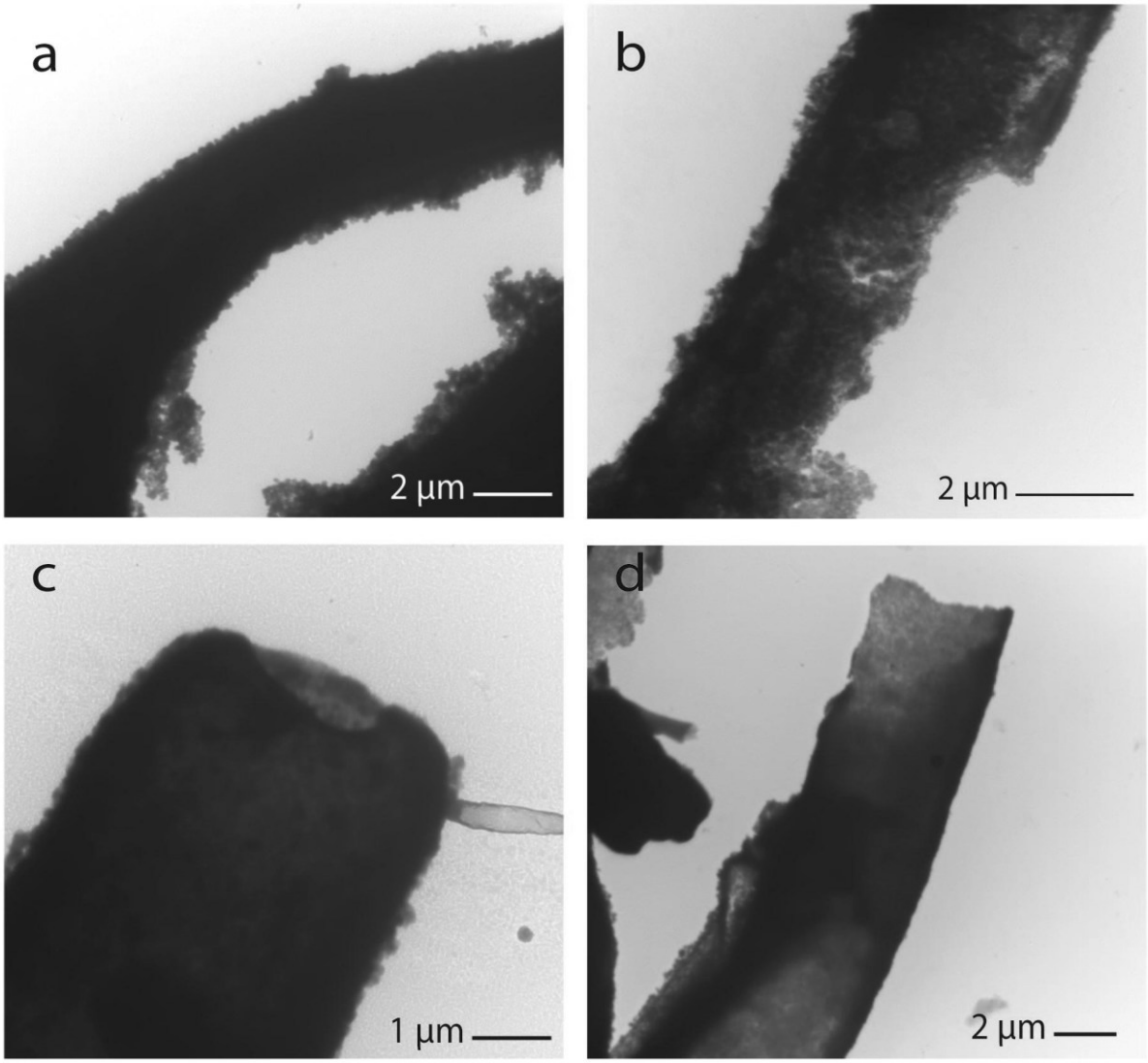

Figure 6.13: Transmission electron photomicrographs of a hypha of *Grosmannia clavigera* from 3-week old mycelium: (a) untreated hypha, note the rough warty layer on the intact wall; (b) a hypha exposed to plasma for 667 s showing erosion of its wall; (c) untreated hypha with a hollow tubular shape, note the globular granules; (d) hypha exposed to plasma for 667 s showing thinning of the wall and loss of electron density

6.4 Discussion

My results confirmed my hypothesis that plasma treatment can increase the effectiveness of sodium hypochlorite bleach at removing the discoloration from blue-stained lodgepole pine sapwood. However, the positive effect of plasma pretreatment on removing blue stain depended on the time that samples were exposed to plasma. My results also showed that the relationship between plasma pretreatment time and the removal of blue stain by bleach is not linear. For example, longer exposure times slightly reduced the effectiveness of bleach at removing blue stain. Plasma treatment on its own removed blue stain, but the combination of plasma treatment for 333 s to 1000 s and bleaching was much more effective at removing blue stain. Nevertheless, the color of the bleached wood was still different from unstained lodgepole pine. In particular, the lightness of plasma pretreated and bleached wood was lower than that of unstained wood.

Plasma treatment increased the wettability and permeability (bleach uptake) of blue-stained lodgepole pine. These findings accord with those of Chen and Zavarin (1990) who found that a radio frequency plasma increased the permeability of Douglas fir wood, and may explain why plasma treatment in combination with bleaching was more effective at removing blue stain than bleaching on its own. Previous research by Lee at al. (1995) showed that the removal of blue stain from ponderosa pine wood was limited by the inability of bleach to penetrate sub-surface layers. Etching of bordered pits and cell walls of plasma treated lodgepole pine explain increases in uptake of bleach. The greater accessibility of the bleach to the sub-surface of blue stained wood may explain why the combination of plasma pre-treatment and bleaching was effective at removing blue stain.

Etching of hyphae by plasma could also account for removal of blue stain by plasma (on its own) and such an effect could have contributed to the ability of the plasma/bleaching treatments

to remove blue stain. The blue-brown color of blue-stain fungal hyphal is due to the presence of melanin granules in the walls of hyphae (Zink and Fengel 1988). Melanins are complex dark-colored polymers that are associated with chitin in hyphal walls (Zink and Fengel 1990, Muzzarelli and Muzzarelli 1998). Breakdown of hyphae's walls and removal of melanin by plasma may explain why plasma treatment shifted the color of blue-stained wood from blue to yellow. The increase in total color difference (delta E) in plasma treated and bleached wood was mainly due to changes in b* (yellowness). Increases in b* values of blue-stained wood bleached with sodium hypochlorite have been observed previously (Evans et al. 2007, Stirling and Morris 2009).

The etching of hyphal cell walls by plasma showed some similarities to the etching of cellulosic fibers. Previous studies have shown that plasma can etch cellulosic microfibrils and change the morphology of fiber surfaces (Sapieha et al. 1988, Yuan et al. 2004, Vander Wielen et al. 2005). These studies showed that exposure to plasma modified the microstructure of fibers by opening up their pits and etching microfibrils. Plasma modification of filter papers resulted in a rougher surface, and fibers in the paper were etched to a depth of a few fibers (~50 μm) (Sapieha et al. 1988). I observed that plasma etched hyphal walls as well as bordered pits and cell walls in wood. Plasma was able to degrade hyphal walls and create new microstructures that extended a few hyphae deep in the hyphal mat. Chitin, like cellulose, is a fibrous polysaccharide and a derivative of glucose although chitin contains nitrogen in addition to carbon, hydrogen and oxygen (Muzzarelli and Muzzarelli 1998). Similarities in the chemical composition of chitin and cellulose, and the fact that both hyphae and fibers are hollow could explain why there are similarities between the etching of hyphae and cellulosic fibers. However, research on the

chemical composition of plasma treated chitin and melanin would be needed to better understand how plasma can remove the blue discoloration from blue-stained wood.

My finding that plasma can alter the color of blue-stained wood suggests further potential applications of plasma treatments for the removal of other types of stains that are found in wood, for example, those occurring due to the migration of extractives during kiln drying of wood (Kollmann and Côté 1968, Fengel and Wegener 1984).

My observations on the etching and modification of hyphal walls may also have practical implications. Hyphae are composed of chitin, which can also be obtained from shellfish (crab or shrimp). Chitin is converted into chitosan and other derivatives of chitin (Carroad and Tom 1978) that are used, for example, as drug carriers by the pharmaceutical industry (Kato et al. 2003). Chitin is industrially deploymerized using conventional wet chemical methods, however, attempts have been made to use more environmentally-friendly processes such as enzymatic depolymerization (Aam et al. 2010). Enzymatic depolymerization of chitin also has some disadvantages, such as the limited accessibility of chitin to enzymes, low yields and difficulties in controlling the process (Muzzarelli and Muzzarelli 1998). My observations of the ability of plasma to decompose hyphae, suggests that plasma-based processing should be explored as a potential alternative to the methods currently used to depolymerize chitin.

6.5 Conclusions

Plasma treatment increased the wettability and permeability of blue-stained lodgepole pine sapwood and removed some of the blue-discoloration from the wood. Plasma also modified the microstructure of pine, as observed above for redwood and yellow cedar (Chapters 3 and 4). Bleaching of blue stained wood by sodium hypochlorite bleach was significantly improved by plasma pre-treatments. The effectiveness of the pretreatment at removing blue stain was

influenced by the duration of plasma treatment. Plasma etched the hyphal walls of a blue-stain fungus and degraded melanin. Therefore I conclude that plasma treatments are able to remove the discoloration from blue stained wood and increase the effectiveness of a bleaching agent because they degrade and remove blue/black fungal hyphae, open-up bordered pits and enable more of the bleach to be absorbed by the wood. The development of plasma processing technologies capable of operating at high speed and at atmospheric pressure would create the opportunity for industry to apply my findings for the removal of the blue discoloration from blue-stained wood.

7 Effect of plasma etching on surface properties of hot-oil modified blue-stained wood[5]

7.1 Introduction

Thermal modification is used to increase the durability and dimensional stability of wood (Stamm et al. 1946, Homan and Tjeerdsma 2005). Thermally modified or heat-treated wood is currently commercially produced and marketed in Europe and North America mostly for non-structural applications (Hill 2006). Heat treatment, however, can adversely affect the mechanical properties of wood and the adhesion of paints and coatings to wood surfaces (Podgorski et al. 2000, Hakkou et al. 2005). Exudation of rosin from heat-treated wood is also a problem (Rapp and Sailer 2001). Therefore attempts have been made to heat-treat wood in the absence of oxygen (in an inert gas atmosphere or under hot oil or molten metal) (Hill 2006). Hot-oil treatments increase the wood's dimensional stability and decay resistance and can also mask the discoloration of wood caused by blue stain fungi (Sailer et al. 2000). Hot-oil treatments show promise as a way of masking the blue-stain in wood attacked by the mountain pine beetle (Wang 2007). However, hot oil treatments deposit oil in the wood's microstructure and this reduces the wood's surface energy, which may interfere with the adhesion of coatings to wood (Petrič et al. 2007). Therefore there has been interest in the development of methods to remove the

---

[5] Part of this Chapter is in a published report. Plasma treatment of oil-modified MPB wood. Jamali, A. and Evans, P.D. In: Coatability of thermal-oil-treated post-MPB, FPInnovations-Forintek Division, Canada (2008), pp. 48-58.

hydrophobic surface layer from wood that has been thermally modified with hot oil or wax (Kurt et al. 2008).

The methods used for the removal of oil and other organic contaminants such as grease, from the surface of wood and other materials, mainly involve the use of wet chemicals such as sodium or calcium hydroxide, hydrogen peroxide and hydroxymethylated resorcinol (Sernek 2002, Kurt et al. 2008). Surfaces are treated with these chemicals, which increase the surface energy of the material. However, the chemical by-products of the cleaning process are costly to dispose of and therefore, dry cleaning techniques such as plasma cleaning are preferred (Egitto 1996; Petrič et al. 2007).

Plasma can increase the surface wettability of wood that has been thermally modified in air (Podgorski et al. 2000), and plasma derived from inorganic gases can remove oils from the surface of materials (Nickerson 1998). Vegetable oils (such as soybean oil) that are used to heat treat wood consist largely of a mixture of triacylglycerols (also called triglycerides) (Voet et al. 1999). Excited particles in plasma can react with the surface layer of such hydrocarbons, and oxidize them to form water and carbon dioxide. These chemicals are desorbed from the surface and removed by the vacuum pump employed by plasma devices (Egitto 1996).

Accordingly, I hypothesized that plasma will be able to break down and etch away vegetable oil deposited at the surface of blue-stained wood that has been thermally modified using hot oil. The removal of residual oil from the thermally modified blue-stained wood surfaces may improve wood properties such as wettability and the adhesion and performance of coatings.

7.2 Materials and methods

7.2.1 Experimental design and statistical analysis

Two experiments were carried out to examine the effect of plasma treatment on the surface properties (Experiment 1) and exterior performance of coatings on hot-oil modified wood (Experiment 2).

The first experiment examined the effect of two fixed factors: (1) plasma treatment and (2) coatings type on the contact angle and adhesion of coatings on hot-oil modified blue-stained lodgepole pine sapwood. A thin veneer of wood was cut from each of five hot-oil modified blue-stained pine sapwood blocks (see below). These blocks provided replication at the higher level. Each veneer was then subdivided into five equally-sized slats, which were allocated at random to the different plasma treatments: (1) 0 s (only vacuum); (2) 33 s; (3) 333 s; (4) 667 s; and (5) 1333 s. Each slat was cut into four specimens which were allocated at random to four different coatings: (1) acrylic latex, (2) polyurethane, (3) supernatural and (4) cetol. Specimens finished with the different coatings were then sawn in two and allocated to either dry or wet adhesion tests (200 specimens in total). The resulting split-plot design accounted for random variation between blocks and between and within specimens. Analysis of variance was used to assess the effect of fixed and random factors on contact angle of water droplets on plasma treated samples, water uptake of specimens and coating adhesion (wet and dry).

A second experiment examined the effect of two fixed factors: (1) treatment (vacuum, plasma treatment, hot-oil treatment, hot-oil/plasma treatment); and (2) coating (five different coating types) on the performance of coated specimens exposed to natural weathering. Four conditioned blue-stained boards (four experimental blocks) were each sawn into two smaller blocks (eight blocks in total). These blocks were randomly assigned to “weathering” (or the non

weathered controls). These smaller blocks were then sawn into four samples and randomly allocated to the following treatments: (1) vacuum; (2) plasma treatment; (3) hot-oil treatment; and (4) hot-oil/plasma treatment. Five equal sized specimens were cut from each sample and were randomly assigned to five different coatings. An appropriate analysis of variance was used to assess the effect of plasma treatment and coating type and random factors on the following response variables: (1) total color change; (2) surface gloss; (3) water uptake of weathered wood; and (4) cracking of weathered samples (see below).

Statistical analysis of data from the abovementioned experiments was performed using Genstat v. 12 (VSN International 2009) after the underlying assumptions of ANOVA, i.e., normality and equal variance of residuals, were tested. As a result of such tests, data for contact angle were transformed into natural logarithms and analyzed as logarithms. Significant results ($p<0.05$) are presented graphically and least significant difference (lsd) bars or ± SED bars on graphs can be used to compare differences between individual means. Appendix 5 contains all of the results of the statistical analysis of data for this Chapter.

7.2.2 Wood samples

Blue-stained lodgepole pine boards with their growth rings oriented tangentially to their wide faces, were purchased from Home Depot in Richmond, British Columbia. Samples measuring 38 (radial) x 89 (tangential) x 240 (longitudinal) mm^3 and free of defects such as knots and cracks, were cut from the boards. The samples were kept in a conditioning room at 20 ± 1°C and 65 ± 5% for one week.

For the first experiment, five conditioned blue-stained pine blocks (described above) were hot-oil modified (see below). One veneer was cut from the tangential face of each of these modified blocks. Each veneer was cut into five samples measuring 3 (radial) x 38 (longitudinal)

x 66 (tangential) mm^3 using a band saw. Then each of these samples was sub-devided into four specimens by sawing three parallel grooves into the surface of each sample to delimit areas measuring 15 x 38 mm^2. Each coated area was sawn into two prior to measuring the dry and wet adhesion of coatings that were applied to the different areas (see below). Figure 7.1 shows a schematic diagram of the cutting pattern used to produce veneers, samples and specimens.

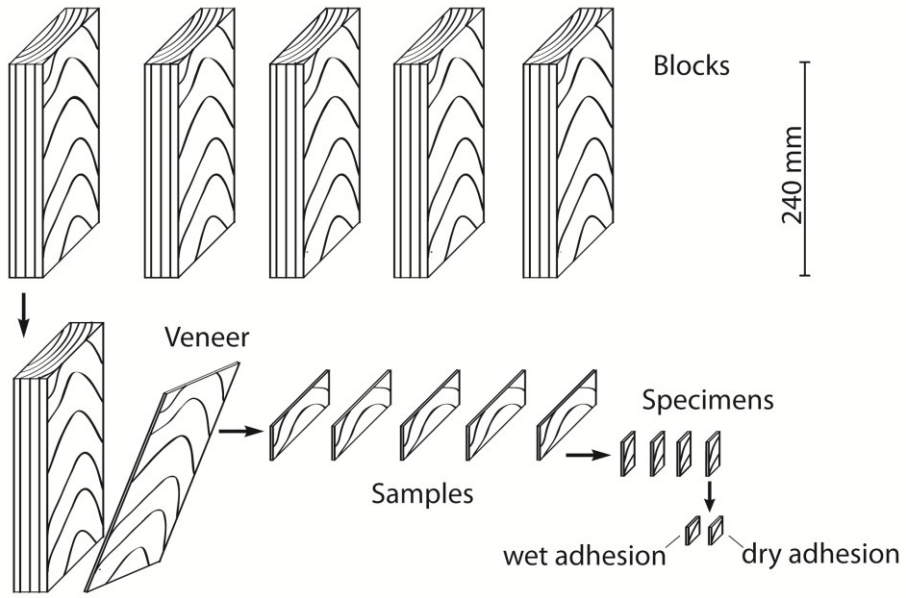

Figure 7.1: Schematic diagram of the cutting pattern used to prepare veneers, samples and specimens from hot-oil modified blue-stained lodgepole pine sapwood blocks

For the second experiment eight conditioned blue-stained lodgepole pine sapwood blocks were cut into four samples measuring 38 (radial) x 89 (tangential) x 55 (longitudinal) mm^3. These samples were assigned to the following treatments: (1) hot-oil modification (on its own); (2) plasma treatment (on its own); (3) hot-oil modification followed by plasma treatment; and (4) untreated control. Each treated sample was sawn using a band saw into a thin veneer measuring 3 (radial) x 55 (tangential) x 89 (longitudinal) mm^3. Four parallel grooves were sawn into the surface of each sample to delimit areas measuring 17 x 55 mm^2. The different coatings were

subsequently applied to these areas. Figure 7.2 shows a schematic diagram of the cutting pattern used to produce samples, veneer and specimens.

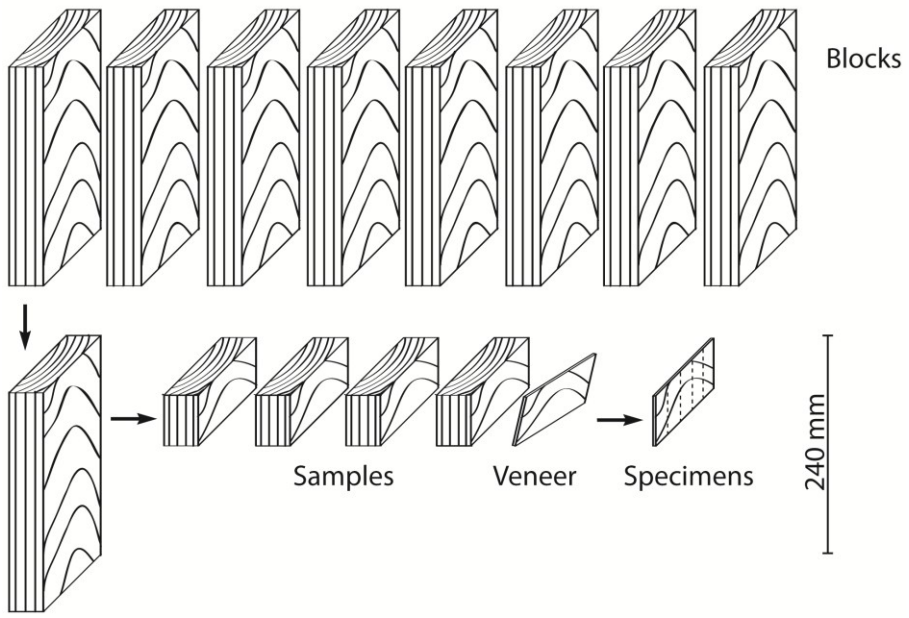

Figure 7.2: Schematic diagram of the cutting pattern used to produce samples, veneer and specimens from blue-stained lodgepole pine sapwood blocks

7.2.3 Hot-oil modification of blue-stained sapwood and plasma treatments

Wood samples were thermally modified by placing them in a pre-heated (220 °C) circulating oil-bath (Thermoline, Australia) containing soybean oil. Wood samples were removed from the oil bath after 2 h and blotted on paper towels to remove excess oil. Each hot-oil modified and unmodified blue-stained wood block was cut into a veneer, 3 mm thick using a band saw (see above). For the first experiment each veneer was then cut in the longitudinal direction to obtain samples for subsequent experimentation (Fig. 7.1). These samples were treated with plasma one at a time. Plasma treatment times varied from 33 s to 1333 s. Samples subjected to vacuum acted as controls. For the second experiment samples were exposed to

plasma for 667 s. After treatment, samples were removed from the plasma chamber, taking care to avoid touching and contaminating their upper surfaces.

7.2.4 Contact angle measurement

The wettability of the hot oil-modified and/or plasma treated wood was assessed by measuring the contact angle of 5 μL droplets of distilled water on three spots on the surface of treated wood (as described in Chapter 6 part 6.2.3). Droplets were wiped from the surface of specimens and each of the four areas within the specimens was brush coated with their assigned coatings.

7.2.5 Scanning electron microscopy and confocal profilometry

Scanning electron microscopy was used to examine the effects of hot-oil modification and plasma treatment on the microstructure of blue-stained sapwood. Four types of specimens were prepared using procedures described in Chapter 3 (part 3.2.1) as follows: (1) hot-oil modified blue-stained sapwood; (2) hot-oil modified blue-stained sapwood that was plasma treated for 333 s; (3) hot-oil modified blue-stained sapwood that was plasma treated for 1333 s; and (4) untreated blue-stained sapwood, which acted as a control. Treated specimens and the control were sputter coated with an ~8 nm layer of gold using a sputter coater (Nanotech SEMPrep II) and they were then examined using a Hitachi S-2600 variable pressure scanning electron microscope at accelerating voltages of 5 or 6 kV.

A chromatic confocal profilometer was used to probe the surface structure of hot-oil modified and plasma treated blue-stained sapwood. Specimens measuring 3 (tangential) x 15 (radial) x 30 (longitudinal) mm^3 were cut from the radial surface of different blocks and an area measuring 1.5 x 1.5 mm^2 was scanned and imaged using an AltiSurf 500 profileometer (as

described in Chapter 4, part 4.2.5). These samples were then treated with plasma, and the same area on the surface of the samples that had been imaged before was re-imaged. The software Papermap was used to produce topographical images of oil-modified and plasma treated wood surfaces.

7.2.6 Application of coatings and measurement of coating adhesion

The wet and dry adhesion of a range of coatings to hot-oil modified wood (first experiment) was assessed. The coatings were applied to the modified wood according to manufacturer's instructions. Table 7.1 summarizes the names and types of coating applied to the surface of hot-oil modified and/or plasma treated specimens.

Table 7.1: Selected coatings that were applied to hot-oil modified blue-stained wood after treating the surface with plasma for different periods of time

Coating type	Carrier	Product	abbreviation	Company
Film forming	Water	Exterior acrylic latex primer (1 coat) and paint (1 coat)	ACL	CIL Dulux
	Solvent	Polyurethane boat finish (2 coats)	PUR	Coelan
Non-film forming	Water	Supernatural semitransparent (2 coats)	SNS	Napier
	Solvent	Cetol 1 (1 coat) + Cetol 23 plus (1coat)	C123	Akzo Nobel

The samples used for the wet adhesion test (100 specimens) were sealed on their uncoated faces and edges with two-part epoxy resin (Industrial Formulators, G2) to reduce water uptake into uncoated areas.

After curing for 2 days, samples were weighed, floated on water on the coated (painted) side for 72 h and reweighed. The dry and wet adhesion of the coatings on plasma treated wood was

assessed using a cross-hatch tape test (ASTM 1976). Specimens were held firmly in a jig and then six cross-cuts, 1 mm apart, were manually inscribed on the coated surface using a scalpel and a steel ruler. Detached flakes or ribbons of coating were removed from coated surfaces with a soft brush. A strip of pressure-sensitive tape (3M Pressure-sensitive adhesive packaging tape) was placed over the cross-hatched area and then pulled off as described in ASTM (D 3359, 1976). The cross-hatched area was scanned using a desktop scanner and digital (TIFF) images were obtained. These images were used to rate the adhesion of coatings on each piece ranking them from 5 to 0 (Table 7.2).

Table 7.2: Description of ASTM (D 3359) classifications for the cross-cut adhesion of coatings to tested substrates

ASTM tape test classification	Area of coating removed from the cross-cut area (%)	Adhesion strength
5	0	Complete adhesion
4	<5	Very good
3	5-15	Good
2	15-35	Poor
1	35-65	Very poor
0	>65	No adhesion

For the evaluation of performance of coatings on modified specimens during natural weathering (second experiment, described above), the five areas within each specimen were brush coated with the coatings listed in Table 7.3 in accord with manufacturer's instructions. Figure 7.3 shows coated samples during conditioning and before the weathering test.

Table 7.3: Selected coatings for the outdoor weathering test that were applied to the blue-stained lodgepole pine sapwood samples, including untreated, hot-oil modified, plasma treated and hot-oil/plasma treated wood

Coating type	Carrier	Product	Abbreviation	Company
Film forming	Water	Exterior acrylic latex primer (1 coat) and paint (1 coat)	ACL	CIL Dulux
Non-film forming	Water	Natural deck oil (2 coats)	NDO	Silva Timber
		Semitransparent wood finish and sealer (1 coat)	SFS	Behr
	Solvent	Natural wood UV plus finish (1 coat)	UVP	Messmer's
		Premium oil-based deck stain (1 coat)	OBS	Behr

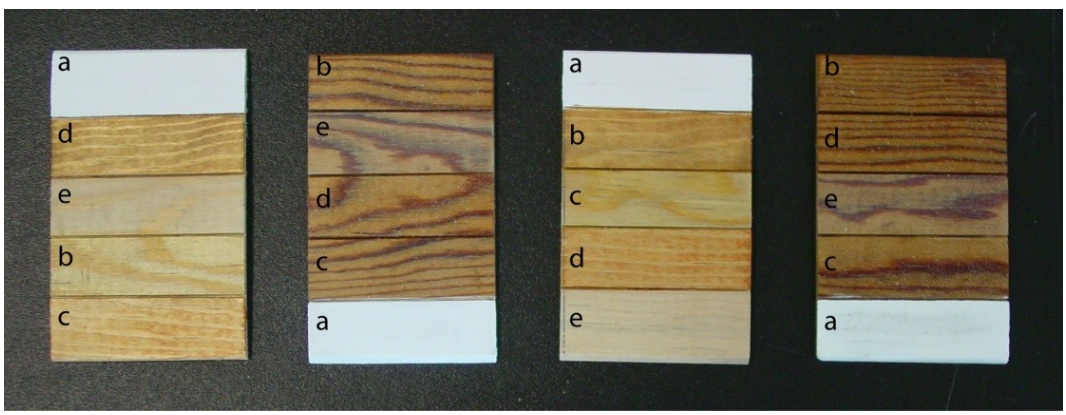

Figure 7.3: A set of specimens including (from left to right) control; hot-oil/plasma treated; plasma treated; and hot-oil modified (five coatings were applied on delimited areas on each specimen at random; a = Acrylic latex; b = Natural deck oil; c = Natural wood UV plus finish; d = Semitransparent wood finish; e = Premium oil-based deck stain)

7.2.7 Exposure of specimens to natural weathering and evaluation of coating performance

Edges and grooves on the coated samples were sealed using epoxy resin (Industrial Formulators, G2). The samples were then attached to glass backing plates (750 mm (L) x 120 mm (W)) and secured against the glass plates by clamping the edges of the samples between two glass strips (~20 mm wide) using alligator clamps. Samples were exposed to the weather on a rack inclined at 45˚ to the vertical and facing south in Vancouver, BC, Canada for a period of 18 months starting August 22nd, 2007. The meteorological conditions during the natural weathering trial are shown in Table 7.4. A matching set of samples was kept in a conditioning room for the duration of the weathering trial.

After the natural weathering trial, specimens were removed from the weathering racks, lightly brushed using a soft brush to remove dust or dirt and then kept in a conditioning room for one week. The surface properties of the coatings on the weathered and non-weathered samples were then evaluated, including, color (L*, a* and b*), gloss (G*), water absorption and presence of cracks.

The color of samples was measured in the middle of each sample using a Minolta CM-2600d spectrophotometer, as described above (Chapter 6, part 6.2.5). Surface gloss was measured using a HWS 5820 gloss meter (Micro-TRI-Gloss meter, USA) using an incident angle of 85º.

The water absorption of coated samples (weathered and controls) was measured as follows. Samples were weighed using an analytical balance and a 100 µL droplet of distilled water was placed on each sample using a single-channel pipette. After 60 seconds, the water droplet was wiped off the surface of the sample with soft paper tissue and the sample was re-weighed. The weight of water absorbed by the surface was calculated (Kiguchi et al. 2005). The total color

changes (ΔE) of coated surfaces were calculated from the measurements of CIE Lab color parameters (L*, a* or b*) made on weathered and non weathered surfaces as described above (Chapter 3, part 6.2.5). Data for surface gloss and water absorption are expressed as the ratio of the values of weathered wood to those of non weathered wood (Table 7.5).

Table 7.4: Meteorological conditions at the site in Vancouver where coated specimens were exposed to the weather (August 2007 to March 2009)

Month	Mean Max Temp (°C)	Mean Temp (°C)	Mean Min Temp (°C)	Highest Temp (°C)	Lowest Temp (°C)	Total Rain (mm)	Total Snow (cm)	Total Precip. (mm)
Aug (07)	21.9	17.8	13.6	26.7	11.3S	8.4	0.0	8.4
Sep	17.6	14.2	10.8	22.4	6.2	73.6	0.0	73.6
Oct	12.4	9.6	6.7	17.3	1.5	155.2	0.0	155.2
Nov	8.9	5.9	2.8	12.8	-3.3S	116.2	Trace	116.2
Dec	5.8	3.2	0.6	12.9	-5.3	181.6	19.6	210.6
Jan (08)	5.5	2.8	0.1	10.3	-4.9	122.2	14.2	137.6
Feb	8.6	5.5	2.4	14.1	-2.9	67.4	0.8	68.6
Mar	9.1	5.9	2.7	11.6	-1.0S	72.8	2.4	75.2
Apr	11.3	7.6	3.8	18.8	-2.1	56.8	2.2	62.2
May	16.6	12.8	8.9	29.0	3.3	43.2	0.0	43.2
Jun	18.0	14.4	10.8	26.9	6.7S	43.0	0.0	43.0
Jul	22.3	17.8	13.2	26.2	10.6	15.8	0.0	15.8
Aug	21.7	17.8	13.8	28.5	9.3	75.8	0.0	75.8
Sep	18.2	14.6	10.8	24.5	6.9	30.6	0.0	30.6
Oct	13.3	10.0	6.6	22.2	0.9	99.6	0.0	99.6
Nov	10.7	8.1	5.5	14.6	-0.3	177.0	0.0	177.0
Dec	3.5	0.9	-1.7	10.3	-15.2	109.6	89.4	197.2
Jan (09)	4.1	2.1	0.1	8.5	-6.5	106.4	17.0	129.4
Feb	7.6	4.0	0.4	12.0	-3.5	54.8	1.6	56.8
Mar	8.3	4.9	1.4	13.8	-5.9	98.8	5.4	104.6
Average	**12.3**	**9.0**	**5.7**	**18.6**	**-0.5**	**85.4**	**8.0**	**94.0**

Source: Environment Canada, National Climate data and Information Archive, www.climate.weatheroffice.gc.ca

The weathered samples were examined for the presence of surface cracks. To quantify the area of each specimen affected by this defect, a transparent sheet, containing a grid of 44 squares was placed on the coated surface. The numbers of squares in the grid that contained cracks were then counted. The resulting figure was divided by the total number of squares in the grid to

obtain a measure (expressed as a percentage) of the frequency of cracks on coated samples (Kiguchi et al. 2005).

Table 7.5: List of parameters that were used to assess the performance of modified and coated blue-stained wood specimens exposed to natural weathering

Performance parameters	Response variable	Abbreviation
Total color change (ΔE)	Color difference of weathered and non weathered	ΔE
Gloss (G*)	Ratio of Weathered (W) to Non weathered (N)	W/N G*
Water uptake	Ratio of Weathered (W) to Non weathered (N)	W/N u.
Cracks	Percent in weathered samples	-

7.3 Results

7.3.1 Effect of hot-oil modification and plasma treatment on the appearance and microstructure of wood

At the end of the hot-oil treatment cycle, when specimens cooled, any oil remaining on the surface of the wood was absorbed by the wood very quickly. Thus the surface of the treated wood appeared to be dry and free of oil. The surface of the treated wood was dark brown after hot-oil treatment (Fig. 7.4) and the treated wood had a smoky smell, which diminished over time. There was no sign of cracks or uneven (spotted) discoloration of the wood after treatment. However, the surface of some of the plasma treated hot oil-modified samples was soft, which became apparent when coatings were brushed onto their surfaces.

Figure7.4: Color of blue-stained lodgepole pinewood; before (left) and after (right) hot-oil treatment (220 ºC) for 2h.

Scanning electron microscopy revealed that the oil treatment deposited oil within the wood's microstructure (Fig. 7.5a-b). Plasma treatment removed oil from the wood and caused pit membranes to balloon through pit openings (Fig. 7.5c). There was significant etching and removal of cell walls in samples exposed to plasma for 1333 s (Fig. 7.5d-f). Appendix 1 contains additional SEM photomicrographs of hot oil and plasma treated surfaces.

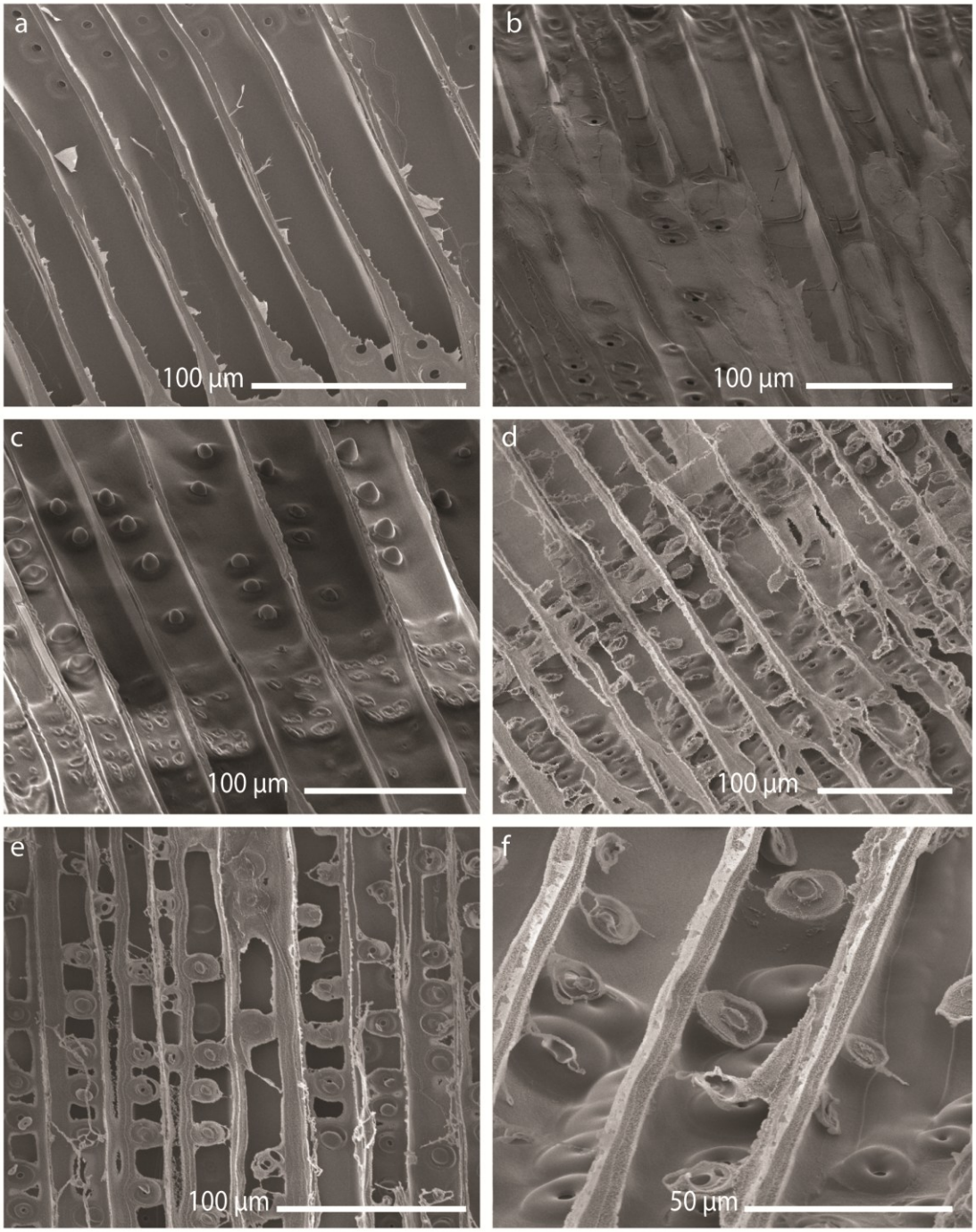

Figure 7.5: SEM photomicrographs of blue-stained lodgepole pine sapwood surfaces before and after hot-oil and plasma treatments: (a) untreated surface showing earlywood tracheids and uniseriate arrangements of bordered pits; (b) hot-oil modified samples, showing deposition of oil on and in tracheid lumens; (c) hot-oil modified blue-stained wood exposed to plasma for 333 s, note removal of oil and ballooning of membranes through pit apertures; (d and e) hot-oil modified blue-stained wood exposed to plasma for 1333 s showing etching of wood cell walls; and (f) high magnification photograph of a hot-oil modified blue-stained sample exposed to plasma for 1333 s showing almost complete removal of upper cell wall layers and exposure of sub-surface layers, note the greater resistance of bordered pits to etching

The changes noted above to the microstructure of wood resulting from exposure to plasma, were confirmed, in part using confocal profileometry. Figure 7.6 shows topographic images of the surface of hot-oil modified wood before and after plasma treatment. A bordered pit in wood that has not been plasma treated shows a raised border around the pit aperture. (Fig. 7.6a and 7.6e). After exposure to plasma the border is etched away, as well as some of the surrounding cell wall material (Fig. 7.6c and 7.6f).

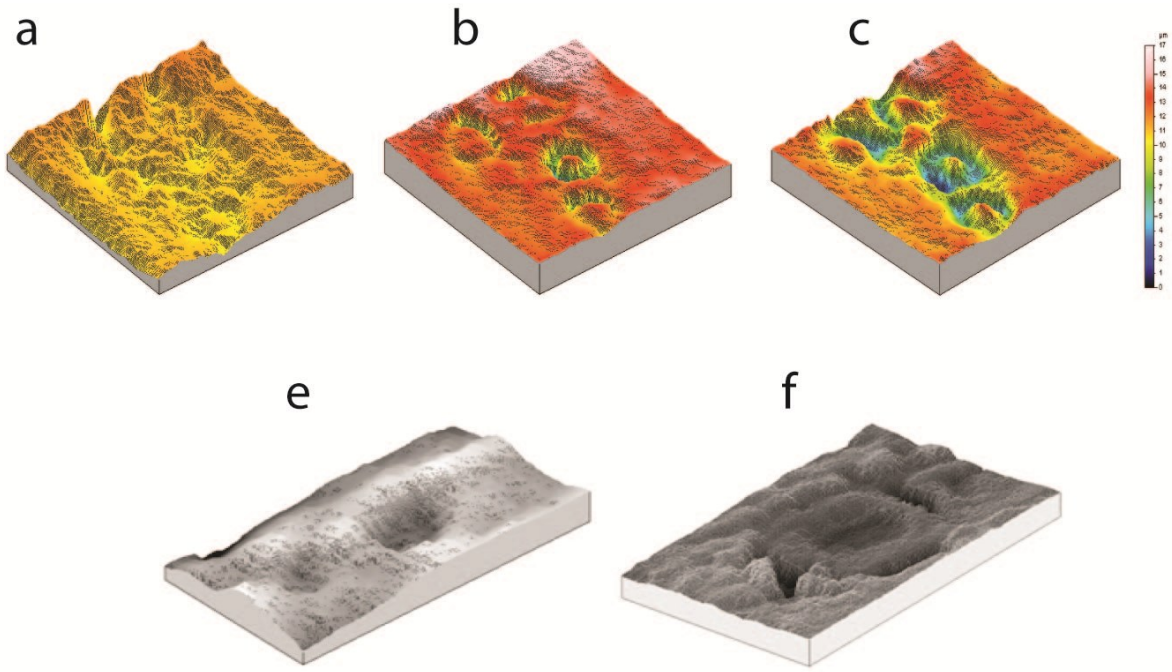

Figure 7.6: Surface topographical maps of the cell wall around pits in hot-oil modified blue-stained lodgepole pine sapwood before and after plasma treatment; (a) hot-oil modified surface before plasma treatment; (b and c) same surface shown in Fig. 7.6a after exposure to plasma for 333 s and 667 s, respectively. (e and f) showing another bordered pit before (e) and after (f) exposure to plasma for 667 s

7.3.2 Wettability, water uptake and adhesion of coatings

There were statistically significant effects of plasma treatments (T) and coating type (C) on contact angle, water uptake and wet and dry adhesion strength of coatings on hot-oil modified wood. There was also a significant interaction of plasma treatment and coating type on the dry adhesion of coatings (Table 7.6).

Table 7.6: Summary of the statistical significance of plasma treatment (T) and coating type (C) on surface wettability, water uptake, and adhesion of coatings to hot-oil modified wood

Experimental Factor	**Response variables**			
	Contact angle (°)	Water uptake (%)	Wet adhesion	Dry adhesion
Plasma treatment (T)	***	NS (0.248)	NS (0.252)	*
Coating type (C)	n/a	***	**	***
T x C	n/a	NS (0.237)	NS (0.879)	**

**** = p<0.05; ** = p<0.01; *** = p<0.001; NS = not significant (p>0.05); n/a = not applicable; data in brackets are associated p-values***

Plasma treatment significantly increased the wettability of uncoated hot-oil modified blue-stained lodgepole pine sapwood. A significant difference ($p<0.05$) was observed between the contact angles of water droplets applied to untreated surfaces and surfaces that were plasma treated (Fig. 7.7). The contact angles of droplets on samples that were plasma treated for 333, 667 and 1333 s were significantly ($p<0.05$) lower than those on samples that were only plasma treated for 33 s, but there was no significant difference ($p>0.05$) in the contact angles of water droplets on samples exposed to plasma for 333 s and longer periods of time (Fig. 7.7).

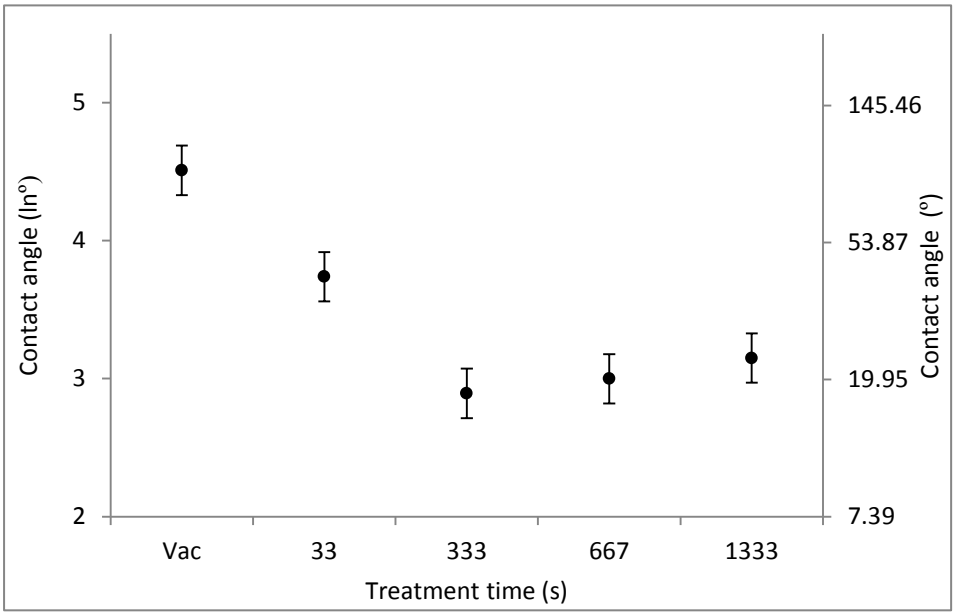

Figure 7.7: The effect of plasma treatment time on contact angles of water droplets on uncoated hot-oil modified blue-stained lodgepole pine sapwood. Note that Y1 axis is expressed on a logarithmic scale, Y2 axis is back transformed to compare results on the natural scale. Error bars are ± standard error of differences of means (from analysis of variance). Non-overlap of these bars indicates that means are significantly different at 5% level (p<0.05)

Plasma treatment had no significant effects on water uptake, and wet adhesion of coatings on hot-oil modified samples, but there were significant ($p<0.01$) effects of coating types on these variables. The effects of coating type on water uptake and wet adhesion are shown in Figures 7.8 and 7.9, respectively. The results are averaged across plasma treated samples because there were no significant interactions of coating type and plasma treatment on water uptake and wet adhesion. Results indicate that the Supernatural semitransparent stain (SNS) was more permeable to water than any of the other applied coatings. Samples coated with the polyurethane (PUR) were the least permeable, however, the difference between their uptake of water and that of samples coated with the acrylic latex (ACL) paint was not statistically significant ($p>0.05$). The water uptake of samples coated with the semi-transparent stain (C123) were significantly ($p<0.05$) higher than those of the acrylic latex paint (ACL) and polyurethane (PUR), but lower than that of the other semi-transparent stain (SNS).

The semitransparent stain (SNS) had the lowest wet adhesion of all the coatings. For example, the wet adhesion of the semitransparent stain was significantly ($p<0.05$) lower than those of the latex paint (ACL) and the other semi-transparent stain (C123), but it was not significantly ($p>0.05$) different from that of the polyurethane (PUR). The wet adhesion of the C123 semi-transparent stain was significantly ($p<0.05$) higher than those of other semi-transparent stain (SNS) and the polyurethane coating, but it was not significantly ($p>0.05$) different from that of the latex paint (ACL) (Fig. 7.9).

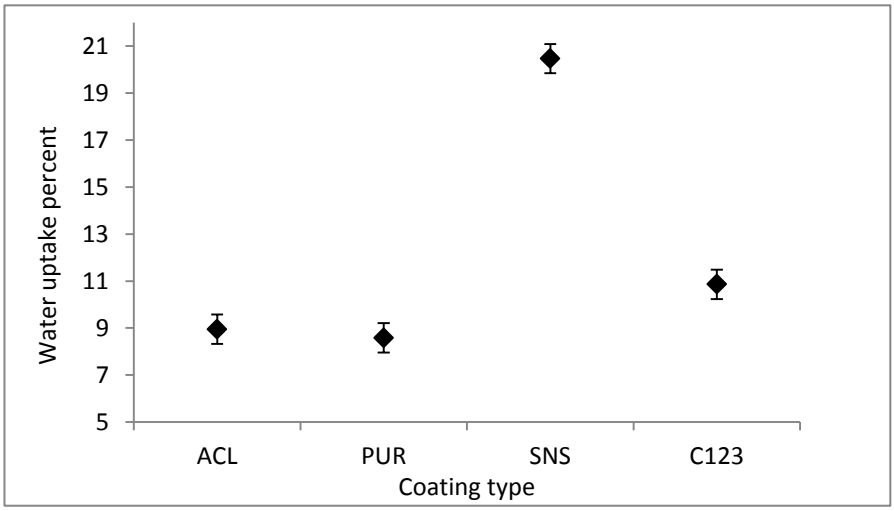

Figure 7.8: Water uptake of hot-oil modified blue-stained lodgepole pine sapwood finished with different coatings (results are averaged across different plasma treatments). ACL = Acrylic latex paint; PUR = Polyurethane; SNS = Supernatural semi-transparent stain; C123 = Cetol 1 and Cetol 23 semi-transparent stain. Error bars are ± standard error of differences of means (from analysis of variance). Non-overlap of these bars indicates that means are significantly different at 5% level ($p<0.05$)

The effect of different plasma treatments and coating types on the dry adhesion of coatings is shown in Figure 7.10. The adhesion of the different coatings was invariably lower on wood that had been modified with plasma except for that of the semi-transparent stain (SNS) that was plasma treated for 33 and 333 s. However, differences in the dry adhesion of the coatings to the control (vacuum) and plasma treated samples were only significant for the polyurethane and the

other semi-transparent stain (C123). The dry adhesion of the semi-transparent stains tended to be higher than those of the film forming coatings (acrylic latex (ACL)) and polyurethane (PUR)), but the dry adhesion of the different coatings varied with plasma treatments as indicated by the significant interaction ($p<0.01$) of coating type and plasma treatment on dry adhesion (Fig. 7.10).

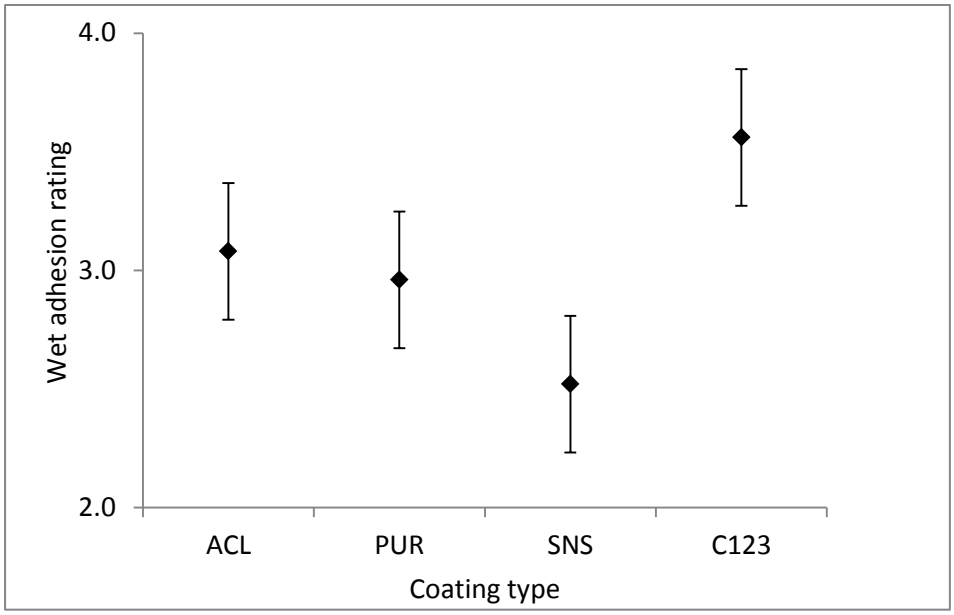

Figure 7.9: Wet adhesion of different coatings to plasma-treated hot-oil modified blue-stained lodgepole pine sapwood (results are averaged across different plasma treatments). ACL = Acrylic latex paint; PUR = Polyurethane; SNS = Supernatural semi-transparent stain; C123 = Cetol 1 and Cetol 23 semi-transparent stain. Error bars are ± standard error of differences of means (from analysis of variance). Non-overlap of these bars indicates that means are significantly different at 5% level ($p<0.05$)

There was a significant ($p<0.05$) reduction in dry adhesion of the polyurethane coating as a result of pre-treating surfaces with plasma for 33 s and 667 s, but there was no significant difference ($p>0.05$) in the dry adhesion of coatings on the control and samples pre-treated with plasma for 1333 s (Fig. 7.10). However, in samples coated with acrylic latex (ACL), significantly lower dry adhesion only occurred in the samples that were pretreated with plasma for 667 s. Plasma pre-treatment for 333s caused a significant reduction in the dry adhesion of the

Cetol semi-transparent stain (C123) (Fig. 7.10) but apart from this effect, plasma pretreatment had no significant effect on the dry adhesion of the semi-transparent stains (SNS and C123).

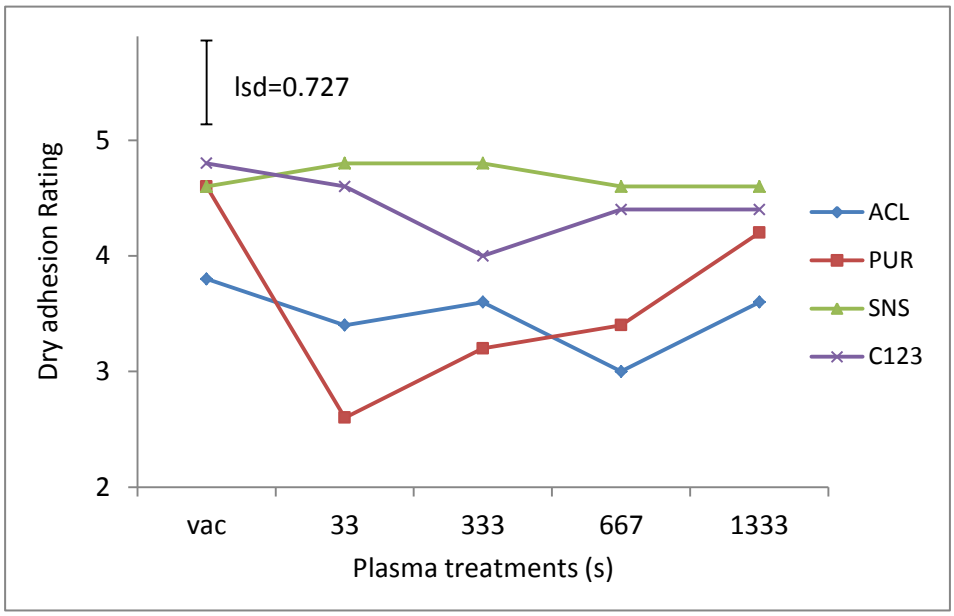

Figure 7.10: Effect of plasma treatment and coating type on dry adhesion of coatings on hot-oil modified blue-stained lodgepole pine sapwood; ACL = Acrylic latex paint; PUR = Polyurethane; SNS = Supernatural semi-transparent stain; C123 = Cetol 1 and Cetol 23 semi-transparent stain. Least significant difference (lsd) bar is based on 95% confidence intervals (from analysis of variance) to estimate the significance of differences between individual means

7.3.2.1 Exterior performance of coatings on hot-oil modified and plasma treated blue-stained sapwood

Exposure to outdoor weathering for eighteen months caused great changes in the appearance of the modified and coated samples, although changes to the acrylic latex paint were less than those observed for the other finishes. Weathering caused surfaces of samples coated with the stains or the polyurethane to become a dull grey color. However such a gray color was more homogenous on hot-oil treated samples (Fig. 7.11).

There were statistically significant effects of oil/plasma treatment (T), coating type (C), and interactions between these factors on the total color change (ΔE), G* (surface gloss), cracking

and water uptake of samples. These effects of and interaction between factors on response variables are summarized in Table 7.7.

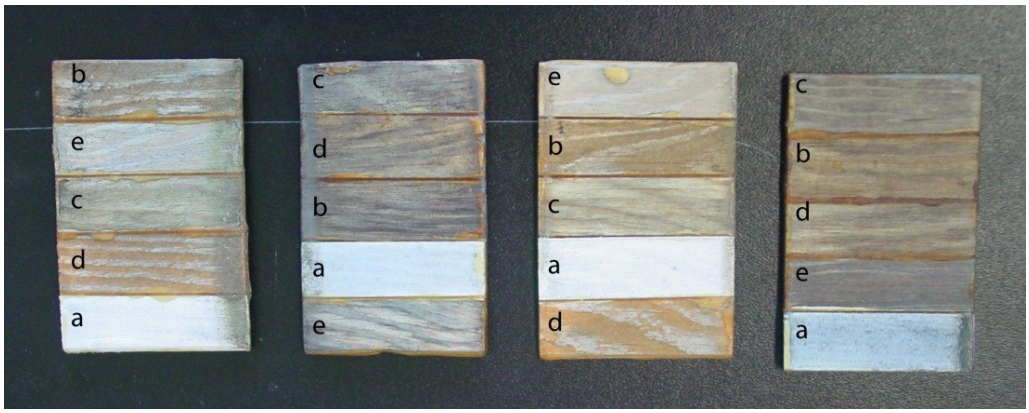

Figure 7.11: Appearance of coated samples after exposure to weathering for 18 month; (from left to right) control, hot-oil/plasma treated, plasma treated and hot-oil modified (five different coatings were applied to delimited areas on each specimen at random; a = Acrylic latex; b = Natural deck oil; c = Natural wood UV plus finish; d = Semitransparent wood finish; e = Premium oil-based deck stain)

Table 7.7: Summary of statistical significance of treatment (T), coating (C) and treatment x coating interactions on response variables measured on coatings on modified blue-stained lodgepole pine wood samples exposed to 18 months of outdoor weathering. Total color change of surface calculated from CIE Lab color parameters on weathered and nonweathered samples; surface gloss and water uptake are expressed as ratios of weathered values to nonweathered values; and crack percent represent the measured values on weathered samples

Experimental Factors	Response variables			
	Total color difference (ΔE)	Gloss 85º (W/N G*)	Water uptake (W/N u.)	Crack percent (W)
Treatment (T)	**	*	***	***
Coating type (C)	**	***	***	***
T x C	***	**	***	NS (0.190)

W/N = ratio of weathered to non-weathered; W = weathered; * = p<0.05; ** = p<0.01; *** = p<0.001; NS = not significant (p>0.05); data in brackets are associated p-values

Treatment by coating type interactions ($p<0.001$) on the ΔE (total color difference) occurred for samples after exposure to weathering (Fig. 7.12). The interaction between coating and treatment type occurred because the behavior of some of the coatings on hot-oil modified and unmodified samples differed from those of the other coatings. Changes in color of most of the

coatings during weathering were smaller on hot-oil modified wood compared to unmodified wood except for the white acrylic latex paint (ACL). Changes in the color of the white acrylic latex coating on hot-oil modified samples became much more pronounced during weathering than the same finish on untreated control samples and the other treated samples. Plasma treatment alone had no significant effect on changes in the color of coated surfaces except for natural UV plus finish (UVP) (Fig. 7.12). Interestingly plasma treatment of hot-oil modified samples reduced the color change of the acrylic latex paint during weathering. In contrast, plasma treatment increased the changes in color of hot-oil modified samples coated with the natural deck oil (NDO). These effects of hot-oil modification and plasma treatment on the color change of the coatings accounts for the significant treatment x coating interaction.

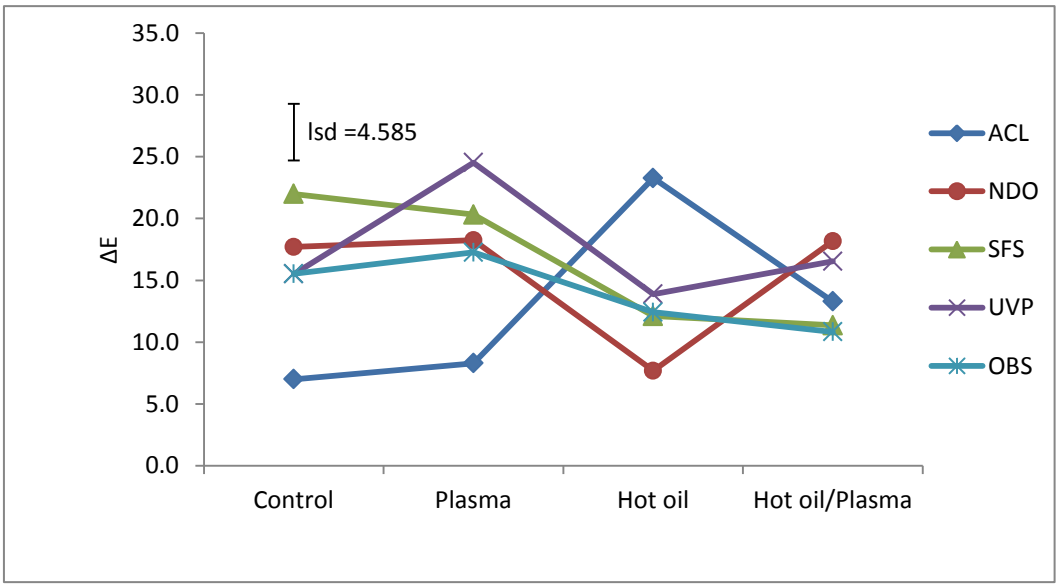

Figure 7.12: Interaction of treatment and coating type on ΔE (total color change) of weathered (18 months) blue-stained lodgepole pine wood; ACL = Acrylic latex; NDO = Natural deck oil; SFS = Semitransparent wood finish; UVP = Natural wood UV plus finish; OBS = Premium oil-based deck stain. Least significant difference (lsd) bar is based on 95% confidence intervals (from analysis of variance) to estimate the significance of differences between individual means

There was also a significant interaction between coating and treatment type on the surface gloss (G*) of the coated samples. Exposure to natural weathering reduced the gloss of all coatings on untreated wood and, as can be seen in Figure 7.13, the ratio of the surface gloss of coated samples after weathering to those of non weathered samples (W/N G* ratio) is smaller than 1.0. Plasma treatment did not have a significant effect ($p>0.05$) on the reductions in gloss of the coatings. The significant interaction between coating type and treatment occurred mainly because the loss in gloss (G*) of most of the coatings during weathering was generally lower on hot-oil modified wood except for the natural UV plus finish. Plasma treatment of hot-oil modified wood generally reversed this effect except for the semi-transparent wood finish.

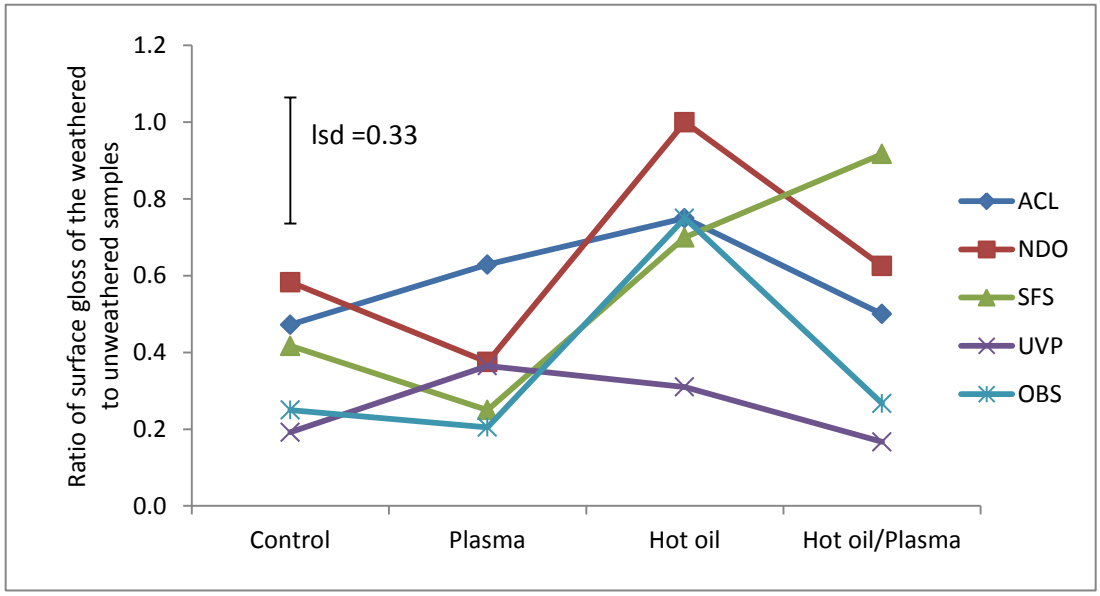

Figure 7.13: Interactions of treatment and coating type on the ratio of G* (surface gloss) of weathered (18 months) blue-stained lodgepole pine wood to that of non weathered wood samples; ACL = Acrylic latex; NDO = Natural deck oil; SFS = Semitransparent wood finish; UVP = Natural wood UV plus finish; OBS = Premium oil-based deck stain. Least significant difference (lsd) bar is based on 95% confidence intervals (from analysis of variance) to estimate the significance of differences between individual means

Analysis of variance revealed a significant ($p<0.001$) interaction of treatment and coating type on the ratio of the water uptake of weathered wood to those of non weathered wood

samples. All samples absorbed more water after exposure to weathering (W/N u. ratio greater than 1.0). The increase in water uptake after weathering on unmodified wood coated with acrylic latex (ACL) or semi-transparent finish (SFS) was significantly lower than those of the other coated samples. Hot-oil treatment (irrespective of plasma treatment) reduced water uptake of coated samples to the levels of the untreated (weathered) ACL and SFS coated samples. Interestingly, plasma treatment alone restricted water uptake of the oil based stain (OBS), natural deck oil (NDO) and (to a lesser extent) the UV plus finish (UVP). However, plasma treatment had no effect on the ratio of water uptake of samples coated with the semi-transparent wood finish (Fig. 7.14).

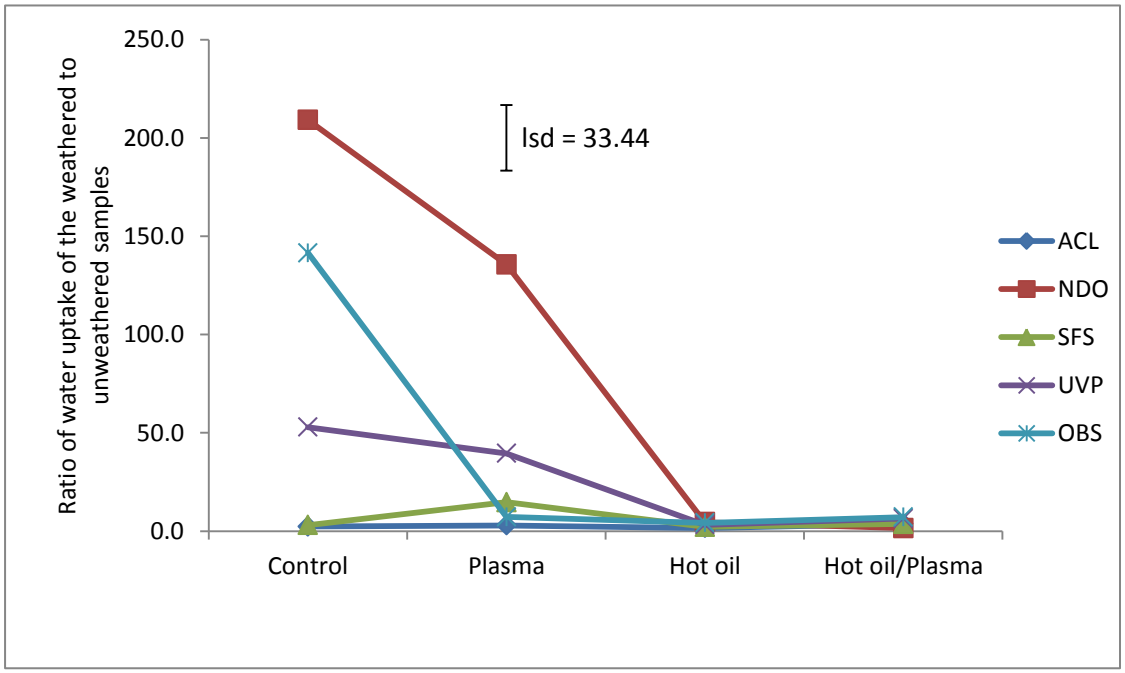

Figure 7.14: Interactions of treatment and coating type on the ratio of water uptake of weathered (18 months) blue-stained lodgepole pine wood to that of non weathered wood samples; ACL = Acrylic latex; NDO = Natural deck oil; SFS = Semitransparent wood finish; UVP = Natural wood UV plus finish; OBS = Premium oil-based deck stain. Least significant difference (lsd) bar is based on 95% confidence intervals (from analysis of variance) to estimate the significance of differences between individual means

Coated samples exposed to natural weathering invariably developed small surface cracks. Analysis of variance revealed a highly significant ($p<0.001$) effect of treatment and coating type on cracking of samples during natural weathering. There was no significant ($p>0.05$) interaction of treatment and coating type on cracking. Plasma treatment significantly ($p<0.05$) increased the tendency of wood to crack, but cracking of hot-oil modified and hot-oil/plasma modified wood was significantly lower than that of the unmodified control (Fig. 7.15). Samples coated with the acrylic latex paint (ACL) cracked significantly ($p<0.05$) less than other coated samples (Fig. 7.16). Samples coated with the natural deck oil (NDO) cracked significantly ($p<0.05$) more than samples coated with the acrylic latex paint (ACL) and the premium oil-based deck stain (OBS). The cracking of samples coated with the natural deck oil was not significantly different from that of samples coated with the semi-transparent wood finish (SFS) or the natural wood UV plus finish (UVP) (Fig. 7.16).

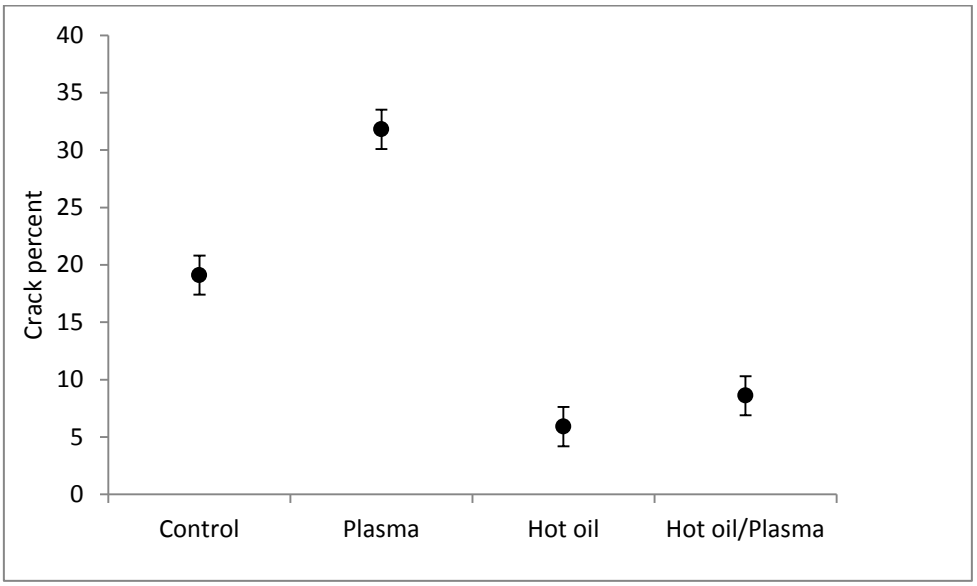

Figure 7.15: Effect of hot-oil and plasma treatments on the surface cracking of coated blue-stained lodgepole pine samples exposed to the weather for eighteen months in Vancouver (results are averaged across coating types). Error bars are ± standard error of differences of means (from analysis of variance). Non-overlap of these bars indicates that means are significantly different at 5% level ($p<0.05$)

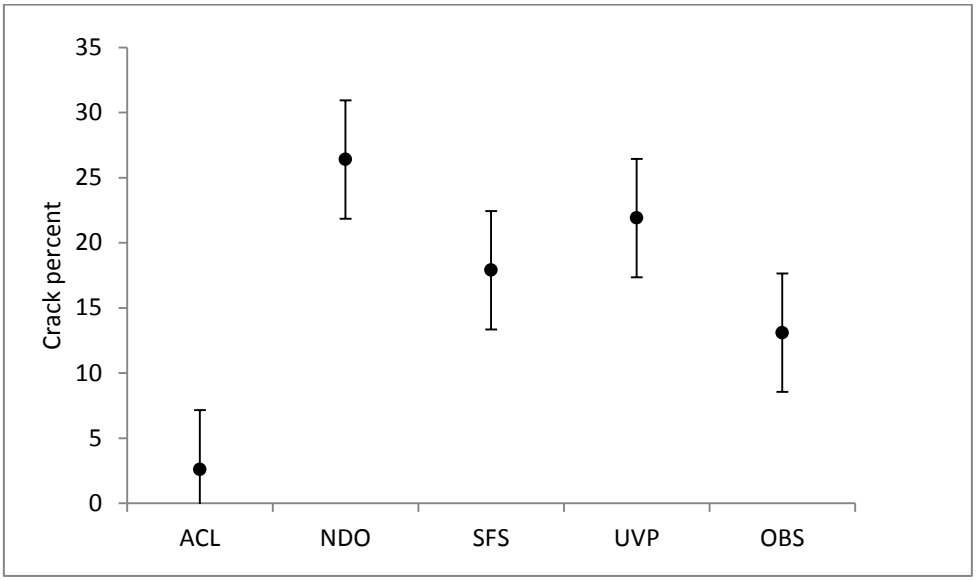

Figure 7.16: Effect of coating type on surface cracking of hot-oil and plasma modified blue-stained lodgepole pine samples exposed to the weather for eighteen months in Vancouver (results are averaged across treatment type); ACL = Acrylic latex; NDO = Natural deck oil; SFS = Semitransparent wood finish; UVP = Natural wood UV plus finish; OBS = Premium oil-based deck stain. Error bars are ± standard error of differences of means (from analysis of variance). Non-overlap of these bars indicates that means are significantly different at 5% level ($p<0.05$)

7.4 Discussion

Hot-oil modification was able to mask the blue color of blue-stained lodgepole pine sapwood and turn it to a uniform golden brown color, as expected. There was no uneven discoloration as has been observed with wood that has been heat-treated in air (Rapp and Sailer 2001). This is one advantage of using soy bean oil as the heat transfer medium to modify blue-stained wood. The smoky smell of the modified treated wood may restrict the use of oil-treated wood inside buildings, although this smell diminished after some time (Vernois, 2001). There was no excess oil on the surface of modified wood that was apparent to the naked eye, which suggests that it could be handled soon after treatment. However, SEM and confocal profilometry showed that oil was present on the surface and within the modified wood. This oil could account for the higher contact angle (lower wettability) of hot-oil modified wood compared to the control. Wang and Cooper (2005) also found that hot oil modified wood was more water repellent than unmodified wood. As I hypothesized, plasma treatment increased the wettability of the hot-oil modified wood. SEM and confocal profilometry suggested that these increases in wettability were due to removal of oil from the wood surfaces by plasma or modification of the oil or wood. Removal of oil from the surfaces of materials by plasma has been reported by Choi et al (2001). They found that plasma treatment was able to remove lubrication oil from the surface of aluminum conductor wires.

The plasma used here also etched wood cell walls as well as removing the deposited oil. Etching of bordered pits may have facilitated the removal of oil because bordered pits are a major flow-path in wood (Buro and Buro 1959). Nickerson (1998) suggested that removal of oil from surfaces by plasma will increase wettability and also adhesion properties (Nickerson 1998).The plasma treatments used here did not increase the adhesion of coatings to hot-oil

modified wood. Liston et al (1994) stated that "even if a surface becomes more wettable after plasma treatment, adhesion of coatings to the surface does not necessarily improve" (Liston et al. 1994). Podgorski et al. (2000) also found that plasma treatment did not improve the adhesion of coatings to heat-treated (torrefied) wood even though the plasma made the surface more wettable. Podgorski et al. (2000) suggested that the incompatibility of the applied coatings with the torrefied wood accounted for their observations. In contrast, Lukowsky and Hora (2002) found that plasma treatment increased the wet adhesion of a waterborne acrylic coating, but had no effect on the adhesion of a solvent borne coating. However, in my experiments there were some instances where plasma treatment reduced the adhesion of coatings to hot-oil modified wood. For example, I found that there was a significant decrease in the adhesion of a solvent-born polyurethane finish on the hot-oil modified wood when the coating was applied to wood that had been plasma treated for a short period of time (33 s). This negative effect of plasma treatment on the adhesion of the polyurethane coating to hot-oil modified wood may be due to the creation of short chain polymeric materials from the plasma-induced chain scission of long chain hydrocarbons in soybean oil at modified surfaces. These lower molecular weight materials may have influenced the adhesion of the polyurethane coating (Wu 1982, Nickerson 1998). Furthermore, migration of soybean oil, retained in sub-surface wood cells, to the interface of wood and coatings may have interfered with the adhesion of coatings (Honary 2003). I observed the etching of pits by plasma, as mentioned above, which may have facilitated the migration and diffusion of the underlying soy bean oil to the surface.

Weathering for 18 months resulted in the degradation of the semi-transparent stains on unmodified wood and the weathering (greying) of the underlying wood. These observations explain changes in surface color (ΔE) and surface gloss of samples finished with satins and

exposed to weathering. Weathering increased the water uptake of coated wood samples and caused cracks to form in the coatings.

I tested the hypothesis that plasma treatment would enhance the performance of coatings on wood that had been modified with hot oil. There was a little evidence that this occurred, with one important exception. The white acrylic coating on hot-oil modified wood discolored badly during exterior exposure. This undesirable effect was not observed in hot-oil modified samples that were pre-treated with plasma. This result suggests that the discoloration of the white acrylic latex finish during weathering was due to the migration of oil from the modified wood through the coating and on to the surface of the coated wood. Migration of oil to surfaces has been observed previously in wood treated with oily wood preservatives (Baileys and Webb 1987). I observed that plasma treatment removed oil from the surface of hot-oil modified wood, which may have prevented oil from migrating through the acrylic latex coating and discoloring coated surfaces. Further research is required to confirm this suggestion.

One unexpected finding was that plasma treatment on its own restricted water uptake of some coated samples during weathering. On the other hand, plasma treatment increased the cracking of coated wood during weathering with exception of samples coated with white acrylic paint. My observations of the performance of coatings on wood modified with hot oil confirm the findings of the previous researchers. Hot-oil treatment was ineffective at restricting the changes in color of most coatings during weathering (with exception of the white acrylic paint). However, as mentioned above the grey color of hot-oil modified wood after weathering was more homogenous than that of plasma treated and control samples possibly because of the presence of oil at the weathered wood surface. Similar observations of the color of wood treated with linseed oil and exposed to artificial weathering were made by Temiz et al. (2007). In

addition, hot oil treatment reduced loss of gloss of some of the water-borne or solvent-borne coatings (i.e. NDO and OBS). The water repellency of hot-oil modified wood explains the lower water uptake of weathered hot-oil treated samples as previously observed by Wang and Cooper (2005) for hot-oil modified white spruce (*Picea glauca* (Moench) Voss). The same property of hot-oil modified wood accounts for the reduced cracking of the hot-oil modified and coated wood samples during natural weathering. A similar effect (for uncoated wood) was reported by Evans et al. (2009). They found that an oil emulsion additive was effective at reducing the checking that develops when CCA-treated wood was exposed outdoors, possibly because the oil migrated to the surface of the wood during natural weathering. My observations of the reduced water uptake and cracking of hot-oil modified and coated blue-stained lodgepole pine wood samples during natural weathering, also accord with those of Dubey (2010) who exposed hot-oil modified radiata pine to accelerated weathering.

7.5 Conclusions

Hot-oil modification deposits oil within the wood's microstructure. Plasma treatment removed oil from the surface of wood and etched the wood surface. I hypothesized that the removal of oil from the surface of modified wood would have beneficial effects on the adhesion and exterior performance of coatings to the modified wood. Plasma treatment increased the surface wettability of hot-oil modified wood, but did not improve the adhesion of coatings or the performance of semi-transparent stains on wood exposed to natural weathering. However, plasma treatment of hot-oil modified wood reduced the discoloration of a white acrylic latex paint exposed to natural weathering. The discoloration of white paints on wood exposed outdoors is regarded as highly undesirable (Bulian and Graystone 2009). Therefore the ability of plasma treatment to reduce the discoloration of white paint on hot oil modified wood is

noteworthy. Thus I conclude that plasma treatment can improve the performance of white film-forming acrylic paint on hot oil modified wood, but not the performance of darker semi-transparent stains or clear finishes.

8 General discussion, conclusions and suggestions for further research

8.1 General discussion

In this thesis I hypothesized that glow-discharge plasma will etch wood surfaces and change their microstructure and chemical composition. I performed experiments to test this hypothesis and examined factors affecting etching of wood by plasma and also some applications of plasma etching for wood processing.

Analysis of wood surface microstructure with scanning electron and light microscopy (Chapter 3) showed that prolonged exposure to plasma etched the cell walls of different wood species and created new surface morphologies. Microscopy revealed that longer exposure to plasma caused greater etching of wood surfaces. Furthermore, regions of cell walls that are rich in lignin such as the middle lamella were etched more slowly by plasma. Etching of wood cell walls in normal and compression wood was quantified using white light confocal profilometry (Chapter 4). This technique was also used to quantify the etching of cellulose and lignin models. Measurements made using confocal profilometry supported observations made using microscopy that plasma is able to etch wood surfaces, and that cellulose is etched more rapidly than lignin. Profilometry measurements also revealed a strong effect of treatment time on etching of wood surfaces by plasma. Plasma altered the surface chemistry of wood as was hypothesized (Chapter 5). Wet chemical analysis showed that plasma treatment reduced the levels of wood carbohydrate and resulted in a relative increase in the lignin content of modified wood surfaces. Plasma also etched fungal hyphae and modified their microstructure (Chapter 6), in accord with observation made of the etching of wood cell walls.

On the other hand exposure of wood to plasma for <u>short periods of time</u> did not cause significant changes in the microstructure of wood (Chapter 3). Accordingly, measurements of the

changes in the volume or mass of wood cell walls after short periods of exposure to plasma did not reveal any significant difference compared to controls that were only exposed to a vacuum (Chapter 4). Quantification of etching of cell walls (Chapter 4) did not show any significant effect of cell wall type (radial v tangential) or wood species on volume/mass losses during exposure to plasma. Furthermore, it was difficult to detect chemical changes at plasma-treated wood surfaces using spectroscopy (FTIR/XPS) and changes were not significant when wood was exposed to plasma for short periods of time (although changes became more evident after longer exposure to plasma).

My observations of wood cell wall microstructure and chemistry (Chapters 3, 4 and 5) confirmed that treatment time is the most important factor affecting the etching of wood surfaces by plasma. Prolonged plasma treatment had profound effects on the structural and chemical properties of wood surfaces. The wood's chemical composition also affects etching. For example, the lignin rich middle lamellae was more resistant to etching than the secondary wall, as mentioned above, and compression wood, which has a high lignin content, was more resistant to etching than 'normal' wood. Thinner-walled wood elements such as tyloses and rays were etched faster than thick-walled cells, although the resin in rays resisted etching. In accord with the former observation plasma rapidly degraded the thin walls of fungal hyphae. These observations point to an effect of cell wall morphology on the etching of wood by plasma.

Two possible applications of plasma etching for wood processing were examined with mixed results. Plasma treatment removed some of the blue stain from blue-stained lodgepole pine, but it was more efficient at enhancing the ability of bleach to remove blue-stain. This finding suggests that plasma treatment may be useful where there is a need to increase the accessibility of chemical reagents to wood surfaces for example staining of wood with dye or

finishing wood with coatings (de Meijer et al. 1998). In contrast plasma pre-treatment had little effect on the adhesion and performance of exterior coatings on hot-oil modified wood, although it significantly reduced the discoloration of a white acrylic latex paint on hot oil modified (blue stained) lodgepole pine exposed to natural weathering.

My findings that plasma etches wood accords with previous studies that have shown that plasma can etch inorganic and some organic materials (Dai et al. 1997). For example, the capacity of plasma to etch silicon is well-known, and plasma etching is being used commercially by the semiconductor industry (Flamm and Herb 1989, Sahoo et al. 2009). The ability of plasma to etch fibers in paper has also been noted (Sapieha et al. 1988, Fricke et al. 2011). My finding that there is a positive correlation between the etching of wood cell walls and the time they are exposed to plasma (Chapter 4) is in agreement with previous findings on the effects of plasma treatment time on the rate of etching of polymers (Yasuda et al. 1973, Gokan et al. 1983, Fricke et al. 2011). The greater resistance of lignin to etching compared to holocellulose in wood accords with previous findings that aromatic polymers are more resistant to etching than non-aromatic polymers (Taylor and Wolf 1980, Pederson 1982, Moss et al. 1986). The changes to the microstructure of wood caused by plasma resembles those caused by exposure wood gamma radiation, and also those caused by bacteria and fungi that selectively degrade hollocellulose (Bamber and Sangster 1997, Tabirih et al. 1977, de Lhoneux et al. 1984, Singh 1997).

A number of my findings are noteworthy because of their practical applications. For example, the increase in lignin content of wood as a result of plasma treatment may assist the development of technologies currently being examined to bond wood without the use of adhesives, ie auto-adhesion and friction-welding (Sakata et al. 1991, Gfeller et al. 2004, Delmotte et al. 2008) because these techniques rely on the thermoplasticization and/or fusion of

lignin at wood surfaces. The technique that I developed to quantify cell wall erosion using white light confocal profilometry is accurate and requires minimal sample preparation. It has a range of possible practical applications from measuring the erosion of wood surfaces during weathering to quantifying the dimensions of anatomical features found in wood (Arnold et al. 1992, Williams et al. 2001). My observation that plasma was able to remove blue stain from wood suggests that plasma treatments could be used (with modification) to remove other types of discoloration from wood, for example, those occurring due to migration of extractives during the kiln drying of wood (Kollmann and Côté 1968, Fengel and Wegener 1984). My observation that fungal hyphae were etched by plasma suggests that the ability of plasma to etch chitin should also be explored. Finally, my finding that plasma treatment reduces the discoloration of white acrylic latex paint on hot oil modified lodgepole pine exposed to natural weathering suggests that plasma pre-treatments may be usefully employed to remove unwanted hydrophobic contaminants from the surface of wood.

8.2 Conclusions

This study demonstrated that prolonged plasma treatment could modify the surface microstructure and chemistry of wood. Etching began in the thinner regions of cell walls at wood surfaces (around pit apertures), and was more pronounced in areas of the cell wall that were rich in cellulose (and less pronounced in areas that were rich in lignin). Prolonged plasma treatment was able to completely remove cell walls at the surface of softwood and hardwoods. Therefore I conclude that all of woods cell wall polymers can be degraded by prolonged exposure to plasma even though cell wall layers that are rich in lignin were etched more slowly than other parts of the cell wall.

My findings showed that the amount of material removed from wood surfaces by plasma mainly depends on the time that they are exposed to plasma and to smaller degrees on the anatomical structure and chemical composition of cell walls. Therefore I conclude that plasma etching of wood depends to a large extent on treatment time, but it is also influenced by the structure and chemical composition of the wood substrate.

Plasma etched fungal hyphal walls, removed some blue stain from wood and enhanced the bleaching of blue-stained wood. Plasma also removed oil and altered the surface microstructure of hot-oil modified wood, but these effects did not translate into better adhesion and outdoor performance of coatings on the oil-modified wood with one important exception, namely plasma treatment reduced the discoloration of a white acrylic latex paint on hot-oil modified wood exposed to natural weathering. Therefore I conclude that plasma treatment is an efficient pretreatment for bleaching and removing the discoloration from blue-stained wood, and also reducing the discoloration of acrylic latex paint on hot-oil modified wood exposed to natural weathering.

Plasma etching is an interesting phenomenon that shows possible applications in areas such as wood finishing and possibly auto-adhesion of lignocellulosics and processing of chitins. Therefore I conclude that practical applications of plasma processing of wood and lignocellulosics should be explored further, and propose some suggestions for research as follows.

8.3 Suggestions for further research

Plasma etching treatments are important in a number of industries and they find practical applications for the processing of a range of different materials (Inagaki 1996, Jama and Delobel 2007, Oehrlein et al. 2011). My findings demonstrate that plasma can etch the surface of wood.

Hence it is possible that plasma etching of wood could find some practical applications, as discussed above. However, before this can occur further research would be needed to develop technologies that could be used by industry.

I demonstrated that the most important factor affecting the etching of wood by plasma was treatment time. However, the treatment times that produced significant etching were too long (20 minutes) to be used industrially. Furthermore, the treatments all required the use of high vacuum to generate the plasma. Industrial treatments would need to be faster and occur at close to atmospheric pressure. Further research using different types of plasmas and reactors would be needed to examine whether wood can be etched in short periods of time and at atmospheric pressure.

Based on my finding that plasma enhanced the ability of bleach to remove blue stain from wood, investigations on the ability of plasma to enhance other treatments that require the surface of wood to be permeable should be carried out.

Furthermore, my observation that plasma can etch fungal hyphae suggests that plasma treatment of chitin could be used as an alternative to processes currently being used by industry. Further research would be needed to explore the etching of chitin by plasma and possible practical applications of plasma etching for chitin rich materials.

I found that plasma treatment of hot-oil modified wood removed oil from the surface of wood and reduced the discoloration of a white acrylic latex paint on hot-oil modified wood exposed to natural weathering. Further research is needed to understand if this effect is related to the ability of plasma treatment to remove oil from the surface of hot-oil modified wood and whether the same beneficial effect occurs with other exterior film-forming paints.

My findings that plasma etching of wood creates a micro-roughened surface that is rich in lignin could enhance attempts being made to bond wood via auto-adhesion (wood friction welding) because this phenomenon relies on the thermoplasticization and melting of lignin to create a 'glue' that can join wood together (Gfeller et al. 2004, Delmotte et al. 2008). Further research would be needed to test this hypothesis.

I finish this section on a strong point. During the course of my experiments I found that plasma treatment of veneers seemed to create veneers that bonded to each other. The underlying mechanism responsible for this effect is not known. Further research is needed to explore this phenomenon and its practical applications.

References

Aam, B.B., Heggset, E.B., Norberg, A.L., Sørlie, M., Vårum, K.M., Eijsink, V.G.H., 2010. Production of chitooligosaccharides and their potential applications in medicine. *Marine Drugs,* 8(5), 1482-1517.

ALTIMET, 2007. Altimet surface metrology; Data sheet, ALTISURF 500. Thonon-les-Bains, Rhône-Alpes, France.

Antoine, R.C., Avella, T., Van Eyseren, J.C., 1971. Studies of wood treated by high doses of γ-irradiation. *IAWA Bulletin,* (4), 11-14.

Aoki, T., Norimoto, M., Yamada, T., 1977. Some physical properties of wood and cellulose irradiated with Gamma rays. *Wood Research,* (62), 19-28.

Arnold, M., Sell, J., Feist, W.C., 1991. Wood weathering in fluorescent ultraviolet and xenon arc chambers. *Forest Products Journal,* 41(2), 40-44.

Arnold, M., Lemaster, R.L., Dost, W.A., 1992. Surface characterization of weathered wood using a laser scanning system. *Wood and Fiber Science,* 24(3), 287-293.

Aschwanden, M.J., 2004. *Physics of the Solar Corona: An Introduction.* Springer, NY, USA, pp. 824.

Ashton, H.E., 1974. Removal of solvent from swollen wood. *Wood Science,* 6(4), 368-374.

ASTM, 2010. D2244; Standard practice for calculation of color tolerances and color differences from instrumentally measured color coordinates. Philadelphia, USA.

ASTM, 1976. D3359; Standard test methods for measuring adhesion by tape test. Philadelphia, USA.

Aveyard, R., Haydon, D.A., 1973. *An Introduction to the Principles of Surface Chemistry.* Cambridge University Press, UK, pp. 232.

Avramidis, G., Nothnick, E., Militz, H., Viöl, W., Wolkenhauer, A., 2011a. Accelerated curing of PVAc adhesive on plasma-treated wood veneers. *European Journal of Wood and Wood Products,* 69(2), 329-332.

Avramidis, G., Scholz, G., Nothnick, E., Militz, H., Viöl, W., Wolkenhauer, A., 2011b. Improved bondability of wax-treated wood following plasma treatment. *Wood Science and Technology,* 45(2), 359-368.

Avramidis, G., Hauswald, E., Lyapin, A., Militz, H., 2009. Plasma treatment of wood and wood-based materials to generate hydrophilic or hydrophobic surface characteristics. *Wood Material Science and Engineering,* 4(1), 52-60.

Azuma, J.I., 1989. Analysis of lignin-carbohydrate complexes of plant cell wall. In: *Plant Fibers. Modern Methods of Plant Analysis. New Series, Volume 10;* Linskens, H.F., Jackson, J.F. (Eds.). Springer-Verlag, Berlin, Germany, pp. 100-126.

Baeza, J., Freer, J., 2001. Chemical characterization of wood and its components. In: *Wood and Cellulosic Chemistry;* Hon, D.N.S., Shiraishi, N. (Eds.). Marcel Dekker, Inc., NY, USA, pp. 275–384.

Baileys, R.T., Webb, D.A., 1987. 1958 Cooperative creosote project-XII: An analysis of creosotes from posts after 26 years in test. In: *Proceedings of the Eighty-Third Annual Meeting of the American Wood-Preservers' Association;*Totronto, Canada, pp. 163-171.

Baird, W., Johnson, M., Parham, R., 1974. Development and composition of the warty layer in Balsam Fir. II. Composition. *Wood and Fiber Science,* 6(3), 211-222.

Bamber, R.K., Sangster, D.F., 1977. Observation on the sectioning characteristics of normal and gamma-irradiated conifer wood. *IAWA Bulletin,* (1), 12-16.

Barnes, G., Gentle, I., 2005. *Interfacial Science.* Oxford University Press, NY, USA, pp. 247.

Belfas, J., Groves, K.W., Evans, P.D., 1993. Bonding surface-modified Karri and Jarrah with resorcinol formaldehyde. *Holz Als Roh-Und Werkstoff,* 51(4), 253-259.

Belgacem, M.N., Czeremuszkin, G., Sapieha, S., Gandini, A., 1995. Surface characterization of cellulose fibres by XPS and inverse gas chromatography. *Cellulose,* 2(3), 145-157.

Belgacem, M.N., Bataille, P., Sapieha, S., 1994. Effect of corona modification on the mechanical properties of polypropylene/cellulose composites. *Journal of Applied Polymer Science,* 53(4), 379-385.

Belkind, A., Zarrabian, S., Engle, F., 1996. Plasma cleaning of metals: Lubricant oil removal. *Metal Finishing,* 94(7), 19-22.

Bente, M., Avramidis, G., Förster, S., Rohwer, E.G., Viöl, W., 2004. Wood surface modification in dielectric barrier discharges at atmospheric pressure for creating water repellent characteristics. *Holz Als Roh-Und Werkstoff,* 62(3), 157-163.

Black, J.M., Mraz, E.A., 1974. Inorganic surface treatments for weather-resistant natural finishes. In: *U.S.D.A. Forest Service Research Paper, FPL 232;* Madison, WIS, USA, pp. 1-39.

Blanchard, V., Blanchet, P., Riedl, B., 2009. Surface energy modification by radiofrequency inductive and capacitive plasmas at low pressures on sugar maple: an exploratory study. *Wood and Fiber Science,* 41(3), 245-254.

Blantocas, G.Q., Ramos, H.J., Wada, M., 2006. Surface modification of narra wood (*Pterocarpus indicus*) by ion shower treatment. *Japanese Journal of Applied Physics. Part1: Regular Papers, Short Notes and Review Papers,* 45(10B), 8498-8501.

Bledzki, A.K., Reihmane, S., Gassan, J., 1998. Thermoplastics reinforced with wood fillers: a literature review. *Polymer-Plastics Technology and Engineering,* 37(4), 451-468.

BMBF., 2001. *Plasma Technology: Process Diversity and Sustainability.* German federal ministry of education and research, Bonn, Germany, pp. 42.

Boenig, H.V., 1982. *Plasma Science and Technology.* Cornell University Press, USA, pp. 299.

Browning, B.L., 1967. *Methods of Wood Chemistry.* Interscience Publishers, New York, USA, pp. 882.

Bulian, F., Graystone, J., 2009. *Wood Coatings: Theory and Practice.* Elsevier, The Netherlands, pp. 320-487.

Buro, A., Buro, E.A., 1959. Pathways for penetration of liquids into pine wood. *Holzforschung,* 13(3), 71-77.

Byrne, T., Stonestreet, C., Peter, B., 2006. Characteristics and utilization of post-mountain pine beetle wood in solid wood products. In: *The Mountain Pine Beetle a Synthesis of Biology, Management, and Impacts on Lodgepole Pine;* Safranyik, L., Wilson, B. (Eds.), Victoria, Canada, pp. 233-253.

Calvimontes, A., Mauersberger, P., Nitschke, M., Dutschk, V., Simon, F., 2011. Effects of oxygen plasma on cellulose surface. *Cellulose,* 18(3), 803-809.

Carlsson, C.M.G., Stroem, G., 1991. Reduction and oxidation of cellulose surfaces by means of cold plasma. *Langmuir,* 7(11), 2492-2497.

Carroad, P.A., Tom, R.A., 1978. Bioconversion of shellfish chitin wastes: process conception and selection of microorganisms. *Journal of Food Science,* 43(4), 1158-1161.

Chang, S.T., Chang, H.T., 2001. Comparisons of the photostability of esterified wood. *Polymer Degradation and Stability,* 71(2), 261-266.

Chapman, B., 1980. *Glow Discharge Processes.* John Willy and Sons, pp. 406.

Chen, H.Y., Zavarin, E., 1990. Interactions of cold radiofrequency plasma with solid wood; I. Nitrogen permeability along the grain. *Journal of Wood Chemistry and Technology,* 10(3), 387-400.

Chen, H. Y., 1989. Effect of low temperature radio frequency oxygen and nitrogen plasmas on lignocellulosic materials. Ph.D. Thesis. University of California, Berkeley, USA.

Cho, D.L., Shin, K.H., Lee, W., Kim, D., 2001. Improvement of paint adhesion to a polypropylene bumper by plasma treatment. *Journal of Adhesion Science and Technology,* 15(6), 653-664.

Choi, I.S., Hwang, S.W., Park, J.C., 2001. Application of medium frequency atmospheric plasma on continuous aluminum wire cleaning for magnet wire manufacturing. In: *Surface and Coatings Technology; Proceedings of the 7th International Conference on Plasma Surface Engineering;* Laube, E., Berg, S., Moller, W., Rie, K.T. (Eds.), Garmisch-Partenkirchen, Germany, pp. 300-305.

Chu, P.K., Chen, J.Y., Wang, L.P., Huang, N., 2002. Plasma-surface modification of biomaterials. *Materials Science & Engineering R,* 36(5-6), 143-206.

CIE., 1976. *Commission Internationale De l'Eclairage, 18th Session.* CIE Publication 36, London, UK.

Cool, J., Hernández, R.E., 2011. Evaluation of four surfacing methods on black spruce wood in relation to poly (venyl acetate) gluing performance. *Wood and Fiber Science,* 43(2), 194-205.

Côté, W.A., Timell, T.E., Zabel, R.A., 1966. Studies on compression wood—Part I: Distribution of lignin in compression wood of red spruce (*Picea rubens* Sarg.). *European Journal of Wood and Wood Products,* 24(10), 432-438.

Cramm, R.H., Bibee, D.V., 1982. The theory and practice of corona treatment for improving adhesion. *Tappi Journal,* 65(8), 75-78.

Custódio, J., Broughton, J., Cruz, H., Winfield, P., 2009. Activation of timber surfaces by flame and corona treatments to improve adhesion. *International Journal of Adhesion and Adhesives,* 29(2), 167-172.

Dai, L., Griesser, H.J., Mau, A.W.H., 1997. Surface modification by plasma etching and plasma patterning. *The Journal of Physical Chemistry B,* 101(46), 9548-9554.

de Lhoneux, B., Antoine, R., Côté, W.A., 1984. Ultrastructural implications of gamma-irradiation of wood. *Wood Science and Technology,* 18(3), 161-176.

de Meijer, M., Thurich, K., Militz, H., 1998. Comparative study on penetration characteristics of modern wood coatings. *Wood Science and Technology,* 32(5), 347-365.

de Moura, L.F., Hernández, R.E., 2006. Effects of abrasive mineral, grit size and feed speed on the quality of sanded surfaces of sugar maple wood. *Wood Science and Technology,* 40(6), 517-530.

de Moura, L.F., Hernández, R.E., 2005. Evaluation of varnish coating performance for two surfacing methods on sugar maple wood. *Wood and Fiber Science,* 37(2), 355-366.

Delmotte, L., Ganne-Chedeville, C., Leban, J.M., Pizzi, A., Pichelin, F., 2008. CP-MAS ^{13}C NMR and FT-IR investigation of the degradation reactions of polymer constituents in wood welding. *Polymer Degradation and Stability,* 93(2), 406-412.

Denes, A.R., Tshabalala, M.A., Rowell, R., Denes, F., Young, R.A., 1999. Hexamethyldisiloxane-plasma coating of wood surfaces for creating water repellent characteristics. *Holzforschung,* 53(3), 318-326.

Denes, A.R., Young, R.A., 1999. Reduction of weathering degradation of wood through plasma-polymer coating. *Holzforschung,* 53(6), 632-640.

Denes, F.S., Cruz-Barba, L.E., Manolache, S., 2005. Plasma treatment of wood. In: *Handbook of Wood Chemistry and Wood Composites;* Rowell, R.M. (Ed.). CRC Press, USA, pp. 447-474.

Denes, F.S., Manolache, S., 2004. Macromolecular plasma-chemistry: an emerging field of polymer science. *Progress in Polymer Science,* 29(8), 815-885.

Denes, F.S., Young, R.A., 1998. Surface modification of polysaccharides under cold plasma conditions. In: *Polysaccharides: Structural Diversity and Functional Versatility;* Dumitriu, S. (Ed.). Marcel Dekker Inc., USA, pp. 1087.

Denes, F.S., 1997. Synthesis and surface modification by macromolecular plasma chemistry. *Trends in Polymer Science,* 5(1), 23-31.

Derbyshire, H., Miller, E., 1981. The photodegradation of wood during solar irradiation. Part I: Effects on the structural integrity of thin wood strips. *Holz Als Roh- Und Werkstoff,* 39(8), 341-350.

Donaldson, L., Frankland, A., 2004. Ultrastructure of iodine treated wood. *Holzforschung,* 58(3), 219-225.

Dong, S., Sapieha, S., Schreiber, H.P., 1993. Mechanical properties of corona-modified cellulose/polyethylene composites. *Polymer Engineering and Science,* 33(6), 343-346.

Dorris, G.M., Gray, D.G., 1978. The surface analysis of paper and wood fibers by ESCA; I. Application to cellulose and lignin. *Cellulose Chemistry and Technology,* (12), 9-23.

Dubey, M. K., 2010. Improvements in stability, durability and mechanical properties of radiata pine wood after heat-treatment in a vegetable oil. Ph.D. Thesis. University of Canterbury, New Zealand.

Durie, R.A., Lynch, B., Sternhell, S., 1960. Comparative studies of brown coal and lignin; I. Infra-red spectra. *Australian Journal of Chemistry,* 13(1), 156–168.

Ebnesajjad, S., Ebnesajjad, C.F., 2006. *Surface Treatment of Materials for Adhesion Bonding.* William Andrew Pub., NY, USA., pp. 260.

Egitto, F.D., 1990. Plasma etching and modification of organic polymers. *Pure & Applied Chemistry,* 62(9), 1699-1708.

Egitto, F.D., Vukanovic, V., Taylor, G.N., 1990. Plasma etching of organic polymers. In: *Plasma Deposition, Treatment, and Etching of Polymers;* d'Agostino, R. (Ed.). Academic press, Inc., USA, pp. 528.

Ehrhardt, S. M., 1984. An investigation of the vibrational spectra of lignin model compounds. Ph.D. Thesis. Georgia Institute of Technology, USA.

Eliezer, S., Eliezer, Y., 2001. *The Forth State of Matter: An Introduction to Plasma Science.* CRC Press, USA, pp. 224.

Evans, P.D., Ramos, M., Senden, T., 2007. Modification of wood using a glow-discharge plasma derived from water. In: *Proceedings of the Third European Conference on Wood Modification;* Hill, C.A.S., Jones, D., Militz, H., Ormondroyd, G.A. (Eds.), Bangor, pp. 123–132.

Evans, P.D., Wingate-Hill, R., Cunningham, R.B., 2009. Wax and oil emulsion additives: How effective are they at improving the performance of preservative-treated wood? *Forest Products Journal,* 59(1-2), 66-70.

Evans, P.D., 2008. Weathering and photoprotection of wood. In: *Development of Commercial Wood Preservatives; Efficacy, Environmental, and Health Issues;* Schultz, T.P., Militz, H., Freeman, M.H., Goodell, B., Nicholas, D.D. (Eds.). American Chemical Society, Washington, D.C., USA, pp. 69-117.

Evans, P.D., Palmer, G., Chowdhury, M., 2007. Bleaching treatments for blue-stained lodgepole pine affected by the mountain pine beetle *Dendroctonus ponderosae*. *European Journal of Wood and Wood Products,* 65(6), 485-486.

Evans, P.D., Thay, P.D., Schmalzl, K.J., 1996. Degradation of wood surfaces during natural weathering. Effects on lignin and cellulose and on the adhesion of acrylic latex primers. *Wood Science and Technology,* 30(6), 411-422.

Evans, P.D., Michell, A.J., Schmalzl, K.J., 1992. Studies of the degradation and protection of wood surfaces. *Wood Science and Technology,* 26(2), 151-163.

Evans, P.D., 1988. A note on assessing the deterioration of thin wood veneers during weathering. *Wood and Fiber Science,* 20(4), 487-492.

Faix, O., 1992. Fourier Transform Infrared spectroscopy. In: *Methods in Lignin Chemistry;* Lin, S.Y., Dence, C.W. (Eds.). Springer, Berlin, Germany, pp. 83-109.

Faix, O., Böttcher, J.H., 1992. The influence of particle size and concentration in transmission and diffuse reflectance spectroscopy of wood. *European Journal of Wood and Wood Products,* 50(6), 221-226.

Falkehag, S.I., Marton, J., Adler, E., 1966. Chromophores in kraft lignin. In: *Advances in Chemistry Series;* Gould, R.F. (Ed.). American Chemical Society, Washington, D.C., USA, pp. 75-89.

Feist, W.C., Hon, D.N.S., 1984. Chemistry of weathering and protection. In: *The Chemistry of Solid Wood;* Rowell, R.M. (Ed.). American Chemical Society, Washington, D.C., USA, pp. 401-451.

Feist, W.C., Mraz, E.A., 1978. Comparison of outdoor and accelerated weathering of unprotected softwoods. *Forest Products Journal,* 28(3), 38-43.

Felby, C., Nielsen, B.R., Olesen, P.O., Skibsted, L.H., 1997. Identification and quantification of radical reaction intermediates by electron spin resonance spectrometry of laccase-catalyzed oxidation of wood fibers from beech (*Fagus sylvatica*). *Applied Microbiology and Biotechnology,* 48(4), 459-464.

Fengel, D., Wegener, G., 1984. *Wood: Chemistry, Ultrastructure, Reactions.* Walter de Gruyter, Berlin, Germany, pp. 613.

Fengel, D., 1966. Electron microscopic contribution to the fine structure of beech wood (*Fagus sylvatica* L.); part III: The fine structure of the pits in beech wood. *European Journal of Wood and Wood Products,* 24(6), 245-253.

Fergus, B.J., Procter, A.R., Scott, J.A.N., Goring, D.A.I., 1969. The distribution of lignin in sprucewood as determined by ultraviolet microscopy. *Wood Science and Technology,* 3(2), 117-138.

Finson, E., Kaplan, S., Wood, L., 1995. Plasma treatment of webs and films. In: *38th Technical Proceeding of Society of Vacuum Coaters;* Chicago, USA, pp. 52-58.

Fitzpatrick, R., 2008. *Introduction to Plasma Physics: A Graduate Level Course.* The University of Texas at Austin, USA, pp. 242.

Flachowsky, G., Bär, M., Zuber, S., Tiroke, K., 1990. Cell wall content and rumen dry matter disappearance of [gamma]-irradiated wood by-products. *Biological Wastes,* 34(3), 181-189.

Flamm, D.L., Herb, G.K., 1989. Plasma etching technology: An overview. In: *Plasma Etching; an Introduction;* Manos, D.M., Flamm, D.L. (Eds.). Academic press Inc., USA, pp. 476.

Fleet, C., Breuil, C., Uzunovic, A., 2001. Nutrient consumption and pigmentation of deep and surface colonizing sapstaining fungi in *Pinus contorta*. *Holzforschung,* 55(4), 340-346}.

Fleury, R.A., Rapson, W.H., 1969. The contribution of alpha-carbonyl compounds to the colour of groundwood. *Pulp and Paper Magazine of Canada,* 70(12), 87-94.

Fogarty, W.M., 1973. Bacteria, enzymes and wood permeability. *Process Biochemistry,* 8(6), 30-34.

Foster, R.C., 1967. Fine structure of tyloses in three species of the Myrtaceae. *Australian Journal of Botany,* (15), 25-34.

Fricke, K., Steffen, H., von Woedtke, T., Schröder, K., Weltmann, K.D., 2011. High rate etching of polymers by means of an atmospheric pressure plasma jet. *Plasma Processes and Polymers,* 8(1), 51-58.

Frihart, C.R., 2005. Wood adhesion and adhesive. In: *Handbook of Wood Chemistry and Wood Composites;* Rowell, R.M. (Ed.). CRC Press, USA, pp. 216-273.

Furuno, T., Uehara, T., Jodai, S., 1990. Histochemical studies of corona-treated wood. *Mokuzai Gakkaishi (Japan Wood Research Society Journal),* 36(4), 323-331.

Gassan, J., Gutowski, V.S., 2000. Effects of corona discharge and UV treatment on the properties of jute-fibre epoxy composites. *Composites Science and Technology,* 60(15), 2857-2863.

Gfeller, B., Pizzi, A., Zanetti, M., Properzi, M., Pichelin, F., Lehmann, M., Delmotte, L., 2004. Solid wood joints by in situ welding of structural wood constituents. *Holzforschung,* 58(1), 45-52.

Gokan, H., Esho, S., Ohnishi, Y., 1983. Dry etch resistance of organic materials. *Journal of the Electrochemical Society,* 130(1), 143-146.

Goldstein, I.S., 1991. Overview of the chemical composition of wood. In: *Wood Structure and Composition;* Lewin, M., Goldstein, I.S. (Eds.). Marcel Dekker Inc., pp. 1-5.

Goswami, L., Eder, M., Gierlinger, N., Burgert, I., 2008. Inducing large deformation in wood cell walls by enzymatic modification. *Journal of Materials Science,* 43(4), 1286-1291.

Grandmaison, J.L., Thibault, J., Kaliaguine, S., Chantal, P.D., 1987. Fourier-transform infrared spectrometry and thermogravimetry of partially converted lignocellulosic materials. *Analytical Chemistry,* 59(17), 2153-2157.

Gray, D.G., 1978. The surface analysis of paper and wood fibres by ESCA; Ⅲ. Interpretation of carbon (1s) peak shape. *Cellulose Chemistry and Technology,* (12), 735-743.

Hachihama, Y., Takamuku, Y.The effects of ionization radiation on lignin and wood. *Journal of the Chemical Society of Japan (Industrial & Chemical Section),* 63(6), 1043-1046.

Hakkou, M., Petrissans, M., Zoulalian, A., Gerardin, P., 2005. Investigation of wood wettability changes during heat treatment on the basis of chemical analysis. *Polymer Degradation and Stability,* 89(1), 1-5.

Hansen, R.H., Pascale, J.V., De Benedictis, T., Rentzepis, P.M., 1965. Effect of atomic oxygen on polymers. *Journal of Polymer Science Part A: General Papers,* 3(6), 2205-2214.

Harrington, K.J., Higgins, H.G., Michell, A.J., 1964. Infrared spectra of *Eucalyptus regnans* F. Muell. and *Pinus radiata* D.Don. *Holzforschung,* 18(4), 108-113.

Haxaire, K., Marechal, Y., Milas, M., Rinaudo, M., 2002. Hydration of polysaccharide hyaluronan observed by IR spectrometry. I. Preliminary experiments and band assignments. *Peptide Science,* 72(1), 10-20.

Heady, R.D., Evans, P.D., 2005. Wood anatomy of *Actinostrobus* (Cupressaceae). *IAWA Journal,* 26(1), 79-92.

Heady, R.D., Evans, P.D., 2000. Callitroid (callitrisoid) thickening in *Callitris*. *IAWA Journal,* 21(3), 293-319.

Heady, R. D., 1997. The wood anatomy of *Callitris* Vent. (Cupressaceae): an SEM study. Ph.D. Thesis. The Australian National University, Australia.

Hergert, H.L., 1971. Infrared spectra. In: *Lignins: Occurrence, Formation, Structure and Reactions;* Sarkanen, K.V., Ludwig, C.H. (Eds.). Wiley-Interscience, NY, USA, pp. 267-297.

Hernández, R.E., Cool, J., 2008. Evaluation of three surfacing methods on paper birch wood in relation to water- and solvent-borne coating. *Wood and Fiber Science,* 40(3), 459-469.

Hihara, T., Okada, Y., Morita, Z., 2000. The reaction of triphenodioxazine dyes with bleaching agents, hypochlorite and hydrogen peroxide, in aqueous solution. *Dyes and Pigments,* 46(3), 181-192.

Hill, C.A.S., 2006. *Wood Modification: Chemical, Thermal and Other Processes.* John Willy and Sons, England, pp. 239.

Homan, W., B. Tjeerdsma., 2005. Control systems, quality assessment and certification of modified wood for market introduction. In: *Proceedings of the Second European Conference on Wood Modification;* Militz, D., Hill, C. (Eds.), Göttingen, Germany, pp. 382-389.

Hon, D.N.S., Minemura, N., 2001. Color and discoloration. In: *Wood and Cellulosic Chemistry;* Hon, D.N.S., Shiraishi, N. (Eds.). Marcel Dekker, Inc., NY, USA, pp. 385-442.

Hon, D.N.S., 1984. ESCA study of oxidized wood surfaces. *Journal of Applied Polymer Science,* 29(9), 2777-2784.

Honary, L.A.T., 2003. Soybean oil impregnation wood preservative process and products. United States patent (US 6641927 B1), USA.

Hua, Z.Q., Sitaru, R., Denes, F.S., Young, R.A., 1997. Mechanisms of oxygen-and argon-RF-plasma-induced surface chemistry of cellulose. *Plasmas and Polymers,* 2(3), 199-224.

Huang, H., Wang, B.J., Dong, L., Zhao, M., 2011. Wettability of hybrid poplar veneers with cold plasma treatments in relation to drying conditions. *Drying Technology,* 29(3), 323-330.

Inagaki, N., Narushima, K., Lim, S.K., 2003. Effects of aromatic groups in polymer chains on plasma surface modification. *Journal of Applied Polymer Science,* 89(1), 96-103.

Inagaki, N., 1996. *Plasma Surface Modification and Plasma Polymerization.* CRC Press, USA, pp. 265.

Inari, G.N., Petrissans, M., Lambert, J., Ehrhardt, J.J., Gerardin, P., 2006. XPS characterization of wood chemical composition after heat-treatment. *Surface and Interface Analysis,* 38(10), 1336-1342.

Jama, C., Delobel, R., 2007. Cold plasma technologies for surface modification and thin film deposition. In: *Multifunctional Barriers for Flexible Structure, Textile, Leather and Paper;* Duquesne, S., Magniez, C., Camino, G. (Eds.). Springer, Berlin, Germany, pp. 109-292.

Jamali, A., Evans, P., 2011. Etching of wood surfaces by glow discharge plasma. *Wood Science and Technology,* 45(1), 169-182.

Janson, J., 1970. Composition of the polysaccharide composition of wood and pulp. *Paperi Ja Puu,* 52(5), 323-329.

Johansson, J., Masuoka, T., 1999. Penetration of pores in membranes by plasma polymer forming species. *Macromolecular Rapid Communications,* 20(1), 12-15.

Johansson, L.S., Campbell, J.M., Koljonen, K., Stenius, P., 1999. Evaluation of surface lignin on cellulose fibers with XPS. *Applied Surface Science,* 144-145, 92-95.

Kamke, F.A., Lee, J.N., 2007. Adhesive penetration in wood-A review. *Wood and Fiber Science,* 39(2), 205-220.

Kan, C.W., Yuen, C.W.M., 2009. Influence of low temperature plasma treatment on the properties of tencel and viscose rayon fibers. *Plasma Science, IEEE Transactions on,* 37(8), 1615-1619.

Kaplan, S.L., Rose, P.S., 2007. Plasma surface treatment. In: *Coatings Technology: Fundamentals, Testing, and Processing Techniques;* Tracton, A.A. (Ed.). CRC Press, USA, pp. 401-406.

Kass, A.J., 1975. Effect of incising on bending properties of redwood dimension lumber. In: *U.S.D.A. Forest Service Research Paper, FPL 232;* Madison, WIS, USA, pp. 1-8.

Kato, Y., Onishi, H., Machida, Y., 2003. Application of chitin and chitosan derivatives in the pharmaceutical field. *Current Pharmaceutical Biotechnology,* 4(5), 303-309.

Kazayawoko, M., Balatinecz, J.J., Matuana, L.M., 1999. Surface modification and adhesion mechanisms in woodfiber-polypropylene composites. *Journal of Materials Science,* 34(24), 6189-6199.

Keith, C.T., Chauret, G., 1988. Anatomical studies of CCA penetration associated with conventional (tooth) and with micro (needle) incising. *Wood and Fiber Science,* 20(2), 197-208.

Kellogg, R.M., Wangaard, F.F., 1969. Variation in the cell-wall density of wood. *Wood and Fiber Science,* 1(3), 180-204.

Kenealy, W., Buschle-Diller, G., Ren, X., 2006. Enzymatic modification of fibers for textile and forest product industries. In: *Modified Fibers with Medical and Specialty Applications;* Edwards, J.V., Buschle-Diller, G., Goheen, S.C. (Eds.). Springer, The Netherlands, pp. 191-208.

Khan, M.A., Khan, R.A., Aliya, B.C., Nasreen, Z., 2006. Effect of the pretreatment with UV and gamma radiations on the modification of plywood surface by photocuring with epoxy acrylate. *Journal of Polymers and the Environment,* 14(1), 111-118.

Kharazipour, A., Hüttermann, A.L., Luedemann, H.D., 1997. Enzymatic activation of wood fibres as a mean for the production of wood composites. *Journal of Adhesion Science and Technology,* 11(3), 419-427.

Kiguchi, M., Kataoka, Y., Suzuki, M., Imamura, Y., 2005. Progress toward the service life prediction of coatings for exterior wood by weathering test trials. In: *Service Life Prediction, Challenging the Status Quo;* Martin, J.W., Ryntz, R.A., Dickie, R.A. (Eds.). Federation of societies for coating technologies, pp. 123-134.

Kiguchi, M., Evans, P.D., 1998. Photostabilisation of wood surfaces using a grafted benzophenone UV absorber. *Polymer Degradation and Stability,* 61(1), 33-45.

Kiguchi, M., 1996. Surface modification and activation of wood. In: *Chemical Modification of Lignocellulosic Materials;* Hon, D.N.-. (Ed.). Marcel Dekker Inc., NY, USA, pp. 197-228.

Kiihamäki, J., Franssila, S., 1999. Pattern shape effects and artefacts in deep silicon etching. *Journal of Vacuum Science & Technology A: Vacuum, Surfaces, and Films,* 17(4), 2280-2285.

Kimura, F., Kimura, T., Gray, D.G., 1994. FT-IR study of the effect of irradiation wavelength on the colour reversion of thermomechanical pulps. *Holzforschung,* 48(4), 343-348.

Kinloch, A.J., 1987. *Adhesion and Adhesives: Science and Technology.* Chapman and Hall, London, UK, pp. 441.

Klarhofer, L., Viol, W., Maus-Friedrichs, W., 2010. Electron spectroscopy on plasma treated lignin and cellulose. *Holzforschung,* 64(3), 331-336.

Kobayashi, M., Konno, K., Nagazoe, H., Yamaguchi, T., Onoe, K., 2006. Decomposition of biomass by microwave plasma process. *Studies in Surface Science and Catalysis,* 159(1), 821-824.

Kobayashi, Y., Iida, I., Imamura, Y., Watanabe, U., 1998. Drying and anatomical characteristics of sugi wood attacked by bacteria during pond storage. *Journal of Wood Science,* 44(6), 432-437.

Kogelschatz, U., 2003. Dielectric-barrier discharges: Their history, discharge physics, and industrial applications. *Plasma Chemistry and Plasma Processing,* 23(1), 1-46.

Kogoma, M., Turban, G., 1986. Mechanism of etching and of surface modification of polyimide in RF and LF SF_6-O_2 discharges. *Plasma Chemistry and Plasma Processing,* 6(4), 349-380.

Kollmann, F.F.P., Côté, W.A.J., 1968. *Principals of Wood Science and Technology. I; Solid Wood.* Springer- Verlag, Heidelberg, Germany, pp. 592.

Kolluri, O.S., 2003. Application of plasma technology for improved adhesion of materials. In: *Handbook of Adhesive Technology;* Pizzi, A., Mittal, K.L. (Eds.). CRC Press, USA, pp. 1-11.

Kotilainen, R.A., Alén, R.J., Toivanen, T.J., 2001. Chemical changes in black alder (*Alnus glutinosa*) and European aspen (*Populus tremula*) during heating at 150-220 °C in a nitrogen atmosphere. *Cellulose Chemistry and Technology,* 35(3-4), 275-284.

KSV Instruments, 2007. CAM 200, 3rd edition. Espoo, Finland.

Kuo, M.L., McClelland, J.F., Luo, S., Chien, P.L., Walker, R., Hse, C.Y., 1988. Applications of infrared photo-acoustic spectroscopy for wood samples. *Wood and Fiber Science,* 20(1), 132-145.

Kurt, R., Krause, A., Militz, H., Mai, C., 2008. Hydroxymethylated resorcinol (HMR) priming agent for improved bondability of wax-treated wood. *European Journal of Wood and Wood Products,* 66(5), 333-338.

Kutner, M.H., Nachtsheim, C.J., Neter, J., Li, W., 2005. *Applied Linear Statistical Models.* McGraw-Hill, New York, USA, pp. 1396.

Kwok, R. W. M., 2000. XPSPEAK, Version 4.1. Department of Chemistry, The Chinese University of Hong Kong, Shatin, Hong Kong.

Laguardia, L., Vassallo, E., Cappitelli, F., Mesto, E., Cremona, A., Sorlini, C., Bonizzoni, G., 2005. Investigation of the effects of plasma treatments on biodeteriorated ancient paper. *Applied Surface Science,* 252(4), 1159-1166.

Lee, B.G., Maristany, A., Brunner, C.C., Morrell, J.J., 1995. Removing fungal stain from ponderosa pine by caustic bleaching. *Forest Products Journal,* 45(3), 56-60.

Lee, C., Gopalakrishnan, R., Nyunt, K., Wong, A., Tan, R.C., Ong, J.W., 1999. Plasma cleaning of plastic ball grid array package. *Microelectronic Reliability,* 39(1), 97-105.

Lee, K., Delille, A., Bismarck, A., 2011. Greener surface treatment of natural fibres for the production of renewable composite materials. In: *Cellulose Fibers: Bio- and Nano-Polymer Composites; Green Chemistry and Technology;* Kalia, S., Kaith, B.S., Kaur, I. (Eds.). Springer, USA, pp. 155-178.

Lehringer, C., Schwarze, F.W.M.R., Militz, H., 2009. A review on promising approaches for liquid permeability improvement on softwoods. *Wood and Fiber Science,* 41(4), 373-385.

Li, H., Costil, S., Barnier, V., Oltra, R., Heintz, O., Coddet, C., 2006. Surface modifications induced by nanosecond pulsed Nd: YAG laser irradiation of metallic substrates. *Surface and Coatings Technology,* 201(3-4), 1383-1392.

Liese, W., 1970. Ultrastructural aspects of woody tissue disintegration. *Annual Review of Phytopathology,* 8(1), 231-258.

Liese, W., 1965. The warty layer. In: *Cellular Ultrastructure of Woody Plants;* Côté, W.A. (Ed.). Syracuse University Press, USA, pp. 251.

Lipska-Quinn, A. E., 1994. The effect of RF plasma on the chemical and physical properties of wood. Ph.D. Thesis. University of California, Berkeley, USA.

Liston, E.M., Martinu, L., Wertheimer, M.R., 1994. Plasma surface modification of polymers for improved adhesion; a critical review. In: *Plasma Surface Modification of Polymers: Relevance to Adhesion;* Strobel, M.C.S., Mittal, K.L. (Eds.). VSP, The Netherlands, pp. 3.

Liu, C., 2011. Use of confocal profilometry to quantify erosion of wood and screen chemicals for their ability to photostabilize wood. M.Sc. Thesis. University of British Columbia, Vancouver, Canada.

Liu, W.J., Guo, X.J., Chuang, C.H., 2005. The effects of plasma surface modification on the molding adhesion properties of film-BGA package. *Surface and Coatings Technology,* 196(1-3), 192-197.

Lukowsky, D., Hora, G., 2002. Pretreatment of wood to enhance the performance of outdoor coatings. *Macromolecular Symposia,* 187(1), 77-85.

Magalhães, W.L.E., de Souza, M.F., 2002. Solid softwood coated with plasma-polymer for water repellence. *Surface & Coatings Technology,* 155(1), 11-15.

Mahlberg, R., Niemi, H.E.M., Denes, F.S., Rowell, R.M., 1999. Application of AFM on the adhesion studies of oxygen-plasma-treated polypropylene and lignocellulosics. *Langmuir,* 15(8), 2985-2992.

Mai, C., Kües, U., Militz, H., 2004. Biotechnology in the wood industry. *Applied Microbiology and Biotechnology,* 63(5), 477-494.

Mater, J., 1957. Chemical effects of high energy irradiation of wood *Forest Product Journal,* 7(6), 208-209.

Matsui, H., Setoyama, K., Kurosu, H., 1992. Surface modification of wood in fluorine-containing gas plasma I. Tetrafluoromethane plasma treatment. *Mokuzai Gakkaishi (Japan Wood Research Society Journal),* 38(1), 73-80.

Mertens, N., Wolkenhauer, A., Leck, M., Viöl, W., 2006. UV laser ablation and plasma treatment of wooden surfaces – a comparing investigation. *Laser Physics. Letter,* 3(8), 380-384.

Microsoft Corporation, 2006. Excel for Windows, 12th edition. Redmond, WA, USA.

Militz, H., 2008. Processes and properties of thermally modified wood manufactured in Europe. In: *Development of Commercial Wood Preservatives; Efficacy, Environmental, and Health Issues;* Schultz, T.P., Militz, H., Freeman, M.H., Goodell, B., Nicholas, D.D. (Eds.). Amirican Chemical Society, Washington, D.C., USA, pp. 372-388.

Militz, H., 1993. Enzymatic pretreatment of spruce posts and sawn boards to improve their treatability with wood preservatives. *Holz Als Roh-Und Werkstoff,* 51(5), 339-346.

Morohoshi, N., Sakakibara, A., 1971. The chemical composition of reaction wood. I. *Mokuzai Gakkaishi (Japan Wood Research Society Journal),* 17(9), 393-399.

Moss, S.J., 1987. Polymer degradation in reactive-gas plasmas. *Polymer Degradation and Stability,* 17(3), 205-222.

Moss, S.J., Jolly, A.M., Tighe, B.J., 1986. Plasma oxidation of polymers. *Plasma Chemistry and Plasma Processing,* 6(4), 401-416.

Murmanis, L., River, B.H., Stewart, H.A., 1986. Surface and subsurface characteristic related to the abrasive-planing condition. *Wood and Fiber Science,* 18(1), 107-117.

Murmanis, L., Stewart, H.A., River, B.H., 1983. Microscopy of abrasive-planed and knife-planed surfaces in wood-adhesive bonds. *Wood and Fiber Science,* 15(2), 102-115.

Muzzarelli, R.A.A., Muzzarelli, B., 1998. Structural and functional versatility of chitins. In: *Polysaccharides: Structural Diversity and Functional Versatility;* Dumitriu, S. (Ed.). Marcel Dekker Inc., USA, pp. 569-594.

Myers Jr, L.S., 1973. Radiation chemistry of nucleic acids, proteins, and polysaccharides. In: *The Radiation Chemistry of Macromolecules;* Dole, M. (Ed.). Academic Press, Inc., NY, USA, pp. 323-374.

Nair, M.N.B., 1987. Occurrence of helical thickenings on the vessel element walls of dicotyledonous woods. *Annals of Botany,* 60(1), 23.

Nakagame, S., Chandra, R.P., Kadla, J.F., Saddler, J.N., 2011. Enhancing the enzymatic hydrolysis of lignocellulosic biomass by increasing the carboxylic acid content of the associated lignin. *Biotechnology and Bioengineering,* 108(3), 538-548.

Nayak, P.L., 1999. Biodegradable polymers: Opportunities and challenges. *Journal of Macromolecular Science; Polymer Reviews,* 39(3), 481-505.

Nickerson, R., 1998. Plasma surface modification for cleaning and adhesion. In: *TAPPI Polymers, Laminations and Coatings Conference Proceedings;* Billerica, MA, USA.

Nzokou, P., Kamdem, D.P., 2005. X-ray photoelectron spectroscopy study of red oak (*Quercus rubra*), black cherry (*Prunus serotina*) and red pine (*Pinus resinosa*) extracted wood surfaces. *Surface and Interface Analysis,* 37(8), 689-694.

Odraskova, M., Rahel, J., Zahoranova, A., Tino, R., Cernak, M., 2008. Plasma activation of wood surface by diffuse coplanar surface barrier discharge. *Plasma Chemistry and Plasma Processing,* 28(2), 203-211.

Oehrlein, G.S., Phaneuf, R.J., Graves, D.B., 2011. Plasma-polymer interactions: A review of progress in understanding polymer resist mask durability during plasma etching for nanoscale fabrication. *Journal of Vacuum Science & Technology B: Microelectronics and Nanometer Structures,* 29(1), 1-35.

Olde Riekerink, M. B., 2001. Structural and chemical modification of polymer surfaces by gas plasma etching. Ph.D. Universiteit Twente, The Netherlands.

Olsson, A.M., Salmén, L., 2004. The association of water to cellulose and hemicellulose in paper examined by FTIR spectroscopy. *Carbohydrate Research,* 339(4), 813-818.

Pabeliņa, K.G., Lumban, C.O., Ramos, H.J., 2011. Plasma impregnation of wood with fire retardants. *Nuclear Instruments and Methods in Physics Research Section B: Beam Interactions with Materials and Atoms,* -, doi:10.1016/j.nimb.2011.01.102.

Pandey, K.K., Pitman, A.J., 2004. Examination of the lignin content in a softwood and a hardwood decayed by a brown-rot fungus with the acetyl bromide method and Fourier transform infrared spectroscopy. *Journal of Polymer Science Part A: Polymer Chemistry,* 42(10), 2340-2346.

Pandey, K.K., Khali, D.P., 1998. Accelerated weathering of wood surfaces modified by chromium trioxide. *Holzforschung,* 52(5), 467-471.

Pandey, K.K., Theagarajan, K.S., 1997. Analysis of wood surfaces and ground wood by diffuse reflectance (DRIFT) and photoacoustic (PAS) Fourier transform infrared spectroscopic techniques. *European Journal of Wood and Wood Products,* 55(6), 383-390.

Pandey, K.K., Pitman, A.J., 2003. FTIR studies of the changes in wood chemistry following decay by brown-rot and white-rot fungi. *International Biodeterioration & Biodegradation,* 52(3), 151-160.

Parameswaran, N., Liese, W., 1982. Ultrastructural localization of wall components in wood cells. *European Journal of Wood and Wood Products,* 40(4), 145-155.

Parham, R.A., Côté, W.A., 1971. Distribution of lignin in normal and compression wood of Pinus taeda L. *Wood Science and Technology,* 5(1), 49-62.

Pederson, L.A., 1982. Structural composition of polymers relative to their plasma etch characteristics. *Journal of the Electrochemical Society,* 129(1), 205-208.

Petrič, M., Knehtl, B., Krause, A., Militz, H., Pavlič, M., Pétrissans, M., Rapp, A.O., Tomažič, M., Welzbacher, C., Gérardin, P., 2007. Wettability of waterborne coatings on chemically and thermally modified pine wood. *Journal of Coatings Technology and Research,* 4(2), 203-206.

Plattner, A. B. L., 2008. Pathology and taxonomy of fungi associated with the mountain pine beetle in British Columbia. M.Sc. Thesis. University of British Columbia, Vancouver, Canada.

Podgorski, L., Bousta, C., Schambourg, F., Maguin, J., Chevet, B., 2001. Surface modification of wood by plasma polymerization. *Pigment and Resin Technology,* 31(1), 33-40.

Podgorski, L., Chevet, B., Onic, L., Merlin, A., 2000. Modification of wood wettability by plasma and corona treatments. *International Journal of Adhesion and Adhesives,* 20(2), 103-111.

Polcin, J., Rapson, W.H., 1969. Interpretation of UV and visible spectrum of lignin. *Pulp and Paper Magazine of Canada,* 70(24), 99-106.

Preston, A.F., 2000. Wood preservation: Trend of today that will influence the industry tomorrow. *Forest Products Journal,* 50(9), 12-19.

Pykonen, M., Lahti, J., 2008. Influence of atmospheric plasma activation on sheet-fed offset print quality. *Nordic Pulp and Paper Research Journal,* 32(2), 181-188.

Ramos, M., 2001. Improving the gluing of eucalypts timber by plasma modification of wood surface. M.Sc. Thesis. The Australian National University, Australia.

Rapp, A.O., Sailer, M., 2001. Heat treatment of wood in Germany–State of the art. In: *Review on Heat Treatments of Wood. Proceedings of the Special Seminar on Heat Treatments;* Rapp, A.O. (Ed.), Antibes, France, pp. 43-60.

Rawlinson, P., 1999. Vacuum plasma processing. *Material World,* 7(5), 276-277.

Rehn, P., Wolkenhauer, A., Bente, M., Förster, S., Viöl, W., 2003. Wood surface modification in dielectric barrier discharges at atmospheric pressure. *Surface and Coatings Technology,* 174-175, 515-518.

Rehn, P., Viöl, W., 2003. Dielectric barrier discharge treatments at atmospheric pressure for wood surface modification. *Holz Als Roh- Und Werkstoff,* 61(2), 145-150.

Reich, L., Stivala, S., 1971. *Elements of Polymer Degradation.* McGraw-Hill, NY, USA, pp. 361.

Richter, G., Herdle, L., Wathera, W., 1957. Cellulose swelling measured by benzene retention. *Industrial & Engineering Chemistry,* 49(5), 907-912.

River, B.H., Vick, C.B., Gillespie, R.H., 1991. Wood as an adherend. In: *Treatise on Adhesion and Adhesives;* Minford, J.D.M. (Ed.). CRC Press, USA, pp. 1-230.

Rodrigues, J., Faix, O., Pereira, H., 1998. Determination of lignin content of *Eucalyptus globulus* wood using FTIR spectroscopy. *Holzforschung,* 52(1), 46-50.

Ross, A., Daisey, G., Jourdain, C., Williams, S., 1998. Cleaners and restorers for wood decks. *The Paint Dealer,* 7(4), 30-33.

Rossell, T. N., 2007. Plasma modification of carbon black surface: From reactor design to final application. Ph.D. Thesis. Universitat Ramon Liull, Barcelona, Spain.

Rowell, R.M., 2005. Chemical modification of wood. In: *Handbook of Wood Chemistry and Wood Composites;* Rowell, R.M. (Ed.). CRC Press, USA, pp. 381-420.

Ruddick, J.N.R., Yamamoto, K., Wong, P.C., Mitchell, K.A.R., 1992. X-ray photoelectron spectroscopic analysis of CCA-treated wood. In: *The International Research Group on Wood Preservation 23rd Annual Meeting;* Harrogate, UK, pp. 1-13.

Sachs, I., Kuntz, J., Ward, J., Nair, G., Schultz, N., 1970. Tyloses structure. *Wood and Fiber,* 2(3), 259-268.

Sahoo, K.C., Lin, M.K., Chang, E.Y., Tinh, T.B., Li, Y., Huang, J.H., 2009. Silicon nitride nanopillars and nanocones formed by nickel nanoclusters and inductively coupled plasma etching for solar cell application. *Japanese Journal of Applied Physics,* 48(12), 126508.

Saka, S., 2001. Chemical composition and distribution. In: *Wood and Cellulosic Chemistry;* Hon, D.N.S., Shiraishi, N. (Eds.). Marcel Dekker, Inc., NY, USA, pp. 51-82.

Sakakibara, A., 1980. A structural model of softwood lignin. *Wood Science and Technology,* 14(2), 89-100.

Sakata, I., Morita, M., Tsuruta, N., Morita, K., 1993. Activation of wood surface by corona treatment to improve adhesive bonding. *Journal of Applied Polymer Science,* 49(7), 1251-1258.

Sakata, I., Morita, M., Furuichi, H., Kawaguchi, Y., 1991. Improvement of plybond strength of paperboard by corona treatment. *Journal of Applied Polymer Science,* 42(7), 2099-2104.

Sapieha, S., Wrobel, A.M., Wertheimer, M.R., 1988. Plasma-assisted etching of paper. *Plasma Chemistry and Plasma Processing,* 8(3), 331-346.

Sarkanen, K.V., Chang, H.M., Ericsson, B., 1967. Species variation in lignins; I. Infrared spectra of guaiacyl and syringyl models. *Tappi,* 50(11), 572-575.

Sawabe, O., Sawabe, T., Kitao, K., Sato, A., 1968. Effects of major wood components on thermal decomposition of wood. *Mokuzai Gakkaishi (Japan Wood Research Society Journal),* 14(2), 104-109.

Scheffer, T.C., 1973. Microbilogical degradation and the causal organisms. In: *Wood Deterioration and its Prevention by Preservative Treatments;* Nicholas, D.D. (Ed.). Syracuse University Press, NY, USA, pp. 31-106.

Schmid, R., Machado, R.D., 1968. Pit membranes in hardwoods-Fine structure and development. *Protoplasma,* 66(1), 185-204.

Schmidt, O., Czeschlik, D., 2006. *Wood and Tree Fungi: Biology, Damage, Protection, and use.* Springer Verlag, Berlin, pp. 334.

Schultz, J., Nardin, M., 1999. Theories and mechanisms of adhesion. In: *Adhesion Promotion Techniques: Technological Applications;* Mittal, K.L., Pizzi, A. (Eds.). CRC Press, USA, pp. 1-15.

Schuman, T., Adolfsson, B., Wikström, M., Rigdahl, M., 2005. Surface treatment and printing properties of dispersion-coated paperboard. *Progress in Organic Coatings,* 54(3), 188-197.

Schwarze, F.W.M.R., Landmesser, H., Zgraggen, B., Heeb, M., 2006. Permeability changes in heartwood of *Picea abies* and *Abies alba* induced by incubation with *Physisporinus vitreus*. *Holzforschung,* 60(4), 450-454.

Schwarze, F.W.M.R., Landmesser, H., 2000. Preferential degradation of pit membranes within tracheids by the basidiomycete *Physisporinus vitreus*. *Holzforschung,* 54(5), 461-462.

Seifert, K., 1964. Zur Chemie gammabestrahlten Holzes (On the chemistry of gamma radiated wood). *European Journal of Wood and Wood Products,* 22(7), 267-275.

Sell, J., Feist, W.C., 1986. Role of density in the erosion of wood during weathering. *Forest Products Journal,* 36(3), 57-60.

Sernek, M., 2002. Comparative analysis of inactivated wood surfaces. Ph.D. Virginia Polytechnic Institute and State University, Virginia, USA.

Setoyama, K., 1996. Surface modification of wood by plasma treatment and plasma polymerization. *Journal of Photopolymer Science and Technology,* 9(2), 243-250.

Shaffner, T.J., Van Veld, R.D., 1971. 'Charging' effects in the scanning electron microscope. *Journal of Physics E: Scientific Instruments,* 4(9), 633-637.

Singh, A.P., Gallagher, S.S., Schmitt, U., Dawson, B.S., Kim, Y.S., 1998. Ponding of radiata pine (*Pinus radiata*); 2. The effect of ponding on coating penetration into wood. In: *The International Research Group on Wood Preservation 29th Annual Meeting;* Maastricht, The Netherlands, pp. 1-8.

Singh, A.P., 1997. Initial pit borders in *Pinus radiata* are resistant to degradation by soft rot fungi and erosion bacteria but not tunnelling bacteria. *Holzforschung,* 51(1), 15-18.

Sinn, G., Reiterer, A., Stanzl-Tschegg, S., 2001. Surface analysis of different wood species using X-ray photoelectron spectroscopy (XPS). *Journal of Materials Science,* 36(19), 4673-4680.

Sjöström, E., 1981. *Wood Chemistry: Fundamental and Applications.* Academic Press, London, UK, pp. 223.

Skvortsov, S.V., 1990. Radiation degradation of lignin. *Chemistry of Natural Compounds,* 26(1), 1-9.

Smith, D.M., Mixer, R.Y., 1959. The effects of lignin on the degradation of wood by gamma irradiation. *Radiation Research,* 11(6), 776-780.

Stamm, A.J., Burr, H.K., Kline, A.A., 1946. Staybwood...Heat-stabilized wood. *Industrial & Engineering Chemistry,* 38(6), 630-634.

Steen, M.L., Jordan, A.C., Fisher, E.R., 2002. Hydrophilic modification of polymeric membranes by low temperature H_2O plasma treatment. *Journal of Membrane Science,* 204(1-2), 341-357.

Steinbruchel, C.H., Curtis, B.J., Lehmann, H.W., Widmer, R., 1986. Diagnostics of low pressure oxygen radio-frequency plasmas and the mechanism for polymer etching: a comparison between reactive sputter etching and magnetron sputter etching. *IEEE Transaction on Plasma Science,* 14(2), 137-144.

Stenius, P., Vuorinen, T., 1999. Direct characterization of chemical properties of fibers. In: *Analytical Methods in Wood Chemistry, Pulping, and Papermaking;* Sjöström, E., Alén, R. (Eds.). Springer, Berlin, pp. 149–192.

Stewart, H.A., Crist, J.B., 1982. SEM [scanning electron microscopic] examination of subsurface damage of wood after abrasive and knife planing. *Wood Science,* 14(3), 106-109.

Stirling, R., Morris, P.L., 2009. Decolorization of blue stain in lodgepole pine sapwood by hypochlorite bleaching and light exposure. *Forest Products Journal,* 59(7-8), 47-52.

Suranyi, G., Gray, D.G., Goring, D.A., 1980. The effect of corona discharge on wettability of aged corrugating medium. *Tappi,* 63(4), 153-154.

Tabirih, P., McGinnes, E., Kay, M., Harlow, C., 1977. A note on anatomical changes of white oak wood upon exposure to gamma radiation. *Wood and Fiber Science,* 9(3), 211-215.

Tan, I.H., Silva, M.L.P., Demarquette, N.R., 2001. Paper surface modification by plasma deposition of double layers of organic silicon compounds. *Journal of Materials Chemistry,* 11(4), 1019-1025.

Tappi, 2000. Tappi Test Methods, T 249 cm-00; Carbohydrate composition of extractive-free wood and wood pulp by gas-liquid chromatography. Atlanta, GA, USA.

Tappi, 1991a. Tappi Test Methods, T 222 om-88; Acid-insoluble lignin in wood and pulp. Atlanta, GA, USA.

Tappi, 1991b. Tappi Useful Methods, UM 250; Acid-soluble lignin in wood and pulp. Atlanta, GA, USA.

Taylor, G.N., Wolf, T.M., 1980. Oxygen plasma removal of thin polymer films. *Polymer Engineering and Science,* 20(16), 1087-1092.

Temiz, A., Terziev, N., Eikenes, M., Hafren, J., 2007. Effect of accelerated weathering on surface chemistry of modified wood. *Applied Surface Science,* 253(12), 5355-5362.

Theocharopoulos, A., Zou, L., Hill, R., Cattell, M., 2010. Wear quantification of human enamel and dental glass-ceramics using white light profilometry. *Wear,* 269(11-12), 930-936.

Timar-Balazsy, A., Eastop, D., 1998. *Chemical Principles of Textile Conservation.* Butterworth-Heinemann, London, UK, pp. 444.

Timell, T.E., 1986. *Compression Wood in Gymnosperms.* Springer-Verlag: Berlin Heidelberg, Germany, pp. 2150.

Timell, T.E., 1982. Recent progress in the chemistry and topochemistry of compression wood. *Wood Science and Technology,* 16(2), 83-122.

Timell, T.E., 1980. Karl Gustav Sanio and the first scientific description of compression wood. *IAWA Bulletin,* 1(4), 147-153.

Timell, T.E., 1978. Helical thickenings and helical cavities in normal and compression woods of *Taxus baccata*. *Wood Science and Technology,* 12(1), 1-15.

Tischer, F.Y., 1939. Method of drying veneers. United States patent (US 2177160), USA.

Tolvaj, L., Faix, O., 1995. Artificial ageing of wood monitored by DRIFT spectroscopy and CIE L* a* b* color measurements; 1. Effect of UV light. *Holzforschung,* 49(5), 397-404.

Tonks, L., 1967. The birth of plasma. *American Journal of Physics,* 35(9), 857-858.

Toriz, G., Denes, F., Young, R.A., 2000. Plasma modification of lignin. In: *Lignin: Historical, Biological, and Materials Perspectives;* Glasser, W.G., Northey, R.A., Schultz, T.P. (Eds.). American Chemical Society, Washington, D.C., USA, pp. 367-389.

Tshabalala, M.A., 2005. Surface characterization. In: *Handbook of Wood Chemistry and Wood Composites;* Rowell, R.M. (Ed.). CRC Press, USA, pp. 187-211.

Uehara, T., 1999. Corona discharge treatment of polymers. In: *Adhesion Promotion Techniques: Technological Applications;* Mittal, K.L., Pizzi, A. (Eds.). CRC Press, USA, pp. 191-204.

Uehara, T., Nishimura, H., Furuno, T., Jodai, S., Sakata, I., 1993. Effect of corona discharge treatment on beech wood meal. *Mokuzai Gakkaishi (Japan Wood Research Society Journal),* 39(6), 729-733.

Uehara, T., Jodai, S., 1987. Gluing of wood by corona treatment. *Mokuzai Gakkaishi (Japan Wood Research Society Journal),* 33(10), 777-784.

Vander Wielen, L.C., Elder, T., Ragauskas, A.J., 2005. Analysis of the topochemical effects of dielectric-barrier discharge on cellulosic fibers. *Cellulose,* 12(2), 185-196.

Vander Wielen, L.C., Östenson, M., Gatenholm, P., Ragauskas, A.J., 2006. Surface modification of cellulosic fibers using dielectric-barrier discharge. *Carbohydrate Polymers,* 65(2), 179-184.

Vaswani, S., Koskinen, J., Hess, D.W., 2005. Surface modification of paper and cellulose by plasma-assisted deposition of fluorocarbon films. *Surface and Coatings Technology,* 195(2-3), 121-129.

Vernois, M., 2001. Heat treatment of wood in France; State of the art. In: *Review on Heat Treatments of Wood. Proceedings of the Special Seminar on Heat Treatments;* Rapp, A.O. (Ed.), Antibes, France, pp. 35-42.

Voet, D., Voet, J.G., Pratt, C.W., 1999. *Fundamentals of Biochemistry.* John Wiley and Sons, Inc., USA, pp. 931.

VSN International Ltd., 2009. Genstat for windows, 12th edition. Hemel Hempstead, HRT, UK.

Wang, J.Y., 2007. Initiating evaluation of thermal oil treatment for post-MPB Lodgepole pine. *FII. Forintek, Vancouver,* 34 pp.

Wang, J.Y., Cooper, P.A., 2005. Properties of hot oil treated wood and possible chemical reaction between wood and soybean oil during the treatment. In: *The International Research Group on Wood Preservation 36rd Annual Meeting;* Bangalore, India.

Ward, P.P., 1996. Plasma cleaning techniques and future applications in environmentally conscious manufacturing. *SAMPE Journal,* 32(1), 51-54.

Warner, S.B., Uhlmann, D.R., Peebles, L.H., 1975. Ion etching of amorphous and semicrystalline fibres. *Journal of Materials Science,* 10(5), 758-764.

Weiland, J.J., Guyonnet, R., 2003. Study of chemical modifications and fungi degradation of thermally modified wood using DRIFT spectroscopy. *European Journal of Wood and Wood Products,* 61(3), 216-220.

Whitney, H.S., Farris, S.H., 1970. Maxillary mycangium in the mountain pine beetle. *Science,* 167(3914), 54-55.

Wilken, L., Hoffmann, V., Wetzig, K., 2003. Erosion rate measurements for GD-OES. *Journal of Analytical Atomic Spectrometry,* 18(9), 1141-1145.

Williams, R.S., Knaebe, M.T., Sotos, P.G., Feist, W.C., 2001. Erosion rates of wood during natural weathering. Part I. Effects of grain angle and surface texture. *Wood and Fiber Science,* 33(1), 31-42.

Williams, R.S., 1999. *Wood Handbook: Wood as an Engineering Material.* Forest Products Laboratory. Madison, WI, USA, pp. 463.

Winandy, J.E., Morrell, J.J., 1998. Effects of incising on lumber strength and stiffness: Relationships between incision density and depth, species, and MSR grade. *Wood and Fiber Science,* 30(2), 185-197.

Wohlfart, E., Fernández-Blázquez, J.P., Knoche, E., Bello, A., Pérez, E., Arzt, E., del Campo, A., 2010. Nanofibrillar patterns by plasma etching: The influence of polymer crystallinity and orientation in surface morphology. *Macromolecules,* 43(23), 9908-9917.

Wolkenhauer, A., Avramidis, G., Cai, Y., Militz, H., Viöl, W., 2007. Investigation of wood and timber surface modification by dielectric barrier discharge at atmospheric pressure. *Plasma Processes and Polymers,* 4(S1), 470-474.

Wolkenhauer, A., Avramidis, G., Hauswald, E., Militz, H., Viöl, W., 2009. Sanding vs. plasma treatment of aged wood: A comparison with respect to surface energy. *International Journal of Adhesion and Adhesives,* 29(1), 18-22.

Worrall, J.J., Anagnost, S.E., Zabel, R.A., 1997. Comparison of wood decay among diverse lignicolous fungi. *Mycologia,* 89(2), 199-219.

Wu, S., 1982. *Polymer Interface and Adhesion.* CRC Press, USA, pp. 630.

Yasuda, H., Lamaze, C.E., Sakaoku, K., 1973. Effect of electrodeless glow discharge on polymers. *Journal of Applied Polymer Science,* 17(1), 137-152.

Yasuda, S., Sakakibara, A., 1975. The chemical composition of lignin from compression wood. *Mokuzai Gakkaishi (Japan Wood Research Society Journal),* 21(6), 363-369.

Yeo, H., Smith, W.B., 2003. Effect of temperature and moisture content on the discoloration of hard maple lumber. In: *Proceedings of the 8th International IUFRO Wood Drying Conference;* Brasov, Romania, pp. 455-458.

Yildiz, S., Gümüşkaya, E., 2007. The effects of thermal modification on crystalline structure of cellulose in soft and hardwood. *Building and Environment,* 42(1), 62-67.

Yoshimoto, T., Hayashi, S., Kishima, T., 1972. Artificial modification of bordered pits in softwoods:(1) Treatment with sodium hydroxide solution. *Wood Research,* (52), 90-105.

Young, R.A., Rammon, R.M., Kelley, S.S., Gillespie, R.H., 1982. Bond formation by wood surface reactions; I. Surface analysis by ESCA. *Wood Science,* 14(3), 110-119.

Young, R.A., Fujita, M., River, B.H., 1985. New approaches to wood bonding; A base-activated lignin adhesive system. *Wood Science and Technology,* 19(4), 363-381.

Yuan, X., Jayaraman, K., Bhattacharyya, D., 2004. Effects of plasma treatment in enhancing the performance of woodfibre-polypropylene composites. *Composites: Part A; Applied Science and Manufacturing,* 35(12), 1363-1374.

Zaman, A., Alén, R., Kotilainen, R., 2000. Thermal behavior of Scots pine (*Pinus sylvestris*) and silver birch (*Betula pendula*) at 200-230 °C. *Wood and Fiber Science,* 32(2), 138-143.

Zanini, S., Riccardi, C., Canevali, C., Orlandi, M., Zoia, L., Tolppa, E.L., 2005. Modifications of lignocellulosic fibers by Ar plasma treatments in comparison with biological treatments. *Surface and Coatings Technology,* 200(1-4), 556-560.

Zink, P., Fengel, D., 1990. Studies on the colouring matter of blue-stain fungi; Part 3. Spectroscopic studies on fungal and synthetic melanins. *Holzforschung,* 44(3), 163-168.

Zink, P., Fengel, D., 1989. Studies on the colouring matter of blue-stain fungi; Part 2. Electron microscopic observations of the hyphae walls. *Holzforschung,* 43(6), 371-374.

Zink, P., Fengel, D., 1988. Studies on the colouring matter of blue-stain fungi; Part 1. General characterization and the associated compounds. *Holzforschung,* 42(4), 217-220.

Appendices

Appendix 1 - Collection of SEM and light microscopy images of untreated and plasma treated samples of studied species (see CD)

Appendix 2 - Statistical analysis: Chapter 4

a) Effect of wood species (poplar or yellow cedar), Plasma treatment time and cell wall type (radial or tangential) and their interaction on etching of wood cell walls (see CD)
b) Effect of wood type (highly lignified compression v. normal wood) on the erosion of cell walls (see CD)
c) Effect of pellet type (cellulose and lignin) and plasma treatment time and their interaction on etching of pellets (see CD)

Appendix 3 - Statistical analysis: Chapter 5

Effect of plasma treatment and wood species and their interaction on chemical composition of wood (see CD)

Appendix 4 - Statistical analysis: Chapter 6

Effect of plasma treatment on contact angle, absorption of bleach, changes in color parameters of blue stained wood (see CD)

Appendix 5 - Statistical analysis: Chapter 7

a) Effect of plasma treatment and coatings type on the contact angle and adhesion of coatings on hot-oil modified blue stained wood (see CD)
b) Effect of treatment type (vacuum, plasma treatment, hot-oil treatment, hot-oil/plasma treatment) and coating on the performance of coated specimens exposed to natural weathering: the ratio of the color parameters, surface gloss, water uptake of the weathered wood to those of non weathered wood, and percentage of cracks on coated weathered samples (see CD)